Master's thesis

NTNU
Norwegian University of Science and Technology
Faculty of Natural Sciences
Department of Chemistry

Sigrid Maria Elisabeth Selmer-Olsen

Palladium Catalyzed Cross-Coupling Reactions on 7-Azaindoles in the Synthesis of CSF1R Inhibitors

Master's thesis in Chemistry
Supervisor: Bård Helge Hoff, IKJ
May 2019

NTNU
Norwegian University of
Science and Technology

Sigrid Maria Elisabeth Selmer-Olsen

Palladium Catalyzed Cross-Coupling Reactions on 7-Azaindoles in the Synthesis of CSF1R Inhibitors

Master's thesis in Chemistry
Supervisor: Bård Helge Hoff, IKJ
May 2019

Norwegian University of Science and Technology
Faculty of Natural Sciences
Department of Chemistry

NTNU
Norwegian University of
Science and Technology

I hereby declare that the work done in this thesis is independent and in accordance with the exam regulations of the Norwegian University of Science and Technology.

Trondheim, May 13th, 2019

Sigrid Maria Elisabeth Selmer-Olsen

Acknowledgements

This master thesis has been carried out in the Department of Chemistry at the Norwegian University of Science and Technology from August 2017 to May 2019. It has been supervised by Professor Bård Helge Hoff and PhD Candidate Thomas Ihle Aarhus.

I want to thank Professor Bård Helge Hoff for the invaluable guidance he has given me throughout the project, and for helping with problems and providing support when necessary. I would also like to thank to PhD Candidate Thomas Ihle Aarhus for always being ready to answer my questions and teaching me so much during my time in the lab. A special note to PhD Susana Vila Gonzalez and Engineer Julie Asmussen for help with the MS analysis, Head Engineer Torun Margareta Melø for all her friendly help with the NMR analysis, and Engineer Roger Aarvik for supplying chemicals.

Lastly, a huge thank you to my family, friends and fellow students for supporting me throughout my studies at NTNU, and making my time here so enjoyable.

Abstract

The overexpression of colony stimulating factor 1 receptor (CSF1R) tyrosine kinase has been linked to numerous diseases, including cancers, bone osteolysis and inflammatory disorders. An emerging treatment strategy for these conditions is the inhibition of the Colony Stimulating Factor 1 Receptor (CSF1R) tyrosine kinase. The aim of this master thesis was to investigate the synthetic strategies towards substituted pyrrolopyridines, as possible CSF1R inhibitor structures.

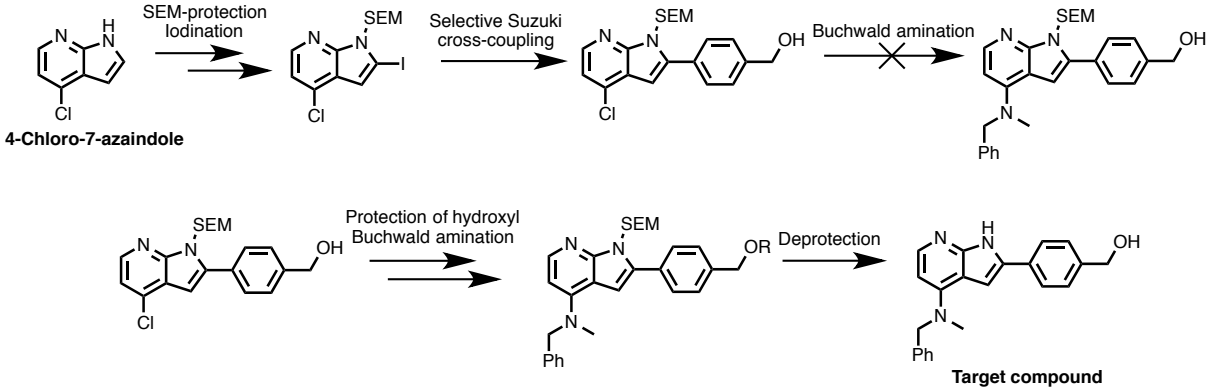

The initial reactions included synthesis of a building block containing a SEM-protecting group and an iodide leaving group. These syntheses proceeded in overall good yields. A selectivity study of the Suzuki-Miyaura cross-coupling reaction was performed, employing various catalysts, ligands and reaction conditions. The most chemoselective catalyst was found to be $Pd(PPh_3)_4$. The selective mono-cross-coupling in C-2 position was conducted giving an isolated yield of 83%.

Several Buchwald-Hartwig aminations were then performed on the mono-cross-coupled product. Various conditions were investigated, yet the amination of a substrate containing a free hydroxyl group remained unsuccessful. The protected substrate analogues gave good results in Buchwald aminations, and the most rewarding reactions provided yields of 89% and 92% of the aminated products.

Removal of the protecting groups was challenging. Two methods of protecting group removal were attempted, providing yields between 3-74% of the target compound.

Sammendrag

Overuttrykk av colony stimulating factor 1 receptor (CSF1R) tyrosin kinase er blitt linket til flere sykdommer, blant annet kreft, benosteolyse og betennelseslidelser. En lovende behandlingsstrategi for disse sykdommene er hemming av Colony Stimulating Factor 1 Receptor (CSF1R) tyrosin kinase. Målet for denne masteroppgaven har vært å undersøke syntetiske strategier mot substituerte pyrrolopyridiner som mulige CSF1R hemmere.

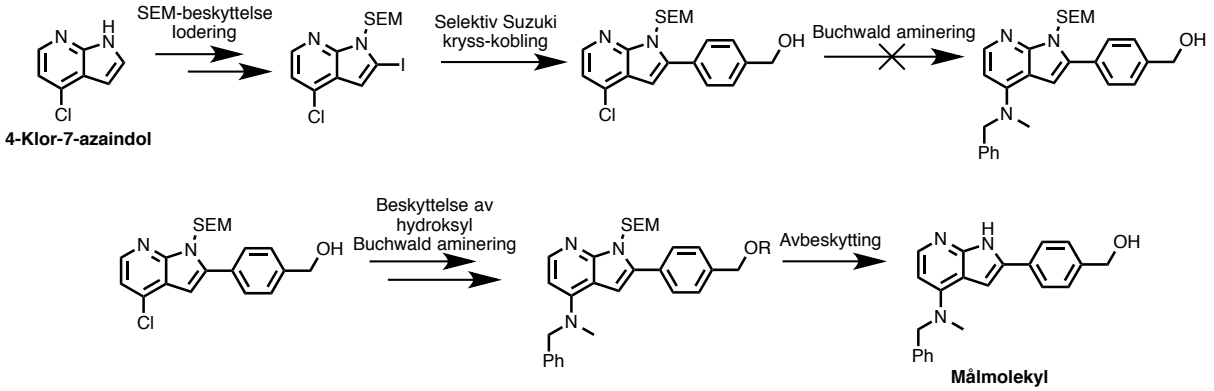

De første reaksjonene var syntese av en byggestein som inneholdt en SEM-beskyttelsesgruppe og jod som utgående gruppe. Disse reaksjonene ble utført med gode utbytter. En selektivitetsstudie av Suzuki-Miyaura-krysskoblinger ble gjennomført, hvor ulike katalysatorer, ligander og reaksjonsbetingelser ble testet. Den mest kjemoselektive katalysatoren viste seg å være $Pd(PPh_3)_4$. Selektiv mono-krysskobling i C-2-posisjon ble utført, og ga et utbytte på 83%.

Flere Buchwald-Hartwig-amineringer ble deretter utført på det mono-krysskoblede produktet. Ulike reaksjonsbetingelser ble utforsket, men aminering av substratet som inneholdt en fri hydroksylgryppe forble mislykket. De beskyttede substratanalogene ga gode resultater i Buchwald amineringer, hvor de mest vellykkede reaksjonene gav utbytter på 89% og 92% av de aminerte produktene.

Avbeskytting av beskyttelsesgruppene var utfordrende. To metoder for fjerning av beskyttelsesgrupper ble utprøvd, og gav utbytter mellom 3-74% av målmolekylet.

Contents

Symbols and abbreviations

ADME-tox	Absorption, Distribution, Metabolism, Excretion, Toxicity
ADP	Adenosine diphosphate
ALK	Anaplastic lymphoma kinase
APCI	Atmospheric-Pressure Chemical Ionization
aq.	Aqueous
Ar	Aryl
ASAP	Atmospheric Solids Analysis Probe
ATP	Adenosine triphosphate
br	Broad signal
BrettPhos	2-(Dicyclohexylphosphino)3,6-dimethoxy-2,4,6-triisopropyl-1,1-biphenyl
cat.	Catalyst
CDK1	Cyclin-dependent kinase 1
COSY	Correlation Spectroscopy
CSF-1	Colony Stimulating Factor 1
CSF1R	Colony Stimulating Factor 1 Receptor
δ	Chemical shift [ppm]
d	Doublet
dba	Dibenzylideneacetone
DMSO	Dimethyl Sulfoxide
DMF	Dimethylformamide
dppf	1,1-Bis(diphenylphosphino)ferrocene
EGFR	Epidermal Growth Factor Receptor
eq.	Equivalent
FTIR	Fourier Transform Infrared Spectroscopy
G2	Generation 2
h	Hour(s)
HMBC	Heteronuclear Multiple Bond Correlation
HPLC	High Performance Liquid Chromatography
HRMS	High Resolution Mass Spectroscopy
HSQC	Heteronuclear Single Quantum Correlation
IC_{50}	Half maximum inhibitory concentration
IR	Infrared
J	Coupling constant [Hz]
JAK	Janus kinase
LDA	Lithium diisopropylamide
lit.	Literature value
m	Multiplet
min	Minute(s)
MOM	Methoxymethyl
mp	Melting point
MS	Mass spectrometry

m/z	Mass per charge
NAS	Nucleophilic Aromatic Substitution
NRTK	Non-Receptor Tyrosine Kinase
^{1}H NMR	Proton nuclear magnetic resonance
^{13}C NMR	Carbon nuclear magnetic resonance
ν	Wave number
PEPPSI™-SIPr	(1,3-Bis(2,6-diisopropylphenyl)imidazolidene)(3-chloropyridyl) palladium(II) dichloride
PK	Protein kinase
ppm	Parts per million
PTK	Protein Tyrosine Kinase
q	Quartet
quin	Quintet
R_f	Retention factor
rt	Room temperature
RTK	Receptor Tyrosine Kinase
RuPhos	2-Dicyclohexylphosphino-2,6-diisopropoxybiphenyl
s	Singlet
SAR	Structure-Activity Relationship
sat.	Saturated
SEM	2-(Trimethylsilyl)ethoxymethyl
sep	Septet
sh	Sharp signal
t	Triplet
TBAF	Tetra-*n*-butylammonium fluoride
TBDMS	*tert*-Butyldimethylsilyl
TFA	Trifluoroacetic acid
THF	Tetrahydrofuran
TLC	Thin Layer Chromatography
XantPhos	4,5-Bis(diphenylphosphino)-9,9-dimethylxanthene
XPhos	2-Dicyclohexylphosphino-2',4',6'-triisopropylbiphenyl

Numbered compounds

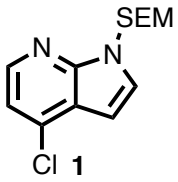

1

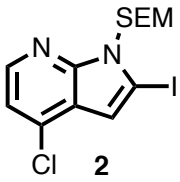

2

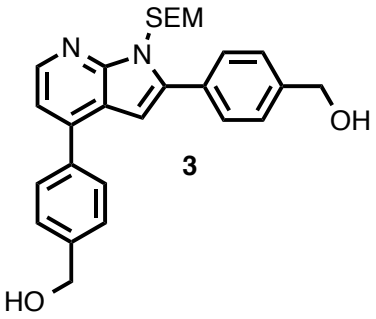

3

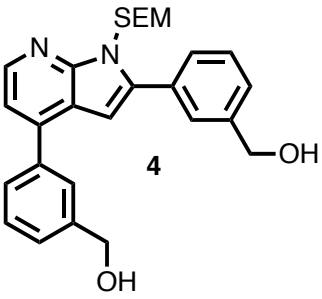

4

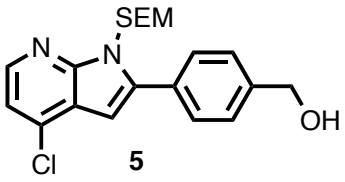

5

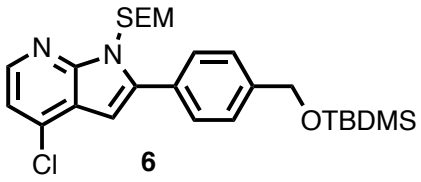

6

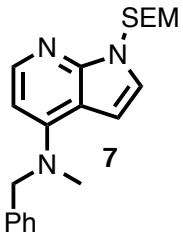

7

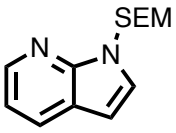

7b

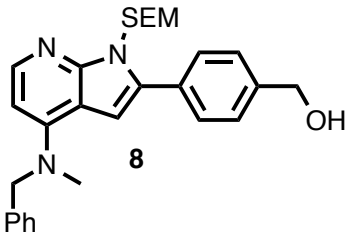

8

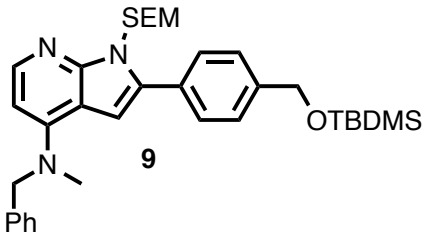

9

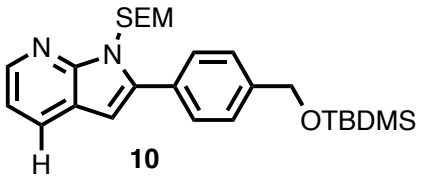

10

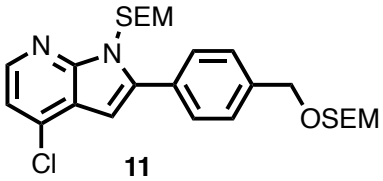

11

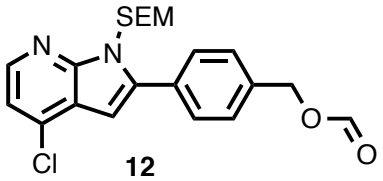

12

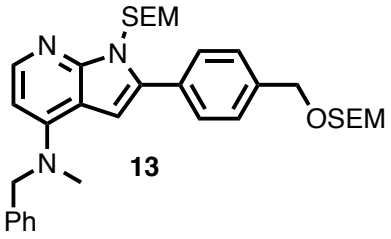

13

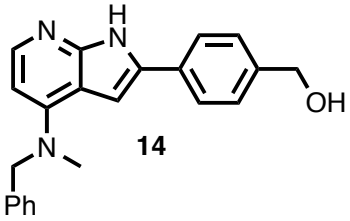

14

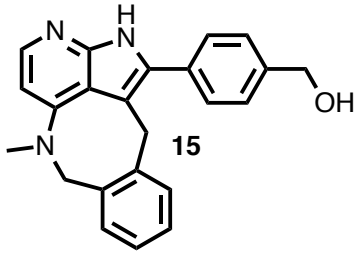

15

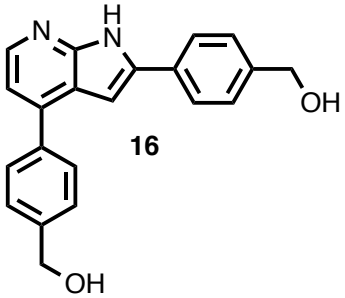

16

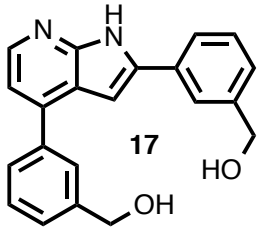

17

1. Background and aim

A total of 12 million people are diagnosed with cancer every year.[1] The search for drugs is vitally important, as this disease is becoming one of the foremost sources of death in developed countries. A promising strategy for developing a treatment is researching the activity of protein kinases in the regulation of cellular processes.[2]

Protein kinases are enzymes that catalyze the phosphorylation of proteins, thereby regulating and controlling their activities.[2] Thus, protein kinases play key roles in controlling cell division, metabolism, survival and differentiation.[3] Mutation or malfunction of the protein kinases has been shown to give rise to several diseases, including various types of cancer, diabetes and inflammatory disorders.[4] Cellular processes and signal transduction in cells are dependent on the functionality of protein kinases, making them attractive drug targets.[2, 5-6] Great amounts of research have been undertaken to investigate the role of the protein kinases in cell regulation.

Colony Stimulating Factor 1 Receptor (CSF1R) is a receptor protein kinase. The overexpression of CSF1R has been linked to several diseases such as cancers and bone osteolysis.[7] Inhibition of CSF1R may therefore be a valuable target for treatment of these diseases, as there are no drugs on the market today.[7-9]

The research group has generated multiple protein kinase inhibitors with pyrrolo-, thieno- and furopyrimidine structures. The main focus has been inhibition of the epidermal growth factor receptor (EGFR) tyrosine kinase.[10] Some of the pyrrolopyrimidine compounds have been found to have inhibitory activity towards CSF1R, see Figure 1.1.[10-11]

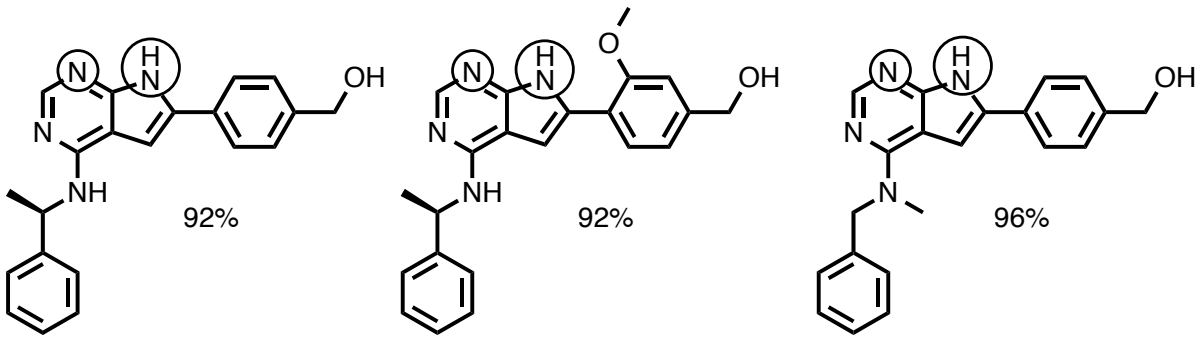

Figure 1.1: Pyrrolopyrimidines possessing activity towards CSF1R, with their respective percent of inhibition at a 500 nM test concentration.[10-11] The encircled nitrogen atoms are believed to be involved in hinge interactions with the CSF1R active site.

It is believed that the nitrogen atoms encircled in Figure 1.1 play a role in interactions with the ATP binding site of CSF1R. The structure-activity relationship (SAR) could be investigated further by replacing the pyrrolopyrimidine scaffold with pyrrolopyridine.

A water-mediated interaction has also been observed between the N-2 nitrogen of the pyrrolopyrimidine inhibitors and a threonine residue of the protein. Investigation of inhibitors with a pyrrolopyridine scaffold, lacking this nitrogen atom, would provide further insight into this interaction and its importance for binding.

This project aims to explore the pyrrolopyridine structure in developing CSF1R inhibitors, and to further investigate the synthetic routes towards 2-aryl-4-aminopyrrolopyridines. The main target molecule is shown in Figure 1.2.

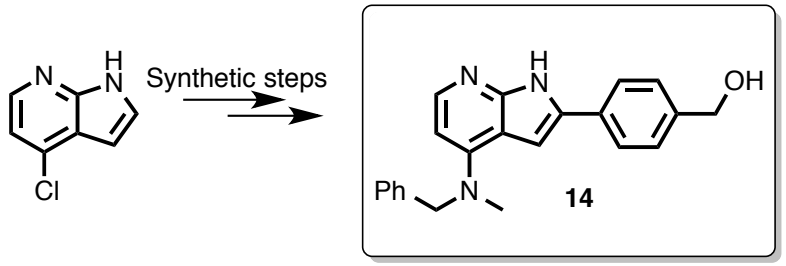

Figure 1.2: Structure of the target (4-(4-(benzyl(methyl)amino)-1*H*-pyrrolo[2,3-*b*]pyridin-2-yl)phenyl)methanol (**14**).

2. Introduction and theory

2.1 Tyrosine kinase

Protein kinases (PKs) are a type of enzymes which catalyze protein phosphorylation. Protein phosphorylation is a highly important process in cell life, as it is a major mechanism through which a protein or enzyme function is regulated.[2] Regulation is important in intracellular processes such as proliferation, apoptosis, angiogenesis and cell replication.[2-3] Mutation or malfunction of the PKs may give rise to multiple diseases including cancer, diabetes and inflammatory disorders.[5] For this reason, the PKs have become important drug targets for medicinal chemists.[2, 4, 6]

PKs are named by the amino acid they phosphorylate in the protein. Protein tyrosine kinases (PTKs) are the enzymes that catalyze the transfer of γ–phosphate from ATP to the hydroxyl group of a tyrosine unit in proteins, leading to a cellular response.[12] The tyrosine kinase activity is illustrated in Figure 2.1.

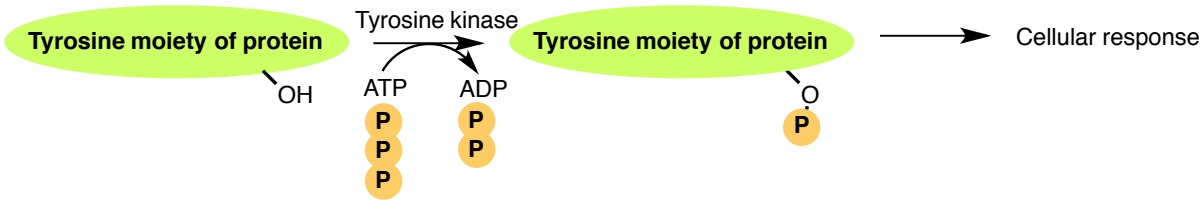

Figure 2. 1: Illustration of the tyrosine kinase activity. Protein tyrosine kinase facilitates the γ-phosphate group transfer from ATP to a tyrosine unit of the protein.

Small molecular inhibitors for the PKs have been classified according to their mechanism of binding to the enzyme. The inhibitors may bind directly in the ATP-binding pocket, next to the ATP-binding site, and they may also bind to either an active or inactive confirmation of the enzyme. Three different types of inhibitors have been distinguished. Type I and type II inhibitors bind in the ATP-pocket. Type I binds to the active conformation, while type II bind to the inactive conformation. Type III binds to an adjacent position to the ATP-pocket, and therefore does not compete with ATP.[4]

One of the primary ways that cells communicate with one another is through binding polypeptide ligands to receptors that possess tyrosine kinase activity.[12] There are two classes of PTKs. The receptor tyrosine kinases (RTKs) cause activation of signaling pathways within the cells, and the non-receptor tyrosine kinases (NRTKs) are components of the signaling pathways instigated by receptors.[12]

The RTKs structure consists of two domains, one extracellular and one intracellular domain which are connected by a transmembrane domain.[13] The activation of the enzyme happens when an extracellular signal ligand (growth factor for cytokine) binds to the extracellular domain.[14-15] The activated enzyme can then catalyze phosphorylation, recruitment and activation of multiple downstream signaling proteins. Overexpression of

RTKs may lead to inflammatory responses and multiple diseases including cancer, psoriasis and diabetes.[16-17]

2.2 CSF1R

Colony Stimulating Factor 1 Receptor (CSF1R) is a type III receptor tyrosine kinase. It is activated by two ligands, the Colony Stimulating Factor 1 (CSF-1) and IL-34.[7, 18] Overexpression of CSF-1 and CSF1R may cause several diseases and disorders, for example inflammatory diseases, bone osteolysis and cancers. CSF1R is significant in microglia differentiation and activation processes, and this indicates that the receptor can be an important target for treating neuroinflammatory and neurodegenerative diseases.[19] It has also been reported to promote growth and metastasis of certain cancer types.[7]

Signal transduction of the CSF1R cascade has been shown to result in survival, proliferation and differentiation of monocyte/macrophage linage.[6-7, 20] Macrophages are a cell type found in every tissue of the body, involved in the immune defense and development of tissue.[21] They can operate as both positive and negative facilitators for the immune system, and promote growth factors, angiogenic factors and proteases to aid tissue repair.[20, 22] If a tumor has been established in the body, macrophages may become pro-tumeral and help to grow and spread the tumor.[23-24] These are often called tumor associated macrophages (TAM).

Thus, CSF1R inhibition may be a promising strategy for treating the above-mentioned diseases.[8-9] Previously, two different courses of inhibition have been described. The first method involves small molecules inhibiting the CSF1R tyrosine kinase activity, while in the second method the binding between the receptor and its stimulating factor CSF-1 is hindered.[6]

Multiple concerns arise from the inhibition of the CSF1R inhibitors, due to the fact that CSF1R is a member of a larger group of similar receptors.[25] Inhibition of CSF1R may therefore offer an effect on the other receptors in the group, if the inhibitor shows low selectivity.[26] Accumulation of CSF-1 in the cells could also be a complication from inhibition.[6]

2.2.1 Previously identified inhibitors

There has already been identified multiple potent CSF1R inhibitors. Ki20227 is an inhibitor reported to be an especially useful agent in treatment of osteolytic diseases and bone diseases.[27] GW2580 is another, more selective inhibitor.[6, 28] PLX3397 is a highly selective inhibitor, reported to slow tumor growth and delay the metastasis of tumor models of mice.[29-30]. It is a derivative of PLX647, where some structural alterations have been made, including changing the phenyl group into a pyridine, and adding a chlorine atom in the 5-position of the 7-azaindole moiety. With these alterations, PLX3397 showed an increased potency towards inhibiting CSF1R and a lower cross-reactivity with other kinases.[31] All four inhibitors are shown in Figure 2.2 with their respective IC_{50}-values.

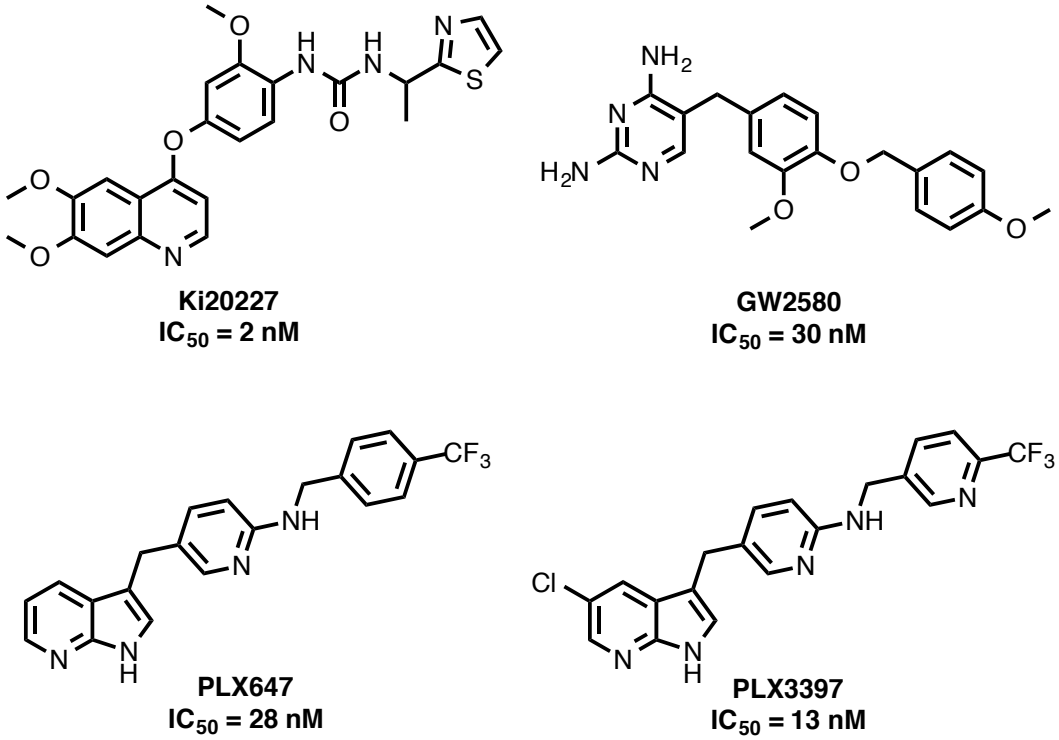

Figure 2.2: CSF1R inhibitors Ki20227[27], GW2580[28], PLX647[32] and PLX3397[31] with their respective IC_{50} values.

2.2.3 Structure of CSF1R

The crystal structure of a kinase inhibitor in complex with the unphosphorylated CSF1R has been reported by Schubert *et al.*, and is shown in Figure 2.3.[33] The binding between the CSF1R backbone and the relevant ligand stimulates the autophosphorylation, dimerization and phosphorylation of the kinase target molecules. In the binding, one or more hydrogen bonds usually arise between the two units.

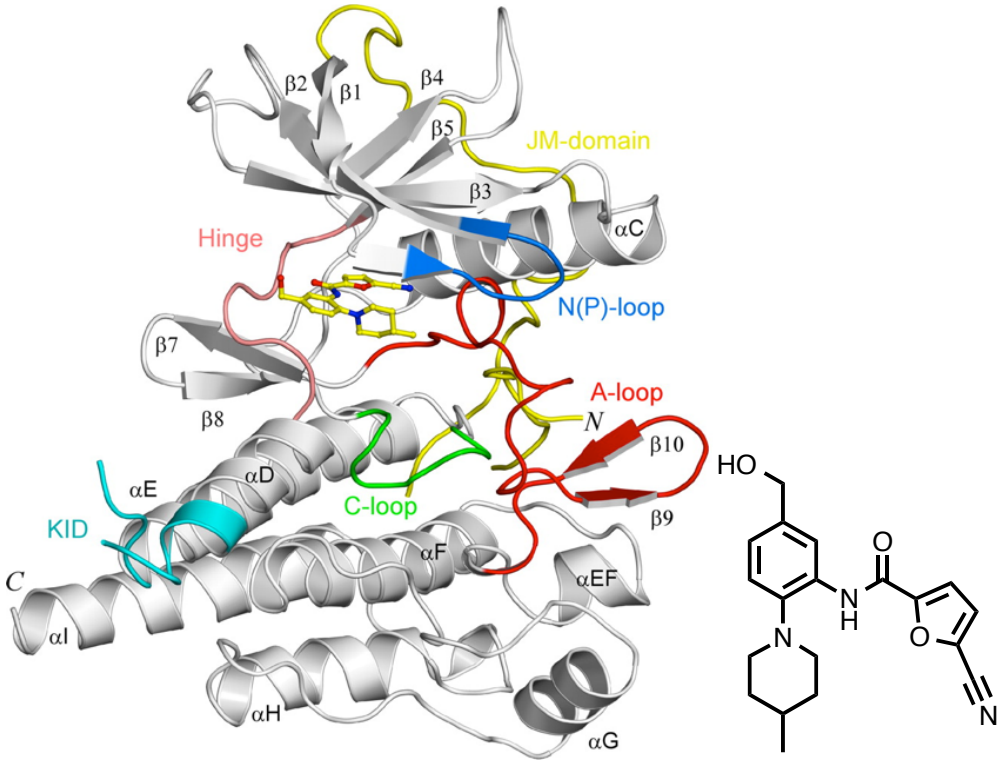

Figure 2.3: The crystal structure of CSF1R with the bound inhibitor on the right. The structural element in blue is the nucleotide binding lobe, red is the activation loop, pink is the hinge region, cyan is the kinase insert domain and yellow is the juxtamembrane domain.[33]

There exists a two-lobe structure in the protein. The N-lobe, on top in Figure 2.3, consists of five twisted β–sheets and one α-helix. The C-lobe, on the bottom of Figure 2.3, consists mostly of α–helix structures. The two lobes are connected to each other by a hinge region. The binding of nucleotide or inhibitor is facilitated by the hinge and the N-lobe, while the C-lobe is responsible for substrate binding. The binding of ATP or inhibitor takes place in a cleft between the N-lobe and the C-lobe.[33]

The activation loop, typically around 22 amino acids long for RTKs, is an essential region for the regulation of kinase activity.[34] Stimulation of RTK activity is dependent on the autophosphorylation of tyrosine residues in the activation loop. When inhibitor structures are introduced, the binding of ATP or substrate is hindered, and the phosphorylation of tyrosine residues is inhibited.[33]

2.3 Substituted pyrrolopyridines

The syntheses in this project are based upon pyrrolopyridines, also named azaindoles. These are fused heterocycles which consist of a pyrrole ring and a pyridine ring. The pyrrole unit is electron rich, and the pyridine ring electron deficient. There are four possible isomers of azaindoles. The isomers are shown in Figure 2.4, as is the atom-numbering of pyrrolo[2,3-*b*]pyridine or 7-azaindole.

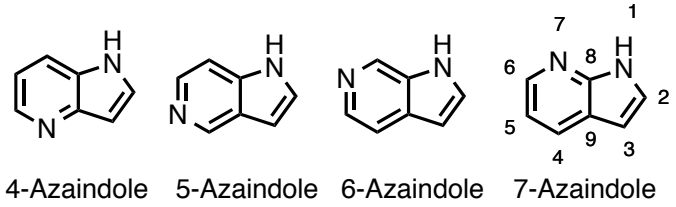

Figure 2.4: The four isomers of azaindoles, with the atom numbering of 7-azaindole.

The azaindoles structures are rare in nature, but the commercial availability has increased in later years.[35-36] One reason for their relevance in drug optimization strategies is that the pK_A, lipophilicity, target binding and ADME-tox (Absorption, Distribution, Metabolism, Excretion, Toxicity) properties of the compounds can be finely adjusted and tuned.[37-39] The 7-azaindole is the azaindole isomer that has generated the largest amount of commercially available molecules, in addition to over 100.000 structures described.[40]

2.3.1 Previous synthesis on 7-azaindoles

Multiple methods have been described for the synthesis of 7-azaindoles. A two-step synthesis of 2-substituted 7-azaindoles was reported by de Mattos *et al*. [41] The first step was a palladium catalyzed Sonogashira coupling, followed by a cyclization with the use of 18-crown-6. Whelligan *et al.* have reported the syntheses of a broad range of aza- and diazaindoles, starting from various chloroamino-*N*-heterocycles.[42] The two-step synthesis of 7-azaindole involved a Suzuki cross-coupling reaction with (2-ethoxyvinyl)borolane, followed by a cyclization catalyzed by acetic acid. Both mentioned syntheses are shown in Scheme 2.1.

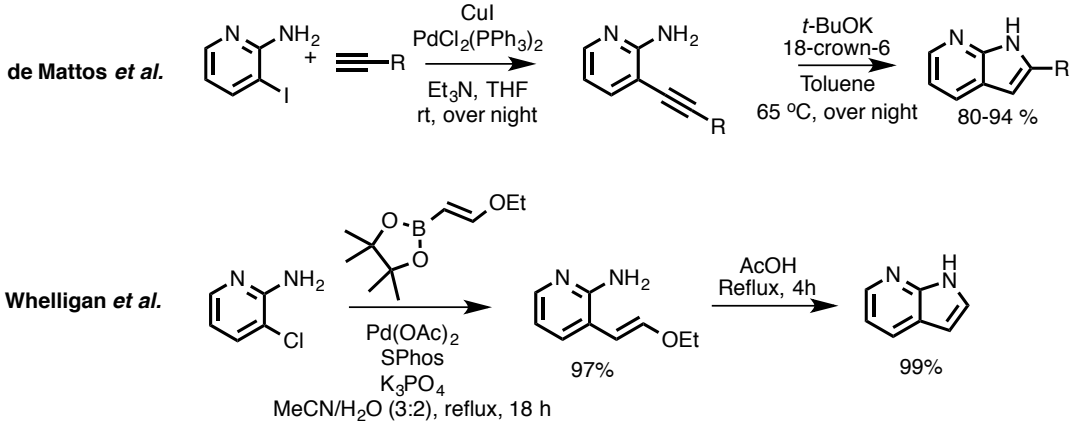

Scheme 2.1: The synthesis of 2-substituted 7-azaindoles as described by de Mattos *et al.*[41], and the synthesis of 7-azaindole as described by Whelligan *et al*.[42]

Many biological targets have been found for 7-azaindoles, amongst them are the kinases.[40, 43] Some examples of kinases that have been reported to be inhibited by 7-azaindole structures are Anaplasmic Lymphoma Kinase (ALK)[44], Aurora kinases[45] and Janus kinases (JAK)[46]. Huang *et al.* reported a synthesis which involved introducing a benzenesulfonyl protecting group to the 7-azaindole, performing a Suzuki cross-coupling reaction and a displacement of chloride to afford an inhibitor of CDK1 (Cyclin-dependent kinase 1).[47] Zhang *et al.* report the synthesis of the KIT/CSF1R dual kinase inhibitor PLX647, by a condensation reaction between 7-azaindole in C-3-position and an aldehyde, followed by a reduction of the secondary alcohol.[32] Farmer *et al.* performed a short synthesis starting with a Suzuki cross-coupling reaction between the 7-azaindole boronate ester and a chloropyrimidine derivative, followed by an amide bond formation which resulted in the JAK inhibitor Decernotinib.[46] The syntheses mentioned are shown in Scheme 2.2.

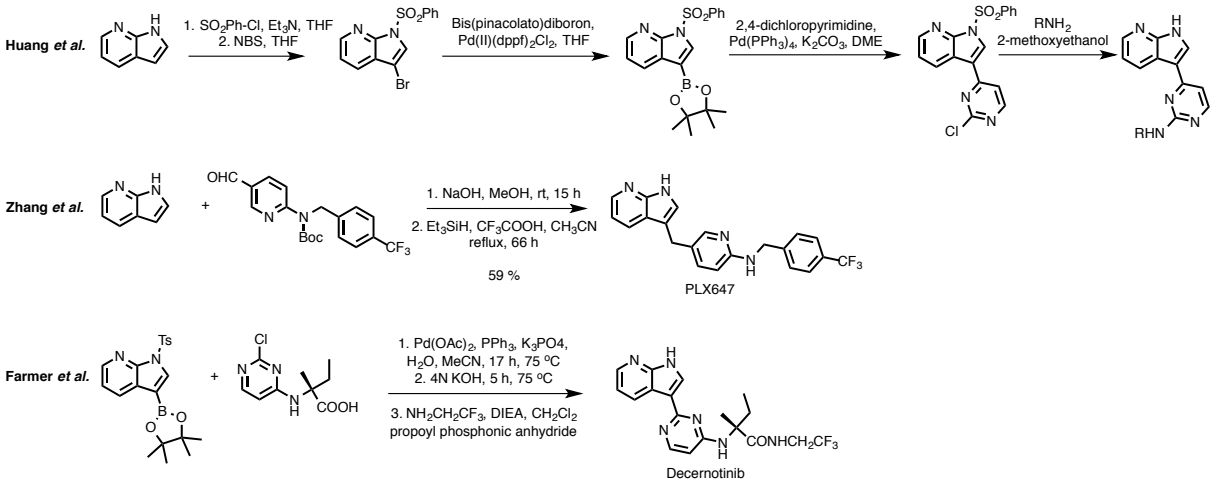

Scheme 2.2: Examples of syntheses of kinase inhibitors from 7-azaindole structures, as described by Huang *et al.*,[47] Zhang *et al.*[32] and Farmer *et al.*[46]

2.3.2 Amination of 7-azaindoles

Different synthetic approaches may be considered when attempting to form 4-amino-7-azaindoles. The corresponding halide may be used in a S_NAr displacement reaction to obtain the aminated product. High temperatures are often necessary, as well as long reaction times and a large excess of amine.[48] Caldwell *et al.* reported a yield of 53% for the thermal amination of an unprotected 4-chloro-7-azaindole substrate.[48] Gehringer *et al.* reported a yield of 63% in the amination reaction of a toluenesulfonyl-protected 5-bromo-4-chloro-7-azaindole substrate.[49] The two examples are shown in Scheme 2.3.

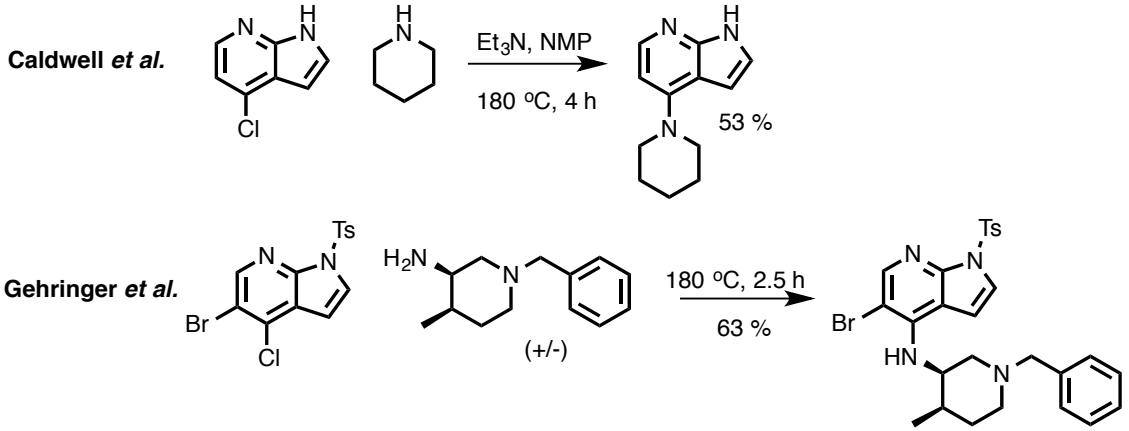

Scheme 2.3: Examples of thermal aminations on 4-chloro-7-azaindole structures, as described by Caldwell *et al.* and Gehringer *et al*.[48-49]

Another synthetic approach utilizes palladium catalysis for the amination reactions. Palladium catalyzed cross-coupling reactions between unprotected halo-azaindoles and amines have been reported by Henderson *et al.,* providing high yields of reactions with both primary and secondary amines.[50] An example is shown in Scheme 2.4. It should be mentioned that Johansen in her master thesis was not able to reproduce this reaction, and that the ^{1}H NMR by Henderson does not match the proposed structure.[50-51]

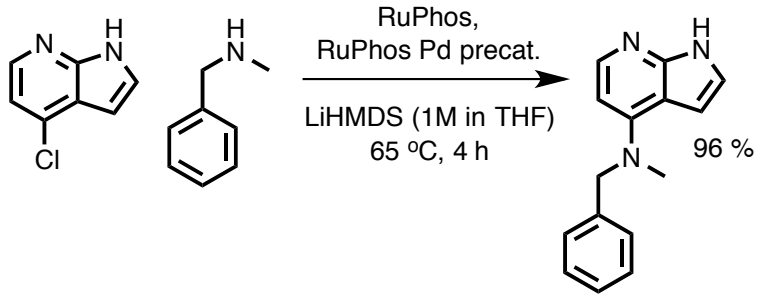

Scheme 2.4: A palladium catalyzed amination reaction on a unprotected 4-chloro-7-azaindole with a secondary amine, as reported by Henderson *et al.*[50]

2.4 Protecting groups

Pyrrolopyridines contain a reactive lone pair on the pyrrole nitrogen. A protecting group in this position causes the reactivity on the pyrrole nitrogen to be reduced and the regioselectivity of subsequent reactions on the pyrrole moiety may be altered.[52] Multiple factors should be contemplated when choosing a protecting group. Some important considerations are the nature of the substrate and the stability of the protecting group under the preferred reaction conditions. The chosen strategy should also allow for protecting group removal without degradation.[53]

Nitrogen protection with an electron withdrawing group will provide the desired effect of decreasing the nucleophilicity and the accessibility of the lone pair of 7-azaindoles. Sulfonyl protecting groups are commonly used for pyrroles and show a great electron

withdrawing ability.[52, 54] Other commonly used protecting groups are silyl groups, including the 2-(trimethylsilyl)ethoxymethyl group (SEM) and the *tert*-butyl-dimethylsilyl group (TBDMS), shown in Figure 2.5.

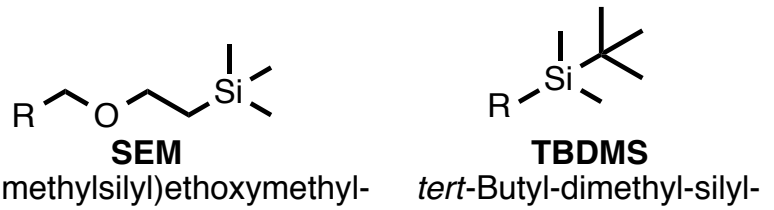

Figure 2.5: The structures of the two protecting groups SEM and TBDMS.

2.4.1 SEM protecting group

The SEM group is useful in settings where a stable protecting group is needed. In Suzuki cross-coupling reactions with pyrrolopyridazinones, a structure which has structural similarities to pyrrolopyridine, the use of SEM protection has resulted in excellent yields.[55] The SEM group has several advantages, amongst others in not being too sterically demanding and being more resistant to decomposing than other common protecting groups. The ability to direct lithiation towards the 2-position of 7-azaindoles is also an attractive feature of the SEM group.[55-56]

The removal strategies of the SEM group may be harsh, as a consequence of its stability under various reaction conditions, and the deprotection often involves fluoride sources.[53] Several papers have reported difficulties with removal of the SEM group.[57-59]

Both one-step and two-step deprotections have been reported. A one-step deprotection by treatment with tetra-*n*-butylammonium fluoride (TBAF) in THF, or aqueous HCl in EtOH, was described by Luo *et al.*[56] In the two-step SEM-removal reactions, the first step has been reported to involve cleaving off $Si(CH_3)_3F$ and formation of a hydroxymethyl protected intermediate. The intermediate is then cleaved under basic conditions in the second step, and formaldehyde is formed.[60-61] Zhou *et al*. reported a two-step deprotection method employing boron trifluoride diethyl etherate (BF_3-OEt_2), followed by aqueous ammonium hydroxide.[60] Hatcher *et al*. have reported deprotection by TFA in CH_2Cl_2, followed by treatment with $NaHCO_3$ in THF for completing the second step.[61] The suggested mechanisms for one-step deprotection and two-step deprotection are shown in Scheme 2.5. If only $Si(CH_3)_3F$ is cleaved off and deprotection is incomplete, the substrate remains protected and this may cause low yields.

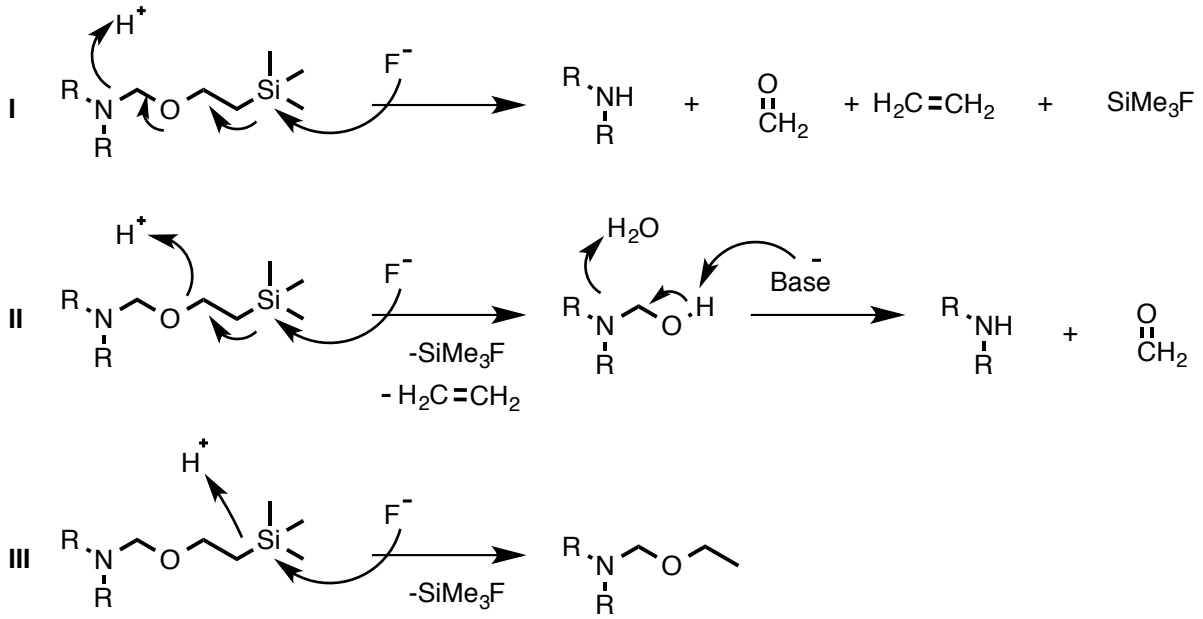

Scheme 2.5: Suggested mechanisms for SEM deprotection: One-step deprotection (I), two-step deprotection (II) and incomplete deprotection (III).[60, 62-63]

2.4.2 TBDMS protecting group

The TBDMS, or TBS, group is known for its ease of removal, as it can be cleaved under conditions that typically do not disturb other groups that are unstable towards acid or base.[64] Its bulkiness provides a selectivity towards primary alcohols. The group is stable towards aqueous base, but can be transformed back to the alcohol if treated with acid. As for the SEM group, fluoride sources are useful in the deprotection. Corey *et al*. suggested in 1972 a deprotection mechanism with TBAF as the fluoride source, as shown in Scheme 2.6.[65] Formation of the strong Si-F bond is the driving force of the deprotection reaction.

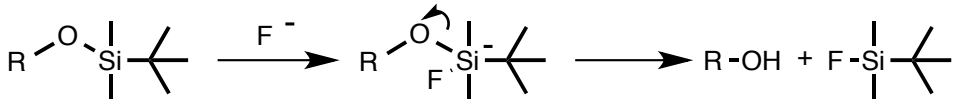

Scheme 2.6: Mechanism suggested by Corey *et al.* for TBDMS protecting group removal.[65]

2.5 Suzuki-Miyaura cross-coupling reaction

The Suzuki-Miyaura cross-coupling reaction (hereafter referred to as the Suzuki cross-coupling) is the palladium cross-coupling of an organoboronic acid and an aryl halide. The reaction forms new sp^2-sp^2 carbon-carbon bonds in good yields.

As a variety of boronic acids and halogenated compounds have become commercially available, the scope of the possible reactant structures has been widely broadened.[66] The Suzuki cross-coupling is catalyzed by palladium, which is often ligated to improve the reactivity and catalytic properties. In many cases, the reaction needs tuning due to low reactivity, formation of by-products or to improve chemo- or regioselectivity.

The removal of inorganic residues and byproducts is made easy as the reaction allows for water being present.[67] Organoboronic acids are generally thermally stable and inert to oxygen and water, and this makes the Suzuki cross-coupling more beneficial than other coupling reactions such as the Grignard reaction.[68] The reaction only requires a catalytic amount of palladium catalyst, together with a suitable base.[69] Enhanced selectivity of coupling organoborons and organic halides is provided when a negatively charged base is used, such as K_2CO_3. This arises from coordination between the negatively charged base and the organoboron, increasing the nucleophilicity of the organoboron.[68]

2.5.1 Mechanism

The mechanism of the Suzuki cross-coupling is suggested to take place in four steps as seen in the catalytic cycle shown in Scheme 2.7.[67-68] Firstly, the aryl/alkenyl/alkyl/alkynyl halide reacts with the Pd(0) catalyst in an oxidative addition step, forming the organopalladium species. The rate of the oxidative addition step is increased with the leaving group ability, in the order I>Br>Cl>F.[70] The metathesis step displaces the halide in the organopalladium complex, forming the more reactive organopalladium alkoxide or hydroxide, depending on the base.[71-73] A reaction with the base is also required for activating the boronic acid reactant, producing the more reactive and nucleophilic boronate anion.[66] The boronate anion is coupled to the organopalladium species in the transmetalation step.[73] The final cross-coupled product is formed in the reductive elimination step, where the Pd(II) returns to its Pd(0) oxidation state.

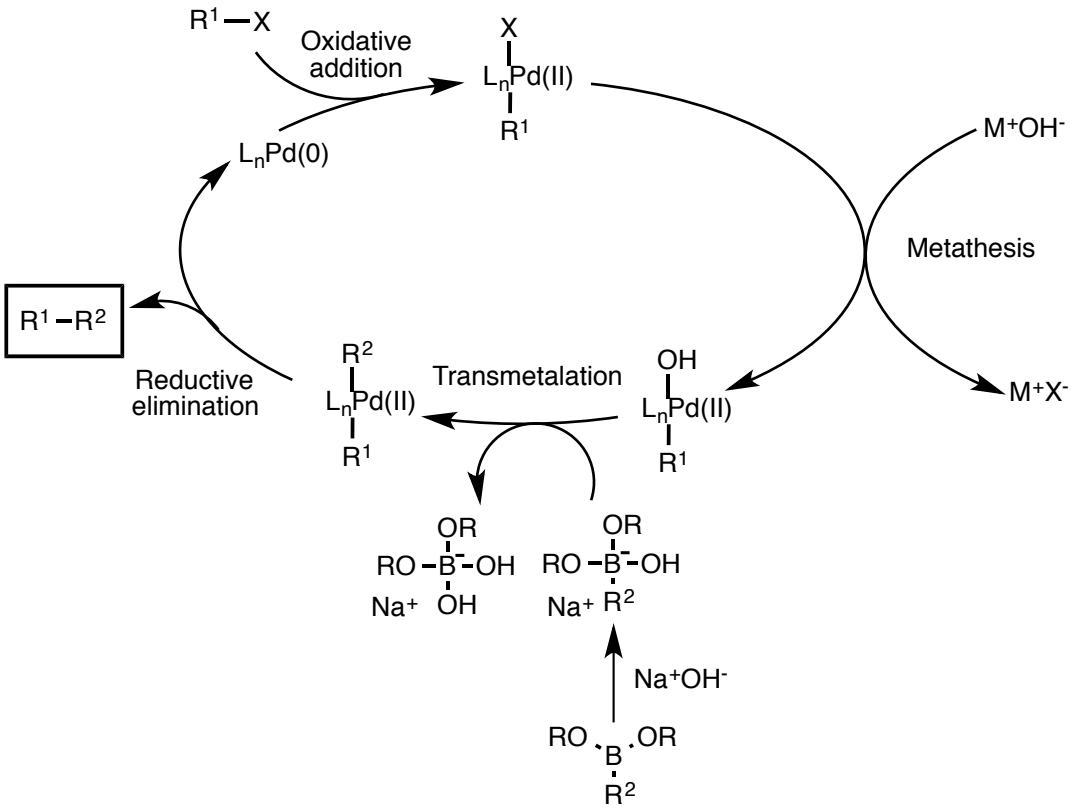

Scheme 2.7: The suggested mechanism of the Suzuki cross-coupling reaction.[67-68]

Which step is rate determining will depend on the reaction system. Schmidt *et al*. suggested that the transmetalation step was the rate determining step in the catalytic cycle, as no change in the rate of reaction was observed when switching from an aryl iodide to an aryl bromide.[74] Smith *et al.* found the rate determining step to change from oxidative addition to transmetalation when the substrate halide was switched from bromide to iodide.[75] The transmetalation step has been reported to proceed faster when the phenylboronic acid contains an electron donating substituent in 4-position.[66] Higher yields, better solubility and more selective reactions were also observed when electron rich boron acids were used.[66]

2.5.2 Byproducts and side reactions

Several side reactions of the Suzuki cross-coupling have been identified. Firstly, side reactions involving the boronic acid moiety will be presented, and they are shown in Scheme 2.8. Oxidative homocoupling of the boronic acid is a consequence of aerobic oxidation, where the boronic acid R-B(OH)$_2$ couples with another boronic acid unit to form R-R.[76] This side reaction is palladium catalyzed and therefore exists as a competing reaction to the Suzuki cross-coupling. In the presence of a base, the oxidation of the boronic acid R-B(OH)$_2$ to RO-B(OH)$_2$ may be catalyzed, and R-OH is formed through hydrolysis.[77] Peroxyboronic acid formed may also oxidize R-B(OH)$_2$ to ROH. Protodeboronation is another side reaction involving the boronic acid moiety, and several pathways of mechanism have been proposed.[77]

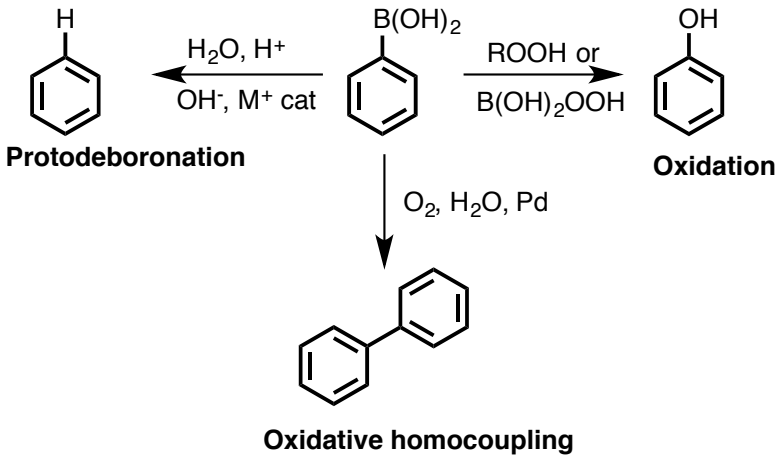

Scheme 2.8: Side reaction of the Suzuki cross-coupling reaction involving the boronic acid.[76-77]

Dehalogenation of the aryl halide is also observed in many Suzuki cross-coupling reactions, shown in Scheme 2.9. As proposed by Navarro *et al*. the dehalogenation and the Suzuki cross-coupling are competing reactions as they share many of the same catalytic steps.[78] They reported that when the substrates are sterically crowded, the rate of transmetalation is decreased and dehalogenation is favored. They observed that the dehalogenated byproduct was formed in the beginning of the reaction, without increasing over time.[78] Jedinák *et al.* proposed that the dehalogenation side reaction of pyrazole halide substrates was promoted by the base.[79] The amount of dehalogenated byproduct has also been reported to decrease with slow addition of the substrate when aryl chlorides are used.[80]

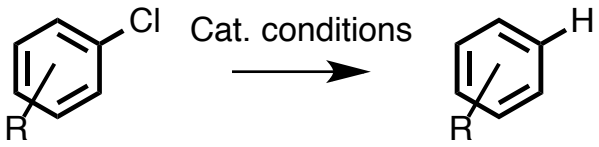

Scheme 2.9: Dehalogenation of the aryl chloride.[80]

2.5.3 Catalysts and ligands

Multiple catalysts for the Suzuki cross-coupling reaction have been developed. An effective ligand should combine steric bulkiness and fitting electronics. The electronics of the ligand are important, as electron rich ligands promote the oxidative addition step, but slow down the reductive elimination step.[81] Optimization of the catalyst and ligand system can be crucial in work to identify the most suitable conditions for a reaction. A selection of common Suzuki cross-coupling catalysts and ligands are shown in Figure 2.6.

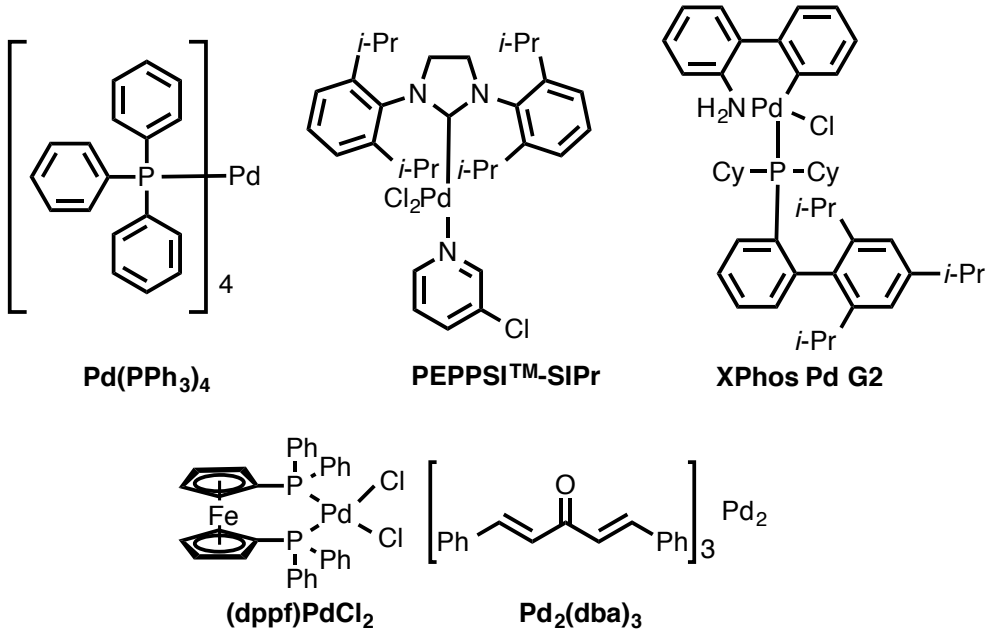

Figure 2.6: The structures of palladium catalysts $Pd(PPh_3)_4$, PEPPSI™-SIPr, XPhos Pd G2, $(dppf)PdCl_2$ and $Pd_2(dba)_3$.

The catalytic cycle for the Suzuki cross-coupling reaction starts with formation of the active Pd(0)-ligand complex, as can be seen in Scheme 2.7. The formation of this complex has been observed to be slow in some cases.[82] To overcome this challenge, pre-ligated Pd(II) compounds, called precatalysts, have been developed.[83-84] These precatalysts are stable towards air and moisture. They are deprotonated in basic conditions and rapidly undergo reductive elimination to form the active Pd(0) catalytic species. An example is the XPhos Pd G2 precatalyst, which is shown together with the XPhos ligand in Figure 2.7.

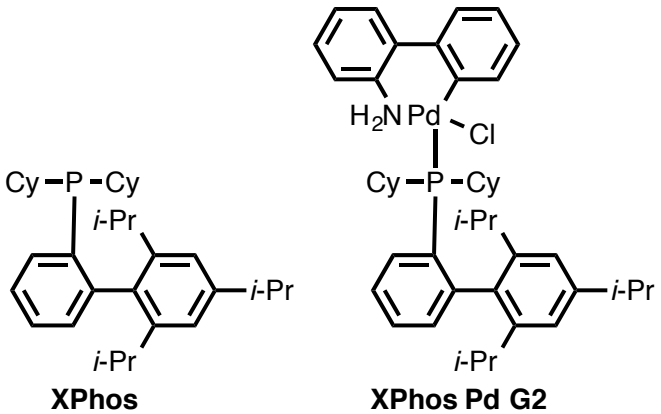

Figure 2.7: The structures of the ligand XPhos and the XPhos Pd G2 precatalyst.[85]

Additionally, the choices of base and solvent are important considerations for a successful reaction. The most suitable solvents for room temperature reactions are THF and 1,4-dioxane.[81] 1,4-Dioxane has been reported to be the best solvent for couplings between arylboronic acids and aryl chlorides.[86]

2.5.4 Regioselectivity and chemoselectivity

In the oxidative addition step, the reactivity is regulated by the nature of the halogen on the aryl halide. The order of reactivity of the halogens are I>Br>Cl>F, providing a difference in selectivity called chemoselectivity.[87] If the substrate is di- or poly-halogenated, the selectivity between the halogens, called regioselectivity or site-selectivity, may be difficult to achieve.[87] The electronic properties of the substrate may be exploited, as the less electron rich position will react first.

The electron density, the chelating effect and the steric bulkiness of the ligand systems have been reported to play key roles for selectivity in reactions with hetereoaryl polyhalide substrates.[88-91] The choice of catalyst system can therefore be important when multiple halides are present in the substrate and a site-selective reaction is required. Especially electron rich ligands with steric bulk have been reported to promote unusual selectivities.[88-90]

Dai *et al.* investigated the site-selectivity of various phosphine ligands in Suzuki cross-coupling reactions with 3,5-dichloropyridazine as substrate.[92] Electron deficient bidentate ligands, such as dppf, favored reaction in the C-3 position, while electron rich monodentate ligands favored C-5. These results are shown in Scheme 2.10.

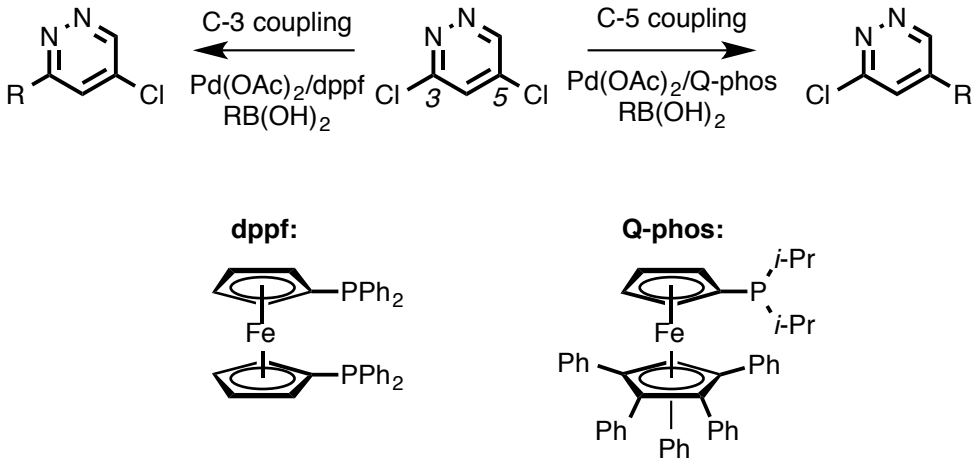

Scheme 2.10: Site-selective Suzuki cross-coupling reactions of 3,5-dichloropyridazine, as reported by Dai *et al*.[92] The bidentate electron deficient ligand dppf favored reaction in C-3 position, and monodentate electron rich ligands such as Q-phos favored reaction in C-5 position.

2.6 Buchwald-Hartwig amination

There are multiple ways of forming new C-N bonds. One strategy is a thermal amination, where a nucleophilic aromatic substitution (NAS) occurs through an S_NAr mechanism. In this mechanism, the aromatic ring needs to be adequately activated (electron deficient) for the reaction to take place.[93-94] When the substrate is not sufficiently activated, the reaction may face several drawbacks, including long reaction times and high temperatures.[48] An alternative to the thermal amination is catalytic amination. Catalytic amination has in several cases been reported to be superior to a thermal amination.[95-96] Aryl halides which are not activated by electron withdrawing groups are best aminated by copper or palladium catalysis. Palladium catalyzed amination of aryl halides are referred to as Buchwald-Hartwig couplings or Buchwald aminations.

2.6.1 Mechanism

The mechanism of the Buchwald amination resembles the Suzuki cross-coupling reaction mechanism. However, the order of some of the catalytic steps may differ for different catalyst systems, ligands and bases. The generalized catalytic cycle, as suggested by Guram and Buchwald in 1994, is shown in Scheme 2.11.[97] This catalytic cycle starts with the reduction of Pd(II) to the active species Pd(0). This oxidative addition step involves the aryl halide connecting to the palladium species. The halide is displaced by the base in the metathesis. The amine is then deprotonated and replaces the hydroxy/alkoxy group in the palladium complex. The coupled product is released in a reductive elimination step, as the Pd(II) returns to the active Pd(0) oxidation state. The C-N bond is formed in this step, as proposed by Paul, Bratt and Hartwig in 1994.[98]

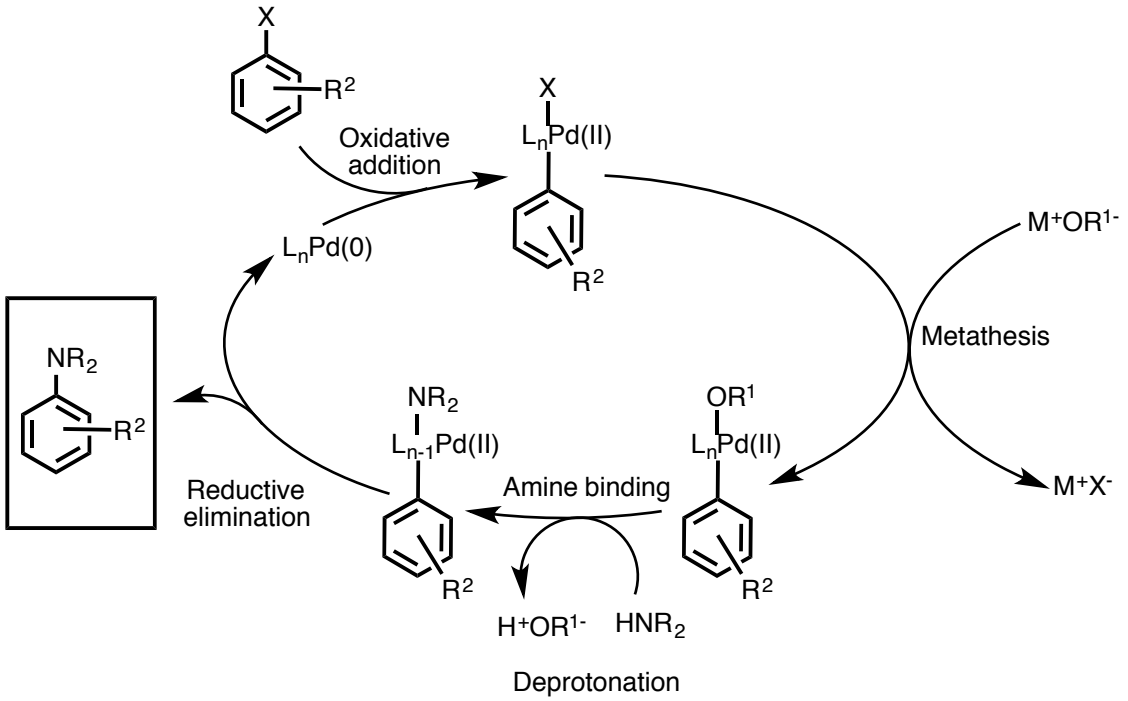

Scheme 2.11: The mechanism of the Buchwald-Hartwig amination, as suggested by Guram and Buchwald in 1994.[97]

Which mechanistic step is rate determining can vary for different substrates, and the reaction conditions can therefore be challenging to optimize.[99] For aryl chlorides, the rate determining step is usually the oxidative addition. Electron rich ligands may improve the rate of the oxidative addition as well as reduce the rate of the reductive elimination step.[81] The rate of the reductive elimination step can be greatly influenced by the introduction of electron withdrawing groups and electron donating groups in certain positions of the ligand. An illustration of this effect is shown in Figure 2.8.[100]

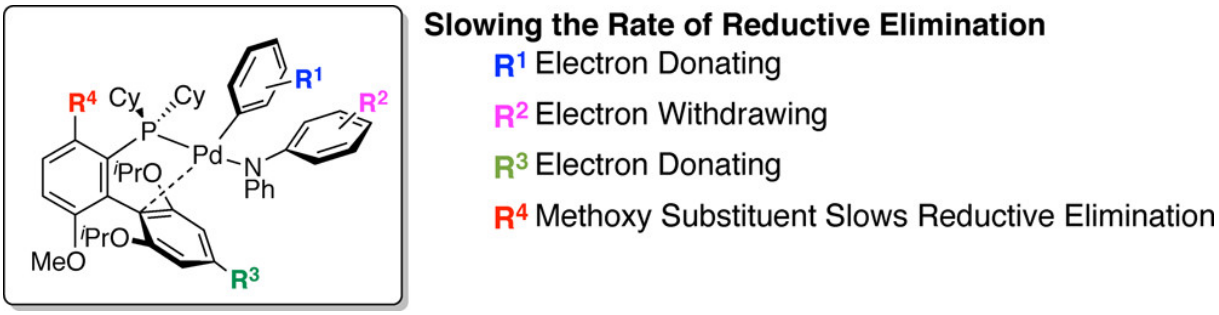

Figure 2.8: The effect of the electronic properties of ligand substituent on the reductive elimination step.[100]

Heteroaryl halides can be especially challenging reactants in Buchwald aminations, as they may show great varieties of electronic properties. This makes it difficult to predict suitable conditions for the Buchwald aminations of such substrates, and the performance of the oxidative addition and reductive elimination steps may vary with different substrates.[99]

2.6.2 Catalysts and ligands

Generating the active Pd(0) complex is a process that can differ greatly in efficiency, and a variety of ligands may be considered when choosing the most suitable conditions for a successful amination. The ligand RuPhos has been suggested to be most advantageous for secondary amines, while BrettPhos is selective for primary amines.[99] Both ligands are also available in precatalyst form, and they are shown in Figure 2.9.

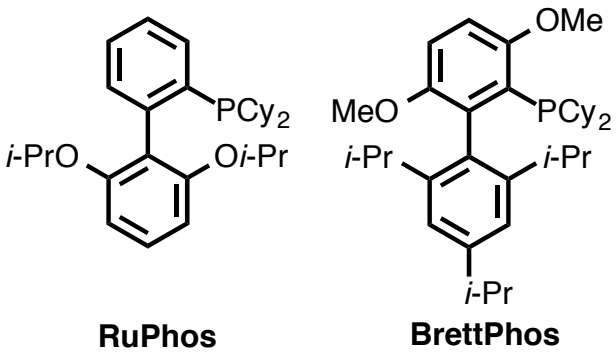

Figure 2.9: The structures of ligands RuPhos and BrettPhos.[99]

Kaspersen *et al*. synthesized 4-*N*-substituted 6-aryl-7*H*-pyrrolo[2,3-*d*]pyrimidine-4-amine structures for inhibition of EGFR (Epidermal Growth Factor Receptor) tyrosine kinase, where one synthesis route involved a Buchwald amination step using primary amines and the $Pd(OAc)_2$/XPhos catalyst system.[101] Yields between 47-71% were obtained of the aminated products, as shown in Scheme 2.12.

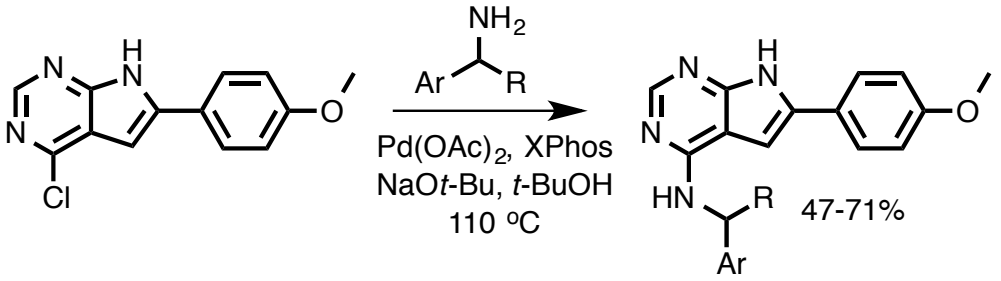

Scheme 2.12: Palladium catalyzed amination reactions between 4-chloro-6-(4-methoxyphenyl)-7*H*-pyrrolo[2,3-*d*]pyrimidine substrates and primary amines using the $Pd(OAc)_2$/XPhos catalyst system, as reported by Kaspersen *et al*.[101]

Guillard *et al*. performed successful Buchwald aminations on 7-azaindoles with secondary amines, using a catalyst system with Pd_2dba_3 and the ligand XantPhos.[102] XantPhos was originally created for regioselective rhodium catalyzed hydroformylation, but has also become a valued ligand in C-N bond forming reactions.[103-104] XantPhos is a bidentate phosphine ligand, providing two coordination sites for palladium, a feature which has been reported to produce less of the reduced arene byproducts.[105] Driver *et al.* reported the use of another bidentate ligand, $(dppf)PdCl_2$, in an amination reaction between 4-bromobenzophenone and a secondary amine.[106] The two reactions are shown in Scheme 2.13, with the structures of the two bidentate ligands on the right.

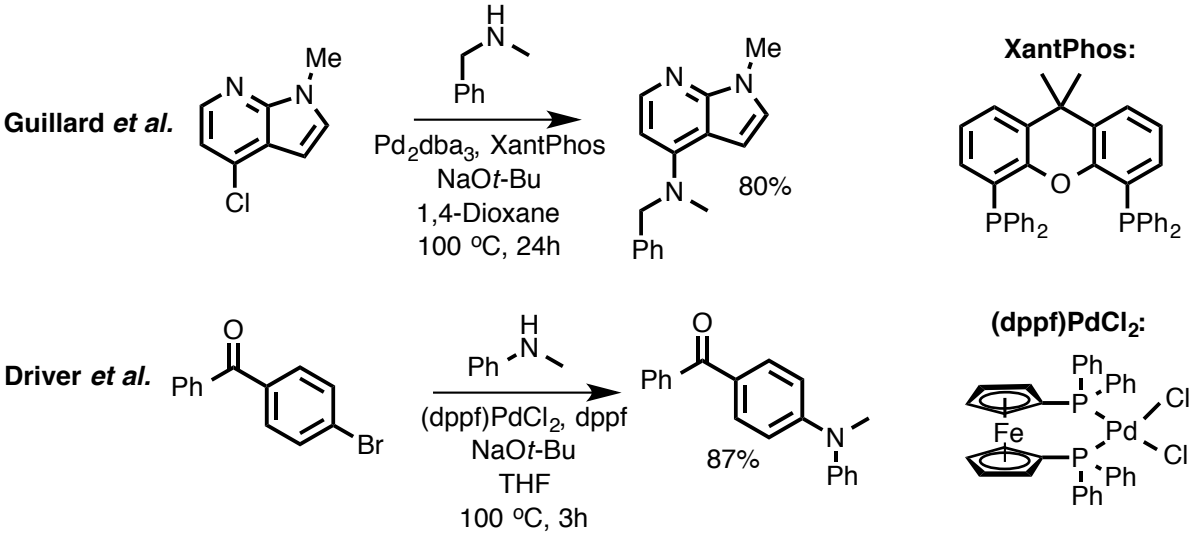

Scheme 2.13: Two examples palladium catalyzed amination reactions using secondary amines and bidentate ligands, as described by Guillard *et al.* for a 1-methyl-4-halo-7-azaindole substrate[102], and Driver *et al.* for a 4-bromobenzophenone substrate.[106] The structures of the ligands XantPhos and $(dppf)PdCl_2$ are shown on the right.

2.6.3 Byproducts and side reactions

Poor nucleophilicity of the amine coupling partners, either as a consequence of steric hindrance or electronic properties, can give slower rates of amine transmetalation. This may cause a side reaction between the alkoxide base and the substrate leading to the formation of an aryl ether (ArO*t*-Bu in the case of NaO*t*-Bu base).[107] Furthermore, β-hydride elimination is a side reaction that may arise from the intermediate Pd(II)-amido-complex. The proposed mechanism for β-hydride elimination is shown in Scheme 2.14.[108] This causes the formation of the reduced arene.[107] The β–hydride elimination is a competitive reaction to the reductive elimination step, and the reaction conditions and catalyst system should be carefully optimized to minimize this side reaction.

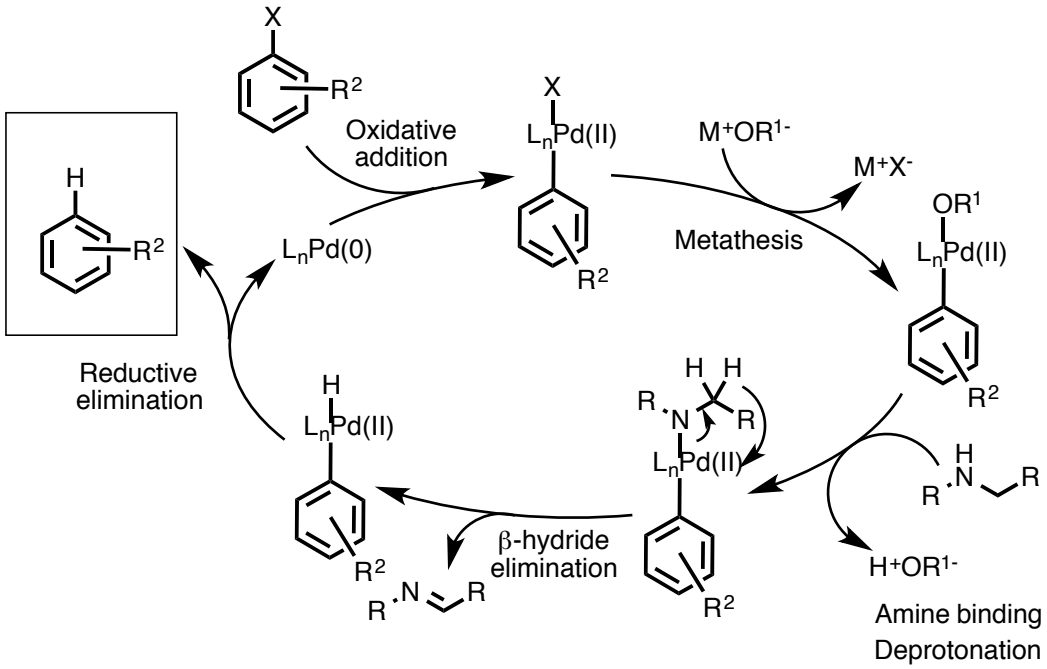

Scheme 2.14: The suggested mechanism of the β-hydride elimination side reaction.[108]

3. Results and discussion

The aim of this master thesis was to develop synthetic protocols towards 4-amino-2-aryl-1*H*-pyrrolo[2,3-*b*]pyridines to be used for CSF1R inhibition. An overview of the synthetic routes to the main target compound is shown in Scheme 3.1.

Protection of the pyrrole nitrogen with a SEM-protecting group and a following iodination offered a route to the first building blocks. A selectivity study of the Suzuki cross-coupling reaction resulted in a chemoselective reaction in the 2-position. The palladium catalyzed Buchwald-Hartwig amination was unsuccessful when the acidic proton of the hydroxyl group was unprotected. This issue was solved by attaching two different protecting groups in this position, and Buchwald aminations were then studied and performed for these protected compounds. The challenging final step was the removal of the protecting groups, yielding the target compound. The syntheses resulted in 15 new compounds, including the identified byproducts.

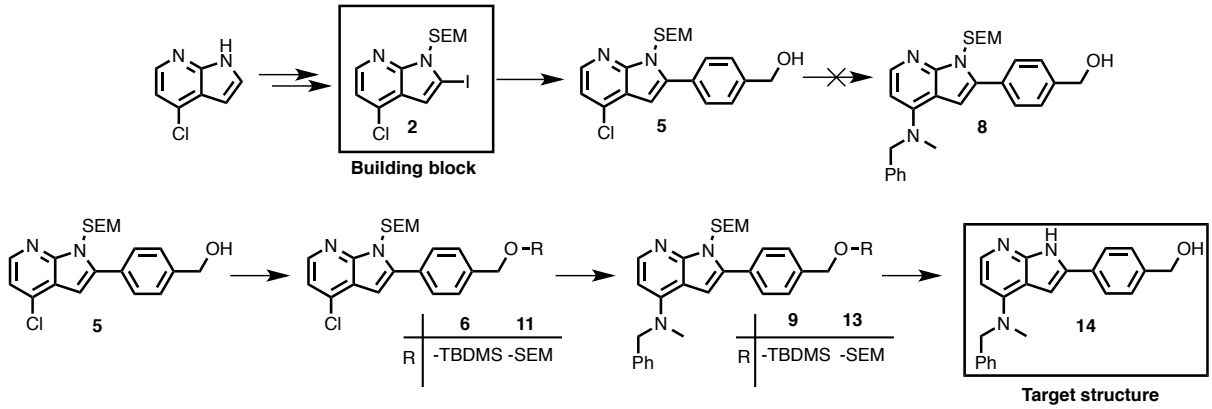

Scheme 3.1: The main synthetic routes leading to the target structure, starting from commercially available 4-chloro-1*H*-pyrrolo[2,3-*b*]pyridine.

This section consists of five main parts. The first part describes the syntheses of the key buildings blocks. The second part covers the Suzuki cross-coupling reactions and findings from the selectivity study. The third part provides an overview of the Buchwald aminations performed in this project, where the encountered problems and synthetic solutions are discussed. The fourth part describes the removal of the protecting groups, the final synthetic step forming the target compound. In the last section, characterizations of the synthesized compounds and byproducts are discussed.

3.1 Building blocks

3.1.1 Synthesis of compound 1 by SEM protection

The first synthesis step was protecting the pyrrole nitrogen with an SEM protecting group. This synthesis has been reported by Nakajima *et al*. and has been successfully executed within the research group.[109]

Compound **1** was synthesized from 4-chloro-1*H*-pyrrolo[2,3-*b*]pyridine in a 3.90 g scale. The starting material was dissolved in dry DMF at 0 °C, NaH was added and the mixture was stirred for 30 minutes. Thereafter followed the dropwise addition of SEM-Cl, before the mixture was left to stir for 2 hours. The mixture had a bright yellow color after addition of the SEM-chloride, and reached a conversion of 84%. After purification with silica gel column chromatography, compound **1** was obtained as a light yellow oil with a yield of 82% (5.45 g). An oil was expected as the SEM group makes it difficult for the molecule to crystallize. The yield corresponds well to the 84% conversion.

The synthesis was later repeated in a 5.43 g scale. The reaction reached full conversion as indicated by TLC and ^{1}H NMR after 3 hours and 45 minutes. Purification with silica gel column chromatography gave compound **1** as a light yellow oil in 90% yield (9.11 g). The synthesis of compound **1** is shown in Scheme 3.2.

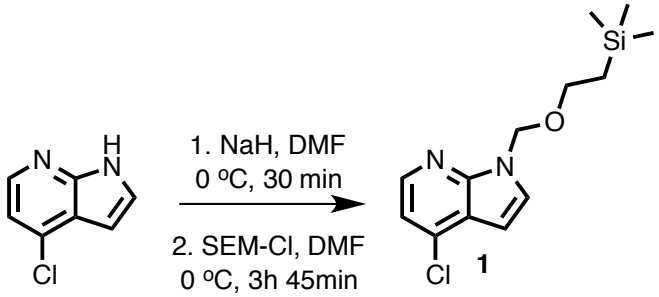

Scheme 3.2: Synthesis of compound **1** by SEM-protection of 4-chloro-1*H*-pyrrolo[2,3-*b*]pyridine.

3.1.2 Synthesis of compound 2 by iodination

Compound **2** had previously been reported in a patent by Kim *et al*.[110] The same procedure was used in this project. The synthesis of compound **2** is shown in Scheme 3.3. The starting material **1** (7.87 g) was dissolved in dry THF and cooled to -78 °C. LDA (2 M in THF) was added dropwise over a period of 45 minutes using a syringe pump. The mixture was left to stir for 1 hour before the dropwise addition of I_2 dissolved in THF. The reaction mixture was stirred for 2 hours after completed addition of I_2, until ^{1}H NMR analysis showed that full conversion had been reached. Solubility issues were encountered during the extraction, leading to the product being partially soluble in the water phase. After a tedious workup including 14 extractions with CH_2Cl_2 and salting out with NaCl, the crude product yield was 82%. The product was purified by silica gel column chromatography, giving compound **2** as a beige powder with a yield of 69% (10.2 g). The

moderate yield can be ascribed to the problems that were encountered during the extraction.

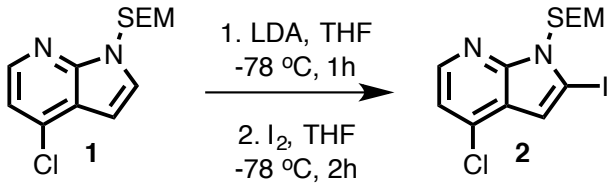

Scheme 3.3: Synthesis of compound **2** by iodination of compound **1**.

The reaction was performed a second time, in a 3.2 g scale. The reaction reached 84% conversion after stirring at -78 °C for 1 hour. The solvent was removed in vacuo and extraction was conducted with CH_2Cl_2. After 3 rounds of extraction, no product **2** remained in the water phase. Compound **2** was isolated in a 50% yield after purification with silica gel column chromatography. The low yield was most likely due to the moderate conversion, and losses during purification. The previously described workup issues were not observed in the second reaction. Possibly, the removal of solvent and amine was more carefully performed, as residues of THF and LDA could have caused the problems in the extraction of the first reaction.

Sufficient amounts of building block **2** had been produced for proceeding to the next synthetic step. The planned synthesis route involved a Suzuki cross-coupling reaction followed by a Buchwald amination.

3.2 Suzuki-Miyaura cross-coupling reactions

The next goal was to develop a chemoselective Suzuki cross-coupling reaction in 2-position of substrate **2**. Multiple side reactions were possible, as shown in Scheme 3.4. Reduction of the aryl halide would give the dehalogenated byproduct **1**. There was also a possibility for di-coupling, where both halides in positions 2 and 4 would couple with the boronic acid, forming compound **3**. The hydroxyl groups of the product **5** and compound **3** could also undergo oxidation to the corresponding aldehydes.

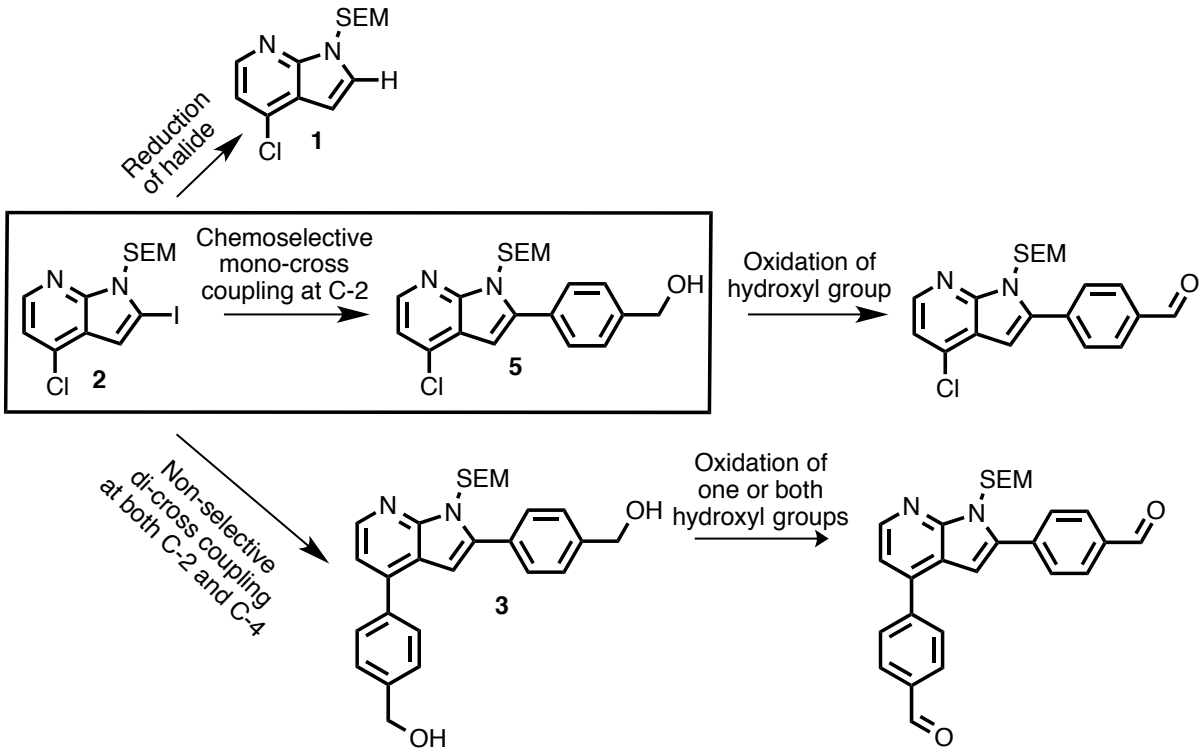

Scheme 3.4: Overview of byproducts formed during synthesis of compound **5** from substrate **3** in a Suzuki cross-coupling reaction. The shown byproducts are results of di-cross-coupling (**3**), reduction of the aryl halide (**1**), and oxidations of the hydroxyl groups of compound **5** and **3**.

To study the chemoselective Suzuki cross-coupling reaction, some reference material was needed. Therefore, the investigation started with synthesis of the di-cross-coupled compound **3**, to obtain the NMR data for reference.

3.2.1 Di-cross-coupling reactions

The XPhos catalyst system was chosen for the di-cross-coupling reactions as it has been reported to be an efficient ligand. The di-arylated compounds **3** and **4** were both successfully synthesized using precatalyst XPhos Pd G2 and XPhos as ligand in a Suzuki cross-coupling reaction, as depicted in Scheme 3.5.

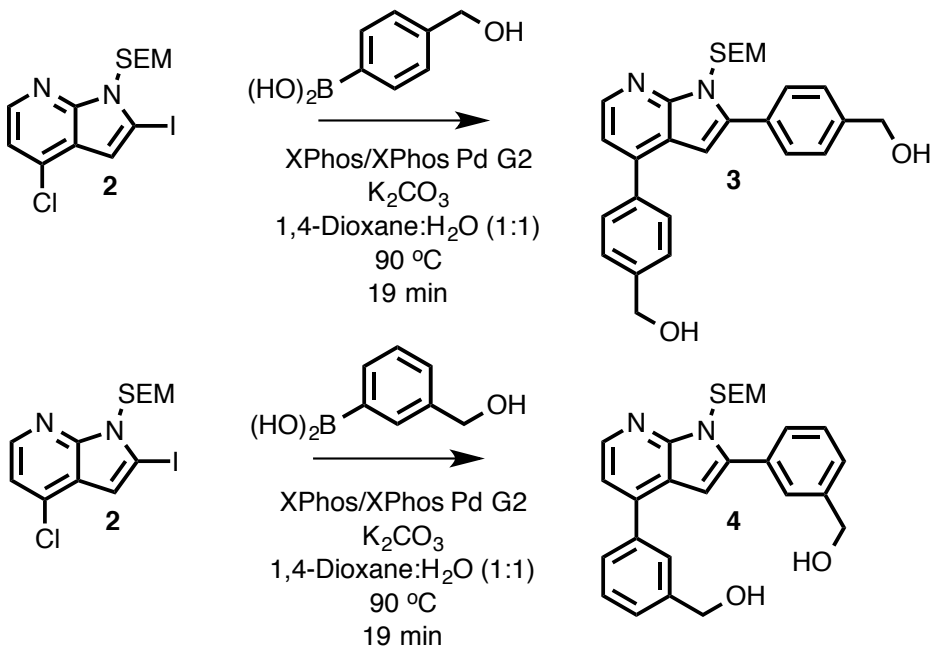

Scheme 3.5: Synthesis of compounds **3** and **4** by Suzuki di-cross-coupling reactions of compound **2**.

Together with base, boronic acid, catalyst and ligand, the starting material was dissolved in degassed 1,4-dioxane and water (1:1) under an N_2 atmosphere. Full conversion had been reached for both reactions after 19 minutes stirring at 90 °C. ^{1}H NMR analysis of the crude materials showed that oxidation of the hydroxyl groups had taken place. Multiple aldehyde signals were observed in both crude materials, indicating that both hydroxyl groups of the products had undergone oxidation, and several different oxidized byproducts were formed. ^{1}H NMR analysis showed that the crude materials of compound **3** and **4** contained 16% and 14% of oxidation byproducts, respectively. After purification with silica gel column chromatography, compound **3** was obtained as an off-white solid in 79% yield (246 mg), and compound **4** as an off-white solid in 80% yield (227 mg).

3.2.2 Selective cross-coupling at C-2

For the synthesis of mono-cross-coupled compound **5,** multiple catalysts and conditions were tested. The general reaction is shown in Scheme 3.6, and the specific results and conditions for each reaction are shown in Table 3.1. The goal was to identify conditions for the Suzuki cross-coupling reaction which allowed a selective mono-cross-coupling in the 2-position, while minimizing formation of the byproducts as shown in Scheme 3.4.

A method using $Pd_2(dba)_3$, which has previously been found useful for an analogous pyrrolopyridine molecule, was initially tested.[51] Reactions with $Pd_2(dba)_3$ are reported in entries 1-3 in Table 3.1. Reactions at different temperatures ranging from 60-100 °C all produced the target compound **5**, the di-cross-coupled byproduct **3** and an unknown byproduct. No oxidation of the hydroxyl groups was seen with the $Pd_2(dba)_3$ reactions. The unknown byproducts proved difficult to remove from product **5** using silica gel column chromatography. Several eluent systems were tested, with both dry loading

application with celite and direct application. Still, the product was not isolated from the impurities.

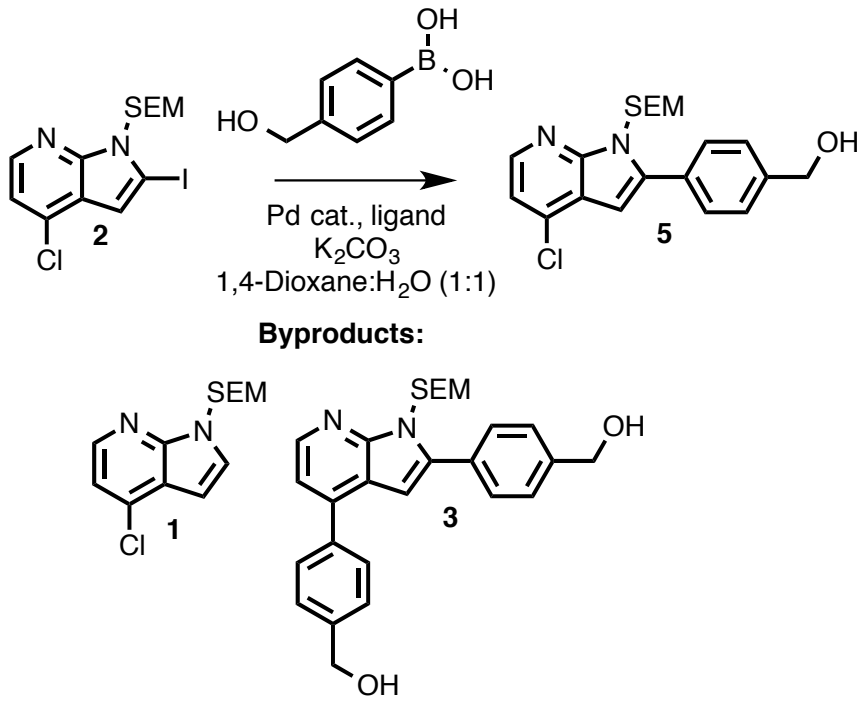

Scheme 3.6: Overview of the synthesis of compound **5**. Multiple Suzuki cross-coupling reactions at various temperatures and with multiple palladium catalyst systems were performed.

In the search of a catalyst system with less formation of byproducts and an easier purification process, the following other catalysts were then evaluated: XPhos, $Pd(OAc)_2$, PEPPSI™-SIPr and $(dppf)PdCl_2$. The specific conditions and amounts of byproducts identified are found in entries 4-7 in Table 3.1. Crude products were retrieved from these reactions in mostly high yields. Byproducts observed by ^1H NMR analysis were: aldehydes from oxidation, reduced compound **1**, di-cross-coupled byproduct **3** and other unknown impurities. With catalysts $Pd_2(dba)_3$ and XPhos/XPhos Pd G2 the formation of the reduced byproduct **1** was avoided, yet other unknown impurities were formed in these reactions. Reactions with certain catalysts gave large amounts of aldehyde impurities from oxidation. This was particularly true for XPhos/XPhos Pd G2 and PEPPSI™-SIPr, indicating that these catalysts were too reactive for this system. Oxidation had already been observed using XPhos in the di-cross-coupling reactions, as mentioned in the previous section. The 49% of oxidation products formed in the XPhos reaction might be ascribed to the reaction time being 2.75 hours, and the high activity of the XPhos catalyst.

The most selective catalyst for this substrate was found to be $Pd(PPh_3)_4$. Reactions using $Pd(PPh_3)_4$ had a significantly longer conversion time than the other catalysts, as seen in entries 8-10 in Table 3.1. However, this catalyst showed a greatly enhanced selectivity towards the desired product **5.** In the 50 mg scale reaction, the crude material consisted solely of the desired product **5** and a minor amount of dehalogenated byproduct **1** (8%). The purification process for the $Pd(PPh_3)_4$ reactions was considerably easier than the

$Pd_2(dba)_3$ reactions, as no other unknown byproducts were formed and a sufficient difference in retention was obtained using silica gel column chromatography for purification. Thus, this catalyst was chosen to move forward with, because of the high selectivity for the mono-cross-coupled product.

The reaction using $Pd(PPh_3)_4$ was scaled up to a 2 g scale which gave an isolated yield of 83% as orange oil, see entry 9 in Table 3.1. A small amount of the reduced byproduct **1** was found from this reaction. A noticeable amount of the di-coupled compound **3** had also been formed, because the reaction was left overnight to stir, allowing time for continued cross-coupling. Another larger scale reaction was then performed, with 1233 mg of starting material **2**, where the reaction was ended right before full conversion had taken place, to minimize the chance of di-coupling. The reaction is shown in entry 10 of Table 3.1, and only gave a minor amount of the dehalogenated impurity **1** (5%), but no other byproducts. Compound **5** was isolated in an 83% yield (972 mg) after purification with silica gel chromatography.

Table 3.1: Results from the selectivity study and optimization of the Suzuki cross-coupling reactions synthesizing compound **5** from compound **2**.

	Catalyst	**Temp [°C]**	**Scale [mg]**	**Cat. load [%Pd]**	**Time [h]**	**Crude product content[a]**				
						5 [%]	**3 [%]**	**Unk.[b] [%]**	**1 [%]**	**Ox.[c] [%]**
1	$Pd_2(dba)_3$	100	100	7.3	1.75	92	4	4	0	0
2	$Pd_2(dba)_3$	80	100	7.2	1.75	89	5	5	0	0
3	$Pd_2(dba)_3$	60	50	7.5	2.5	87	6	7	0	0
4	XPhos/ XPhos Pd G2	80	50	6.9	2.75	15	23	13	0	49
5	$Pd(OAc)_2$	80	50	11	2.75	63	12	8	5	12
6	PEPPSI™-SIPr	87	50	15.9	0.3	43	15	10	7	25
7	$(dppf)PdCl_2$	87	50	12.8	0.3	69	10	6	7	8
8	$Pd(PPh_3)_4$	80	50	8.1	5	92	0	0	8	0
9	$Pd(PPh_3)_4$	90	2087	5.5	22	85	9	0	6	0
10	$Pd(PPh_3)_4$	80	1233	5.1	9	95	0	0	5	0

[a]Analysis by ^1H NMR

[b]Unidentified byproducts

[c]Products of oxidations of hydroxyl groups of compounds **5** and **3**

In conclusion for the optimization of the Suzuki cross-coupling reactions for this system, the $Pd(PPh_3)_4$ catalyst was certainly the most selective of the systems that were tested. The purification process was significantly easier than for the other reactions, considering that lower amounts of byproducts were formed. Small impurities of the reduced byproduct **1** are to be expected, but in contrast to reactions with the other catalyst systems, significant formation of the di-cross-coupled compound **3** was not observed before full conversion was reached. Ending the reaction at the right time is therefore crucial, as the di-cross-coupling reaction becomes significant once full conversion is reached if there is an excess of boronic acid present.

3.2.3 Synthesis of compound 6

The chemoselective Suzuki cross-coupling conditions described in Section 3.2.2 were applied to synthesize the TBDMS-protected compound **6** from compound **2**. The reaction was performed in a 901 mg scale, and is shown in Scheme 3.7. A minor amount of reduced byproduct **1** (6%) was observed in the crude mixture. After purification with silica gel column chromatography, 991 mg (90%) of compound **6** was obtained as a white powder.

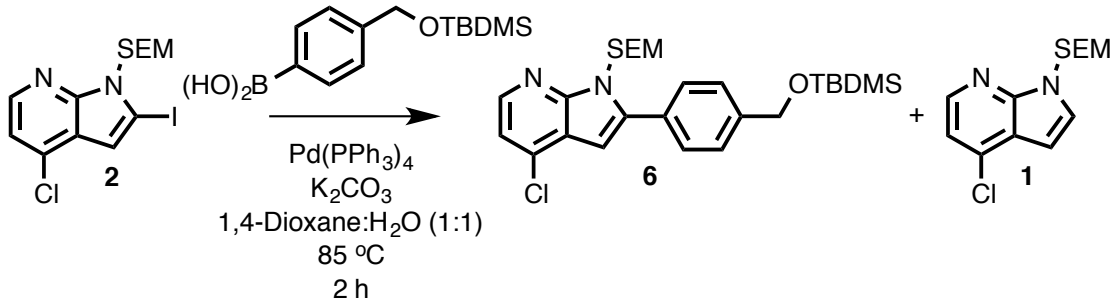

Scheme 3.7: The synthesis of compound **6** by Suzuki cross-coupling reaction of compound **2**.

At a later time, compound **6** was synthesized by TBDMS protection of the hydroxyl group of compound **5**. This reaction is described in Section 3.3.3.1.

3.3 Buchwald-Hartwig amination

Buchwald aminations have been performed previously in the research group on substituted 7-azaindoles, with varying results. Poor results were reported when the pyrrole nitrogen was unprotected. Different protecting groups have been introduced in this position, and the best results were found with the SEM-group protecting the pyrrole nitrogen.[51] The most successful Buchwald aminations were conducted with the substrate shown in Figure 3.1. For this project, the initial goal of this synthesis step was to aminate compound **5**, containing a hydroxymethyl group in place of the methoxy group of the compound shown in Figure 3.1.

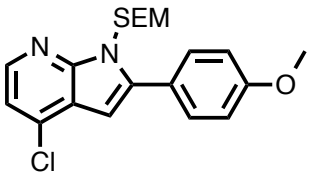

Figure 3.1: Substrate structure for a previously successful Buchwald amination of 2-substituted 7-azaindole.[51]

3.3.1 Test of palladium sources and reaction conditions

One of the most frequently reported ligands used in Buchwald aminations with secondary amines is RuPhos.[50, 111-112] For the palladium source, various options are reported, including a RuPhos precatalyst, RuPhos Pd G2, and $Pd(OAc)_2$.

Two test reactions were conducted, shown in Scheme 3.8. The goal of these model reactions was to investigate which catalyst system was best suited for a Buchwald amination on a pyrrolopyridine substrate. The experiments would also show whether the reaction conditions and dryness of the system were sufficient for a successful amination. Compound **1** was the starting material for these test reactions, as it is a simple pyrrolopyridine molecule.

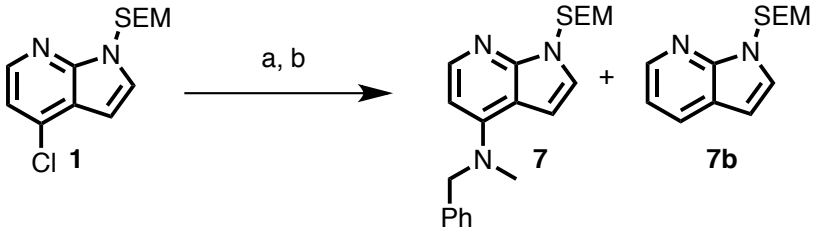

Scheme 3.8: Test reactions A and B synthesizing compound **7** and the assumed byproduct **7b**.
(a) *N*-Benzylmethylamine, RuPhos, $Pd(OAc)_2$, NaO*t*-Bu, *t*-BuOH, 85 °C, 5 min;
(b) *N*-Benzylmethylamine, RuPhos, RuPhos Pd G2, NaO*t*-Bu, *t*-BuOH, 85 °C, 2 h.

Starting material **1**, NaO*t*-Bu, palladium catalyst, RuPhos and 5-6 eq. of amine were dissolved in degassed and anhydrous *t*-BuOH and stirred at 85 °C in an oven dried Schlenk tube. Test reaction A was performed in an 80 mg scale, with $Pd(OAc)_2$ as a palladium source and the ligand RuPhos. Test reaction B was performed in a 110 mg scale, using RuPhos Pd G2 precatalyst as the palladium source and the ligand RuPhos. As precatalysts are often thought to be a more efficient and active catalyst species than $Pd(OAc)_2$, this reaction would show if the precatalyst was a more fitting palladium source for this amination.

The results of both test reactions are shown in Table 3.2. ^{1}H NMR analysis showed that reaction A reached full conversion after 5 minutes. ^{1}H NMR analysis of the crude product proved that the substrate had undergone amination with 94% of the crude mixture consisting of product **7**. A minor byproduct was observed in the crude material (6%). This

was suggested to be the reduced aryl chloride **7b**, after observing the crude ^{1}H NMR spectrum. After purification by silica gel column chromatography, the product **7** was obtained as a light yellow oil in a 68% yield.

For test reaction B with RuPhos Pd G2 precatalyst, only 50% conversion had been reached after 20 minutes. ^{1}H NMR analysis showed that full conversion had been reached after 2 hours, when the reaction was stopped. This observation contrasted with the initial suspicion that the precatalyst species would be a more reactive palladium source. As reported in Table 3.2, 81% of the crude product consisted of the desired aminated target **7**. Byproducts observed were the suggested reduced aryl chloride **7b** (11%) and an unidentified impurity (8%).

Table 3.2. Results of the two test reactions forming compound **7**.

	Pd source	**Time [min]**	**Crude material content[a]**		
			7 [%]	**7b [%]**	**Unknown byproduct [%]**
Test reaction A	$Pd(OAc)_2$	20	94	6	0
Test reaction B	RuPhos Pd G2	120	81	11	8

[a]Analysis of crude product by ^{1}H NMR

After these test reactions, it could be concluded that $Pd(OAc)_2$ was a satisfactorily active palladium source in these reactions. There was a significant difference in reactivity between the catalysts, as the reaction B with RuPhos Pd G2 precatalyst took almost 2 hours to reach full conversion, in contrast to the conversion time of 5 minutes for $Pd(OAc)_2$. There had also been formed lower amounts of byproducts in reaction A than in reaction B. The reaction temperature and dryness of the system showed to be sufficient for a successful Buchwald coupling of compound **1**.

3.3.2 Aminations of compound 5 with the unprotected -OH group

The initial goal was to perform a Buchwald amination on compound **5**, which contained an acidic proton in the form of an unprotected hydroxyl group. The identified conditions found most ideal from the previous section were applied, however, the amination of compound **5** was not successful. An overview of the reaction is shown in Scheme 3.9. Several attempts were made using the $Pd(OAc)_2$/RuPhos catalyst system, where the conversions were all below 40%, and the desired aminated target **8** was not observed even after 24 hours. According to ^{1}H NMR analysis after workup, the crude product mixtures consisted mostly of starting material **5** and multiple unknown byproducts.

A variety of ligands and catalyst systems were tested using the same reaction conditions. These included XantPhos/$Pd(OAc)_2$, PEPPSI™-SIPr precatalyst, tri(o-tolyl)phosphine and $(dppf)PdCl_2$. All of these catalyst systems gave similarly low conversions (<40%) and complex mixtures were formed with no observation of product **8**.

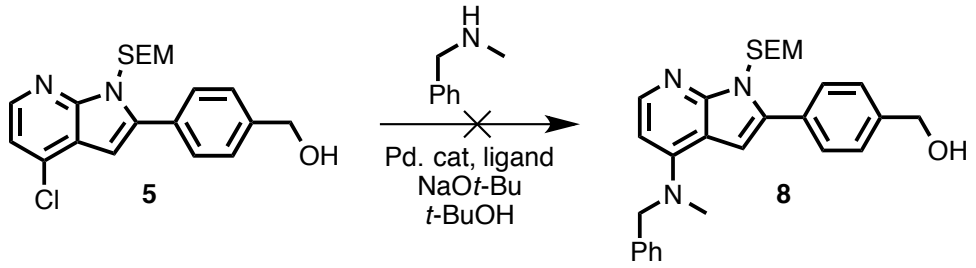

Scheme 3.9: An illustration of the attempted amination of compound **5**, which remained unsuccessful after testing a variety of catalyst systems and reaction conditions.

A reaction was also conducted at a 65 ^{o}C, to investigate whether a lower reaction temperature would enhance the selectivity and performance of the reaction. ^{1}H NMR analysis showed that the rate of reaction had dramatically decreased. After 28 hours, the reaction had reached 39% conversion, creating a complex mixture of unidentified byproducts, and again product **8** was not observed.

As the amination of this substrate **5** was unsuccessful with all the different catalysts/ligand systems, and at a lower temperature, it was concluded that compound **5** was unfit as a substrate in the Buchwald aminations under these conditions. The substrate **5** contained an acidic proton in the form of an unprotected hydroxyl group, which could possibly be the source of the problem. It was therefore decided to approach the Buchwald amination using other substrates, where the acidic proton of this hydroxyl group was protected.

3.3.3 Synthesis and aminations of compounds 6 and 11

As the amination of compound **5** was unsuccessful, two alternative routes were explored. This entailed protecting the hydroxyl group of compound **5** with two different groups, TBDMS and SEM. The protection reactions are discussed in Section 3.3.3.1. An overview of the amination reactions is seen in Scheme 3.10, and the Buchwald amination studies are discussed in Sections 3.3.3.2 and 3.3.3.3.

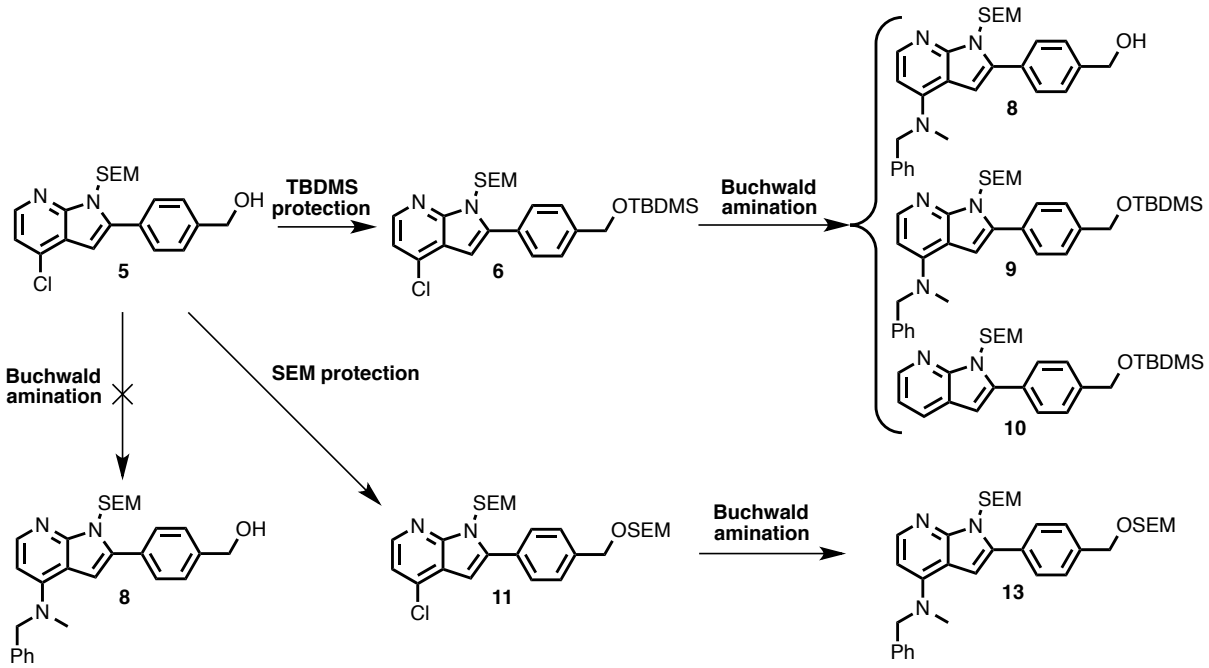

Scheme 3.10: Overview of Buchwald aminations.

3.3.3.1 Protection of the hydroxyl group

A SEM protection reaction was performed to protect the hydroxyl group of compound **5**. The reaction was conducted in a 1 gram scale, and is shown in Scheme 3.11. The substrate **5** was dissolved in DMF and added NaH, before stirring for 30 minutes at 0 °C. After dropwise addition of SEM-chloride, the reaction mixture was stirred at 0 °C for 4 hours and 45 minutes. The course of the reaction was monitored using TLC, and the reaction was quenched when no more changes could be observed. From ^{1}H NMR analysis of the crude product, 87% conversion had been reached at this point.

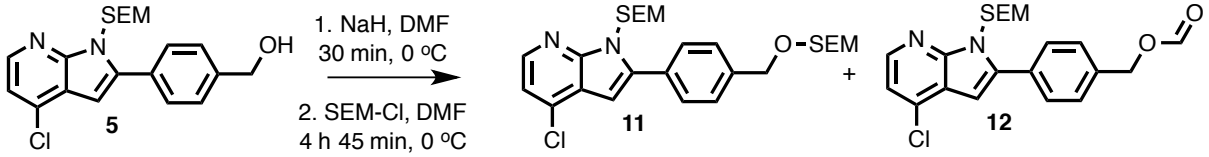

Scheme 3.11: The SEM-protection reaction forming compound **11** and byproduct **12**.

After purification with silica gel column chromatography, compound **11** was obtained in a 51% yield (717 mg) as a clear oil. The low yield was a result of the incomplete conversion, and the formation of a byproduct, compound **12**. ^{1}H NMR analysis showed that the crude product contained 18% of byproduct **12**, but due to losses during purification, only 15 mg (2%) was collected after purification by silica gel column chromatography. NMR, IR and MS analyses of compound **12** confirmed the identity of the byproduct, most likely resulting from the substrate reacting with the solvent, DMF. The formation of byproduct **12** is shown in Scheme 3.12.

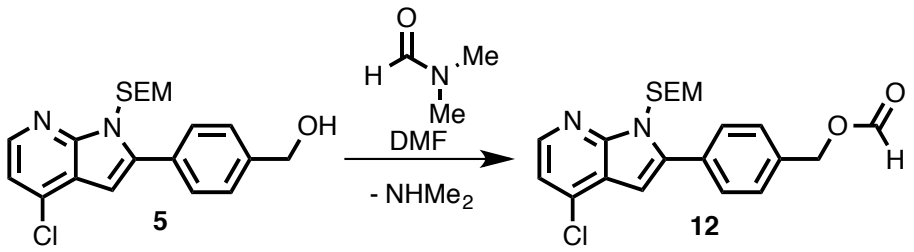

Scheme 3.12: Formation of byproduct **12**.

The formation of byproduct **12** could have been avoided by using another solvent. This was attempted in the analogous protection reaction, where the hydroxyl group of compound **5** was protected with a TBDMS group to produce compound **6**. The reaction was performed using the same procedure as described for the synthesis of compound **11**, but THF replaced DMF as solvent. The reaction is shown in Scheme 3.13. After 4 hours of stirring at 0 °C, ^{1}H NMR showed only 7% conversion into compound **6**, and no further changes were observed when monitoring the reaction using TLC and ^{1}H NMR analysis. The mixture was then warmed to 50 °C and stirred for 10 minutes. After workup and extraction, ^{1}H NMR analysis was conducted on the crude product, and showed that full conversion had been reached and product **6** had been formed. After purification with silica gel column chromatography, compound **6** was obtained as a white solid in a 75% yield (888 mg).

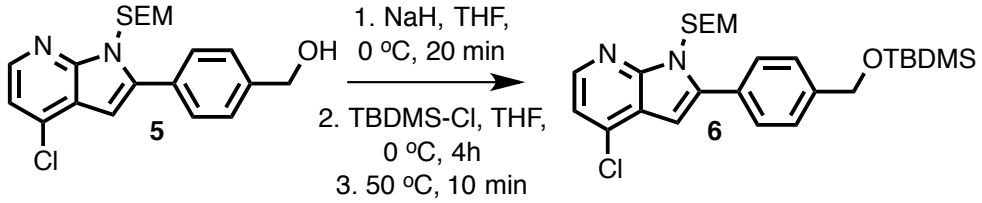

Scheme 3.13: The TBDMS-protection reaction forming compound **6**, performed in THF as solvent. A 7% conversion was reached after 4 hours of stirring at 0 °C, and the reaction was completed to 100% conversion after heating to 50 °C for 10 minutes.

Patchinski *et al.* report the protection reaction to be catalyzed by DMF, which can explain the poor result of the reaction conducted in THF at 0 °C.[113] The reaction proceeded rapidly to completion when the temperature was increased. In conclusion, both compounds **6** and **11** were successfully synthesized from compound **5** in moderate yields. The side reaction forming byproduct **12** was avoided when THF was used as solvent instead of DMF, but this reaction was not successful at 0 °C. Heat was necessary to complete the reaction.

3.3.3.2 Aminations of compound 6 with the -OTBDMS group

Multiple Buchwald aminations on the TBDMS-protected substrate **6** were performed. The starting material **6**, NaO*t*-Bu, amine, catalyst and ligand were stirred in anhydrous and degassed *t*-BuOH at 85 °C until ^{1}H NMR analysis showed full conversion. The solvent was removed in vacuo, before workup and purification by silica gel column chromatography.

The reaction conditions are shown in Scheme 3.14, as are the structures of the observed byproducts **8** and **10**.

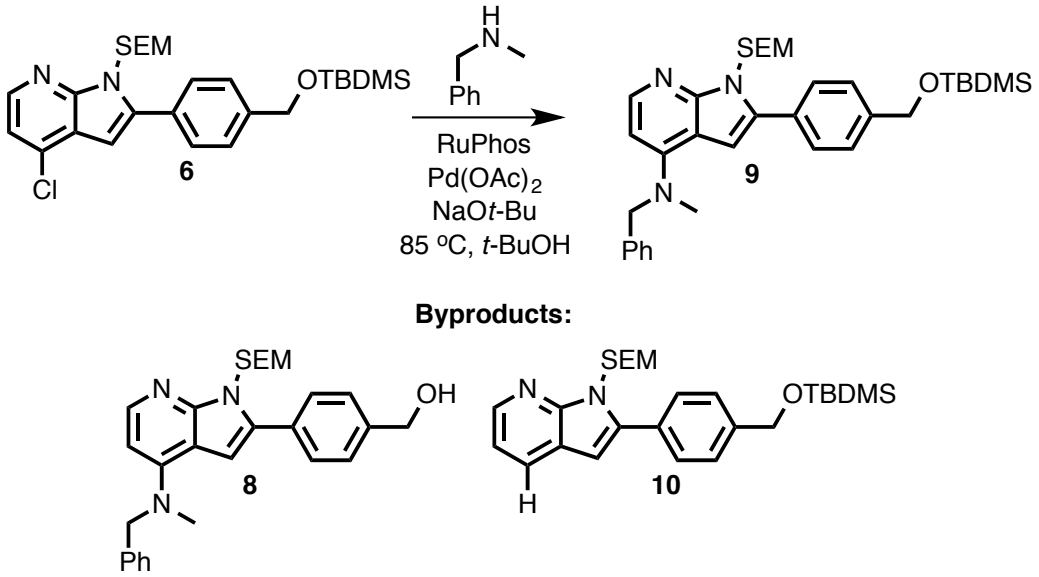

Scheme 3.14: The synthesis of compound **9** and the structures of byproducts **8** and **10**, formed by loss of the TBDMS group and β–hydride elimination, respectively.

The Buchwald amination with substrate **6** was successfully reproduced several times, and the results are reported in Table 3.3, entries 1-4. The yields after isolation of compound **9** varied from 34-89%. The product was obtained as a clear oil. Low yields in the initial reactions were primarily due the formation of several byproducts and overlap on the column. Side reactions occurring were β–hydride elimination of the palladium complex, resulting in byproduct **10**, and cleavage of the TBDMS group, giving compound **8** with an unprotected hydroxyl group. The loss in yield due to byproduct **8** shows that the TBDMS protecting group was evidently not sufficiently stable under the reaction conditions. There was a significant reduction in amounts of byproducts formed when the reaction time was shortened. Entry 4 in Table 3.3 shows that the largest scale reaction with the shortest reaction time gave the most selective amination and highest isolated yield of compound **9**.

Table 3.3: Results from the Buchwald amination synthesis of compound **9**.

	Reaction time [h]	**Scale [mg]**	**Conversion [%]**	**Crude product content[a]**			**Yield[b]** [%]
				Product **9** [%]	Byproduct **8** [%]	Byproduct **10** [%]	
1	1.3	104	>99	74	18	8	34
2	2.2	42	>99	80	8	12	55
3	0.7	156	>99	86	6	8	69
4	0.5	816	>99	90	6	4	89
5[c]	2.5	53	35	12	12	11	-
6[c]	24	393	33	0	0	23	-

[a]Analysis by ^{1}H NMR

[b]Isolated yield of **9**

[c]Reaction performed with non-anhydrous solvent and non-dried glass equipment

Several problematic issues were encountered in dealing with the Buchwald reactions, such as the reactions sensitivity to water. The Buchwald aminations were performed with all glass equipment properly oven-dried, and anhydrous degassed solvent was used. Buchwald aminations were also attempted on compound **6** using non-anhydrous *t*-BuOH, and without properly drying the glass equipment. These reactions resulted in conversions below 35%, and 0-12% formation of the aminated product **9,** as shown in entries 5-6 of Table 3.3. These observations indicated that the Buchwald aminations of these compounds are highly sensitive to water and other impurity residues.

In an attempt to increase the selectivity of the reaction, and reduce the amounts of byproducts formed, a test reaction with substrate **6** was also conducted at 65 ^{o}C. After 28 hours, the TBDMS-group had been completely cleaved off. Only trace amounts of the aminated target **9** was formed. It therefore appears that below a certain temperature, the amination reaction rate will be slower than the rate of removal of the TBDMS-group, giving an unsuccessful amination.

The results from the deprotection of the SEM- and TBDMS-groups are discussed in Section 3.4.1.

3.3.3.3 Amination of compound 11 with the -OSEM group

The initial substrate **5** contained an acidic proton in the form of a hydroxyl group, which gave an unsuccessful amination. The TBDMS-protected substrate **6** provided a route to the desired product, but an issue was encountered where the TBDMS group was not sufficiently stable and would fall off during the course of the reaction. To investigate an

alternative approach to the target structure, a SEM protecting group was installed in this position. The hypothesis was that as the SEM group has higher stability, it would not cleave off as easily as TBDMS, so that higher yields would be reached in the Buchwald amination.

Compound **11** was aminated using the same conditions as described for the synthesis of compound **9**. The results of these reactions are reported in Table 3.4, and the reaction is shown in Scheme 3.15.

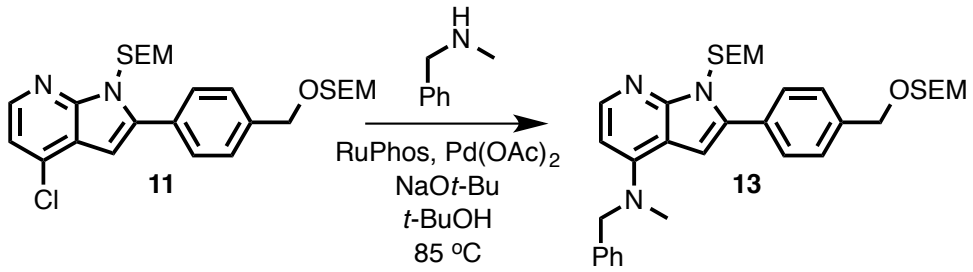

Scheme 3.15: The synthesis of compound **13** by amination of compound **11**.

The first amination was performed in a 111 mg scale. The reaction mixture was stirred at 85 °C for 5 hours. ^{1}H NMR analysis of the crude material showed that >99% conversion had been reached, and that around 95% of the crude mixture consisted of the product compound **13**. After purification with silica gel column chromatography, the target **13** was obtained as a clear oil, 118 mg (92%).

This amination reaction was also performed in a larger scale, starting with 455 mg of compound **11**. The reaction mixture was stirred at 85 °C for a total of 20 minutes before solvent removal. After purification with silica gel column chromatography, compound **13** was obtained as a clear oil, 471 mg (89%).

Table 3.4: Results from synthesis of compound **13** by Buchwald amination of compound **11**.

Entry	Scale [mg]	Reaction time [min]	Isolated yield of compound 13 [%]
1	111	300	92
2	455	20	89

As mentioned in Sections 3.3.2 and 3.3.3, compound **5**, with its unprotected hydroxyl group, would not undergo a Buchwald amination under the applied conditions. Compound **6** was adequate as a substrate in the Buchwald aminations, though the TBDMS group would cleave off during the reaction and expose the hydroxyl group. Neither of the reactions with substrates **5** or **6** provided the high selectivity that the reactions with the SEM-protected substrate **11** showed. In conclusion, compound **11** proved to be the most robust substrate in Buchwald aminations. The absence of acidic protons in the substrate,

as well as the stability of the SEM group, ensured a high yield of the reaction and minimized the formation of byproducts. In addition, the Buchwald amination reactions proved to be exceptionally sensitive to water residues, as the presence of water in the reaction gave low conversions or simply no reaction.

3.4 Removal of protecting groups

3.4.1 Synthesis of target compound 14

Two methods were tested for the deprotection of compounds **9** and **13**. Both methods were performed on both substrates **9** and **13**, and the results are summarized in Table 3.5.

The first procedure involved dissolving the starting material in dry acetonitrile at 0 ^{o}C, before BF_3-OEt_2 was added dropwise to the solution. After stirring at room temperature, water and later NH_3 (12.5% in H_2O) was added, before further stirring at room temperature overnight. This has previously been reported to be an efficient SEM-removal procedure.[60, 114] In general, these conditions produced low amounts of product **14,** and multiple unidentified byproducts were formed, resulting in low yields. The low yields were also the result of a difficult purification process, with poor separation and large losses during purification. The specific reactions employing this method are discussed in Section 3.4.1.1.

The second procedure entailed dissolving the starting material in dry CH_2Cl_2 before adding 2,2,2-trifluoroacetic acid (TFA). After stirring, the volatiles were removed, the mixture was dissolved in THF and added *sat. aq.* $NaHCO_3$ before stirring at room temperature overnight. This method generally gave fewer byproducts, and the crude products showed clearly the formation of compound **14** as the major product. The purification process was still problematic, as a very polar eluent system was required, and tailing of trace impurities made isolation of pure product challenging**.** Low yields of product **14** were therefore obtained in some cases. The specific reactions using this method are discussed in Sections 3.4.1.1. and 3.4.1.2.

Table 3.5: Results from the deprotections of compound **9** and **13.**

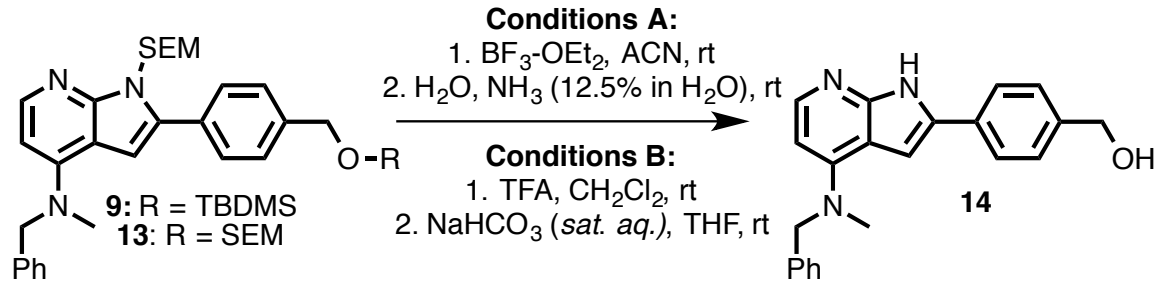

Entry	Conditions	Substrate	Scale [mg]	Isolated yield of compound 14 [%]
1	A	**9**	119	22
2		**13**	158	3
3	B	**9**	430	74
4[a]		**13**	182	13

[a]First reaction step performed at 50 °C

3.4.1.1 Deprotection of compounds 9 and 13 using BF_3-OEt_2

The first deprotection reaction of compound **9** (Table 3.5, entry 1) was performed using BF_3-OEt_2. The starting material **9** was dissolved in dry acetonitrile at 0 °C and BF_3-OEt_2 was added dropwise, before the reaction was left to stir at room temperature for 1 hour and 30 minutes. When ^1H NMR analysis showed full conversion of the starting material, water and later ammonia (12.5% in water) was added at 0 °C, before the mixture was left to stir at room temperature for 36 hours. After workup and purification with silica gel column chromatography, compound **14** was obtained in a 22% yield (15.1 mg) as an off-white solid. The low yield was a result of the challenging purification process, as purification required three rounds of column chromatography. Multiple side-reactions had also taken place. The reaction is shown in Scheme 3.16.

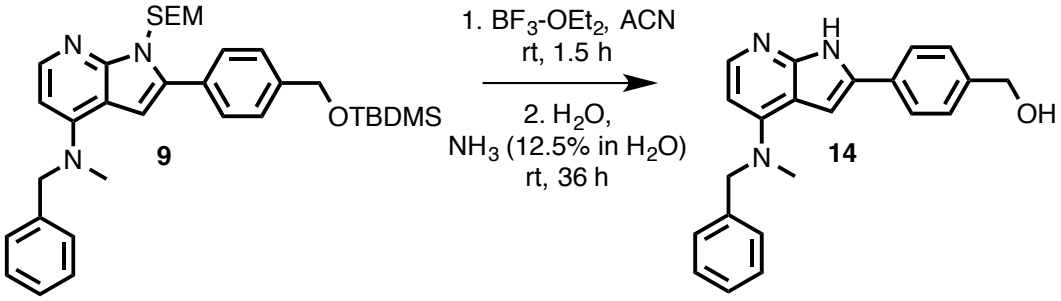

Scheme 3.16: Synthesis of compound **14** by deprotection of compound **9** using BF_3-OEt_2.

The BF_3-OEt_2 deprotection of compound **13** (Table 3.5, entry 3) is shown in Scheme 3.17. The reaction was conducted using the same conditions as described above for the deprotection of compound **9**. During the addition of NH_3, a light yellow solid precipitated.

The mixture was stirred overnight, before 53 mg of the light yellow solid was isolated by filtration.

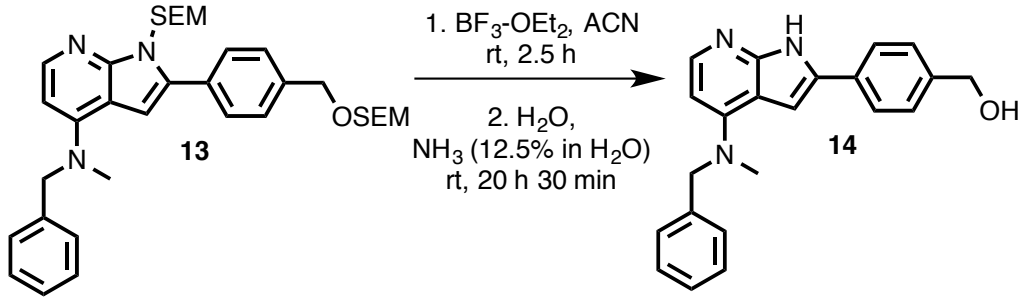

Scheme 3.17: Synthesis of compound **14** by deprotection of compound **13** using BF_3-OEt_2.

^{1}H NMR and TLC analysis of this crude compound showed that many impurities and byproducts were present. The mixture was attempted purified by silica gel column chromatography, and a fraction containing only 3 mg (3%) of compound **14** was collected from the column. Impurities were still present in this sample, but as only a small amount was obtained, no further purification was done. Another fraction collected from the column contained 27 mg of a yellow powder. TLC analysis showed that multiple byproducts were present in this sample. Characterization of the byproducts was problematic as ^{1}H NMR analysis showed over 10 different signals in the region between 4.1-4.9 ppm, where only the benzylic protons were typically seen.

It was evident that the SEM group protecting the hydroxyl group in compound **13** was more challenging to remove than the TBDMS group of compound **9** in the same position. It was clear from the NMR spectra of the BF_3-OEt_2 mediated reactions that many side reactions had taken place, making purification difficult. This strategy offered low yields of the target **14** for the reactions of both substrates.

3.4.1.2 Deprotection of compounds 9 and 13 using TFA

The deprotection reaction of compound **9** with TFA (Table 3.5, entry 2) is shown in Scheme 3.18. Compound **9** was dissolved in dry CH_2Cl_2 before TFA was added dropwise under an N_2 atmosphere. The mixture was stirred for 4 hours and 30 minutes at room temperature, before the solvent was removed. The product was dissolved in THF and added *sat. aq.* $NaHCO_3$ dropwise over a period of 10 minutes. A light yellow powder precipitated from the solution when *sat. aq.* $NaHCO_3$ was added. After stirring overnight at room temperature, the solvent was removed, and the mixture was dissolved in CH_2Cl_2 and MeOH (2:1). The mixture was stirred at room temperature for 1 hour and 30 minutes before filtration and concentration in vacuo to give the crude product as a light yellow powder.

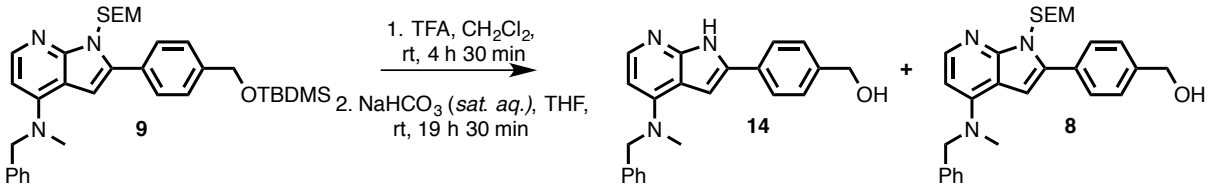

Scheme 3.18: Synthesis of compound **14** by deprotection of compound **9** using TFA. Byproduct **8** was also collected from the column, as a result of incomplete SEM-deprotection.

^{1}H NMR analysis of the crude product showed that the TBDMS group had been completely removed, and no starting material **9** was observed. This was expected, as the TBDMS group had previously shown to be more easily cleaved off than the SEM group. The crude product contained mostly target **14** (94% by ^{1}H NMR analysis). A small impurity of compound **8** (6% by ^{1}H NMR analysis) was also observed, where the TBDMS group had been cleaved off and the SEM group was still present. The crude mixture was purified by silica gel column chromatography, giving the target **14** as an off-white powder, 186 mg (74%).

As described in the previous section, using the BF_3-OEt_2 strategy for the deprotection of compound **13** gave poor results and a low 3% yield of compound **14**. The TFA procedure for the deprotection of compound **13** (entry 4, Table 3.5) is shown in Scheme 3.19. Compound **13** was dissolved in dry CH_2Cl_2 and TFA was added dropwise. After 2 hours of stirring at 50 ^{o}C, the solvent was removed and the mixture was dissolved in THF for the second step. $NaHCO_3$ (*sat. aq.)* was added dropwise over the course of 10 minutes, and the mixture was stirred overnight. The product was then dissolved in CH_2Cl_2 and MeOH, and stirred at room temperature for 2 hours before filtration and concentration in vacuo. A prominent byproduct was observed in the ^{1}H NMR spectrum, and it was suspected that the second step of the deprotection had not been completed at this point. The material was therefore dissolved in MeOH, added NH_3 (12.5% in water) and stirred at room temperature for 18 hours and 30 minutes. No change in the composition was observed after treatment with NH_3, neither with TLC or ^{1}H NMR analysis. The volatiles were then removed, and the crude product (219 mg, 211%) was collected as a yellow powder.

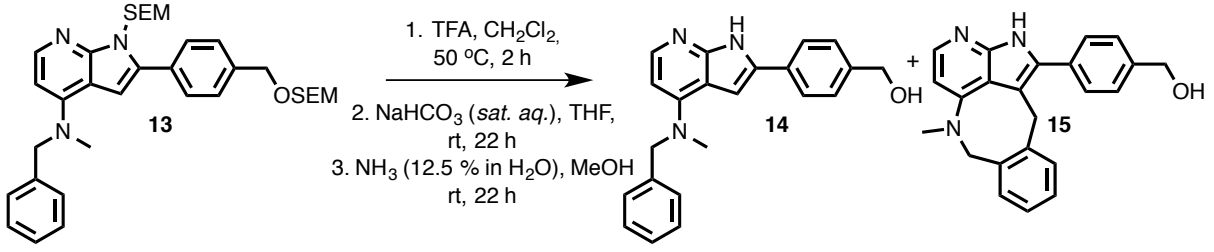

Scheme 3.19: Synthesis of compound **14** and byproduct **15** by deprotection of compound **9** using TFA. The structure for compound **15** was deduced using NMR and MS analysis.

^{1}H NMR analysis showed full conversion of the starting material, and the desired target **14** had been formed as the main product. The crude mixture contained the target **14** and the byproduct **15** in a 2:1 ratio. After isolation, the structure of byproduct **15** was deduced

from NMR and MS analysis, and is shown in Scheme 3.19. The rare eight-membered ring system might have been formed in a side-reaction between product **14** and formaldehyde, which is formed during the SEM group removal. This byproduct was not observed in any of the other deprotection reactions, which could indicate that the reaction temperature of 50 °C was necessary for the formation of byproduct **15**. The byproduct was first observed after the second reaction step, when *sat. aq.* $NaHCO_3$ was added. No changes in the crude material were observed after treatment with NH_3. The byproduct **15** was therefore most likely formed in one of the first two steps, either after the addition of TFA or base.

The crude mixture was purified by silica gel column chromatography, giving the target **14** in a 13% yield (13 mg). Byproduct **15** was collected from the column in a 11% yield (12 mg). The low yields obtained of both compounds after purification are the results of overlap on the column, and losses during purification.

In conclusion, the TFA method proved superior to the BF_3-OEt_2 method, due to the lower amounts of byproducts formed and the more selective formation of target **14**. The TFA reactions both gave compound **14** as the major product. A high yield of 74% was obtained for the deprotection of compound **9** using TFA, and this reaction was the most successful of the performed deprotection reactions. The large scale was beneficial in making the purification process easier, so a higher yield could be reached. For the deprotection of the twice SEM-protected compound **13**, the TFA method also proved superior to BF_3-OEt_2, again forming target **14** as the major product. However, the formation of byproduct **15** lowered the end yield of the target **14** to 13%. It is possible that the formation of compound **15** could have been avoided by lowering the reaction temperature, as it was not observed in the room temperature reactions.

3.4.2 Deprotection of compound 3 and 4

The diarylated compounds **16** and **17** were synthesized by deprotection of compound **3** and **4,** respectively. The deprotection reactions were performed using the BF_3-OEt_2 method, with substrate **3** in a 150 mg scale, and substrate **4** in a 148 mg scale.

Both starting materials **3** and **4** showed poor solubility in dry acetonitrile at 0 °C. After the mixtures were warmed to room temperature and BF_3-OEt_2 was added, all material dissolved. During the course of the reaction, some material had solidified in the reaction flasks. When ^1H NMR analysis showed that no starting material remained, water was added and later NH_3 (12.5% in water). The mixtures were left to stir for 19 hours. Scheme 3.20 shows the deprotections of **3** and **4**.

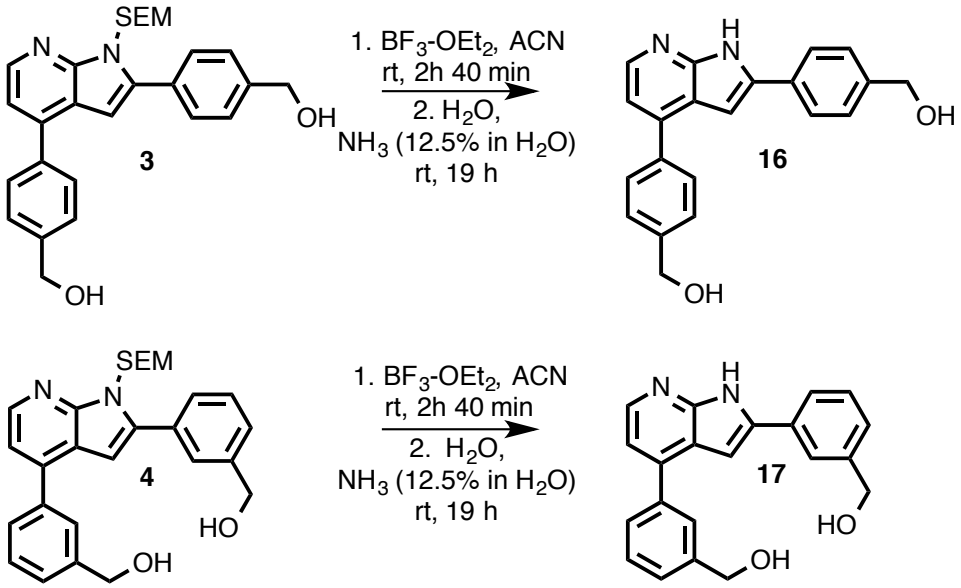

Scheme 3.20: Synthesis of compounds **16** and **17** from deprotection of compounds **3** and **4**, respectively.

After purification with silica gel column chromatography, product **17** was obtained as a yellow solid in a 32% yield (34 mg) with a purity of 97% as judged by HPLC analysis. A lot of product was lost during purification, as the compound showed low solubility in the mobile phase.

Product **16** showed many of the same solubility issues as described for compound **17**. After purification by silica gel column chromatography and drying, there were still impurities present. To remove more of the impurities, acetonitrile was added to the product and the mixture was stirred at room temperature for 2 hours. After filtering and drying, 35 mg compound **16** was obtained as a light yellow powder in a 33% yield, with a purity of 91% by HPLC.

3.5 Structural elucidation

Of the 17 compounds synthesized in this master thesis, 15 were not reported in literature. NMR, HRMS and IR analysis have been used to verify the structures of these compounds. Chemical shifts have been assigned using the 1D ^{1}H NMR and ^{13}C NMR, 2D ^{1}H-^{1}H COSY, ^{1}H-^{13}C HSQC and ^{1}H-^{13}C HMBC experiments. MS was used to verify the identities of the compounds. All NMR, IR and MS spectra are given in Appendix A-Q. The assigned chemical shifts are presented for the new compounds **3**-**17** in Sections 3.5.2-3.5.16. All NMR spectra were conducted using DMSO-d_6 as solvent, and all spectra were calibrated relative to DMSO-d_6 (2.50 ppm in ^{1}H NMR and 39.52 ppm in ^{13}C NMR). Some NMR spectra contains signals corresponding to solvent residues and grease. An overview of the chemical shifts of these trace impurities can be seen in Table 3.6.

Table 3.6: NMR chemical shifts of common solvents and trace impurities in DMSO-d_6.

	Proton	**Carbon**	**^{1}H DMSO-d_6**	**^{13}C DMSO-d_6**
DMSO residue	-	-	2.50 (quin)	39.52 (sep)
H_2O	-	-	3.33 (s)	-
EtOAc	$CH_3C\underline{H_2}$	$CH_3\underline{C}H_2$	4.03 (q)	59.74
	$C\underline{H_3}CH_2$	$\underline{C}H_3CH_2$	1.17 (t)	14.40
	CH_3CO	$\underline{C}H_3CO$	1.99 (s)	20.68
	-	CO	-	170.31
CH_2Cl_2	CH_2	CH_2	5.76 (s)	54.84
MeOH	CH_3	CH_3	3.17 (d)	48.59
	OH	-	4.10 (q)	-
Grease	-	-	1.24 (br, s)	-
	-	-	0.88-0.82 (m)	-
Acetone	-	CO	-	206.31
	CH_3	CH_3	2.09 (s)	30.56

3.5.1 General remarks

The assignments of quaternary carbons were done using ^{1}H-^{13}C long range coupling observed in the HMBC spectra. Long range couplings were in most cases detected between H-6/C-8, H-6/C-4, H-5/C-9, H-5/C-6, H-5/C-3 and H-3/C-9. The concentration of the NMR-samples varied, and for some of the compounds it was therefore difficult to distinguish the mentioned carbon signals from noise in the ^{13}C NMR spectra. In these cases, the 2D spectra signals were used to determine the shifts of these signals. For the N-CH_3 group present in compounds **7-9**, **14** and **15**, the ^{1}H signal (3.19-3.40 ppm) could overlap with the H_2O residue signal, and the ^{13}C signal (39.6-40.2 ppm) was usually hidden behind the DMSO-d_6 residue signal. In the cases where these signals were concealed in the spectra, the 2D spectra were used for assigning the chemical shifts. In a

few of the HSQC spectra, flipping was observed. Signals corresponding to carbon signals below 0 ppm appeared above 200 ppm in these cases.

3.5.2 Compound 3

A detailed demonstration of the structural elucidation of compound **3** will be given in this section. The structures of the other compounds synthesized in this project were confirmed using the same method, and will be presented in a less detailed manner in Sections 3.5.3-3.5.16.

Compound **3** is presented in Figure 3.2, with atom numbering. HRMS gave *m/z* 461.2259 [M+H$^+$] for compound **3**. With a calculated value of 461.2260, thus the molecular formula $C_{27}H_{33}N_2O_3Si$ was confirmed. From IR analysis, some signals were useful in confirming the correct structure. Examples were: 3404 cm^{-1} (w, br, O-H stretch), 2919 cm^{-1} (w, CH_2 asymmetrical stretch), 2858 cm^{-1} (w, CH_2 symmetrical stretch), 1585 cm^{-1} (m, aromatic C=C stretch), 1082 cm^{-1} (s, C-O hydroxyl stretch) and 833 cm^{-1} (s, =C-H out-of-plane-bending, para substitution). All spectra for compound **3** can be found in Appendix C.

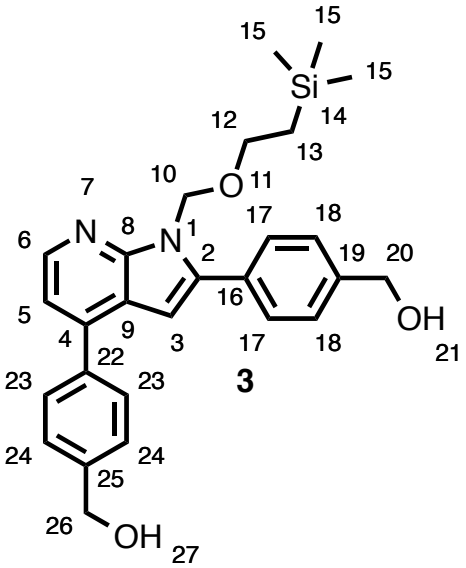

Figure 3.2: The structure of compound **3** with atom numbering.

The ^{1}H NMR spectrum showed a doublet at 8.36 ppm (J = 5.0 Hz) with an integral of 1. This signal must represent H-6, due to the high chemical shift and the multiplicity. The corresponding carbon C-6 was found from the HSQC spectrum as shown in Figure 3.3, with a ^{13}C shift at 143.2 ppm. One ^{1}H-^{1}H coupling was observed for H-6 in the COSY spectrum, see Figure 3.4. This was a doublet at 7.32 ppm (J = 5.0 Hz) with the integral of 1, and this signal was assigned to originate from H-5. The corresponding carbon C-5 was found to be at 115.7 ppm from the HSQC spectrum, also visible in Figure 3.3. All following corresponding carbon and proton signal pairs were assigned using the HSQC spectrum in the same manner.

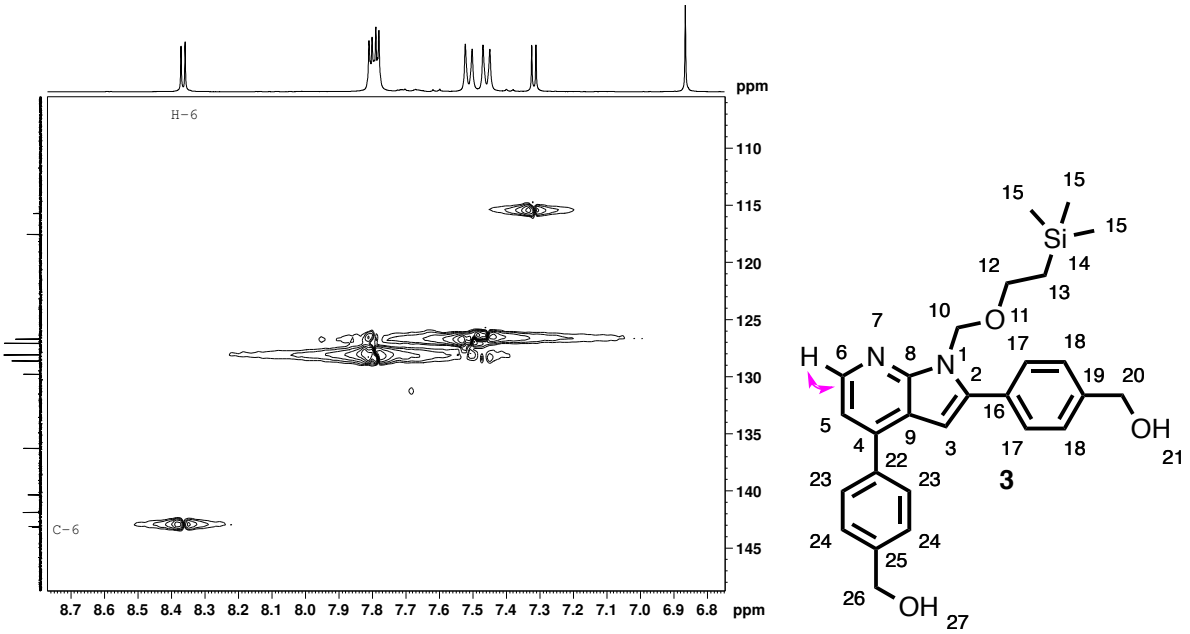

Figure 3.3: Part of the HSQC spectrum of compound **3**, used to determine the chemical shift of C-6 from the proton shift of H-6. The ^{1}H-^{13}C coupling is shown by the pink arrow on the right.

A signal of chemical shift -0.07 ppm with the integral of 9 was observed in the ^{1}H NMR spectrum. This was assigned to H-15, due to the multiplicity, integral and the fact that the silicon atom has a shielding effect on neighboring atoms. The corresponding carbon C-15 signal was found at -1.4 ppm. ^{1}H-^{13}C long range coupling was seen in the HMBC spectrum between C-15 and a triplet signal at 0.88 ppm (J = 8.1 Hz) with integral 2. This signal was assigned to H-13, and the ^{13}C chemical shift from the HSQC spectrum was found to be at 17.4 ppm. Selected examples of ^{1}H-^{13}C long range couplings can be found in Figure 3.5.

Furthermore, ^{1}H-^{1}H coupling was seen in the COSY spectrum between H-13 and a triplet signal with integral 2 at 3.67 ppm (J = 8.1 Hz), as shown in Figure 3.4. This signal was assigned to H-12, with the corresponding carbon signal at 65.8 ppm. The signal C-12 showed ^{1}H-^{13}C long range coupling to a singlet peak at 5.68 ppm with integral 2, which was assigned as H-10, corresponding to C-10 at 70.5 ppm. All signals of the SEM protecting group moiety had at this point been assigned.

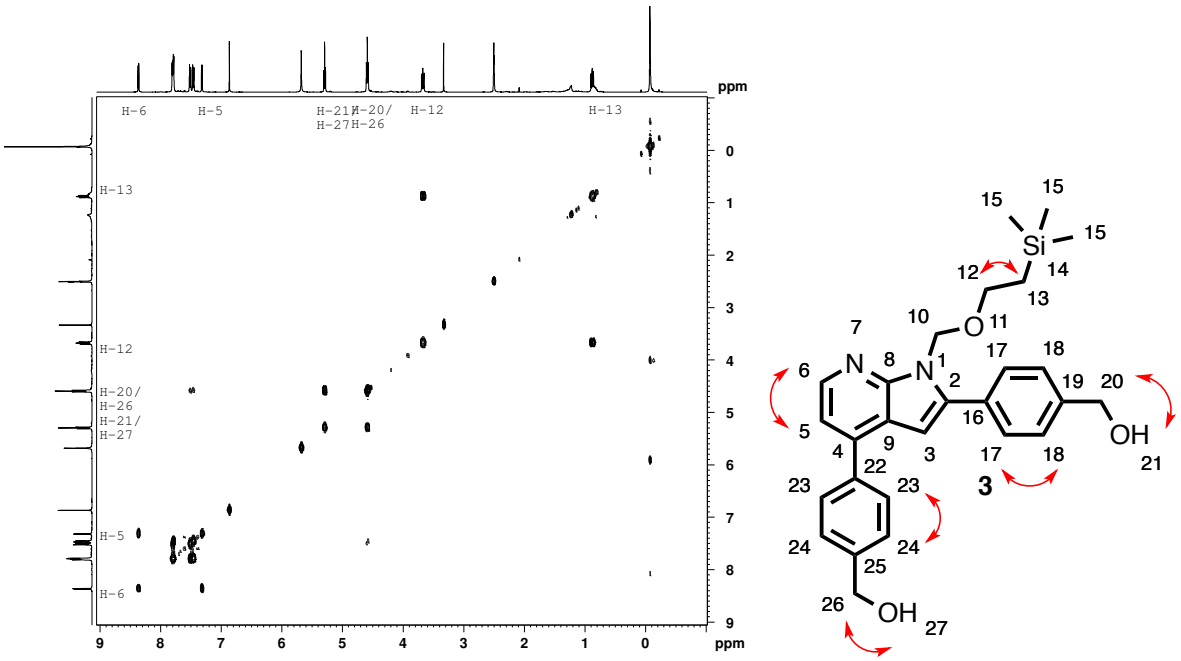

Figure 3.4: COSY spectrum of compound **3**, showing ^{1}H-^{1}H coupling between neighboring protons. The red arrows on the right represent ^{1}H-^{1}H-coupling as shown in the spectrum.

The signal H-10 displayed ^{1}H-^{13}C long range coupling to two other carbon atoms, which showed to be quaternary due to the lack of coupling in the HSQC spectrum. These signals were at 150.1 ppm and 141.9 ppm, and should belong to C-8 and C-2. As C-8 is located between two nitrogen atoms, it must have the highest chemical shift. The H-6 signal also showed long range coupling to 150.1 ppm. The signal at 150.1 ppm was therefore assigned to C-8, and 141.9 ppm to C-2. The C-8 signal showed ^{1}H-^{13}C coupling to the singlet at 6.86 ppm with integral 1, which also coupled to C-2. The multiplicity, integral and long range coupling supported the assignment of 6.86 ppm to H-3. The corresponding carbon ^{13}C shift was found to be 99.7 ppm. The signal H-3 coupled to another quaternary carbon with ^{13}C shift at 117.5 ppm. As the signal at 117.5 ppm also showed coupling to H-5 and weak coupling to H-6, it was assigned to C-9.

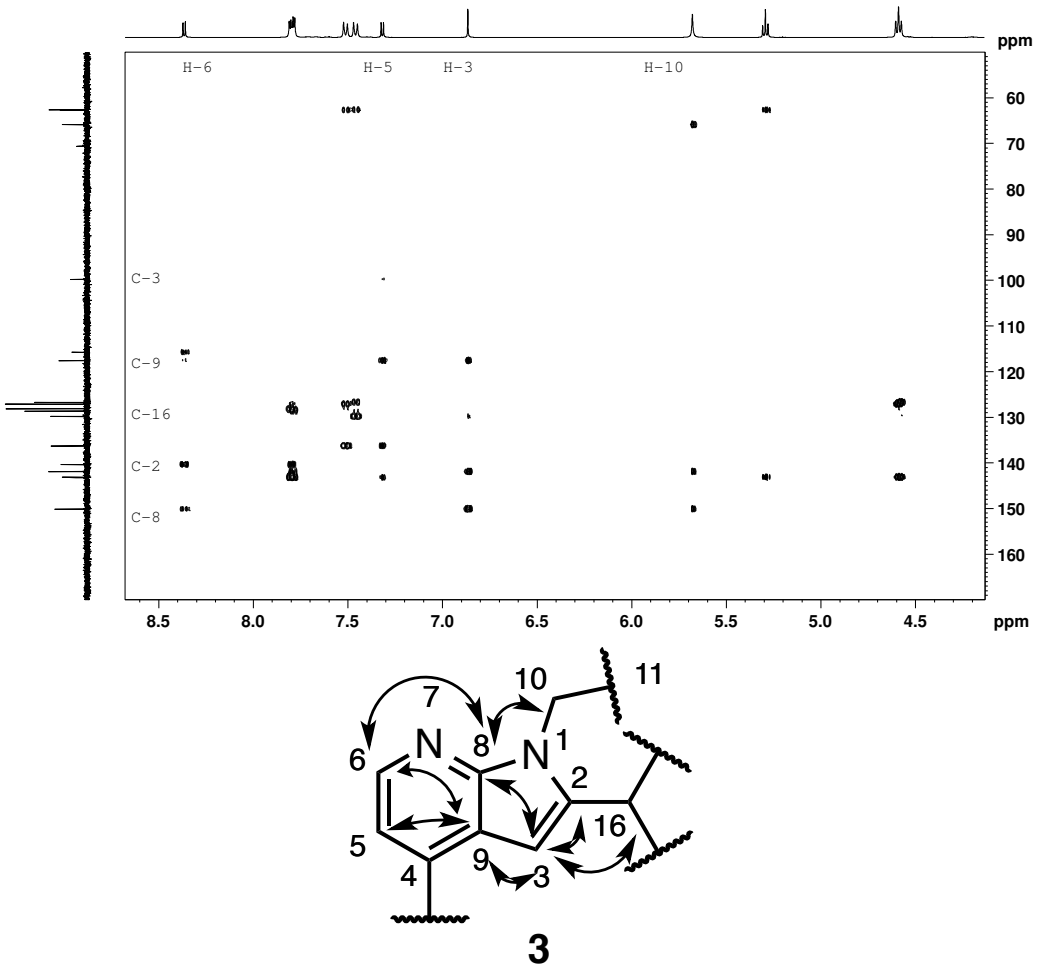

3

Figure 3.5: Part of the HMBC spectrum of compound **3**, showing ^{1}H-^{13}C long range coupling between protons and carbon atoms 2, 3 and 4 bonds away. The bottom structure illustrates the ^{1}H-^{13}C long range coupling observed for H-3, C-8 and C-9.

On the SEM-protected pyrrolopyridine skeleton, only one carbon signal remained to be assigned at this point. The H-6 doublet showed long range coupling to the carbon at 140.3 ppm, and this signal was assigned to C-4. The remaining signals would at this point belong to the two *para*-hydroxymethylphenyl substituents. H-5 showed ^{1}H-^{13}C long range coupling to 136.2 ppm. This carbon shift is situated in the aromatic region, and as it is a quaternary carbon, it is assigned to C-22. H-3 showed weak ^{1}H-^{13}C long range coupling to a quaternary carbon at 129.8 ppm, which in turn was assigned to C-16.

As the solvent was DMSO-d_6, the hydroxyl protons signals would be expected to appear as triplets in the ^{1}H spectrum. The hydroxyl groups neighboring environments are quite similar and the triplets would be expected to appear close to one another, if not completely overlapping. A triplet signal with the integral of 2 was found in the ^{1}H spectrum at 5.29 ppm (J = 5.7 Hz). This signal had no carbon atom coupling in the HSQC spectrum, and was assigned to H-21/H-27. The signal showed ^{1}H-^{1}H coupling with to overlapping doublet at 4.59 ppm with integral 4 (J = 6.0 Hz), as seen in the COSY spectrum in Figure 3.4. The signals were assigned to H-20 and H-26. The corresponding carbon

signals for C-20 and C-26 were found in the HSQC spectrum at 62.5 and 62.6 ppm. As the doublets overlapped in the ^{1}H spectrum and the ^{13}C signals were close, the shifts were interchangeable.

The carbon signal at 143.1 ppm showed ^{1}H-^{13}C long range coupling to H-20, H-21, H-26 and H-27, and was therefore assigned to both quaternary carbons C-19 and C-25.

For the phenyl group protons, the remaining signals were 7.81-7.78 ppm (4H, m), 7.51 ppm (2H, *J* = 8.2 Hz, d) and 7.46 ppm (2H, *J* = 8.2 Hz, d). Due to the structure of the molecule, and resonance arguments, it was suspected that the phenyl protons closer to the pyrrolopyridine ring (H-17 and H-23), would have higher proton shifts than H-18 and H-24. The 7.81-7.78 ppm signal showed ^{1}H-^{13}C long range coupling to both C-4 and C-2, as well as to C-19 and C-25, and it was therefore assigned to belong to both proton groups at H-17 and H-23. These proton signals are interchangeable as they appeared so close together in the spectrum. The corresponding ^{13}C signals were found to be at 128.1 and 128.6 ppm, though it was not possible to distinguish the C-17 and C-23 signals. Long range couplings between *meta*-positions of the phenyl rings were observed in the HMBC spectrum. The 7.51 ppm doublet showed ^{1}H-^{13}C long range coupling to C-22, and was therefore assigned H-24. The corresponding C-22 was found at 127.1 ppm. The 7.46 ppm doublet coupled to C-16, and was assigned to H-18 along with the corresponding C-18 found at 126.7 ppm.

Assigned ^{1}H and ^{13}C NMR shifts for compound **3** are summarized in Table 3.7.

Table 3.7: ^{1}H and ^{13}C NMR for compound **3** (DMSO-d_6, 400 MHz).

Position	^{1}H [ppm]	^{13}C [ppm]	COSY	HMBC
2	-	141.9		3, 10, 17
3	6.86 (s, 1H)	99.7		2, 8, 9, 16
4	-	140.3		1, 11
5	7.32 (d, *J* = 5.0 Hz, 1H)	115.7	6	6, 9, 22
6	8.36 (d, *J* = 5.0 Hz,1H)	143.2	5	4, 5, 8, 9
8	-	150.1		3, 6, 10
9	-	117.5		3, 5, 6
10	5.68 (s, 2H)	70.5		2, 8, 12
12	3.67 (t, *J* = 8.1 Hz, 2H)	65.8	13	10, 13
13	0.88 (t, *J* = 8.1 Hz, 2H)	17.4	12	12, 15
15	-0.07 (s, 9H)	-1.4		13, 15
16	-	129.8		3, 18
17	7.81-7.78 (m, 4H)	128.6/128.1[a]	18	8, 19
18	7.46 (d, *J* = 8.2 Hz, 2H)	126.7	17	16, 18, 20
19	-	143.1[c]		17, 20, 21
20	4.59 (t, *J* = 6.0 Hz, 4H)	62.5/62.6[b]	18, 21	18, 19
21	5.29 (t, *J* = 5.7 Hz, 2H)	-	20	19, 20
22	-	136.2		5, 24
23	7.81-7.78 (m, 4H)	128.6/128.1[a]	24	4, 24, 25
24	7.51 (d, *J* = 8.2 Hz, 2H)	127.1	23	22, 24, 26
25	-	143.1[c]		23, 26, 27
26	4.59 (t, *J* = 6.0 Hz, 4H)	62.5/62.6[b]	23, 27	24, 25
27	5.29 (t, *J* = 5.7 Hz, 2H)	-	26	25, 26

[a, b]Might be interchanged

[c]Overlapping signals

3.5.3 Compound 4

The structure of compound **4** with numbered positions is given in Figure 3.6. Assigned ^{1}H and ^{13}C NMR shifts are given in Table 3.8. HRMS gave *m/z* 461.2256 $[M+H]^{+}$]. With a calculated value of 461.2260, the molecular formula $C_{27}H_{33}N_2O_3Si$ was confirmed. ^{1}H and ^{13}C NMR, MS and IR spectra for compound **4** can be found in Appendix D.

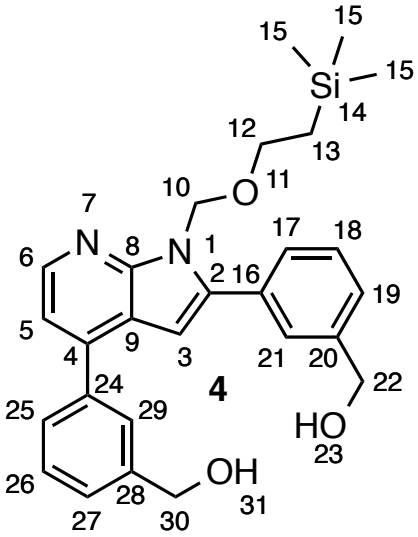

Figure 3.6: The structure of compound **4** with atom numbering.

Table 3.8: ^{1}H and ^{13}C NMR for compound **4** (DMSO-d_6, 400 MHz).

Position	^{1}H [ppm]	^{13}C [ppm]	COSY	HMBC
2	-	142.1		3, 17, 21
3	6.86 (s, 1H)	99.9		2, 8, 9, 16
4	-	140.7		6, 25, 29
5	7.32 (d, *J* = 4.9 Hz, 1H)	115.8	6	3, 6, 9, 24
6	8.39 (d, *J* = 4.9 Hz, 1H)	143.3[a]	5	4, 5, 6, 9
8	-	150.0		3, 6, 10
9	-	117.5		3, 5, 6
10	5.69 (s, 2H)	70.5		6, 8, 12
12	3.63 (t, *J* = 8.2 Hz, 2H)	65.7	13	10, 13
13	0.87 (t, *J* = 8.2 Hz, 2H)	17.4	12	12, 15
15	-0.08 (s, 9H)	-1.4		13, 15
16	-	131.2		3, 18
17	7.70-7.68 (m, 2H)	126.9		2, 19, 21/25/27
18	7.48 (t, *J* = 7.5 Hz, 1H)	127.1		16, 17, 20
19	7.44-7.42 (m, 2H)	128.5	22	21/25/27, 22
20	-	143.3[a]		18, 22, 23
21	7.72 (s, 1H)	126.69/126.67/126.64[c]	22	2, 17, 22
22	4.58 (d, *J* = 5.8 Hz, 2H)	62.7/62.8[b]	19, 21, 23	20, 17
23	5.27 (t, *J* = 5.9 Hz, 1H)	-	22	20, 22
24	-	137.7		5, 26
25	7.70-7.68 (m, 2H)	126.69/126.67/126.64[c]	30	4, 21/25/27
26	7.53 (t, *J* = 7.7 Hz, 1H)	128.9		24, 28, 29
27	7.44-7.42 (m, 2H)	126.69/126.67/126.64[c]	30	21/25/27, 30
28	-	143.5		26, 30, 31
29	7.77 (s, 1H)	126.2	30	4, 21/25/27, 30
30	4.62 (d, *J* = 5.9 Hz, 2H)	62.7/62.8[b]	27, 29, 31	28, 29
31	5.30 (t, *J* = 5.9 Hz, 1H)	-	30	28, 30

[a]Overlapping signals

[b, c]Might be interchanged

3.5.4 Compound 5

The structure of compound **5** with numbered positions is given in Figure 3.7. Assigned ^{1}H and ^{13}C NMR shifts are given in Table 3.9. HRMS gave *m/z* 389.1445 $[M+H]^{+}$]. With a calculated value of 389.1452, the molecular formula $C_{20}H_{26}N_2O_2SiCl$ was confirmed. ^{1}H and ^{13}C NMR, MS and IR spectra for compound **5** can be found in Appendix E.

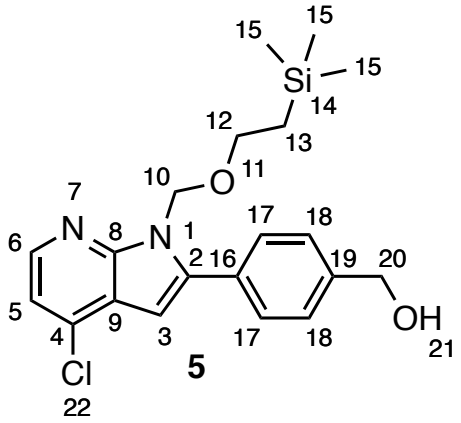

Figure 3.7: The structure of compound **5** with atom numbering.

Table 3.9: ^{1}H and ^{13}C NMR for compound **5** (DMSO-d_6, 400 MHz).

Position	^{1}H [ppm]	^{13}C [ppm]	COSY	HMBC
2	-	142.5		3, 10, 17
3	6.75 (s, 1H)	98.2		2, 4, 8, 9, 16
4	-	133.8		3, 5, 6
5	7.33 (d, *J* = 5.2 Hz, 1H)	116.9	6	3, 5, 6, 9
6	8.27 (d, *J* = 5.2 Hz, 1H)	143.6	5	4, 5, 8, 9
8	-	149.8		3, 6
9	-	118.9		3, 5, 6, 8
10	5.63 (s, 2H)	70.8		9, 12, 16
12	3.61 (t, *J* = 8.0 Hz, 2H)	65.9	13	10, 13
13	0.84 (t, *J* = 8.0 Hz, 2H)	17.3	12	12, 15
15	-0.11 (s, 9H);	-1.4		13
16	-	129.2		3, 18
17	7.77 (d, *J* = 8.3 Hz, 2H)	128.7	18	2, 17, 18, 19, 20
18	7.47 (d, *J* = 8.3 Hz, 2H)	126.7	17	17, 18, 20
19	-	143.4		17, 20, 21
20	4.58 (d, *J* = 5.7 Hz, 2H)	62.5	21	17, 18, 19
21	5.31 (t, *J* = 5.7 Hz, 1H)	-	20	19, 20

3.5.5 Compound 6

The structure of compound **6** with numbered positions is given in Figure 3.8. Assigned ^{1}H and ^{13}C NMR shifts are given in Table 3.10. HRMS gave *m/z* 503.2315 $[M+H]^{+}$]. With a calculated value of 503.2317, the molecular formula $C_{26}H_{40}N_2O_2Si_2Cl$ was confirmed. ^{1}H and ^{13}C NMR, MS and IR spectra for compound **6** can be found in Appendix F.

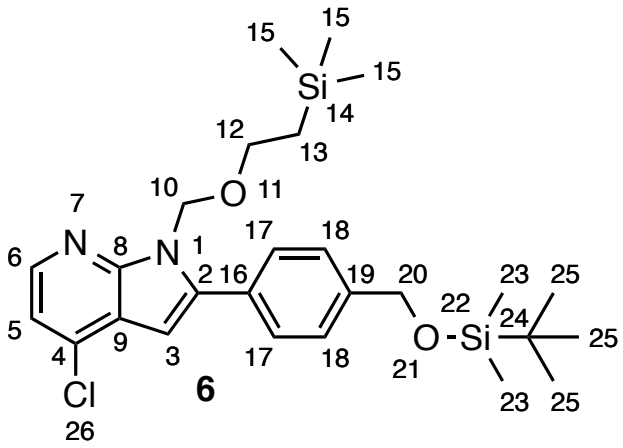

Figure 3.8: The structure of compound **6** with atom numbering.

Table 3.10: ^{1}H and ^{13}C NMR for compound **6** (DMSO-d_6, 400 MHz).

Position	^{1}H [ppm]	^{13}C [ppm]	COSY	HMBC
2	-	142.4		3, 10
3	6.76 (s, 1H)	98.3		2, 4, 8, 9, 10
4	-	133.9		3, 5, 6
5	7.33 (d, *J* = 5.2 Hz, 1H)	117.0	6	4, 6, 9
6	8.27 (d, *J* = 5.2 Hz, 1H)	143.5	5	4, 5, 8, 9
8	-	149.8		3, 6, 10
9	-	118.9		3, 5, 6
10	5.64 (s, 2H)	70.8		2, 8, 12
12	3.59 (t, *J* = 8.0 Hz, 2H)	65.9	13	10, 13
13	0.82 (t, *J* = 8.0 Hz, 2H)	17.3	12	12, 15
15	-0.11 (s, 9H)	-1.5		13, 15
16	-	129.4		18, 20
17	7.79 (d, *J* = 8.3 Hz, 2H)	128.8	18, 20	17, 18, 19
18	7.46 (d, *J* = 8.3 Hz, 2H)	126.3	17, 20	16, 18, 20
19	-	142.2		17, 20
20	4.80 (s, 2H)	63.9	17, 18	16, 18, 19
23	0.11 (s, 6H)	-5.3		24, 25
24	-	18.0		23, 25
25	0.93 (s, 9H)	25.8		24, 25

3.5.6 Compound 7

The structure of compound **7** with numbered positions is given in Figure 3.9. Assigned ^{1}H and ^{13}C NMR shifts are given in Table 3.11. HRMS gave *m/z* 368.2157 $[M+H]^{+}$]. With a calculated value of 368.2158, the molecular formula $C_{21}H_{30}N_3OSi$ was confirmed. ^{1}H and ^{13}C NMR, MS and IR spectra for compound **7** can be found in Appendix G.

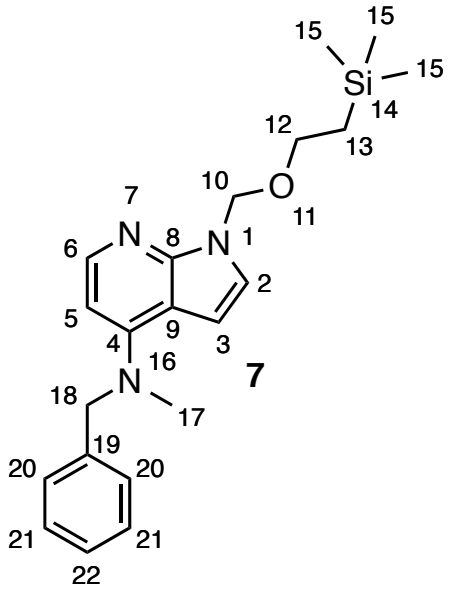

Figure 3.9: The structure of compound **7** with atom numbering.

Table 3.11: ^{1}H and ^{13}C NMR for compound **7** (DMSO-d_6, 400 MHz).

Position	^{1}H [ppm]	^{13}C [ppm]	COSY	HMBC
2	7.25 (m, 4H)[a]	124.3	3	3, 8, 9, 10
3	6.49 (d, *J* = 3.8 Hz, 1H)	101.1	2	2, 8, 9, 10
4	-	149.7		5, 6, 17, 18
5	6.28 (d, *J* = 5.7 Hz, 1H)	99.8	6	3, 4, 6, 9
6	7.88 (d, *J* = 5.7 Hz, 1H)	143.9	5	4, 5, 8, 9
8	-	149.4		2, 3, 6, 10
9	-	107.3		2, 3, 5, 6
10	5.52 (s, 2H)	72.3		2, 8, 12
12	3.49 (t, *J* = 8.1 Hz, 2H)	65.1	13	10, 13
13	0.81 (t, *J* = 8.1 Hz, 2H)	17.2	12	12, 15
15	-0.09 (s, 9H)	-1.4		13, 15
17	3.19 (s, 3H)	39.6[b]	18	4, 5, 18
18	4.81 (s, 2H)	56.1	17	4, 17, 19, 20, 21
19	-	138.4		18, 20, 21
20	7.26-7.23 (m, 4H)[a]	126.5	21	18, 19, 22
21	7.34-7.31 (m, 2H)	128.5	20, 22	19, 20, 21, 22
22	7.26-7.23 (m, 4H)[a]	126.9	21	20, 21

[a]Overlapping signals

[b]Overlapping with solvent signal

3.5.7 Compound 8

The structure of compound **8** with numbered positions is given in Figure 3.10. Assigned ^{1}H and ^{13}C NMR shifts are given in Table 3.12. HRMS gave *m/z* 474.2571 $[M+H]^{+}$]. With a calculated value of 474.2577, the molecular formula $C_{28}H_{36}N_3O_2Si$ was confirmed. ^{1}H and ^{13}C NMR, MS and IR spectra for compound **8** can be found in Appendix H.

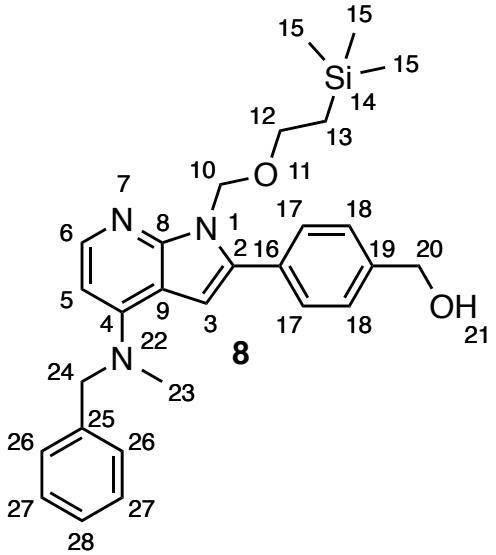

Figure 3.10: The structure of compound **8** with atom numbering.

Table 3.12: ^{1}H and ^{13}C NMR for compound **8** (DMSO-d_6, 400 MHz).

Position	^{1}H [ppm]	^{13}C [ppm]	COSY	HMBC
2	-	136.6		3, 10, 17
3	6.68 (s, 1H)	101.3		2, 8, 9, 16
4	-	149.4		6, 23, 24
5	6.34 (d, *J* = 5.7 Hz, 1H)	100.5	5	6, 9
6	7.91 (d, *J* = 5.7 Hz, 1H)	143.9	6	4, 5, 8
8	-	151.1		3, 6, 10
9	-	107.4		3, 5
10	5.55 (s, 2H)	70.4		2, 8, 12
12	3.63 (t, *J* = 8.2 Hz, 2H)	65.5	13	10, 13
13	0.85 (t, *J* = 8.2 Hz, 2H)	17.4	12	12, 15
15	-0.08 (s, 9H)	-1.4		13, 15
16	-	130.3		3, 18
17	7.64 (d, *J* = 8.2 Hz, 2H)	128.2	18	2, 17, 19
18	7.39 (d, *J* = 8.2 Hz, 2H)	126.6/126.5[b]	17, 20	16, 18, 20
19	-	142.3		17, 20, 21
20	4.54 (d, *J* = 5.7 Hz, 2H)	62.6	27, 21	18, 19
21	5.24 (t, *J* = 5.7 Hz, 1H)	-	20	20, 19
23	3.25 (s, 3H)	39.8[c]		4, 24
24	4.85 (s, 2H)	56.1	26	4, 23, 25, 26
25	-	138.4		24, 27
26	7.27-7.24 (m, 3H)[a]	126.6/126.5[b]	24, 27	24, 28
27	7.35-7.31 (m, 2H)	128.6	26, 28	25, 27
28	7.27-7.24 (m, 3H)[a]	126.9	27	26

[a]Overlapping signals

[b]Might be interchanged

[c]Overlapping with solvent signal

3.5.8 Compound 9

The structure of compound **9** with numbered positions is given in Figure 3.11. Assigned ^{1}H and ^{13}C NMR shifts are given in Table 3.13. HRMS gave *m/z* 588.3446 $[M+H]^{+}$]. With a calculated value of 588.3442, the molecular formula $C_{34}H_{50}N_3O_2Si_2$ was confirmed. ^{1}H and ^{13}C NMR, MS and IR spectra for compound **9** can be found in Appendix I.

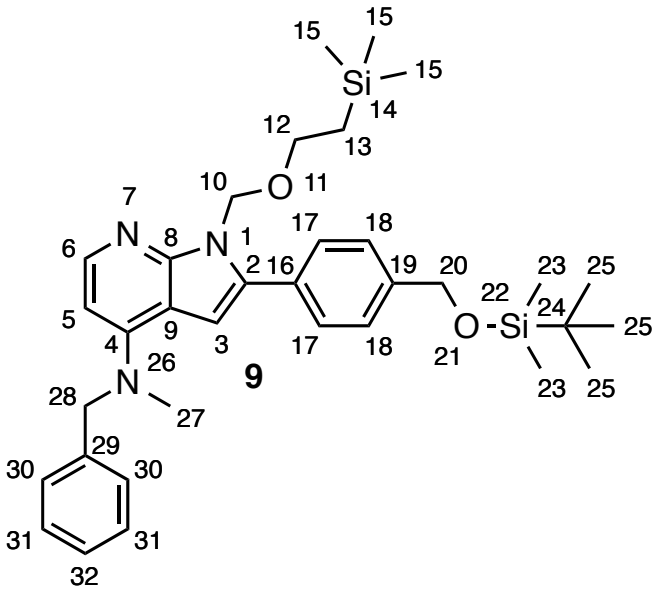

Figure 3.11: The structure of compound **9** with atom numbering.

Table 3.13: ^{1}H and ^{13}C NMR for compound **9** (DMSO-d_6, 400 MHz).

Position	^{1}H [ppm]	^{13}C [ppm]	COSY	HMBC
2	-	136.4		3, 10, 17
3	6.69 (s, 1H)	101.5		2, 8, 9, 16
4	-	149.4		6, 27, 28
5	6.33 (d, *J* = 5.8 Hz, 1H)	100.5	6	6, 9
6	7.91 (d, *J* = 5.8 Hz, 1H)	144.0	5	4, 5, 8
8	-	151.1		3, 6, 10
9	-	107.4		3, 5
10	5.55 (s, 2H)	70.4		2, 8, 10
12	3.60 (t, *J* = 8.1 Hz, 2H)	65.5	13	10, 13
13	0.83 (t, *J* = 8.0 Hz, 2H)	17.4	12	12, 15
15	-0.09 (s, 9H)	-1.4		13, 15
16	-	130.6		3, 18
17	7.65 (d, *J* = 8.3 Hz, 2H)	128.3	18	2, 17, 19
18	7.39-35 (m, 2H)	126.1	17	16, 17, 18, 20
19	-	140.9		17, 20
20	4.75 (s, 2H)	63.9		18, 19
23	0.09 (s, 6H)	-5.3		23, 24
24	-	18.0		23, 25
25	0.92 (s, 9H)	25.8		24, 25
27	3.25 (s, 3H)	39.9[b]		4, 28
28	4.85 (s, 2H)	56.1		4, 27, 29, 30
29	-	138.4		28, 31
30	7.24-7.27 (m, 3H)[a]	126.6	31	28, 32
31	7.33-31 (m, 2H)	128.6	30, 32	29, 31
32	7.24-7.27 (m, 3H)[a]	126.9	31	30

[a]Overlapping signals

[b]Overlapping with solvent signal

3.5.9 Compound 10

The structure of compound **10** with numbered positions is given in Figure 3.12. Assigned ^{1}H and ^{13}C NMR shifts are given in Table 3.14. HRMS gave *m/z* 469.2704 $[M+H]^{+}$]. With a calculated value of 469.2707, the molecular formula $C_{26}H_{41}N_2O_2Si_2$ was confirmed. ^{1}H and ^{13}C NMR, MS and IR spectra for compound **10** can be found in Appendix J.

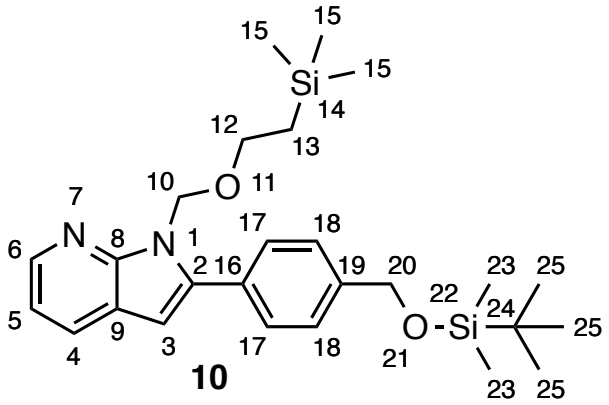

10

Figure 3.12: The structure of compound **10** with atom numbering.

Table 3.14: ^{1}H and ^{13}C NMR for compound **10** (DMSO-d_6, 400 MHz).

Position	^{1}H [ppm]	^{13}C [ppm]	COSY	HMBC
2	-	141.3		3, 10
3	6.70 (s, 1H)	100.5		2, 8, 9, 16, 17
4	8.00 (dd, 1.54 Hz/7.8 Hz, 1H)	128.2	5	6, 8
5	7.18 (dd, *J* = 4.7/7.8 Hz, 1H)	117.0	4, 6	6, 9
6	8.30 (dd, *J* = 1.54 Hz/4.7 Hz, 1H)	142.7	5	4, 5, 8
8	-	149.3		3, 4, 6, 10
9	-	119.9		3, 5
10	5.63 (s, 2H)	70.3		2, 8, 12
12	3.59 (t, *J* = 8.0 Hz, 2H)	65.6	13	10, 13
13	0.83 (t, *J* = 8.0 Hz, 2H)	17.3	12	12, 15
15	-0.11 (s, 9H)	-1.5		13, 15
16	-	130.1		3, 18
17	7.76 (d, *J* = 8.3 Hz, 2H)	128.6	18	17, 19
18	7.45 (d, *J* = 8.3 Hz, 2H)	126.2	17, 20	16, 18, 20
19	-	141.7		17, 20
20	4.79 (s, 2H)	63.9	18	18, 19
23	0.11 (s, 6H)	-5.3		23, 24
24	-	18.0		23, 25
25	0.93 (s, 9H)	25.8		24, 25

3.5.10 Compound 11

The structure of compound **11** with numbered positions is given in Figure 3.13. Assigned ^{1}H and ^{13}C NMR shifts are given in Table 3.15. HRMS gave *m/z* 519.2262 $[M+H]^{+}$]. With a calculated value of 519.2266, the molecular formula $C_{26}H_{40}N_2O_3Si_2Cl$ was confirmed. ^{1}H and ^{13}C NMR, MS and IR spectra for compound **11** can be found in Appendix K.

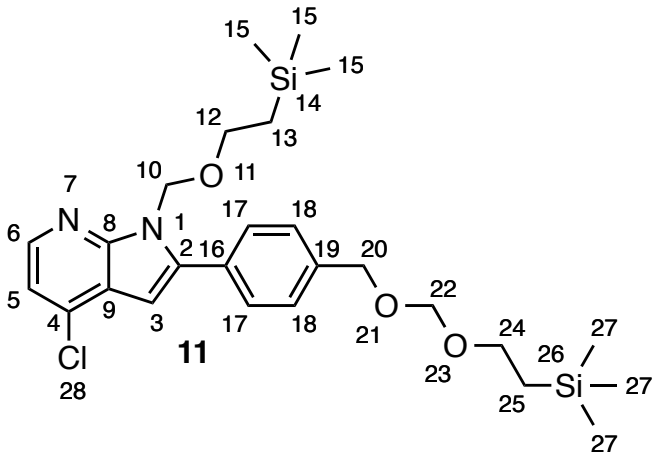

Figure 3.13: The structure of compound **11** with atom numbering.

Table 3.15: ^{1}H and ^{13}C NMR for compound **11** (DMSO-d_6, 400 MHz).

Position	^{1}H [ppm]	^{13}C [ppm]	COSY	HMBC
2	-	142.2		3, 10, 17
3	6.77 (s, 1H)	98.5		2, 4, 8, 9, 16
4	-	133.9		3, 5, 6
5	7.34 (d, *J* = 5.2 Hz, 1H)	117.0	6	3, 4, 6, 9
6	8.28 (d, *J* = 5.2 Hz, 1H)	143.6	5	4, 5, 8, 9
8	-	149.8		3, 6, 10
9	-	118.8		3, 5, 6
10	5.65 (s, 2H)	70.8		2, 8, 12
12	3.60 (t, *J* = 8.0 Hz, 2H)	65.9	13	10, 13
13	0.83 (t, *J* = 8.0 Hz, 2H)	17.3	12	12, 15
15	-0.11 (s, 9H)	-1.5		13, 15
16	-	129.9		3, 18
17	7.80 (d, *J* = 8.2 Hz, 2H)	128.9		2, 17, 19
18	7.48 (d, *J* = 8.2 Hz, 2H)	127.9	20	16, 18, 20
19	-	139.3		17, 20
20	4.62 (s, 2H)	68.2	18	18, 19, 22
22	4.73 (s, 2H)	93.9		20, 24
24	3.62 (t, *J* = 8.2 Hz, 2H)	64.4	25	22, 25
25	0.90 (t, *J* = 8.2 Hz, 2H)	17.6	24	24,27
27	0.01 (s, 9H)	-1.3		25, 27

3.5.11 Compound 12

The structure of compound **12** with numbered positions is given in Figure 3.14. Assigned ^{1}H and ^{13}C NMR shifts are given in Table 3.16. HRMS gave *m/z* 417.1398 $[M+H]^{+}$]. With a calculated value of 417.1401, the molecular formula $C_{21}H_{26}N_2O_3SiCl$ was confirmed. ^{1}H and ^{13}C NMR, MS and IR spectra for compound **12** can be found in Appendix L.

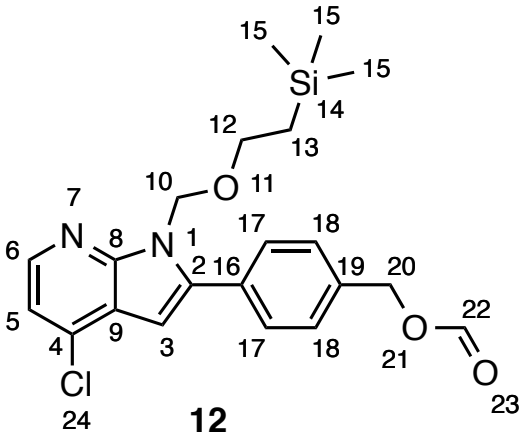

Figure 3.14: The structure of compound **12** with atom numbering.

Table 3.16: ^{1}H and ^{13}C NMR for compound **12** (DMSO-d_6, 400 MHz).

Position	^{1}H [ppm]	^{13}C [ppm]	COSY	HMBC
2	-	142.0		3, 10, 17
3	6.81 (s, 1H)	98.7		2, 4, 8, 10, 16
4	-	134.0		3, 5, 6
5	7.34 (d, *J* = 5.2 Hz, 1H)	117.0	6	4, 6, 9
6	8.28 (d, *J* = 5.2 Hz, 1H)	143.7	5	4, 5, 8, 9
8	-	149.9		3, 6, 10
9	-	118.8		5, 6
10	5.65 (s, 2H)	70.8		2, 8, 12
12	3.60 (t, *J* = 8.1 Hz, 2H)	65.9	13	10, 13
13	0.83 (t, *J* = 8.0 Hz, 2H)	17.3	12	12, 15
15	-0.11 (s, 9H)	-1.5		13, 15
16	-	130.7		3, 18
17	7.83 (d, *J* = 8.3 Hz, 2H)	129.0	18	2, 16, 18
18	7.55 (d, *J* = 8.3 Hz, 2H)	128.5	17	16, 18, 20
19	-	136.5		17, 20
20	5.26 (s, 2H)	64.4	22	18, 19, 22
22	8.37 (s, 1H)	162.0	20	20

3.5.12 Compound 13

The structure of compound **13** with numbered positions is given in Figure 3.15. Assigned ^{1}H and ^{13}C NMR shifts are given in Table 3.17. HRMS gave *m/z* 604.3390 $[M+H]^{+}$]. With a calculated value of 604.3391, the molecular formula $C_{34}H_{50}N_3O_3Si_2$ was confirmed. ^{1}H and ^{13}C NMR, MS and IR spectra for compound **13** can be found in Appendix M.

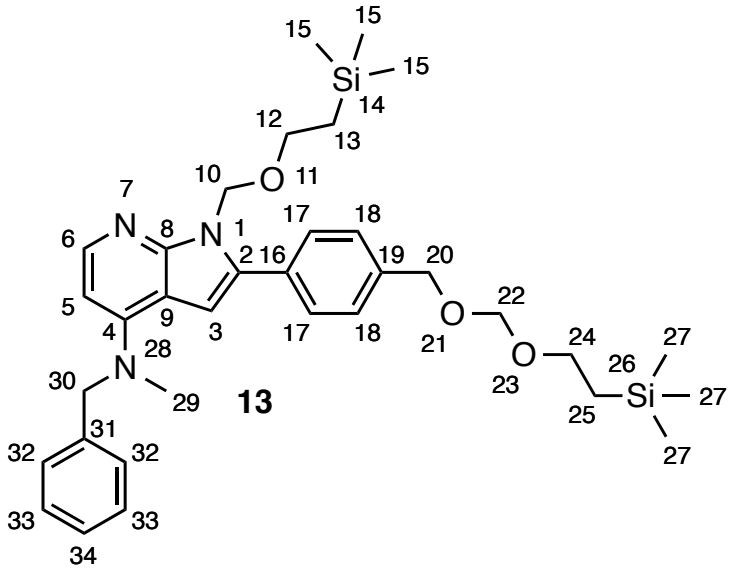

Figure 3.15: The structure of compound **13** with atom numbering.

Table 3.17: ^{1}H and ^{13}C NMR for compound **13** (DMSO-d_6, 400 MHz).

Position	^{1}H [ppm]	^{13}C [ppm]	COSY	HMBC
2	-	136.3		3, 10, 17
3	6.70 (s, 1H)	101.6		2, 8, 9, 16
4	-	149.4		30, 33
5	6.35 (d, *J* = 5.8 Hz, 1H)	100.5	6	3, 6, 9
6	7.91 (d, *J* = 5.7 Hz, 1H)	144.1	5	5, 8, 9, 31
8	-	151.1		3, 6, 10
9	-	107.3		3, 5, 6
10	5.55 (s, 2H)	70.4		2, 8, 12
12	3.62 (t, *J* = 3.9 Hz, 2H)	65.5	13	10, 13
13	0.84 (t, *J* = 7.9 Hz, 2H)	17.4	12	12, 15
15	-0.09 (s, 9H)	-1.4		13, 15
16	-	131.1		3, 18
17	7.66 (d, *J* = 8.2 Hz, 2H)	128.3	18	2, 17, 19
18	7.39 (d, *J* = 8.2 Hz, 2H)	127.8	17, 20	16, 18, 20
19	-	137.9		17, 20
20	4.57 (s, 2H)	68.2	20	18, 19, 22
22	4.71 (s, 2H)	93.8		20, 24
24	3.59 (t, *J* = 4.4 Hz, 2H)	64.4	25	22, 25
25	0.88 (t, *J* = 8.2 Hz, 2H)	17.5	24	24, 27
27	0.00 (s, 9H)	-1.3		25, 27
29	3.25 (s, 3H)	39.9[a]	30	5, 30, 31
30	4.86 (s, 2H)	56.1	29, 33	4, 29, 31, 32
31	-	138.4		6, 29, 30
32	7.27-7.24 (m, 3H)[b]	126.6	30, 33	30, 34
33	7.35-7.31 (m, 2H)	128.6	32, 34	31, 33
34	7.27-7.24 (m, 3H)[b]	126.9	33	32

[a]Overlapping with solvent signal

[b]Overlapping signals

3.5.13 Compound 14

The structure of compound **14** with numbered positions is given in Figure 3.16. Assigned ^{1}H and ^{13}C NMR shifts are given in Table 3.18. HRMS gave *m/z* 344.1757 $[M+H]^{+}$]. With a calculated value of 344.1763, the molecular formula $C_{22}H_{22}N_3O$ was confirmed. ^{1}H and ^{13}C NMR, MS and IR spectra for compound **14** can be found in Appendix N.

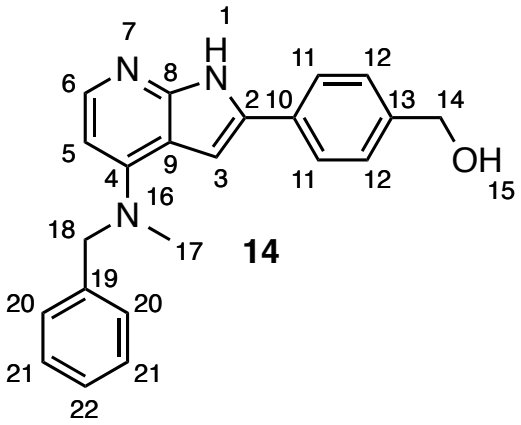

Figure 3.16: The structure of compound **14** with atom numbering.

Table 3.18: ^{1}H and ^{13}C NMR for compound **14** (DMSO-d_6, 600 MHz).

Position	^{1}H [ppm]	^{13}C [ppm]	COSY	HMBC
1	11.84 (s, 1H)	-		
2	-	133.5		3, 11
3	6.97 (s, 1H)	98.0		2, 8, 9, 10
4	-	149.6		17, 18
5	6.24 (d, *J* = 5.8 Hz, 1H)	99.5	6	3, 6, 9
6	7.83 (d, *J* = 5.8 Hz, 1H)	143.0[a]	5	5, 8, 9
8	-	150.5[a]		3, 6
9	-	108.6		3, 5, 6
10	-	130.3		3, 12
11	7.77 (d, *J* = 8.2 Hz, 2H)	124.4	12	2, 11, 12, 13
12	7.36-7.32 (m, 4H)[b]	126.8	11	10, 11, 14
13	-	141.5		11, 14, 15
14	4.50 (d, *J* = 5.7 Hz, 2H)	62.6	15	12, 13
15	5.17 (t, *J* = 5.7 Hz, 1H)	-	14	13, 14
17	3.27 (s, 3H)	40.1[c]		4, 18
18	4.87 (s, 2H)	56.1		4, 17, 19, 21
19	-	138.4		18, 20, 21, 22
20	7.28-7.25 (m, 3H)[d]	126.7	21	18, 19, 22
21	7.36-7.32 (m, 4H)[b]	128.6	20, 22	19, 21
22	7.28-7.25 (m, 3H)[d]	126.9	21	20

[a]Not visible in ^{13}C NMR spectrum

[b,d]Overlapping signals

[c]Overlapping with solvent signal

3.5.14 Compound 15

The structure of compound **15** with numbered positions is given in Figure 3.17. HRMS gave *m/z* 356.1759 $[M+H]^+$]. With a calculated value of 356.1763, the molecular formula $C_{23}H_{22}N_3O$ was confirmed. ^1H and ^{13}C NMR, MS and IR spectra for compound **15** can be found in Appendix O.

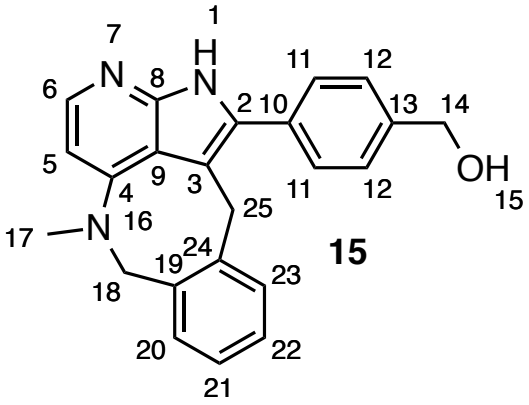

Figure 3.17: The suggested structure of compound **15** with atom numbering.

As compound **15** contained a rare eight-membered ring, the details of the structural elucidation of this structure will be presented in this section.

Firstly, the broad singlet with integral 1 at 11.65 ppm was assigned to the H-1 amine proton. A signal at 5.30 ppm with integral 1 showed no coupling in the HSQC spectrum, and was therefore assigned to the hydroxyl group H-15. This hydroxyl signal showed coupling in the COSY spectrum to a doublet at 4.61 ppm (J = 4.2 Hz, 2H) which was assigned to H-14, and the corresponding C-14 signal was found at 62.7 ppm. This benzylic CH_2-group showed ^1H-^{13}C long range coupling in the HMBC spectrum to a quaternary carbon at 142.0 ppm, which was assigned to C-13. Long range coupling was also seen between H-14 and a carbon signal at 126.6 ppm. This signal corresponded to the doublet signal with integral 2 at 7.50 ppm (J = 8.1 Hz), and was assigned to H-12. The COSY spectrum revealed coupling between H-12 and a multiplet signal with integral 3 at 7.60-7.56 ppm. This multiplet contained two doublet signals overlapping, and one of these doublets was assigned to H-11. The corresponding C-11 signal was found at 129.5 ppm. ^1H-^{13}C long range coupling was observed between H-12 and 131.0 ppm, a quaternary carbon which was assigned to C-10. A quaternary carbon signal at 131.6 ppm showed long range coupling to H-11, and was assigned to C-2.

A broad doublet at 7.81 ppm with integral 1 was assigned to H-6 because of the high chemical shift, and because the signal at H-6 was typically observed in this region. The corresponding C-6 signal was found from the HSQC spectrum at 142.1 ppm, though this signal was too weak to be observed in the ^{13}C NMR spectrum. Weak long range coupling was seen between H-6 and a carbon signal at 150.3 ppm, which was assigned to C-8. The H-6 peak showed ^1H-^1H coupling in the COSY spectrum to a doublet at 6.20 ppm (J = 5.8 Hz). This signal was in turn assigned to H-5, and the corresponding C-5 was found at 99.0

ppm. H-5 showed ^{1}H-^{13}C long range coupling to two carbon signals at 41.0 and 106.4 ppm. The signal at 106.4 ppm was assigned to C-9.

The HSQC spectrum revealed that the signal at 41.0 ppm corresponded to a proton signal overlapping with the water residue signal in the proton spectra, at 3.25 ppm. The chemical shifts of these signals indicated that they corresponded to the methyl group in position 17. Long range coupling was seen between H-17 and carbon signals at 149.7 and 54.0 ppm. The signal at 149.7 ppm was assigned to C-4, and the signal at 54.0 ppm was assigned to C-18. The HSQC spectrum showed that the singlet at 4.71 ppm with integral 2 belonged to H-18.

The C-9 signal showed long range coupling to a singlet at 4.16 ppm containing two protons. Such a peak in this region had not been observed in any of the spectra in this thesis. The corresponding carbon was found from the HSQC spectrum at 31.7 ppm. This peak showed coupling to several aromatic signals, as well as C-9, C-2 and 110.9. The signal at 110.9 ppm was assigned to C-3. In the other compounds identified this thesis, the 3-position had contained a proton signal between 6.7-7.0 ppm. In compound **15**, the C-3 signal appeared as a quaternary carbon. The mentioned signals at 4.16 ppm/31.7 ppm were therefore assumed to be connected in this position, and were assigned to position 25.

The CH_2-group at position 25 showed long range coupling to two quaternary carbons at 136.9 and 140.4 ppm, which also showed coupling to H-18. The CH_2-group was therefore clearly connected to the pyrrole-unit in position 3, and the amine benzyl group. The splitting and coupling pattern of the remaining signals in the aromatic region indicated that an *ortho*-substitution had taken place in the amine phenyl group. This confirmed the suspicion of an eight-membered-ring formation. A part of the HMBC spectrum is shown in Figure 3.18, depicting the long-range couplings observed for H-25.

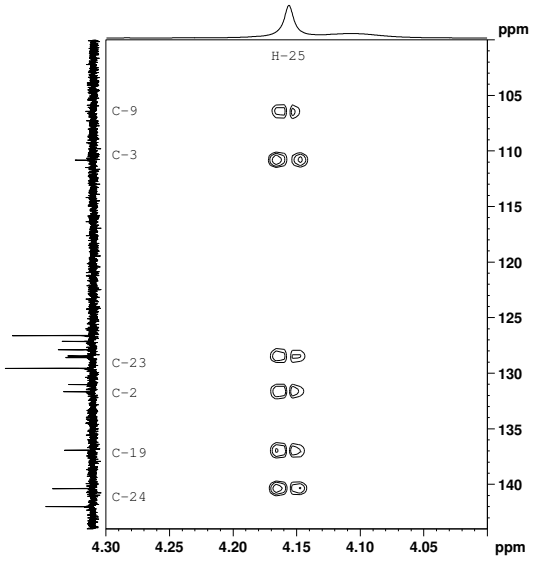

Figure 3.18: Part of the HMBC spectrum showing the ^{1}H-^{13}C long range couplings of the singlet at 4.16 ppm, assigned to position 25.

Remaining signals in the aromatic region were at this point two triplets at 7.24 ppm (J = 7.4 Hz) and 7.14 ppm (J = 7.3 Hz), one doublet at 7.00 ppm (J = 7.3 Hz), as well as the remaining doublet overlapping in the multiplet at 7.60-7.56 ppm (1H). Long range coupling was detected between C-18 and the multiplet at 7.60-7.56 ppm, which was assigned to H-20. The corresponding C-20 signal was found at 128.6 ppm. Long range coupling was also observed between C-25 and the doublet at 7.00 ppm, which was assigned to H-23. The corresponding carbon signal was found at 128.4 ppm. From ^{1}H-^{1}H couplings observed in the COSY spectrum, the signals at 7.24 ppm/127.1 ppm and 7.14 ppm/127.9 ppm were assigned to positions 21 and 22, respectively. Long range coupling between all *meta*-positions of the phenyl ring was observed in the HMBC spectrum. This observation provided the basis for assigning the signal at 140.4 ppm to C-24, and 136.9 ppm to C-19. A part of the HMBC spectrum showing long range couplings in the aromatic region is shown in Figure 3.19. A selection of significant couplings that helped identify the structure is shown in Figure 3.20.

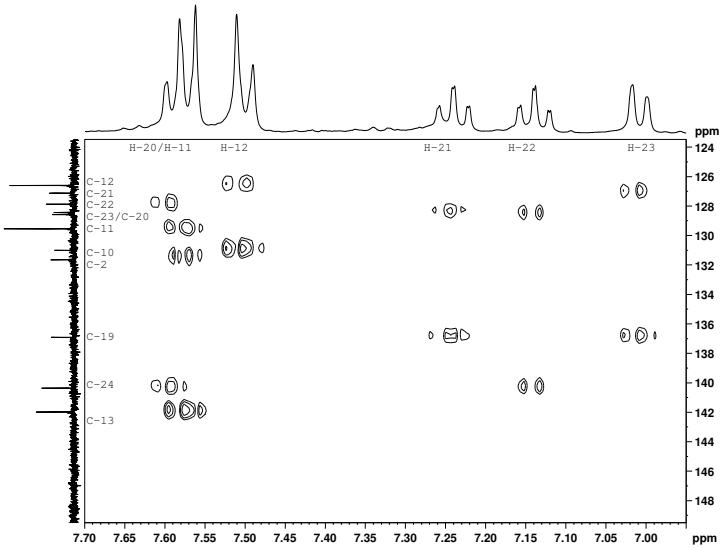

Figure 3.19: Part of the HMBC spectrum showing ^{1}H-^{13}C long range couplings of the aromatic region.

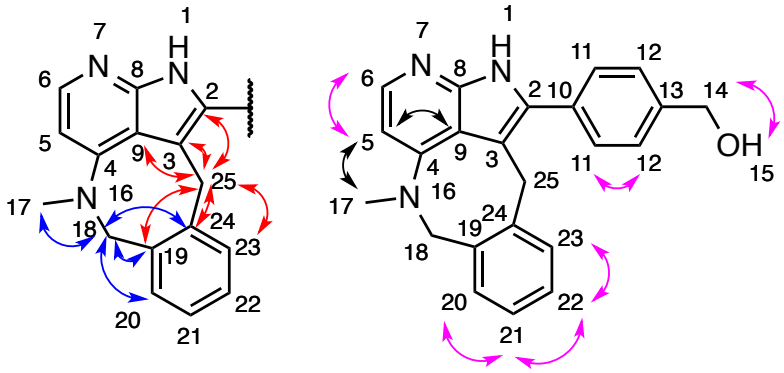

Figure 3.20: Left: The ^{1}H-^{13}C long range coupling observed in the HMBC spectra for H-18 (blue arrows) and H-25 (red arrows). Right: ^{1}H-^{1}H couplings observed in the COSY spectrum (pink arrows), and ^{1}H-^{13}C long range coupling of H-5 (black arrows).

All assigned ^{1}H and ^{13}C NMR shifts of compound **15** are given in Table 3.19.

Table 3.19: ^{1}H and ^{13}C NMR for compound **15** (DMSO-d_6, 400 MHz).

Position	^{1}H [ppm]	^{13}C [ppm]	COSY	HMBC
1	11.65 (s, 1H)	-		-
2	-	131.6		11, 25
3	-	110.8		25
4	-	149.7[a]		17, 18
5	6.20 (d, *J* = 5.8 Hz, 1H)	99.0	5	9, 17
6	7.81 (m, 1H)	142.1[a]	6	-
8	-	150.3[a]		-
9	-	106.4		5, 25
10	-	131.0		12
11	7.60-7.56 (m, 3H)[b]	129.5	12	2, 11, 13
12	7.50 (d, *J* = 8.1 Hz, 2H)	126.6	11, 14	10, 12, 14
13	-	142.0		11, 14
14	4.61 (d, *J* = 4.2 Hz, 2H)	62.7	12, 15	12, 13
15	5.30 (m, 1H)	-	14	-
17	3.25 (s, 3H)[c]	41.0		4, 5, 18
18	4.71 (s, 2H)	54.0		4, 17, 19, 20, 24
19	-	136.9		18, 21, 23, 25
20	7.60-7.56 (m, 3H)[b]	128.6	21	18, 22, 24
21	7.24 (t, *J* = 7.4 Hz, 1H)	127.1	20, 22	19, 23
22	7.14 (t, *J* = 7.3 Hz, 1H)	127.9	21, 23	20, 24
23	7.00 (d, *J* = 7.3 Hz, 1H)	128.4	22	19, 21, 25
24	-	140.4		18, 20, 22, 25
25	4.16 (s, 2H)	31.7		2, 3, 9, 19, 23, 24

[a]Not visible in ^{13}C NMR spectrum

[b]Overlapping signals

[c]Overlapping with water residue signal

3.5.15 Compound 16

The structure of compound **16** with numbered positions is given in Figure 3.21. Assigned ^{1}H and ^{13}C NMR shifts are given in Table 3.20. HRMS gave *m/z* 331.1446 $[M+H]^{+}$]. With a calculated value of 331.1447, the molecular formula $C_{21}H_{19}N_2O_2$ was confirmed. ^{1}H and ^{13}C NMR, MS and IR spectra for compound **16** can be found in Appendix P.

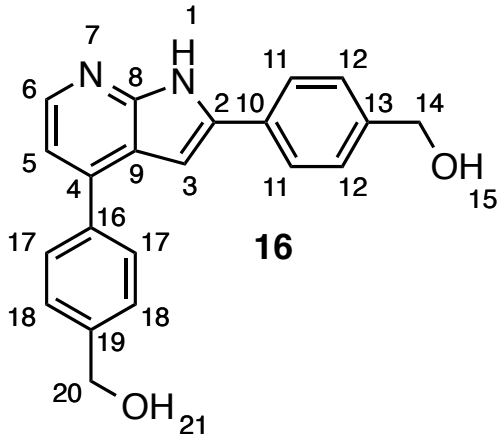

Figure 3.21: The structure of compound **16** with atom numbering.

Table 3.20: ^{1}H and ^{13}C NMR for compound **16** (DMSO-d_6, 400 MHz).

Position	^{1}H [ppm]	^{13}C [ppm]	COSY	HMBC
1	12.25 (s, 1H)	-	3	-
2	-	138.8		3, 11
3	7.09 (s, 1H)	96.1	1	2, 8, 9
4	-	139.7		6, 17
5	7.18 (d, *J* = 5.0 Hz, 1H)	114.7	6	6, 9, 16
6	8.26 (d, *J* = 5.0 Hz, 1H)	143.1	5	4, 5, 8
8	-	150.4		6
9	-	118.7		3, 5
10	-	129.9		12
11	7.94 (d, *J* = 8.3 Hz, 2H)	125.2	12	2, 11, 13
12	7.39 (d, *J* = 8.3 Hz, 2H)	126.9	11, 14	10, 12, 14
13	-	142.9		11, 14
14	4.54 (s, 1H)	62.60	12, 15	12, 13
15	5.25 (m, 1H)	-	14	-
16	-	136.7		5, 18
17	7.79 (d, *J* = 8.2 Hz, 2H)	128.0	18	3, 4, 19
18	7.52 (d, *J* = 8.2 Hz, 2H)	127.0	17, 20	16, 18, 20
19	-	142.6		17, 20
20	4.60 (s, 2H)	62.64	18, 21	18, 19
21	5.31 (m, 1H)	-	20	-

3.5.16 Compound 17

The structure of compound **17** with numbered positions is given in Figure 3.22. Assigned ^{1}H and ^{13}C NMR shifts are given in Table 3.21. HRMS gave *m/z* 331.1441 $[M+H]^{+}$]. With a calculated value of 331.1447, the molecular formula $C_{21}H_{19}N_2O_2$ was confirmed. ^{1}H and ^{13}C NMR, MS and IR spectra for compound **17** can be found in Appendix Q.

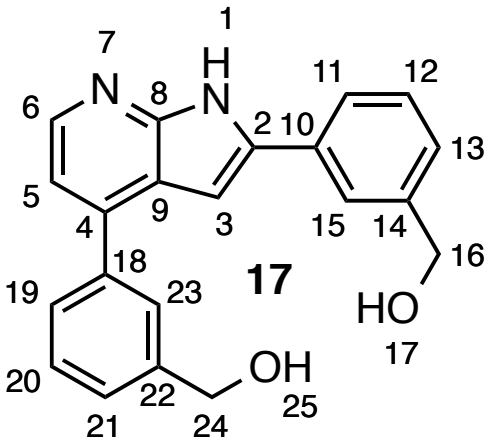

Figure 3.22: The structure of compound **17** with atom numbering.

Table 3.21: ^{1}H and ^{13}C NMR for compound **17** (DMSO-d_6, 400 MHz).

Position	^{1}H [ppm]	^{13}C [ppm]	COSY	HMBC
1	12.29 (s, 1H)	-	3	-
2	-	138.9		3, 11, 15
3	7.08 (s, 1H)	96.3	1	2, 8, 9
4	-	140.1		6, 19, 23
5	7.18 (d, *J* = 5.0 Hz, 1H)	114.7	6	6, 9 18
6	8.28 (d, *J* = 5.0 Hz, 1H)	143.19	5	4, 5, 8, 9
8	-	150.4		3, 6
9	-	118.6		3, 5, 6
10	-	131.2		12
11	7.85 (d, *J* = 7.8 Hz, 1H)	123.8	12, 13	2, 13, 15
12	7.44-7.41 (m, 2H)[a]	128.8	11	10, 11, 14, 16/24
13	7.32 (d, *J* = 7.6 Hz, 1H)	126.3	12	11, 16/24
14	-	143.24		12, 16, 17
15	7.92 (s, 1H)	123.6		2, 11, 13, 16/24
16	4.56 (d, *J* = 5.8 Hz, 1H)	62.9/62.8[b]	17	13, 14, 15
17	5.26 (t, *J* = 5.8 Hz, 1H)	-	16	14, 16/24
18	-	138.2		5, 20
19	7.69 (d, *J* = 7.8 Hz, 1H)	126.6	20	4, 21
20	7.54 (t, *J* = 7.6 Hz, 1H)	128.7	19	18, 22
21	7.44-7.41 (m, 2H)[a]	126.5	20	19, 22, 16/24
22	-	143.4		20, 21, 24, 25
23	7.77 (s, 1H)	126.2		4, 19, 16/24
24	4.64 (d, *J* = 5.8 Hz, 2H)	62.9/62.8[b]	25	21, 22
25	5.31 (t, *J* = 5.8 Hz, 1H)	-	24	22, 16/24

[a]Overlapping signals

[b]Might be interchanged

4. Conclusion

The aim of this thesis was to develop the synthetic strategies towards 2-aryl-4-aminopyrrolopyridines, and synthesize the target molecule **14** as seen in Scheme 4.1.

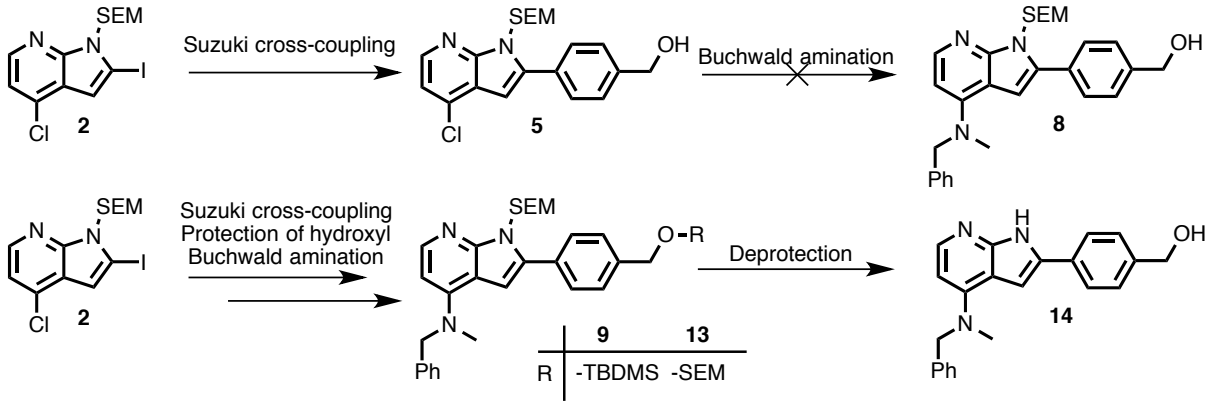

Scheme 4.1: Synthetic pathways leading to the target compound **14**.

The two initial synthetic steps were SEM-protection of the pyrrole nitrogen and iodination in 2-position, both reactions giving satisfactory yields and forming building block **2**. Although the iodination chemistry proceeded with excellent regioselectivity and conversion, work should be done on improving the work-up.

A selectivity study was performed for optimizing the chemoselective Suzuki cross-coupling of compound **2**, leading to compound **5**. Multiple catalysts and conditions were tested, and a selective mono-cross-coupling in 2-position was developed by the use of $Pd(PPh_3)_4$. This catalyst gave a longer reaction time, but offered a highly selective cross-coupling, with minimal formation of byproducts.

The Buchwald amination of compound **5** proved unsuccessful. Several catalyst systems and conditions were tested, yet no aminated product was observed. Other routes were therefore explored with the aim of achieving amination in 4-position. Compound **5** contained an acidic proton in the form of a hydroxyl group. This hydroxyl group was protected with TBDMS and SEM groups, both protection reactions giving moderate yields. The TBDMS group of substrate **6** proved unstable under the amination conditions, and was partly cleaved off during the course of reaction. This was avoided by the use of the more stable SEM group in substrate **11**, providing minimal amounts of byproducts and higher yields in the aminations. The Buchwald aminations with TBDMS-protected compound **6** gave at most an 89% yield of the aminated product, while the SEM-protected compound **11** proved most valuable as substrate with a 92% yield obtained. A significant observation was that the Buchwald aminations are very sensitive to water. The presence of water or impurity residues in either the solvent, substrate or glass equipment gave conversions below 35%, and 0-12% formation of the aminated product.

The most challenging step was the deprotection reactions of the aminated compounds **9** and **13**. Two methods were tested, where the best result was obtained using TFA and *sat. aq.* $NaHCO_3$. In these reactions, the target **14** was formed as the major product in deprotections of both compounds **9** and **13**. As expected, the TBDMS group of compound **9** proved easier to remove than the SEM groups. The best result was obtained in a larger scale deprotection of compound **9**, which gave a 74% yield of the target **14**. Low yields were obtained from many of the deprotection reactions, as scales were low and multiple byproducts were formed, making the purification process difficult. Poor separation and large losses were observed using silica gel column chromatography.

Overall, 15 new compounds have been synthesized in this master project. The main target **14** was synthesized with the most beneficial route giving an overall yield of 37%. Hopefully, evaluation of compound **14** as an inhibitor towards CSF1R might aid further structure-activity understanding of this kinase.

5. Future work

The work described in this master project has produced 15 new compounds, including one new potential CSF1R inhibitor. Many of the syntheses have been performed in good yields, yet there is room for improvement in several of the reactions and synthetic steps.

Problems were encountered with the workup in the iodination reaction producing the SEM-protected 4-chloro-2-iodo-7-azaindole building block, where the product was partially soluble in the water phase. Further optimizations of the workup and extraction procedures should be made.

A selectivity study of Suzuki cross-coupling reactions in C-2 position was performed, and while good yields were obtained for the $Pd(PPh_3)_4$ catalyst system, the reaction conditions can be optimized further. A minor amount of the dehalogenated byproduct was observed in these reactions. Slow addition of the substrate to the reaction mixture has been reported to mend this issue.[80]

The Buchwald amination in C-4 position proved successful when no acidic protons were present in the substrate. If acidic aryl groups are desired in the C-2 position, the reaction conditions should be carefully tested to allow for the presence of these groups. The introduction of protecting groups was a successful solution in this project. This strategy could be explored further with other protecting groups. An alternative could be the use of a benzoic ester, which may be reduced to the benzyl alcohol in the final step. Further insights into this reaction could be gained by testing other reaction conditions and catalysts. Bidentate ligands such as dppf and XantPhos have been reported to give good results in Buchwald aminations of pyrrolopyridines.[102, 106] A methodical investigation of the water sensitivity could also be beneficial. The introduction of the amine in C-4 prior to the aryl group in C-2 has been attempted previously in the research group, and is a possibility that could be explored further.

The deprotection reaction was the most challenging synthetic step. To further this investigation, optimizations can be made to the procedure with TFA and *sat aq.* $NaHCO_3$. A screening of other procedures could also be performed to find a better method of deprotecting the SEM-group on the pyrrole nitrogen. The use of $LiBF_4$ has given high yields in SEM deprotection reactions of pyrrolopyrimidines.[60] Luo *et al.* utilized TBAF in the SEM deprotections of indazoles in good yields.[56] Another solution would be to replace the SEM protecting group all together, if a suitable displacement group could be found that allows an easier and more selective deprotection. Using the methoxymethyl (MOM) protecting group with pyrrolopyridines has been reported with good results by several papers.[115-116] It is quite stable, yet can easily be removed with acid. The formation of formaldehyde and byproducts as is observed in the SEM deprotection, may be avoided when using the MOM group. Poor results from the deprotection reactions were also due to the suboptimal purification process. Recrystallization could be a good alternative.

Synthesizing key building blocks using other methods could also be beneficial. de Mattos *et al.* have reported a method for synthesizing various 2-aryl-7-azaindole structures.[41] Scheme 5.1 shows a suggested pathway to the 2-aryl-4-chloro-7-azaindole building block employing this method.

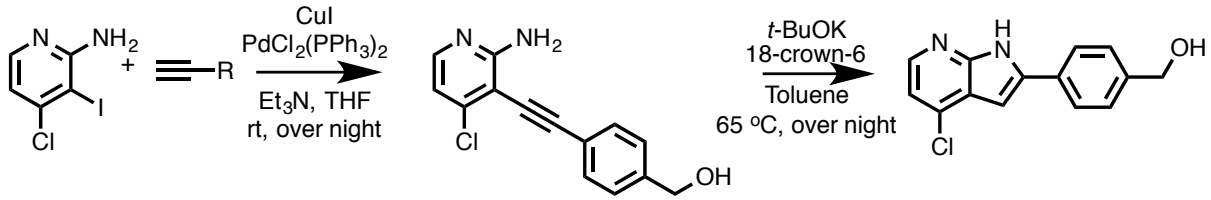

Scheme 5.1: A suggested synthesis route to a 4-chloro-2-aryl-7-azaindole building block, employing the method as reported by de Mattos *et al.*[41]

The introduction of various other aryl groups and amines in positions C-4 and C-2 can give further insight into the chemistry and CSF1R activity of the pyrrolopyridine scaffold.

6. Experimental

6.1 General information

All reagents and solvents used in the experiments were commercially available, and were used without further purification. All reagents were purchased from Sigma Aldrich, except for 4-chloro-7-azaindole, which was purchased from 1Click Chemistry. When reactions were conducted above room temperature (22 ^{o}C), an oil bath was used for heating. Ice and water were used for cooling to 0 ^{o}C, and dry ice and acetone were used for cooling to -78 ^{o}C. A Teflon coated magnetic stir bar was used in all reactions. Dry solvents were collected from a Braun MB SPS-800 Solvent Purification System, and filtered and deionized water was used. All reactions were monitored using thin layer chromatography (TLC, silica gel on aluminum plates, F_{254}, Merck). The plates were visualized using UV-light (wave length 254 nm and 365 nm). Column chromatography was performed using silica gel (40-63 mesh, 60 Å) as the stationary phase, and eluent systems are specified for each separation.

Spectroscopic analysis:

^{1}H NMR and ^{13}C NMR spectra were recorded on a Bruker Avance III HD instrument operating at 400 or 600 MHz for proton and 100 MHz or 150 MHz for carbon. Deuterated DMSO-d_6 was used as solvent. Chemical shifts are reported in δ (ppm), calibrated to the solvent signal in DMSO-d_6 (2.50 ppm in ^{1}H and 39.52 in ^{13}C). Coupling constants, *J*, are expressed in Hz. Signals are defined according to their multiplicity: s (singlet), d (doublet), dd (doublet of doublets), t (triplet), br is used when peak broadening is seen. Multiplets (m) are defined as an interval. Missing signals in the ^{13}C spectra are marked by *.

Accurate mass determination in positive and negative mode was performed on a "Synapt G2-S" Q-TOF instrument from Water™. Samples were ionized by the use of ASAP probe (APCI) or ESI probe. No chromatographic separation was used previous to the mass analysis. Calculated exact mass and spectra processing was done by Waters™ Software Masslynx V4.1 SCN871.

6.2 Synthesis of compound 1[109]

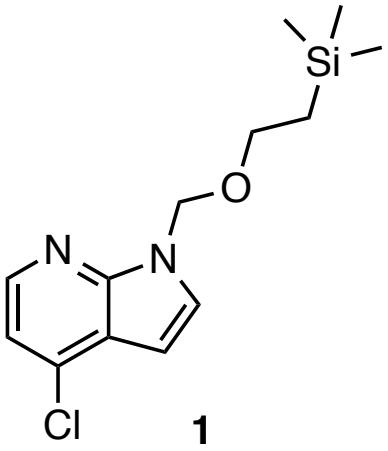

1

4-Chloro-1*H*-pyrrolo[2,3-*b*]pyridine (5.43 g, 35.6 mmol) was dissolved in dry DMF (47 mL). Then NaH (1.24 g, 51.8 mmol) was added to the reaction flask under an N_2 atmosphere at 0 °C. After stirring for 30 minutes at 0 °C, 2-(trimethylsilyl)ethoxymethyl chloride (7.1 mL, 40.7 mmol) was added dropwise over a period of 10 minutes. The reaction mixture was stirred at 0 °C for 3 hours and 45 minutes, before being allowed to warm to room temperature. The mixture then was quenched with sat. aq. NH_4Cl (100 mL) and extracted with EtOAc (3×100 mL). The combined organic phases were washed with brine (100 mL), dried over anhydrous Na_2SO_4, filtered and concentrated in vacuo. The product was purified by silica gel column chromatography (*n*-pentane:EtOAc, 96:4, R_f = 0.38) to give compound **1** as a light-yellow oil, 9.11 g (32.2 mmol, 90%).

Spectroscopic data for compound **1** (Appendix A):
^{1}H NMR (400 MHz, DMSO-d_6) δ: 8.25 (d, *J* = 5.2 Hz, 1H), 7.78 (d, *J* = 3.6 Hz, 1H), 7.28 (d, *J* = 5.2 Hz, 1H), 6.60 (d, *J* = 3.6 Hz, 1H), 5.64 (s, 2H), 3.51 (t, *J* = 7.9 Hz, 2H), 0.81 (t, *J* = 7.9 Hz, 2H), -0.11 (s, 9H). The reported shifts correspond well with previously reported data.[109]

6.3 Synthesis of compound 2[110]

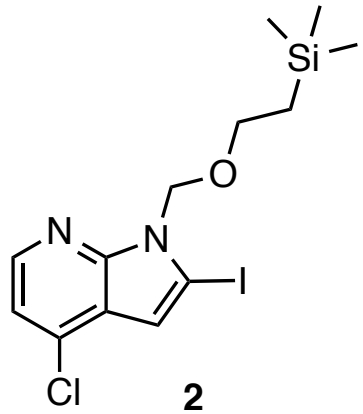

2

4-Chloro-1-((2-(trimethylsilyl)ethoxy)methyl)-1*H*-pyrrolo [2,3-*b*]pyridine (**1**) (7.87 g, 27.8 mmol) was dissolved in dry THF (120 mL) under an N_2 atmosphere before cooling to -78 °C. Lithium diisopropylamide (2M in THF/*n*-heptane/ethylbenzene) (20 mL, 40 mmol) was added dropwise over a period of 45 minutes using a syringe pump. The reaction mixture was stirred at -78 °C for 1 hour. I_2 (9.11 g, 35.9 mmol) was dissolved in dry THF (40 mL) and added to the reaction mixture dropwise over a period of 45 minutes using a syringe pump. The mixture was then stirred for 2 hours at -78 °C before being warmed to room temperature. The reaction was then quenched with sat. aq. NH_4Cl (2 mL). The solvent was removed in vacuo before addition of CH_2Cl_2 (200 mL) and water (200 mL). The two layers were separated and the aqueous phase was extracted with CH_2Cl_2 (6×50 mL). The combined organic phases were washed with brine (100 mL), dried over anhydrous Na_2SO_4, filtered and concentrated in vacuo. The crude product was dissolved in CH_2Cl_2 (100 mL), and added aq. $Na_2S_2O_3$ (10%, 50 mL). The water phase was extracted with CH_2Cl_2 (3×50 mL). The combined organic phases were dried over anhydrous Na_2SO_4, filtered and concentrated in vacuo. The

product was purified by silica gel column chromatography (*n*-pentane:EtOAc, 97.5:2.5, R_f = 0.37 to give compound **2** as a beige powder, 10.2 g (24.5 mmol, 69%); mp 47.5-48.5 °C

Spectroscopic data for compound **2** (Appendix B):
^{1}H NMR (400 MHz, DMSO-d_6) δ: 8.19 (d, *J* = 5.2 Hz, 1H), 7.27 (d, *J* = 5.2 Hz, 1H), 6.99 (s, 1 H), 5.63 (s, 1H), 3.52 (t, *J* = 8.0 Hz, 2H), 0.81 (t, *J* = 8.0 Hz, 2H), -0.12 (s, 9H); ^{13}C NMR (100 MHz, DMSO-d_6) δ: 149.4, 143.6, 132.9, 120.5, 116.9, 109.0, 89.8, 73.3, 65.8, 17.1, -1.3 (3C). IR (cm^{-1}, neat) ν: 3129 (w), 2950 (w), 2908 (w), 1589 (m), 1556 (s), 1455 (s), 1381 (s), 1365 (s), 1074 (s, br), 850 (s, br), 755 (s), 740 (s), 676 (m), 530 (m). HRMS (APCI/ASAP, *m/z)*: detected 409.0000 (calcd. $C_{13}H_{19}N_2OSiClI$, 409.0000, $[M+H]^+$). Spectrocopic data have not been reported in the literature.[110]

6.4 Synthesis of compound 3

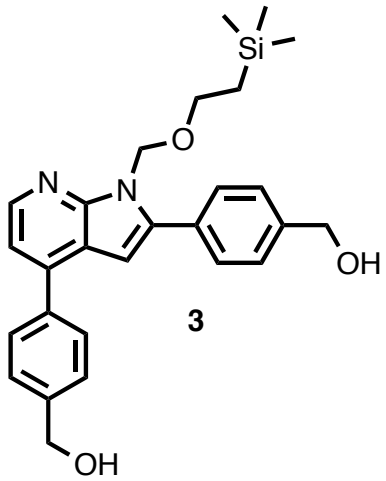

3

A mixture of 4-chloro-2-iodo-1-((2-(trimethylsilyl)-ethoxy)methyl)-1*H*-pyrrolo[2,3-*b*]pyridine (**2**) (277 mg, 0.678 mmol), (4-(hydroxymethyl)phenyl)boronic acid (227 mg, 1.50 mmol), XPhos (24.0 mg, 0.036 mmol), XPhos Pd G2 precatalyst (24 mg, 0.030 mmol) and K_2CO_3 (349 mg, 2.56 mmol) was added degassed 1,4- dioxane:water (1:1, 5 mL) under an N_2 atmosphere. The reaction mixture was stirred at 90 °C for 19 minutes before cooling to room temperature. The solvent was removed in vacuo. CH_2Cl_2 (50 mL) and water (50 mL) was added to the flask and the layers were separated. The water phase was extracted with CH_2Cl_2 (3×20 mL). The combined organic phases were washed with brine (20 mL), dried over anhydrous Na_2SO_4, filtered and concentrated in vacuo. The product was purified by silica gel column chromatography (CH_2Cl_2:MeOH, 95:5, R_f= 0.45) to give compound **3** as an off-white solid, 246 mg (0.534 mmol, 79%); mp 142.5-144 °C

Spectroscopic data for compound **3** (Appendix C):
^{1}H NMR (400 MHz, DMSO-d_6) δ: 8.36 (d, *J* = 5.0 Hz, 1H), 7.81-7.78 (m, 4H), 7.51 (d, *J* = 8.2 Hz, 2H), 7.46 (d, *J* = 8.2 Hz, 2H), 7.32 (d, *J* = 5.0 Hz, 1H), 6.86 (s, 1H), 5.68 (s, 2H), 5.29 (t, *J* = 5.7 Hz, 2H), 4.59 (t, *J* = 6.0 Hz, 4H), 3.67 (t, *J* = 8.1 Hz, 2H), 0.88 (t, *J* = 8.1 Hz, 2H), -0.07 (s, 9H); ^{13}C NMR (100 MHz, DMSO-d_6) δ: 150.1, 143.2, 143.1 (2C), 141.9, 140.3, 136.2, 129.8, 128.6 (2C), 128.1 (2C), 127.1 (2C), 126.7 (2C), 117.5, 115.7, 99.7, 70.5, 65.8, 62.6, 62.5, 17.4, -1.4 (3C). IR (cm^{-1}, neat) ν: 3404 (w, br), 2919 (w), 2858 (w), 1730 (w), 1585 (m), 1364 (m), 1245 (m), 1082 (s), 833 (s), 636 (m). HRMS (APCI/ASAP, *m/z*): detected 461.2259 (calcd. $C_{27}H_{33}N_2O_3Si$, 461.2260 $[M+H]^+$).

6.5 Synthesis of compound 4

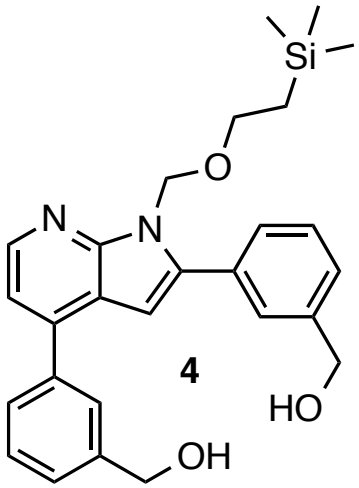

A mixture of 4-chloro-2-iodo-1-((2-(trimethylsilyl)-ethoxy)methyl)-1*H*-pyrrolo[2,3-*b*]pyridine (**2**) (252 mg, 0.617 mmol), (4-(hydroxymethyl)phenyl)boronic acid (211 mg, 1.39 mmol), XPhos (23.0 mg, 0.034 mmol), XPhos Pd G2 precatalyst (25.0 mg, 0.031 mmol) and K_2CO_3 (298 mg, 2.16 mmol) was added degassed 1,4-dioxane:water (1:1, 5 mL) under an N_2 atmosphere. The reaction mixture was stirred at 90 °C for 19 minutes before cooling to room temperature. The solvent was removed in vacuo. CH_2Cl_2 (50 mL) and water (50 mL) were added to the flask and the layers were separated. The water phase was extracted with CH_2Cl_2 (3×20 mL). The combined organic phases were washed with brine (20 mL), dried over anhydrous Na_2SO_4, filtered and concentrated in vacuo. The product was purified by silica gel column chromatography (CH_2Cl_2:MeOH, 97:3, R_f= 0.28) to give compound **4** as an off-white solid, 227 mg (0.493 mmol, 80%); mp 149-151 °C

Spectroscopic data for compound **4** (Appendix D):
^{1}H NMR (400 MHz, DMSO-d_6) δ: 8.39 (d, *J* = 4.9 Hz, 1H), 7.77 (s, 1H), 7.72 (s, 1H), 7.70-7.68 (m, 2H), 7.53 (t, *J* = 7.7 Hz, 1H), 7.48 (t, *J* = 7.5 Hz, 1H), 7.44-7.42 (m, 2H), 7.32 (d, *J* = 4.9 Hz, 1H), 6.86 (s, 1H), 5.69 (s, 2H), 5.30 (t, *J* = 5.9 Hz, 1H), 5.27 (t, *J* = 5.9 Hz, 1H), 4.62 (d, *J* = 5.9 Hz, 2H), 4.58 (d, *J* = 5.8 Hz, 2H), 3.63 (t, *J* = 8.2 Hz, 2H), 0.87 (t, *J* = 8.2 Hz, 2H), -0.08 (s, 9H); ^{13}C NMR (100 MHz, DMSO-d_6) δ: 150.0, 143.5, 143.3 (2C), 142.1, 140.7, 137.7, 131.2, 128.9, 128.5, 127.1, 126.9, 126.69, 126.67, 126.64, 126.2, 117.6, 115.8, 99.9, 70.5, 65.7, 62.8, 62.7, 17.4, -1.4 (3C). IR (cm^{-1}, neat) ν: 3284 (w, br), 3055 (w), 2871 (m), 1583 (m), 1399 (m), 1325 (m), 1246 (s), 1066 (s, br), 1018 (s, br), 831 (s), 764 (m), 701 (s). HRMS (APCI/ASAP, *m/z*): detected 461.2256 (calcd. $C_{27}H_{33}N_2O_3Si$, 461.2260 $[M+H]^+$).

6.6 Synthesis of compound 5

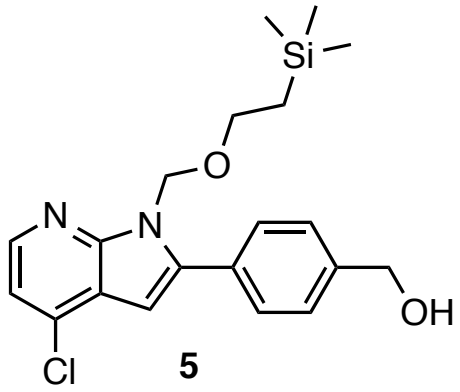

5

Multiple screening reactions were performed which led to compound **5**. A general procedure is described below. The amounts of reagents, solvents and products, and the specific reaction conditions, are listed for each conducted reaction.

General procedure:
A mixture of 4-chloro-2-iodo-1-((2-trimethylsilyl)-ethoxy)methyl)-1*H*-pyrrolo[2,3-*b*]pyridine (**2**), (4-(hydroxymethyl)phenyl)boronic acid, K_2CO_3, palladium source and ligand was added degassed 1,4-dioxane:water (1:1) under an N_2 atmosphere. The reaction mixture was stirred at an elevated temperature before being cooled to room temperature. The solvent was removed in vacuo.

*For reactions with <150 mg of compound **2**:* EtOAc (10 mL) and water (10 mL) were added to the flask and the layers were separated. The water phase was extracted with EtOAc (3×10 mL). The combined organic phases were washed with brine (10 mL).

*For reactions with >1 g of compound **2**:* EtOAc (100 mL) and water (100 mL) were added to the flask and the layers were separated. The water phase was extracted with EtOAc (3×75 mL). The combined organic phases were washed with brine (75 mL).

The combined organic phases were dried over anhydrous Na_2SO_4, filtered and concentrated in vacuo. After drying, the reaction gave a crude product of compound **5** as a yellow oil.

Spectroscopic data for compound **5** (Appendix E):
^{1}H NMR (400 MHz, DMSO-d_6) δ: 8.27 (d, *J* = 5.2 Hz, 1H), 7.77 (d, *J* = 8.3 Hz, 2H), 7.47 (d, *J* = 8.3 Hz, 2H), 7.33 (d, *J* = 5.2 Hz, 1H), 6.75 (s, 1H), 5.63 (s, 2H), 5.31 (t, *J* = 5.7 Hz, 1H), 4.58 (d, *J* = 5.7 Hz, 2H), 3.61 (t, *J* = 8.0 Hz, 2H), 0.84 (t, *J* = 8.0 Hz, 2H), -0.11 (s, 9H); ^{13}C NMR (100 MHz, DMSO-d_6) δ: 149.8, 143.6, 143.4, 142.5, 133.8, 129.2, 128.7 (2C), 126.7 (2C), 118.9, 116.9, 98.2, 70.8, 65.9, 62.5, 17.3, -1.4 (3C). IR (cm^{-1}, neat) ν: 3330 (w, br), 2950 (m), 2893 (m), 1558 (m), 1368 (m), 1286 (s), 1120 (s), 930 (s, br), 909 (m, br), 831 (s, br), 791 (s), 694 (s), 581 (m). HRMS (APCI/ASAP, *m/z*): detected 389.1445 (calcd. $C_{20}H_{26}N_2O_2SiCl$, 389.1452 $[M+H]^+$).

$Pd(PPh_3)_4$
Compound **2** (1.23 g, 3.02 mmol); (4-(hydroxymethyl)phenyl)boronic acid (539 mg, 3.55 mmol); $Pd(PPh_3)_4$ (180 mg, 0.156 mmol); K_2CO_3 (1560 mg, 11.3 mmol); 1,4-dioxane:water

(1:1, 50 mL). 80 °C; 9 hours; crude **5 (**1.47 g, 3.78 mmol, 125%). The product was purified by silica gel column chromatography (*n*-pentane:EtOAc, 80:20, R_f = 0.27) to give compound **5** as a light-yellow oil, 936 mg (2.50 mmol, 79%).

(dppf)$PdCl_2$

Compound **2** (48.4 mg, 0.118 mmol); (4-(hydroxymethyl)phenyl)boronic acid (20.3 mg, 0.134 mmol); (dppf)$PdCl_2$ (11.1 mg, 0.015 mmol); K_2CO_3 (70.7 mg, 0.512 mmol); 1,4-dioxane:water (1:1, 3 mL). 87 °C, 17 min; crude **5** (49.0 mg, 0.126 mmol, 107%). The product was purified by silica gel column chromatography (*n*-pentane:EtOAc, 75:25, R_f =0.52) to give compound **5** as a clear oil, 14.7 mg (0.054 mmol, 46%).

$Pd_2(dba)_3$

Compound **2** (104 mg, 0.253 mmol); (4-(hydroxymethyl)phenyl)boronic acid (51.4 mg, 0.338 mmol); $Pd_2(dba)_3$ (7.2 mg, 0.008 mmol); K_2CO_3 (125 mg, 0.904 mmol); 1,4-dioxane:water (1:1, 2.6 mL). 100 °C, 1 h 45 min; crude **5** (90.5 mg, 0.233 mmol, 92%).

Compound **2** (100 mg, 0.244 mmol); (4-(hydroxymethyl)phenyl)boronic acid (52.0 mg, 0.340 mmol); $Pd_2(dba)_3$ (8.1 mg, 0.009 mmol); K_2CO_3 (151 mg, 1.09 mmol); 1,4-dioxane:water (1:1, 2.6 mL). 80 °C, 1 h 45 min; crude **5** (86.0 mg, 0.221 mmol, 90%).

Compound **2** (53.1 mg, 0.130 mmol); (4-(hydroxymethyl)phenyl)boronic acid (29.3 mg, 0.193 mmol); $Pd_2(dba)_3$ (4.5 mg, 0.005 mmol); K_2CO_3 (75.3 mg, 0.545 mmol); 1,4-dioxane:water (1:1, 2.6 mL). 60 °C, 2 h 27 min; crude **5 (**41.6 mg, 0.107 mmol, 82%).

XPhos/XPhos Pd G2 precatalyst

Compound **2** (55.5 mg, 0.136 mmol); (4-(hydroxymethyl)phenyl)boronic acid (24.3 mg, 0.160 mmol); XPhos (7.6 mg, 0.016 mmol); XPhos Pd G2 precatalyst (7.4 mg, 0.009 mmol); K_2CO_3 (75.8 mg, 0.548 mmol); 1,4-dioxane:water (1:1, 2.6 mL). 60 °C, 2 h 27 min; crude **5** (46.6 mg, 0.120 mmol, 87%).

$Pd(OAc)_2$

Compound **2** (52.4 mg, 0.128 mmol); (4-(hydroxymethyl)phenyl)boronic acid (24.7 mg, 0.163 mmol); $Pd(OAc)_2$ (3.2 mg, 0.014 mmol); K_2CO_3 (75.7 mg, 0.548 mmol); 1,4-dioxane:water (1:1, 3 mL). 100 °C, 2 h 45 min; crude **5** (21.7 mg, 0.056 mmol, 43%).

PEPPSI™-SIPr precatalyst

Compound **2** (50.1 mg, 0.123 mmol); (4-(hydroxymethyl)phenyl)boronic acid (22.1 mg, 0.145 mmol); PEPPSI™-SIPr precatalyst (13.3 mg, 0.019 mmol); K_2CO_3 (76.0 mg, 0.550 mmol); 1,4-dioxane:water (1:1, 3 mL). 87 °C, 17 min; crude **5** (44.6 mg, 0.115 mmol, 93%).

6.7 Synthesis of compound 6

6.7.1 Synthesis of compound 6 by Suzuki cross-coupling

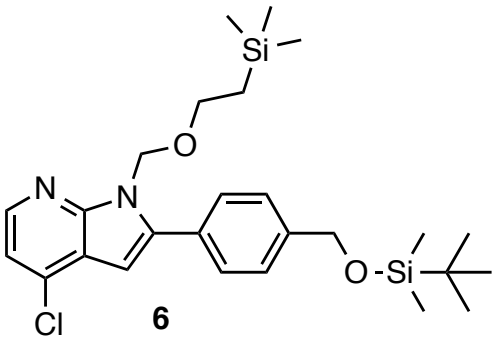

6

A mixture of 4-chloro-2-iodo-1-((2-trimethylsilyl)-ethoxy)methyl)-1*H*-pyrrolo[2,3-b]pyridine (**2**) (901 mg, 2.2 mmol), (4-(((*tert*-butyldimethyl silyl)oxy) methyl)phenyl)boronic acid (644 mg, 2.42 mmol), $Pd(PPh_3)_4$ (127 mg, 0.110 mmol), and K_2CO_3 (1110 mg, 8.03 mmol) was added degassed 1,4-dioxane:water (1:1, 70 mL) under an N_2 atmosphere. The mixture was stirred at 85 °C for 2 hours before being cooled to room temperature. The solvent was removed in vacuo. CH_2Cl_2 (100 ml) and water (100 mL) were added to the flask and the layers were separated. The water phase was extracted with CH_2Cl_2 (3×50 mL). The combined organic phases were washed with brine (75 mL), dried over anhydrous Na_2SO_4, filtered and concentrated in vacuo. After drying, the reaction gave a crude material as a yellow oil, 1.43 mg (2.85 mmol, 130%). The product was purified by silica gel column chromatography (*n*-pentane:EtOAc, 97:3, R_f =0.11) to give compound **6** as a white powder, 991 mg (1.97 mmol, 90%); mp 48.5-50 °C

Spectroscopic data for compound **6** (Appendix F):
^{1}H NMR (400 MHz, DMSO-d_6) δ: 8.27 (d, *J* = 5.2 Hz, 1H), 7.79 (d, *J* = 8.3 Hz, 2H), 7.46 (d, *J* = 8.3 Hz, 2H), 7.33 (d, *J* = 5.2 Hz, 1H), 6.76 (s, 1H), 5.64 (s, 2H), 4.80 (s, 2H), 3.59 (t, *J* = 8.0 Hz, 2H), 0.93 (s, 9H), 0.82 (t, *J* = 8.0 Hz, 2H), 0.11 (s, 6H), -0.11 (s, 9H); ^{13}C NMR (100 MHz, DMSO-d_6) δ: 149.8, 143.5, 142.4, 142.2, 133.9, 129.4, 128.8 (2C), 126.3 (2C), 118.9, 117.0, 98.3, 70.8, 65.9, 63.9, 25.8 (3C), 18.0, 17.3, -1.5 (3C), -5.3 (2C). IR (cm^{-1}, neat) ν: 2951 (m), 2926 (m), 2883 (w), 2853 (w), 1554 (m), 1471 (m), 1458 (m), 1375 (m), 1249 (s), 1074 (s), 918 (m), 829 (s, br), 767 (s, br), 584 (m). HRMS (APCI/ASAP, *m/z*): detected 503.2315 (calcd. $C_{26}H_{40}N_2O_2Si_2Cl$, 503.2317 $[M+H]^+$).

6.7.2 Synthesis of compound 6 by TBDMS protection

(4-(4-Chloro-1-((2-(trimethylsilyl)ethoxy)methyl)-1*H*-pyrrolo[2,3-*b*]pyridin-2-yl)phenyl)methanol (**5**) (914 mg, 2.35 mmol) was dissolved in dry DMF (40 mL). NaH (128 mg, 5.34 mmol) was then added to the reaction flask under an N_2 atmosphere at 0 °C, and the mixture was stirred for 20 minutes. *tert*-Butyldimethylsilyl chloride (593 mg, 3.93 mmol) was dissolved in dry THF (10 mL), and was added to reaction mixture dropwise over a period of 10 minutes. The reaction mixture was stirred at 0 °C for 4 hours, before stirring at 50 °C for 10 minutes. The solvent was removed in vacuo. The mixture was added $(NH_4)_2SO_4$ (50 mL, 30% in water) and EtOAc (50 mL), and the layers were separated. The water phase was extracted with EtOAc (3×50 mL). The combined organic phases were washed with brine (50 mL), dried over anhydrous Na_2SO_4, filtered and concentrated in vacuo. The product was purified by silica gel column chromatography (*n*-pentane:EtOAc, 97:3, R_f = 0.11) to give compound **6** as a white powder, 888 mg (1.77 mmol, 75%); mp 48.5-50 °C

6.8 Synthesis of compound 7

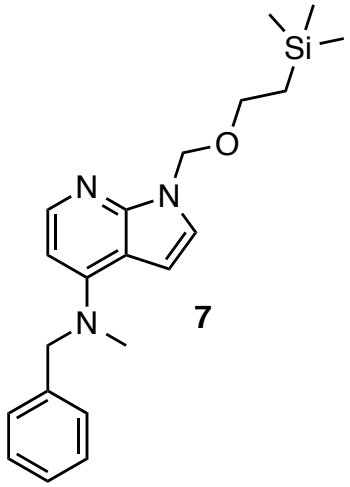

7

A mixture of 4-chloro-1-((2-(trimethylsilyl)ethoxy)methyl)-1*H*-pyrrolo[2,3-*b*]pyridine (**1**) (81.0 mg, 0.286 mmol), *N*-methyl-1-phenylmethylamine (0.2 mL, 1.55 mmol), NaO*t*-Bu (95.4 mg, 0.990 mmol), RuPhos (7.5 mg, 0.016 mmol) and $Pd(OAc)_2$ (7.0 mg, 0.031 mmol) was added degassed *t*-BuOH (4 mL), under an N_2 atmosphere. The reaction mixture was stirred at 85 °C for 20 minutes before allowing to cool to room temperature. The solvent was removed in vacuo. CH_2Cl_2 (15 mL) and water (15 mL) were added to the flask and the layers were separated. The water phase was adjusted to pH 7 with *sat. aq*. NH_4Cl, and extracted with CH_2Cl_2 (3×15 mL). The combined organic phases were washed with brine (15 mL), dried over anhydrous Na_2SO_4, filtered and concentrated in vacuo. After drying, the reaction gave a crude product of compound **7** as a dark green oil 111 mg, (0.302 mmol, 105%). The product was purified by silica gel column chromatography (*n*-pentane:EtOAc, 7:3, R_f =0.47) to give compound **7** as a light-yellow oil, 71.0 mg (0.193 mmol, 68%).

Spectroscopic data for compound **7** (Appendix G):
^{1}H NMR (400 MHz, DMSO-d_6) δ: 7.88 (d, *J* = 5.7 Hz, 1H), 7.34-7.31 (m, 2H), 7.26-7.23 (m, 4H), 6.49 (d, *J* = 3.8 Hz, 1H), 6.28 (d, *J* = 5.7 Hz, 1H), 5.52 (s, 2H), 4.81 (s, 2H), 3.49 (t, *J* = 8.1 Hz, 2H), 3.19 (s, 3H), 0.81 (t, *J* = 8.1 Hz, 2H), -0.09 (s, 9H); ^{13}C NMR (100 MHz, DMSO-d_6) δ: 149.7, 149.4, 143.9, 138.4, 128.5 (2C), 126.9, 126.5 (2C), 124.3, 107.3, 101.1, 99.8, 72.3, 65.1, 56.1, 39.6, 17.2, -1.4 (3C). IR (cm^{-1}, neat) ν: 2950 (w), 2893 (w, br), 1703 (w), 1574 (s), 1503 (m), 1373 (m), 1246 (s), 1072 (s, br), 832 (s), 696 (s). HRMS (APCI/ASAP, *m/z*): detected 368.2157 (calcd. $C_{21}H_{30}N_3OSi$, 368.2158 $[M+H]^+$).

6.9 Isolation of compound 8

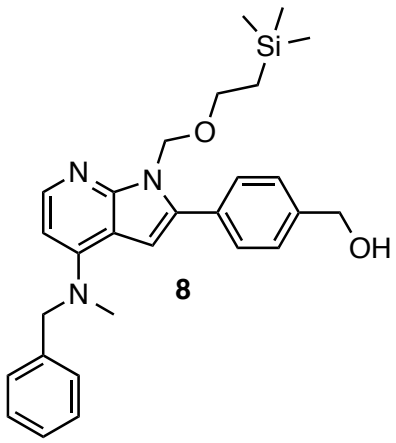

Compound **8** was isolated as a minor product of the reaction described in Section 6.10. Purification by silica gel column chromatography (*n*-pentane:EtOAc, 9:1, R_f = 0.01) gave compound **8** as a brown wax, 45 mg (0.095 mmol, 6%)

Spectroscopic data for compound **8** (Appendix H):
^{1}H NMR (400 MHz, DMSO-d_6) δ: 7.91 (d, *J* = 5.7 Hz, 1H), 7.64 (d, *J* = 8.2 Hz, 2H), 7.39 (d, *J* = 8.2 Hz, 2H), 7.35-7.31 (m, 2H), 7.27-7.24 (m, 3H), 6.68 (s, 1H), 6.34 (d, *J* = 5.7 Hz, 1H), 5.55 (s, 2H), 5.24 (t, *J* = 5.7 Hz, 1H), 4.85 (s, 2H), 4.54 (d, *J* = 5.7 Hz, 2H), 3.63 (t, *J* = 8.2 Hz, 2H), 3.25 (s, 3H), 0.85 (t, *J* = 8.2 Hz, 2H), -0.08 (s, 9H); ^{13}C NMR (100 MHz, DMSO-d_6) δ: 151.1, 149.4, 143.9, 142.3, 138.4, 136.6, 130.3, 128.6 (2C), 128.2 (2C), 126.9, 126.6 (2C), 126.5 (2C), 107.4, 101.3, 100.5, 70.4, 65.5, 62.6, 56.1, 39.8, 17.4, -1.4 (3C); IR (cm^{-1}, neat) ν: 3400 (w, br), 2927 (w), 2853 (w), 1737 (w), 1578 (s), 1496 (m), 1354 (m), 1245 (s, sh), 1205 (m), 1064 (s, br), 832 (s, sh), 695 (s); HRMS (APCI/ASAP, *m/z*): detected 474.2571 (calcd. $C_{28}H_{36}N_3O_2Si$, 474.2577 $[M+H]^+$).

6.10 Synthesis of compound 9

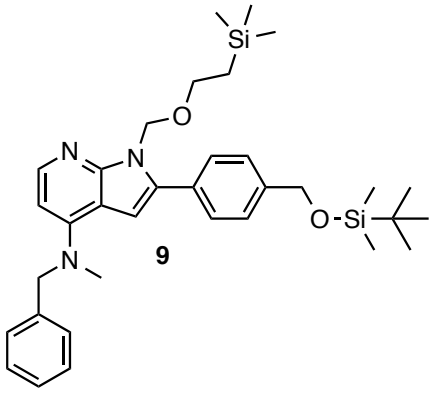

A mixture of 2-(4-(((*tert*-butyldimethylsilyl)oxy) methyl)phenyl)-4-chloro-1-((2-(trimethylsilyl)ethoxy) methyl)1*H*-pyrrolo[2,3-*b*]pyridine (**6**) (816 mg, 1.62 mmol), N-methyl-1-phenylmethylamine (1.5 mL, 11.6 mmol), NaO*t*-Bu (470 mg, 4.89 mmol), RuPhos (51 mg, 0.109 mmol) and $Pd(OAc)_2$ (24 mg, 0.107 mmol) was added degassed *t*-BuOH (28 mL), under an N_2 atmosphere. The reaction mixture was stirred at 85 °C for 30 minutes before being allowed to cool to room temperature. The pH was adjusted to 6 with $(NH_4)_2SO_4$ (30% in H_2O). The solvent was removed in vacuo. CH_2Cl_2 (50 mL) and water (50 mL) were added to the flask and the layers were separated. The water phase was extracted with CH_2Cl_2 (3×50 mL). The combined organic phases were washed with brine (50 mL), dried over anhydrous Na_2SO_4, filtered and concentrated in vacuo. After drying, the reaction gave the crude material as a dark yellow oil 1.47 gr (2.50 mmol, 154%). The product was purified by silica gel column chromatography (*n*-pentane:EtOAc, 9:1, R_f = 0.27) to give compound **9** as a light-yellow oil, 847 mg (1.44 mmol, 89%).

Spectroscopic data for compound **9** (Appendix I):
^{1}H NMR (400 MHz, DMSO-d_6) δ: 7.91 (d, J = 5.8 Hz, 1H), 7.65 (d, J = 8.3 Hz, 2H), 7.39-35 (m, 2H), 7.33-31 (m, 2H), 7.27-7.24 (m, 3H), 6.69 (s, 1H), 6.33 (d, J = 5.8 Hz, 1H), 5.55 (s, 2H), 4.85 (s, 2H), 4.75 (s, 2H), 3.60 (t, J = 8.1 Hz, 2H), 3.25 (s, 3H), 0.92 (s, 9H), 0.83 (t, J = 8.0 Hz, 2H), 0.09 (s, 6H), -0.09 (s, 9H); ^{13}C NMR (100 MHz, DMSO-d_6) δ: 151.1, 149.4, 144.0, 140.9, 138.4, 136.4, 130.6, 128.6 (2C), 128.3 (2C), 126.9, 126.6 (2C), 126.1 (2C), 107.4, 101.5, 100.5, 70.4, 65.5, 63.9, 56.1, 39.9 25.8 (3C), 18.0, 17.4, -1.4 (3C), -5.3 (2C). IR (cm^{-1}, neat) ν: 2951 (m), 2928 (m), 2887 (w), 2855 (w), 1702 (w), 1577 (m), 1496 (m), 1248 (m), 1072 (s, br), 831 (s, br), 774 (s, br), 694 (m). HRMS (APCI/ASAP, *m/z*): detected 588.3446 (calcd. $C_{34}H_{50}N_3O_2Si_2$, 588.3442 $[M+H]^+$).

6.11 Isolation of compound 10

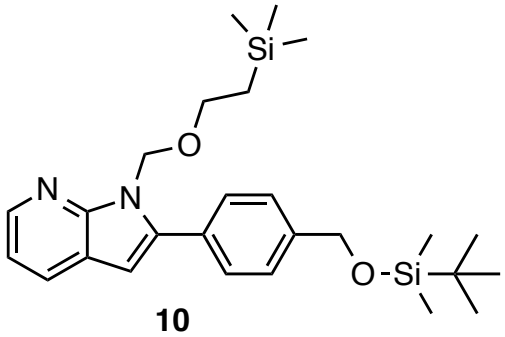

10

Compound **10** was isolated as a minor product of the reaction described in Section 6.10. Purification by silica gel column chromatography (*n*-pentane:EtOAc, 9:1, R_f = 0.51) gave compound **10** as a yellow oil, 29 mg (0.062 mmol, 4%)

Spectroscopic data for compound **10** (Appendix J):
^{1}H NMR (400 MHz, DMSO-d_6) δ: 8.30 (dd, J = 1.54 Hz/4.7 Hz, 1H), 8.00 (dd, J = 1.54 Hz/7.8 Hz, 1H), 7.76 (d, J = 8.3 Hz, 2H), 7.45 (d, J = 8.3 Hz, 2H), 7.18 (dd, J = 4.7/7.8 Hz, 1H), 6.70 (s, 1H), 5.63 (s, 2H), 4.79 (s, 2H), 3.59 (t, J = 8.0 Hz, 2H), 0.93 (s, 9H), 0.83 (t, J = 8.0 Hz, 2H), 0.11 (s, 6H), -0.11 (s, 9H); ^{13}C NMR (100 MHz, DMSO-d_6) δ: 149.3, 142.7, 141.6, 141.3, 130.1, 128.6 (2C), 128.2, 126.2 (2C), 119.9, 117.0, 100.5, 70.3, 65.6, 63.9, 25.8 (3C), 18.0, 17.3, -1.5 (3C), -5.3 (2C); IR (cm^{-1}, neat) ν: 2951 (m), 2627 (m), 2893 (w), 2855 (m), 1725 (w), 1593 (w), 1500 (w), 1429 (w), 1248 (s), 1076 (s, br), 835 (s, br), 775 (s, sh); HRMS (APCI/ASAP, *m/z*): detected 469.2704 (calcd. $C_{26}H_{41}N_2O_2Si_2$, 469.2707 $[M+H]^+$).

6.12 Synthesis of compound 11

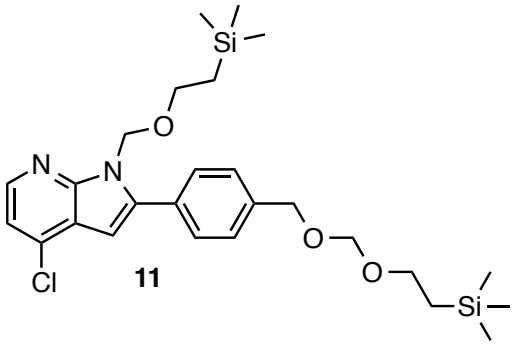

11

(4-(4-Chloro-1-((2-(trimethylsilyl)ethoxy) methyl)-1*H*-pyrrolo[2,3-*b*]pyridin-2-yl)phenyl) methanol (**5**) (1.05 g, 2.70 mmol) was dissolved in dry DMF (11 mL). NaH (114 mg, 4.75 mmol) was added to the reaction flask under an N_2 atmosphere at 0 °C. After stirring for 30 minutes at 0 °C, 2-(trimethylsilyl)ethoxymethyl chloride (0.7 mL, 3.96 mmol) was added dropwise over a period of 10 minutes. The reaction mixture was stirred at 0 °C for 4 hours and 45 minutes,

before being allowed to warm to room temperature. The mixture was quenched with sat. aq. NH_4Cl (100 mL) and extracted with EtOAc (3×100 mL). The combined organic phases were washed with brine (100 mL), dried over anhydrous Na_2SO_4, filtered and concentrated in vacuo. The product was purified by silica gel column chromatography (*n*-pentane:EtOAc, 96:4, R_f = 0.19) to give compound **11** as a clear oil, 717 mg (1.38 mmol, 51%).

Spectroscopic data for compound **11** (Appendix K):
^{1}H NMR (400 MHz, DMSO-d_6) δ: 8.28 (d, *J* = 5.2 Hz, 1H), 7.80 (d, *J* = 8.2 Hz, 2H), 7.48 (d, *J* = 8.2 Hz, 2H), 7.34 (d, *J* = 5.2 Hz, 1H), 6.77 (s, 1H), 5.65 (s, 2H), 4.73 (s, 2H), 4.62 (s, 2H), 3.62 (t, *J* = 8.2 Hz, 2H), 3.60 (t, *J* = 8.0 Hz, 2H), 0.90 (t, *J* = 8.2 Hz, 2H), 0.83 (t, *J* = 8.0 Hz, 2H), 0.01 (s, 9H), -0.11 (s, 9H); ^{13}C NMR (100 MHz, DMSO-d_6) δ: 149.8, 143.6, 142.2, 139.3, 133.9, 129.9, 128.9 (2C), 127.9 (2C), 118.8, 117.0, 98.5, 93.9, 70.8, 68.2, 65.9, 64.4, 17.6, 17.3, -1.3 (3C), -1.5 (3C) IR (cm^{-1}, neat) ν: 2951 (w), 2892 (w, br), 1557 (w), 1369 (m), 1248 (s), 1157 (m), 1055 (s, br), 1023 (s, br), 910 (m), 855 (s), 830 (s), 756 (m), 585 (w). HRMS (APCI/ASAP, *m/z*): detected 519.2262 (calcd. $C_{26}H_{40}N_2O_3Si_2Cl$, 519.2266 $[M+H]^+$).

6.13 Isolation of compound 12

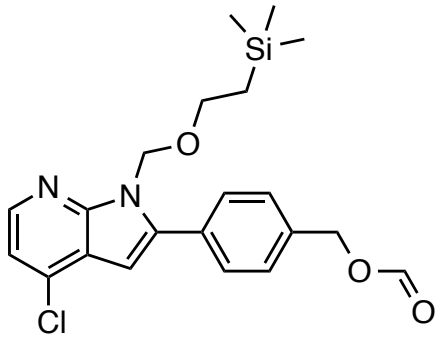

12

Compound **12** was isolated as a minor product of the reaction described in Section 6.12. Purification by silica gel column chromatography (*n*-pentane:EtOAc, 96:4, R_f = 0.13) gave compound **12** as a clear oil, 25 mg (0.060 mmol, 2%)

Spectroscopic data for compound **12** (Appendix L):
^{1}H NMR (400 MHz, DMSO-d_6) δ: 8.37 (s, 1H), 8.28 (d, *J* = 5.2 Hz, 1H), 7.83 (d, *J* = 8.3 Hz, 2H), 7.55 (d, *J* = 8.3 Hz, 2H), 7.34 (d, *J* = 5.2 Hz, 1H), 6.81 (s, 1H), 5.65 (s, 2H), 5.26 (s, 2H), 3.60 (t, *J* = 8.1 Hz, 2H), 0.83 (t, *J* = 8.0 Hz, 2H), -0.11 (s, 9H); ^{13}C NMR (100 MHz, DMSO-d_6) δ: 162.0, 149.9, 143.7, 142.0, 136.5, 134.0, 130.7, 129.0 (2C), 128.5 (2C), 118.8, 117.0, 98.7, 70.8, 65.9, 64.4, 17.3, -1.5 (3C). IR (cm^{-1}, neat) ν: 2950 (w), 2983 (w, br), 1724 (s, sh), 1557 (m), 1368 (m), 1248 (m), 1156 (s, br), 1075 (s, br), 856 (s), 833 (s). HRMS (APCI/ASAP, *m/z*): detected 417.1398 (calcd. $C_{21}H_{26}N_2O_3SiCl$, 417.1401 $[M+H]^+$).

6.14 Synthesis of compound 13

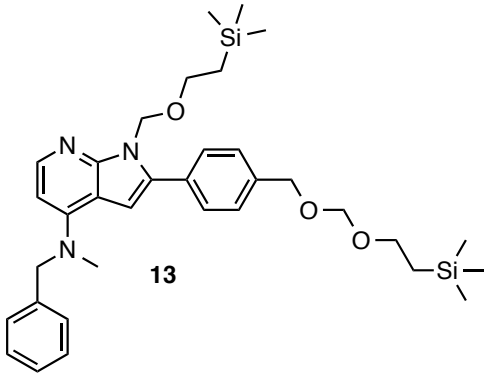

A mixture of 4-chloro-2-(4-(((2-(trimethylsilyl) ethoxy)methoxy)methyl)phenyl)-1-((2-(trimethyl-silyl)ethoxy)methyl)-1*H*-pyrrolo[2,3-*b*]pyridine (**11**) (111 mg, 0.213 mmol), *N*-methyl-1-phenylmethylamine (0.2 mL, 1.55 mmol), NaO*t*-Bu (71 mg, 0.739 mmol), RuPhos (6 mg, 0.013 mmol) and $Pd(OAc)_2$ (4 mg, 0.018 mmol) was added degassed *t*-BuOH (3 mL), under an N_2 atmosphere. The reaction mixture was stirred at 85 °C for 5 hours before being cooled to room temperature. The solvent was removed in vacuo. CH_2Cl_2 (15 mL) and water (15 mL) were added to the flask and the layers were separated. The water phase was then adjusted to pH 7 with *sat. aq*. NH_4Cl, and extracted with CH_2Cl_2 (3×15 mL). The combined organic phases were washed with brine (15 mL), dried over anhydrous Na_2SO_4, filtered and concentrated in vacuo. After drying, the reaction gave a crude material of compound **13** as a dark green oil, 200 mg (0.331 mmol, 155%). The product was purified by silica gel column chromatography (*n*-pentane:EtOAc, 9:1, R_f = 0.19) to give compound **13** as an off-white oil, 118 mg (0.196 mmol, 92%).

Spectroscopic data for compound **13** (Appendix M):
^{1}H NMR (400 MHz, DMSO-d_6) δ: 7.91 (d, *J* = 5.7 Hz, 1H), 7.66 (d, *J* = 8.2 Hz, 2H), 7.39 (d, *J* = 8.2 Hz, 2H), 7.35-7.31 (m, 2H), 7.27-7.24 (m, 3H), 6.70 (s, 1H), 6.35 (d, *J* = 5.8 Hz, 1H), 5.55 (s, 2H), 4.86 (s, 2H), 4.70 (s, 2H), 4.57 (s, 2H), 3.62 (t, *J* = 3.9 Hz, 2H), 3.59 (t, *J* = 4.4 Hz, 2H), 3.25 (s, 3H), 0.88 (t, *J* = 8.2 Hz, 2H), 0.84 (t, *J* = 7.9 Hz, 2H), 0.00 (s, 9H), -0.09 (s, 9H); ^{13}C NMR (100 MHz, DMSO-d_6) δ: 151.1, 149.4, 144.1, 138.4, 137.9, 136.3, 131.1, 128.6 (2C), 128.3 (2C), 127.8 (2C), 126.9, 126.6 (2C), 107.3, 101.6, 100.5, 93.8, 70.4, 68.2, 65.5, 64.4, 56.1, 39.9, 17.5, 17.4, -1.3 (3C), -1.4 (3C); IR (cm^{-1}, neat) ν: 2950 (w), 2883 (w, br), 1576 (s), 1495 (m), 1452 (m), 1245 (m), 1100 (s, br), 832 (s, br), 693 (m). HRMS (APCI/ASAP, *m/z*): detected 604.3390 (calcd. $C_{34}H_{50}N_3O_3Si_2$, 604.3391 $[M+H]^+$).

6.15 Synthesis of compound 14

6.15.1 Synthesis of compound 14 by deprotection of compound 9

6.15.1.1 Deprotection of compound 9 by BF_3-OEt_2

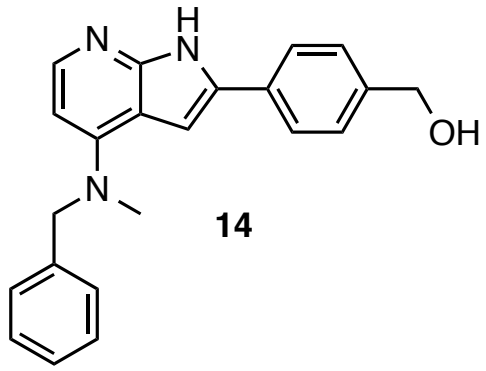

N-benzyl-2-(4-(((*tert*-butyldimethylsilyl)oxy) methyl)phenyl)-*N*-methyl-1-((2-(trimethylsilyl) ethoxy)methyl)-1*H*-pyrrolo[2,3-*b*]pyridin-4-amine (**9**) (119 mg, 0.202 mmol) was dissolved in dry acetonitrile (3 mL) and stirred at 0 °C for 5 minutes under an N_2 atmosphere. Boron trifluoride diethyl etherate (0.15 mL, 1.22 mmol) was then added dropwise over the course of 5 minutes. The mixture was stirred at room temperature for 1 hour and 25 minutes. The reaction flask was lowered into an icebath holding 0 °C, and water (2 mL) was then added dropwise over a period of 5 minutes. The mixture was then stirred at room temperature for 35 minutes, before NH_3 (6 mL, 12.5% in water, 40.1 mmol) was added. The reaction mixture was stirred at room temperature for 36 hours. The solvent was removed in vacuo, and the crude product was obtained as a yellow powder (205 mg, 0.597 mmol). The product was purified by silica gel column chromatography (CH_2Cl_2:MeOH, 94:6, R_f= 0.10) to give compound **14** as an off white solid, 15.1 mg, (0.044 mmol, 22%); mp 199-200.5 °C

Spectroscopic data for compound **14** (Appendix N):
^{1}H NMR (600 MHz, DMSO-d_6) δ: 11.84 (s, 1H), 7.83 (d, *J* = 5.8 Hz, 1H), 7.77 (d, *J* = 8.2 Hz, 2H), 7.36-7.32 (m, 4H), 7.28-7.25 (m, 3H), 6.97 (s, 1H), 6.24 (d, *J* = 5.8 Hz, 1H), 5.17 (t, *J* = 5.7 Hz, 1H), 4.87 (s, 2H), 4.50 (d, *J* = 5.7 Hz, 2H), 3.27 (s, 3H); ^{13}C NMR (150 MHz, DMSO-d_6) δ: 150.5*, 149.6, 143.0*, 141.5, 138.4, 133.5, 130.3, 128.6 (2C), 126.9, 126.8 (2C), 126.7 (2C), 124.4 (2C), 108.6, 99.5, 98.0, 62.6, 56.1, 40.1; IR (cm^{-1}, neat) ν: 3204 (m, br), 3063 (m, br), 3023 (m, br), 2919 (m), 2852 (m), 1574 (s), 1518 (s), 1499 (m), 1371 (m), 1294 (m), 1199 (s), 1027 (s), 1013 (s), 1013 (s, sh), 767 (s, br), 723 (s, sh), 695 (s, sh). HRMS (APCI/ASAP, *m/z*): detected 344.1757 (calcd. $C_{22}H_{22}N_3O$, 344.1763 $[M+H]^+$).

6.15.1.2 Deprotection of compound 9 by TFA

N-benzyl-2-(4-(((*tert*-butyldimethylsilyl)oxy)methyl)phenyl)-*N*-methyl-1-((2-(trimethylsilyl)ethoxy)methyl)-1*H*-pyrrolo[2,3-*b*]pyridin-4-amine (**9**) (430 mg, 0.731 mmol) was dissolved in dry CH_2Cl_2 (30 mL) and 2,2,2-trifluoroacetic acid (5 mL, 65.3 mmol) was added dropwise over a period of 5 minutes under an N_2 atmosphere. The reaction mixture was stirred at room temperature for 4 hours and 30 minutes. The solvent was removed in vacuo. The mixture was dissolved in THF (30 mL) and added $NaHCO_3$ (*sat. aq.*, 40 mL) dropwise over the course of 10 minutes. The reaction mixture was then stirred at room temperature for 19 hours and 30 minutes, before the solvent was removed in vacuo. The product mixture was added CH_2Cl_2:MeOH (2:1, 75 mL) and stirred at room temperature for 1 hour and 30 minutes, before filtration. The solvent was

removed in vacuo to give the crude product as a light-yellow powder. The product **14** was purified by silica gel column chromatography (CH_2Cl_2:MeOH, 9:1, R_f= 0.15) to give compound **14** as an off-white powder, 186 mg, (0.542 mmol, 74%); mp 200.8 °C

6.15.2 Synthesis of compound 14 by deprotection of compound 13

6.15.2.1 Deprotection of compound 13 by BF_3-OEt_2

N-benzyl-*N*-methyl-2-(4-(((2-(trimethylsilyl)ethoxy)methoxy)methyl)phenyl)-1-((2-(trimethylsilyl)ethoxy)methyl)-1*H*-pyrrolo[2,3-*b*]pyridin-4-amine (**13**) (158 mg, 0.262 mmol) was dissolved in dry acetonitrile (6 mL) and stirred at 0 °C for 10 minutes under an N_2 atmosphere. Boron trifluoride diethyl etherate (0.1 mL, 0.810 mmol) was added dropwise over a period of 10 minutes. The mixture was stirred at 0 °C for 5 minutes and then at room temperature for 2 hours and 20 minutes. The reaction flask was lowered into an icebath holding 0 °C and water (4 mL) was added dropwise over a period of 5 minutes. The mixture was stirred at room temperature for 1 hour and 30 minutes. NH_3 (10 mL, 12.5% in water, 66.8 mmol) was added dropwise over the course of 5 minutes and the mixture was stirred at room temperature for 20 hours. After filtration, the crude product of compound **14** was obtained as a yellow powder (0.154 mmol, 59%). The product was purified by silica gel column chromatography (CH_2Cl_2:MeOH:NH_3(25% in water), 95:5:0-90:9:1, R_f= 0.09 (90:10:0)) to give compound **14** as a beige oil, 3 mg (0.009 mmol, 3%)

6.15.2.2 Deprotection of compound 13 by TFA

N-benzyl-*N*-methyl-2-(4-(((2-(trimethylsilyl)ethoxy)methoxy)methyl)phenyl)-1-((2-(trimethylsilyl)ethoxy)methyl)-1*H*-pyrrolo[2,3-*b*]pyridin-4-amine (**13**) (182 mg, 0.301 mmol) was dissolved in dry CH_2Cl_2 (40 mL) and added 2,2,2-trifluoroacetic acid (2 mL, 26.2 mmol) under an N_2 atmosphere. The reaction mixture was stirred at 50 °C for 2 hours, before it was cooled to room temperature and the solvent was removed in vacuo. The mixture was dissolved in THF (20 mL), before $NaHCO_3$ (*sat. aq.*, 20 mL), was added dropwise over the course of 10 minutes. The mixture was then stirred at room temperature for 22 hours. The solvent was removed in vacuo, and the mixture was dissolved in CH_2Cl_2 (40 mL) and MeOH (20 mL) and stirred at room temperature for 1 hour and 30 minutes. The reaction mixture was then filtered, and solvent was removed in vacuo. The mixture was dissolved in MeOH (10 mL) before NH_3 (12.5% in water, 20 mL, 133.6 mmol) was added dropwise over a period of 10 minutes. The mixture was stirred at room temperature for 22 hours. The solvent was removed in vacuo, and the crude product was obtained as a yellow powder, 218 mg (0.636 mmol, 211%). The product was purified using silica gel column chromatography (CH_2Cl_2, 9:1, R_f = 0.21) and gave compound **14** as a white powder, 13 mg (0.038 mmol, 13%); mp 199-200.5 °C

6.16 Isolation of compound 15

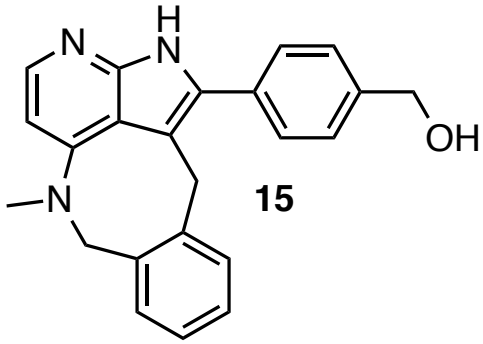

Compound **15** was isolated as a minor product of the reaction described in Section 6.15.2.2. Purification by silica gel column chromatography (CH_2Cl_2, 9:1, R_f = 0.08) gave compound **15** as a white solid, 12 mg (0.034 mmol, 11%).

Spectroscopic data for compound **15** (Appendix O):
^{1}H NMR (600 MHz, DMSO-d_6) δ: 11.65 (s, 1H), 7.81 (m, 1H), 7.60-7.56 (m, 3H), 7.50 (d, *J* = 8.1 Hz, 2H), 7.24 (t, *J* = 7.4 Hz, 1H), 7.14 (t, *J* = 7.3 Hz, 1H), 7.00 (d, *J* = 7.3 Hz, 1H), 6.20 (d, *J* = 5.8 Hz, 1H), 5.30 (m, 1H), 4.71 (s, 2H), 4.61 (d, *J* = 4.2 Hz, 2H), 4.16 (s, 2H), 3.25 (s, 3H); ^{13}C NMR (100 MHz, DMSO-d_6) δ: 150.3*, 149.7*, 142.1*, 142.0, 140.4, 136.9, 131.6, 131.0, 129.5 (2C), 128.6, 128.4, 127.9, 127.1, 126.6 (2C), 110.8, 106.4, 99.0, 62.7, 54.0, 41.0, 31.7; IR (cm^{-1}, neat) ν: 3606 (w), 3460 (w, br), 3102 (w), 3024 (w), 3000 (w), 2947 (w), 2842 (m), 1596 (s), 1557 (s), 1540 (s), 1518 (s), 1460 (m), 1376 (m), 1342 (m), 1206 (m), 1097 (m), 1043 (s, br), 1015 (m), 917 (s, sh), 783 (s, sh), 756 (s, sh), 467 (m, br); HRMS (APCI/ASAP, *m/z*): detected 356.1759 (calcd. $C_{23}H_{22}N_3O$, 356.1763 $[M+H]^+$).

6.17 Synthesis of compound 16

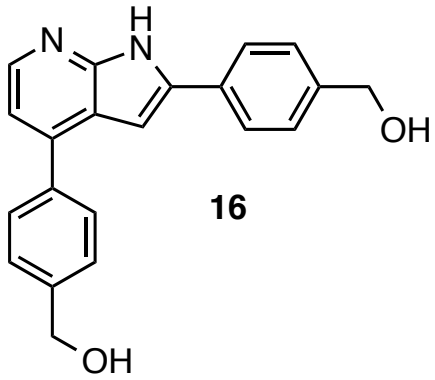

((1-((2-(Trimethylsilyl)ethoxy)methyl)-1pyrrolo[2,3-*b*]pyridine-2,4-diyl)bis(4,1-phenylene))dimethanol(**3**) (150 mg, 0.325 mmol) was added dry acetonitrile (4 mL) and stirred at 0 °C for 15 minutes under an N_2 atmosphere. Boron trifluoride diethyl etherate (0.15 mL, 1.22 mmol) was added dropwise over a period of 5 minutes. The mixture was stirred at room temperature for 2 hours and 40 minutes. The reaction flask was lowered into an icebath holding 0 °C. Water (2 mL) was then added dropwise over the course of 5 minutes, before the mixture was stirred at room temperture for 30 minutes. Then NH_3 (6 mL, 12.5% in water, 40.1 mmol) was added and the reaction was stirred at room temperature for 19 hours. The solvent was removed in vacuo, and the crude product was obtained as a yellow powder. The product was purified by silica gel column chromatography (CH_2Cl_2:MeOH, 90:10, R_f =0.24) to give compound **16** as a light yellow powder, 35 mg (0.105 mmol, 32%, purity 91% by HPLC); mp 230-233 °C (decomposition)

Spectroscopic data for compound **16** (Appendix P):
^{1}H NMR (400 MHz, DMSO-d_6) δ: 12.25 (s, 1H), 8.26 (d, *J* = 5.0 Hz, 1H), 7.94 (d, *J* = 8.3 Hz, 2H), 7.79 (d, *J* = 8.2 Hz, 2H), 7.52 (d, *J* = 8.2 Hz, 2H), 7.39 (d, *J* = 8.3 Hz, 2H), 7.18 (d, *J* = 5.0 Hz, 1H), 7.09 (s, 1H), 5.31 (m, 1H), 5.25 (m, 1H), 4.60 (s, 2H), 4.54 (s, 1H); ^{13}C NMR (100

MHz, DMSO-d_6) δ: 150.4, 143.1, 142.9, 142.6, 139.7, 138.8, 136.7, 129.9, 128.0 (2C), 127.0 (2C), 126.9 (2C), 125.2 (2C), 118.7, 114.7, 96.1, 62.64, 62.60. IR (cm^{-1}, neat) ν: 3206 (m, br), 3133 (m, br), 2918 (m), 2850 (m), 1599 (m), 1439 (m), 1207 (m), 1034 (s, br), 1015 (s), 813 (s, sh), 793 (s, sh), 578 (w). HRMS (APCI/ASAP, *m/z*): detected 331.1446 (calcd. $C_{21}H_{19}N_2O_2$, 331.1447 $[M+H]^+$).

6.18 Synthesis of compound 17

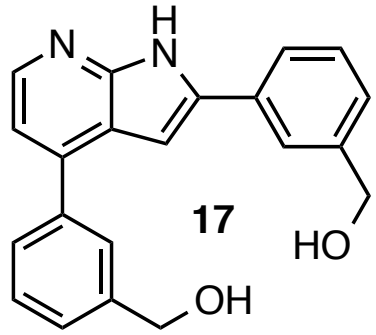

((1-((2-(Trimethylsilyl)ethoxy)methyl)-1*H*-pyrrolo[2,3-*b*]pyridine-2,4-diyl)bis(3,1-phenylene))dimethanol (**4**) (148 mg, 0.320 mmol) was added 2 mL dry acetonitrile and stirred at 0 °C for 15 minutes under an N_2 atmosphere. Boron trifluoride diethyl etherate (0.15 mL, 1.22 mmol) was added dropwise over a period of 5 minutes. The mixture was stirred at room temperature for 2 hours and 40 minutes. The reaction flask was lowered into an icebath holding 0 °C. Water (2 mL) was added dropwise over the course of 5 minutes, before the mixture was stirred at room temperture for 30 minutes. NH_3 (6 mL, 12.5% in water, 40.1 mmol) was added and the reaction was stirred at room temperature for 19 hours. The solvent was removed in vacuo, and the crude product was obtained as a yellow powder. The product was purified by silica gel column chromatography (CH_2Cl_2:MeOH, 93:7, R_f =0.43) to give compound **17** as a yellow powder, 34.3 mg (0.104 mmol, 32%, purity 97% by HPLC); mp 172.0-175.0 °C (decomposition)

Spectroscopic data for compound **17** (Appendix Q):
^{1}H NMR (400 MHz, DMSO-d_6) δ: 12.29 (s, 1H), 8.28 (d, *J* = 5.0 Hz, 1H), 7.92 (s, 1H), 7.85 (d, *J* = 7.8 Hz, 1H), 7.77 (s, 1H), 7.69 (d, *J* = 7.8 Hz, 1H), 7.54 (t, *J* = 7.6 Hz, 1H), 7.44-7.41 (m, 2H), 7.32 (d, *J* = 7.6 Hz, 1H), 7.18 (d, *J* = 5.0 Hz, 1H), 7.08 (s, 1H), 5.31 (t, *J* = 5.8 Hz, 1H), 5.26 (t, *J* = 5.8 Hz, 1H), 4.64 (d, *J* = 5.8 Hz, 2H), 4.56 (d, *J* = 5.8 Hz, 1H); ^{13}C NMR (100 MHz, DMSO-d_6) δ: 150.4, 143.4, 143.24, 143.19, 140.1, 138.9, 138.2, 131.2, 128.8, 128.7, 126.6, 126.5, 126.3, 126.2, 123.8, 123.6, 118.6, 114.7, 96.3, 62.9, 62.8. IR (cm^{-1}, neat) ν: 3127 (m, br), 3094 (m, br), 3062 (m, br), 2919 (m), 2851 (m), 1599 (m), 1477 (m), 1449 (m), 1326 (m), 1252 (m), 1051 (s), 1017 (s, br), 786 (s), 775 (s), 700 (s), 688 (s). HRMS (APCI/ASAP, *m/z*): detected 331.1441 (calcd. $C_{21}H_{19}N_2O_2$, 331.1447 $[M+H]^+$).

7. Literature

1. Popat, K.; McQueen, K.; Feeley, T. W., *Pract. Res. Clin. Anaesthesiol.* **2013,** *27* (4), 399-408.
2. Avendano, C.; Menendez, J. C., *Medicinal Chemistry of Anticancer Drugs* **2015**, Elsevier, 391–402.
3. Ruetten, H.; Thiemermann, C., *Br. J. Pharmacol.* **1997,** *122*, 59-70.
4. Roskoski, R., *Pharmacol. Res.* **2016,** *103*, 26-48.
5. Cohen, P., *Nat. Rev. Drug. Discov.* **2002,** *1*, 309.
6. Hume, D. A.; MacDonald, K. P., *Blood* **2011,** *119* (8), 1810-1820.
7. El-Gamal, M. I.; Anbar, H. S.; Yoo, K. H.; Oh, C. H., *Med. Res. Rev.* **2012,** *33* (3), 599-636.
8. Xu, J.; Escamilla, J.; Mok, S.; David, J.; Priceman, S.; West, B.; Bollag, G.; McBride, W.; Wu, L., *Cancer Res.* **2013,** *73* (9), 2782-2794.
9. Sluijter, M.; van der Sluis, T. C.; van der Velden, P. A.; Versluis, M.; West, B. L.; van der Burg, S. H.; van Hall, T., *PLoS One* **2014,** *9* (8), e104230.
10. Kaspersen, S. J.; Han, J.; Nørsett, K. G.; Rydså, L.; Kjøbli, E.; Bugge, S.; Bjørkøy, G.; Sundby, E.; Hoff, B. H., *Eur. J. Pharm. Sci.* **2014,** *59*, 69-82.
11. Larsen, K. U., Synthesis of Pyrrolopyrimidines as CSF-1R Kinase Inhibitors, M.Sc. thesis, NTNU, 2016.
12. Hubbard, S. R.; Till, J. H., *Annu. Rev. Biochem.* **2000,** *69* (1), 373-398.
13. Lemmon, M. A.; Schlessinger, J., *Cell* **2010,** *141*, 1117–1134.
14. Paul, M. K.; Mukhopadhyay, A. K., *Int. J. Med. Sci.* **2004,** *1*, 101–115.
15. Ichiro, N. M., *Cells* **2014,** *3*, 304-330.
16. Levitzki, A.; Gazit, A., *Science* **1995,** *267*, 1782-1788.
17. Dan, R. R.; Yi-Mi, W.; Su-Fang, L., *Oncogene* **2000,** *19*, 5548-5557.
18. Stanley, E. R.; Chitu, V., *Cold Spring Harb. Perspect. Biol.* **2014,** *6*, 1-21.
19. Gómez-Nicola, D.; Fransen, N. L.; Suzzi, S.; Perry, V. H., *J. Neurosci.* **2013,** *33* (6), 2481.
20. Pixley, F. J.; Stanley, E. R., *Trends Cell. Biol.* **2004,** *14*, 628–638.
21. Pollard, J. W., *Encyclopedia of Cancer, Vol. 5* **2012**, 2130–2133.
22. Jeffrey, W. P., *Nat. Rev. Cancer* **2004,** *4*, 71.
23. Gouon-Evans, V.; Lin, E.; Pollard, J. W., *Breast Cancer Res.* **2002,** *4*, 155-164.

24. Noy, R.; Pollard, J. W., *Immunity* **2014,** *41*, 49-61.
25. Blanc, J.; Geney, R.; Menet, C., *Anticancer Agents Med. Chem.* **2013,** *13* (731-747).
26. Force, T.; Kolaja, K. L., *Nat. Rev. Drug. Discov.* **2011,** *10*, 111-126.
27. Ohno, H.; Kubo, K.; Murooka, H.; Kobayashi, Y.; Nishitoba, T.; Shibuya, M.; Yoneda, T.; Isoe, T., *Mol. Cancer Ther.* **2006,** *5*, 2634-43.
28. Conway, J. G.; McDonald, B.; Parham, J.; Keith, B.; Rusnak, D. W.; Shaw, E.; Jansen, M.; Lin, P.; Payne, A.; Crosby, R. M.; Johnson, J. H.; Frick, L.; Lin, M.-H. J.; Depee, S.; Tadepalli, S.; Votta, B.; James, I.; Fuller, K.; Chambers, T. J.; Kull, F. C.; Chamberlain, S. D.; Hutchins, J. T., *Proc. Natl. Acad. Sci.* **2005,** *102* (44), 16078.
29. Moskowitz, C. H.; Younes, A.; de Vos, S.; Bociek, R. G.; Gordon, L. I.; Witzig, T. E.; Gascoyne, R. D.; West, B.; Nolop, K.; Steidl, C., *Blood* **2012,** *120* (21), 1638.
30. Rugo, H.; Sharma, N.; Reebel, L.; Rodal, M.; Peck, A.; West, B.; Marimuthu, A.; Karlin, D.; Dowlati, A.; Le, M.; Coussens, L.; Wesolowski, R., *Ann. Oncol.* **2014,** *25*, iv148.
31. Tap, W. D.; Wainberg, Z. A.; Anthony, S. P.; Ibrahim, P. N.; Zhang, C.; Healey, J. H.; Chmielowski, B.; Staddon, A. P.; Cohn, A. L.; Shapiro, G. I.; Keedy, V. L.; Singh, A. S.; Puzanov, I.; Kwak, E. L.; Wagner, A. J.; Von Hoff, D. D.; Weiss, G. J.; Ramanathan, R. K.; Zhang, J.; Habets, G.; Zhang, Y.; Burton, E. A.; Visor, G.; Sanftner, L.; Severson, P.; Nguyen, H.; Kim, M. J.; Marimuthu, A.; Tsang, G.; Shellooe, R.; Gee, C.; West, B. L.; Hirth, P.; Nolop, K.; van de Rijn, M.; Hsu, H. H.; Peterfy, C.; Lin, P. S.; Tong-Starksen, S.; Bollag, G., *N. Engl. J. Med.* **2015,** *373* (5), 428-437.
32. Zhang, C.; Ibrahim, P. N.; Zhang, J.; Burton, E. A.; Habets, G.; Zhang, Y.; Powell, B.; West, B. L.; Matusow, B.; Tsang, G.; Shellooe, R.; Carias, H.; Nguyen, H.; Marimuthu, A.; Zhang, K. Y. J.; Oh, A.; Bremer, R.; Hurt, C. R.; Artis, D. R.; Wu, G.; Nespi, M.; Spevak, W.; Lin, P.; Nolop, K.; Hirth, P.; Tesch, G. H.; Bollag, G., *Proc. Natl. Acad. Sci. U.S.A.* **2013,** *110* (14), 5689-5694.
33. Schubert, C.; Schalk-Hihi, C.; Struble, G. T.; Ma, H.-C.; Petrounia, I. P.; Brandt, B.; Deckman, I. C.; Patch, R. J.; Player, M. R.; Spurlino, J. C.; Springer, B. A., *J. Biol. Chem.* **2007,** *282* (6), 4094-4101.
34. Hubbard, S. R., *Front. Biosci.* **2002,** *7*, 330-340.
35. Paulo, A.; Gomes, E. T.; Houghton, P. J., *J. Nat. Prod.* **1995,** *58* (10), 1485-1491.
36. Cao, S.; Kingston, D. G. I., *Pharm. Biol.* **2009,** *47* (8), 809-823.
37. Prudhomme, M., *Eur. J. Med. Chem.* **2003,** *38* (2), 123-140.

38. Zhang, H.-C.; Ye, H.; Conway, B. R.; Derian, C. K.; Addo, M. F.; Kuo, G.-H.; Hecker, L. R.; Croll, D. R.; Li, J.; Westover, L.; Xu, J. Z.; Look, R.; Demarest, K. T.; Andrade-Gordon, P.; Damiano, B. P.; Maryanoff, B. E., *Bioorganic Med. Chem. Lett.* **2004,** *14* (12), 3245-3250.
39. Fonquerna, S.; Miralpeix, M.; Pagès, L.; Puig, C.; Cardús, A.; Antón, F.; Vilella, D.; Aparici, M.; Prieto, J.; Warrellow, G.; Beleta, J.; Ryder, H., *Bioorganic Med. Chem. Lett.* **2005,** *15* (4), 1165-1167.
40. Mérour, J.-Y.; Buron, F.; Plé, K.; Bonnet, P.; Routier, S., *Molecules* **2014,** *19* (12), 19935-19979.
41. de Mattos, M. C.; Alatorre-Santamaría, S.; Gotor-Fernández, V., *Synthesis* **2007,** *14*, 2149-2152.
42. Whelligan, D. K.; Thomson, D. W.; Taylor, D.; Hoelder, S., *J. Org. Chem.* **2010,** *75* (1), 11-15.
43. Zuccotto, F.; Ardini, E.; Casale, E.; Angiolini, M., *J. Med. Chem.* **2010,** *53* (7), 2681-2694.
44. Gummadi, V. R.; Rajagopalan, S.; Looi, C.-Y.; Paydar, M.; Renukappa, G. A.; Ainan, B. R.; Krishnamurthy, N. R.; Panigrahi, S. K.; Mahasweta, K.; Raghuramachandran, S.; Rajappa, M.; Ramanathan, A.; Lakshminarasimhan, A.; Ramachandra, M.; Wong, P.-F.; Mustafa, M. R.; Nanduri, S.; Hosahalli, S., *Bioorg. Med. Chem. Lett.* **2013,** *23* (17), 4911-4918.
45. Adams, N. D.; Adams, J. L.; Burgess, J. L.; Chaudhari, A. M.; Copeland, R. A.; Donatelli, C. A.; Drewry, D. H.; Fisher, K. E.; Hamajima, T.; Hardwicke, M. A.; Huffman, W. F.; Koretke-Brown, K. K.; Lai, Z. V.; McDonald, O. B.; Nakamura, H.; Newlander, K. A.; Oleykowski, C. A.; Parrish, C. A.; Patrick, D. R.; Plant, R.; Sarpong, M. A.; Sasaki, K.; Schmidt, S. J.; Silva, D. J.; Sutton, D.; Tang, J.; Thompson, C. S.; Tummino, P. J.; Wang, J. C.; Xiang, H.; Yang, J.; Dhanak, D., *J. Med. Chem.* **2010,** *53* (10), 3973-4001.
46. Farmer, L. M.-B., G.; Pierce, A.; Salituro, F.; Wang, J.; Wannamker, M.; Wang, T. , **2007**, Patent WO2007084557.
47. Huang, S.; Li, R.; Connolly, P. J.; Emanuel, S.; Middleton, S. A., *Bioorg. Med. Chem. Lett.* **2006,** *16* (18), 4818-4821.
48. Caldwell, J. J.; Cheung, K.-M.; Collins, I., *Tetrahedron Lett.* **2007,** *48* (9), 1527-1529.

49. Gehringer, M.; Pfaffenrot, E.; Bauer, S.; Laufer, S. A., *ChemMedChem* **2014,** *9* (2), 277-281.
50. Henderson, J. L.; McDermott, S. M.; Buchwald, S. L., *Org. Lett.* **2010,** *12* (20), 4438-4441.
51. Johansen, C., Synthetic Strategies Towards Substituted Pyrrolopyridines as Possible CSF1R Inhibitors, M.Sc. thesis, NTNU, 2017.
52. Jolicoeur, B.; Chapman, E. E.; Thompson, A.; Lubell, W. D., *Tetrahedron* **2006,** *62* (50), 11531-11563.
53. Carey, A. F., Sundberg, R. J. , *Advanced Organic Chemistry, Part B: Reactions and Synthesis* **2007**, Fifth edition; Springer: Virginia, 258-267.
54. Thompson, A.; Butler, R. J.; Grundy, M. N.; Laltoo, A. B. E.; Robertson, K. N.; Cameron, T. S., *J. Org. Chem.* **2005,** *70* (9), 3753-3756.
55. Nair, R. N.; Bannister, T. D., *Org. Process Res. Dev.* **2016,** *20* (7), 1370-1376.
56. Luo, G.; Chen, L.; Dubowchik, G., *J. Org. Chem.* **2006,** *71* (14), 5392-5395.
57. Zeng, Q.; Bailey, S.; Wang, T.-Z.; Paquette, L. A., *J. Org. Chem.* **1998,** *63* (1), 137-143.
58. Kobayashi, T.; Regens, C. S.; Denmark, S. E., *Strategies and Tactics in Organic Synthesis* **2012,** *8*, Chapter 4 - Total Synthesis of Papulacandin D, 79-126.
59. Parsons, T. B.; Spencer, N.; Tsang, C. W.; Grainger, R. S., *Chem. Commun.* **2013,** *49* (23), 2296-2298.
60. Zhou, J.; Liu, P.; Lin, Q.; Metcalf, B. W.; Meloni, D.; Pan, Y.; Xia, M.; Li, M.; Yue, T.-Y.; Rodgers, J. D.; Wang, H. P., **2010**, WO 2010/083283 A2.
61. Hatcher, J. M.; Zhang, J.; Choi, H. G.; Ito, G.; Alessi, D. R.; Gray, N. S., *ACS Med. Chem. Lett.* **2015,** *6* (5), 584-589.
62. Kan, T.; Hashimoto, M.; Yanagiya, M.; Shirahama, H., *Tetrahedron Lett.* **1988,** *29* (42), 5417-5418.
63. Lipshutz, B. H.; Pegram, J. J., *Tetrahedron Lett.* **1980,** *21* (35), 3343-3346.
64. Ogilvie, K. K., *Can. J. Chem.* **1973,** *51* (22), 3799-3807.
65. Corey, E. J.; Venkateswarlu, A., *J. Am. Chem. Soc.* **1972,** *94* (17), 6190-6191.
66. Lima, C. F. R. A. C.; Rodriguez-Borges, J. E.; Santos, L. M. N. B. F., *Tetrahedron* **2011,** *67* (4), 689-697.
67. Moreno-Mañas, M.; Pérez, M.; Pleixats, R., *J. Org. Chem.* **1996,** *61* (7), 2346-2351.
68. Miyaura, N.; Suzuki, A., *Chem. Rev.* **1995,** *95*, 2457-2483.

69. Miyaura, N.; Yanagi, T.; Suzuki, A., *Synth. Commun.* **1981,** *11*, 513-519.
70. Schomaker, J. M.; Delia, T. J., *J. Org. Chem.* **2001,** *66* (21), 7125-7128.
71. Kotha, S.; Lahiri, K.; Kashinath, D., *Tetrahedron* **2002,** *58*, 9633–9695.
72. Amatore, C.; Jutand, A.; Le Duc, G., *Chem. Eur. J.* **2011,** *17* (8), 2492-2503.
73. Carrow, B. P.; Hartwig, J. F., *J. Am. Chem. Soc.* **2011,** *133* (7), 2116-2119.
74. Schmidt, A. F.; Kurokhtina, A. A.; Smirnov, V. V.; Larina, E. V.; Chechil, E. V., *Kinet. Catal.* **2012,** *53* (2), 214-221.
75. Smith, G. B.; Dezeny, G. C.; Hughes, D. L.; King, A. O.; Verhoeven, T. R., *J. Org. Chem.* **1994,** *59* (26), 8151-8156.
76. Adamo, C.; Amatore, C.; Ciofini, I.; Jutand, A.; Lakmini, H., *J. Am. Chem. Soc.* **2006,** *128* (21), 6829-6836.
77. Lennox, A. J. J.; Lloyd-Jones, G. C., *Isr. J. Chem.* **2010,** *50* (5-6), 664-674.
78. Navarro, O.; Marion, N.; Oonishi, Y.; Kelly, R. A.; Nolan, S. P., *J. Org. Chem.* **2006,** *71* (2), 685-692.
79. Jedinák, L.; Zátopková, R.; Zemánková, H.; Šustková, A.; Cankař, P., *J. Org. Chem.* **2017,** *82* (1), 157-169.
80. Navarro, O.; Kelly, R. A.; Nolan, S. P., *J. Am. Chem. Soc.* **2003,** *125* (52), 16194-16195.
81. Wolfe, J. P.; Singer, R. A.; Yang, B. H.; Buchwald, S. L., *J. Am. Chem. Soc.* **1999,** *121* (41), 9550-9561.
82. Bruno, N. C.; Buchwald, S. L., *Org. Lett.* **2013,** *15* (11), 2876-2879.
83. Bruno, N. C.; Buchwald, S. L., **2013**, WO2013184198.
84. Biscoe, M. R.; Fors, B. P.; Buchwald, S. L., *J. Am. Chem. Soc.* **2008,** *130* (21), 6686-6687.
85. Kinzel, T.; Zhang, Y.; Buchwald, S. L., *J. Am. Chem. Soc.* **2010,** *132* (40), 14073-14075.
86. Littke, A. F.; Fu, G. C., *Angew. Chem. Int. Ed.* **1999,** *37* (24), 3387-3388.
87. Wang, J. R.; Manabe, K., *Synthesis* **2009,** *9*, 1405-1427.
88. Almond-Thynne, J.; Blakemore, D. C.; Pryde, D. C.; Spivey, A. C., *Chem. Sci.* **2017,** *8* (1), 40-62.
89. Zhang, Y.; Handy, S. T., *Open Org. Chem. J.* **2008,** *2*, 58-64.
90. Handy, S. T.; Zhang, Y., *Chem. Commun.* **2006,** (3), 299-301.
91. Christmann, U.; Vilar, R., *Angew. Chem. Int. Ed.* **2005,** *44* (3), 366-374.

92. Dai, X.; Chen, Y.; Garrell, S.; Liu, H.; Zhang, L.-K.; Palani, A.; Hughes, G.; Nargund, R., *J. Org. Chem.* **2013,** *78* (15), 7758-7763.
93. Moors, S. L. C.; Brigou, B.; Hertsen, D.; Pinter, B.; Geerlings, P.; Van Speybroeck, V.; Catak, S.; De Proft, F., *J. Org. Chem.* **2016,** *81* (4), 1635-1644.
94. Fernández, I.; Frenking, G.; Uggerud, E., *J. Org. Chem.* **2010,** *75* (9), 2971-2980.
95. Kim, Y. M.; Yu, S., *J. Am. Chem. Soc.* **2003,** *125* (7), 1696-1697.
96. Jaime-Figueroa, S.; Liu, Y.; Muchowski, J. M.; Putman, D. G., *Tetrahedron Lett.* **1998,** *39* (11), 1313-1316.
97. Guram, A. S.; Buchwald, S. L., *J. Am. Chem. Soc.* **1994,** *116*, 7901-7902.
98. Paul, F.; Patt, J.; Hartwig, J. F., *J. Am. Chem. Soc.* **1994,** *116* (5969-5970).
99. Surry, D. S.; Buchwald, S. L., *Chem. Sci.* **2011,** *2* (1), 27-50.
100. Arrechea, P. L.; Buchwald, S. L., *J. Am. Chem. Soc.* **2016,** *138* (38), 12486-12493.
101. Kaspersen, S. J.; Sørum, C.; Willassen, V.; Fuglseth, E.; Kjøbli, E.; Bjørkøy, G.; Sundby, E.; Hoff, B. H., *Eur. J. Med. Chem.* **2011,** *46* (12), 6002-6014.
102. Guillard, J.; Decrop, M.; Gallay, N.; Espanel, C.; Boissier, E.; Herault, O.; Viaud-Massuard, M.-C., *Bioorg. Med. Chem. Lett.* **2007,** *17* (7), 1934-1937.
103. Kranenburg, M.; van der Burgt, Y. E. M.; Kamer, P. C. J.; van Leeuwen, P. W. N. M.; Goubitz, K.; Fraanje, J., *Organometallics* **1995,** *14* (6), 3081-3089.
104. Audisio, D.; Messaoudi, S.; Peyrat, J.-F.; Brion, J.-D.; Alami, M., *Tetrahedron Lett.* **2007,** *48* (39), 6928-6932.
105. Tasler, S.; Mies, J.; Lang, M., *Adv. Synth. Catal.* **2007,** *349* (14-15), 2286-2300.
106. Driver, M. S.; Hartwig, J. F., *J. Am. Chem. Soc.* **1996,** *118* (30), 7217-7218.
107. Park, N. H.; Vinogradova, E. V.; Surry, D. S.; Buchwald, S. L., *Angew. Chem. Int. Ed.* **2015,** *54* (28), 8259-8262.
108. Hartwig, J. F.; Richards, S.; Barañano, D.; Paul, F., *J. Am. Chem. Soc.* **1996,** *118* (15), 3626-3633.
109. Nakajima, Y.; Tojo, T.; Morita, M.; Hatanaka, K.; Shirakami, S.; Tanaka, A.; Sasaki, H.; Nakai, K.; Mukoyoshi, K.; Hamaguchi, H.; Takahashi, F.; Moritomo, A.; Higashi, Y.; Inoue, T., *Chem. Pharm. Bull.* **2015,** *63* (5), 341-353.
110. Kim, T. S.; Lee, E.; Kim, D.; Park, B.; Park, J.; Joo, J., **2015**, Patent US 8957102.
111. Maiti, D.; Fors, B. P.; Henderson, J. L.; Nakamura, Y.; Buchwald, S. L., *Chem. Sci.* **2011,** *2* (1), 57-68.

112. Topchiy, M. A.; Asachenko, A. F.; Nechaev, M. S., *Eur. J. Org. Chem.* **2014,** *2014* (16), 3319-3322.
113. Patschinski, P.; Zhang, C.; Zipse, H., *J. Org. Chem.* **2014,** *79* (17), 8348-8357.
114. Bekkevard, P. U., Synthesis of Pyrrolopyrimidines for Investigation of JAK2 inhibition, M.Sc. thesis, NTNU, 2015.
115. Juchum, M.; Günther, M.; Döring, E.; Sievers-Engler, A.; Lämmerhofer, M.; Laufer, S., *J. Med. Chem.* **2017,** *60* (11), 4636-4656.
116. Elsayed, M. S. A.; Nielsen, J. J.; Park, S.; Park, J.; Liu, Q.; Kim, C. H.; Pommier, Y.; Agama, K.; Low, P. S.; Cushman, M., *J. Med. Chem.* **2018,** *61* (23), 10440-10462.

Appendix A Compound 1

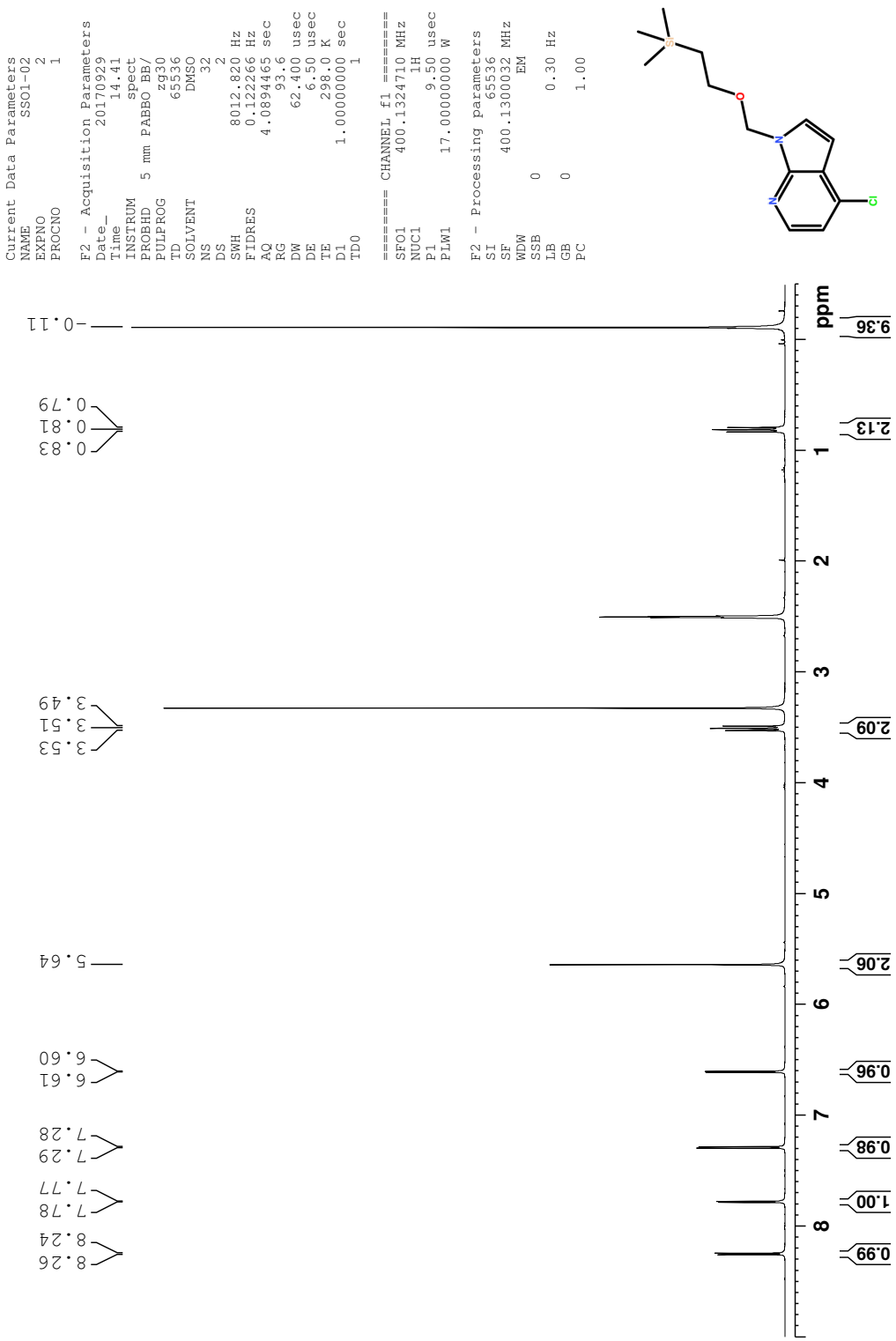

Figure A.1: ^{1}H NMR spectrum of compound **1**.

Appendix B Compound 2

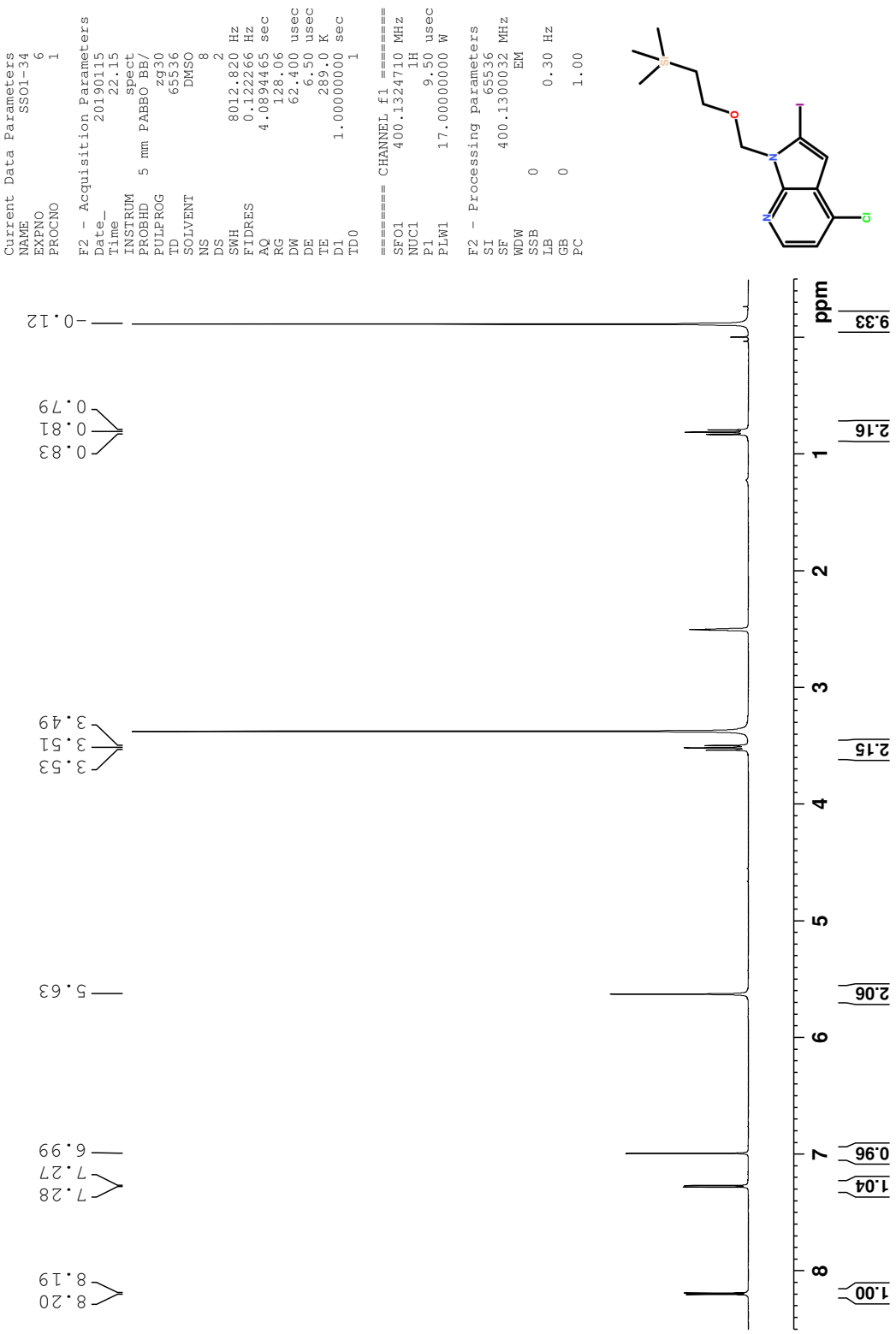

Figure B.1: ^{1}H NMR spectrum of compound **2**.

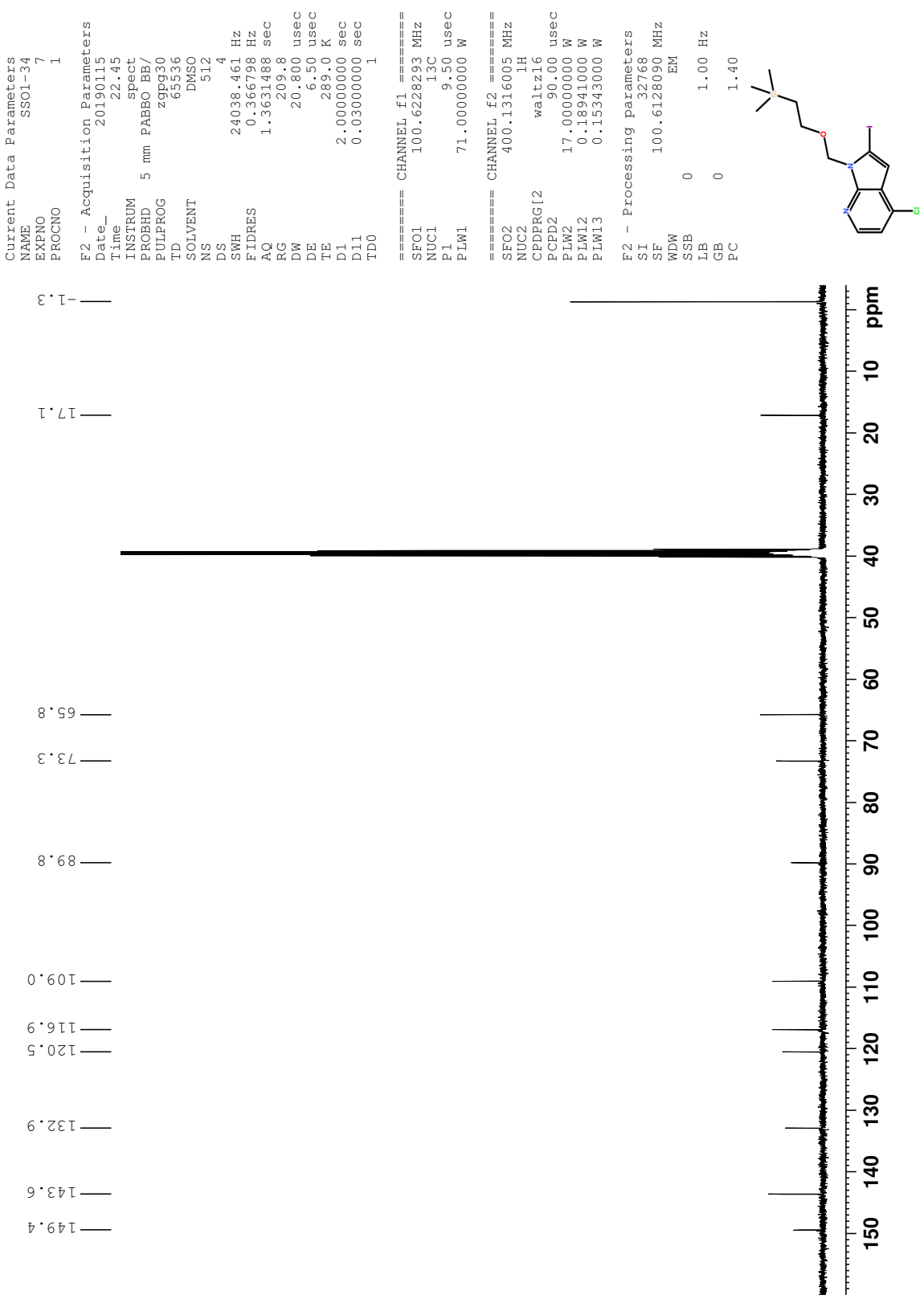

Figure B.2: ^{13}C NMR spectrum of compound **2**.

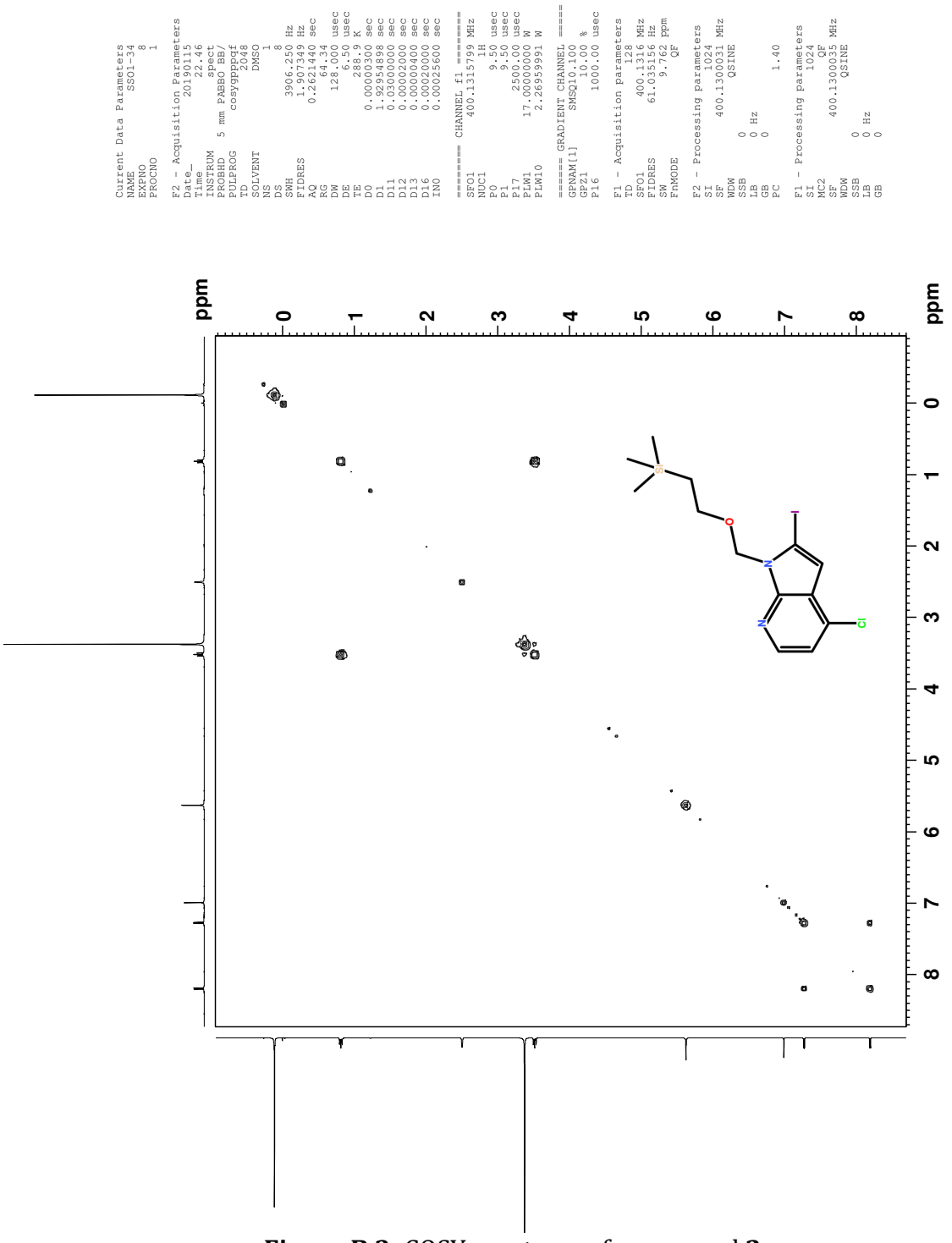

Figure B.3: COSY spectrum of compound **2**.

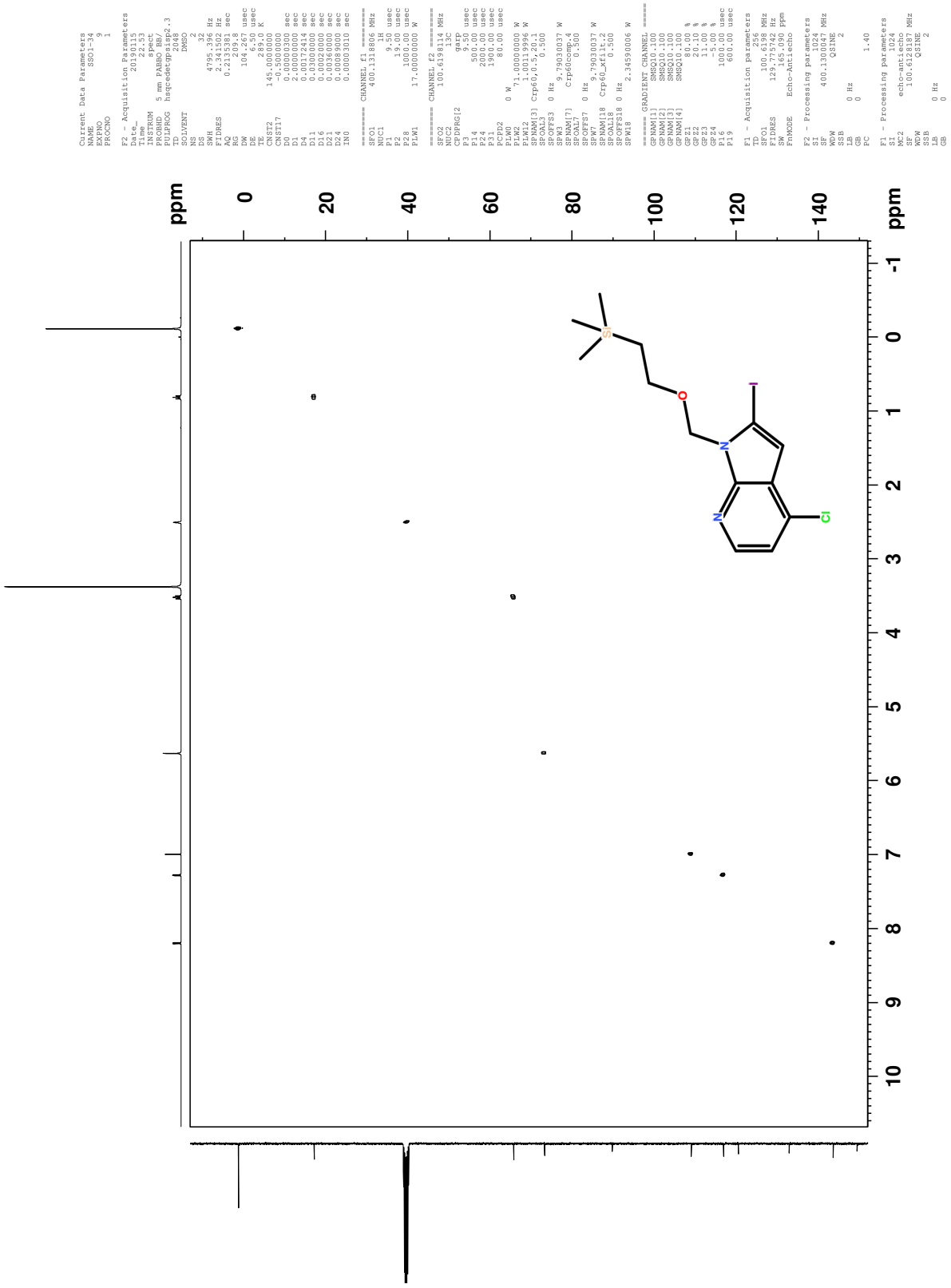

Figure B.4: HSQC spectrum of compound **2**.

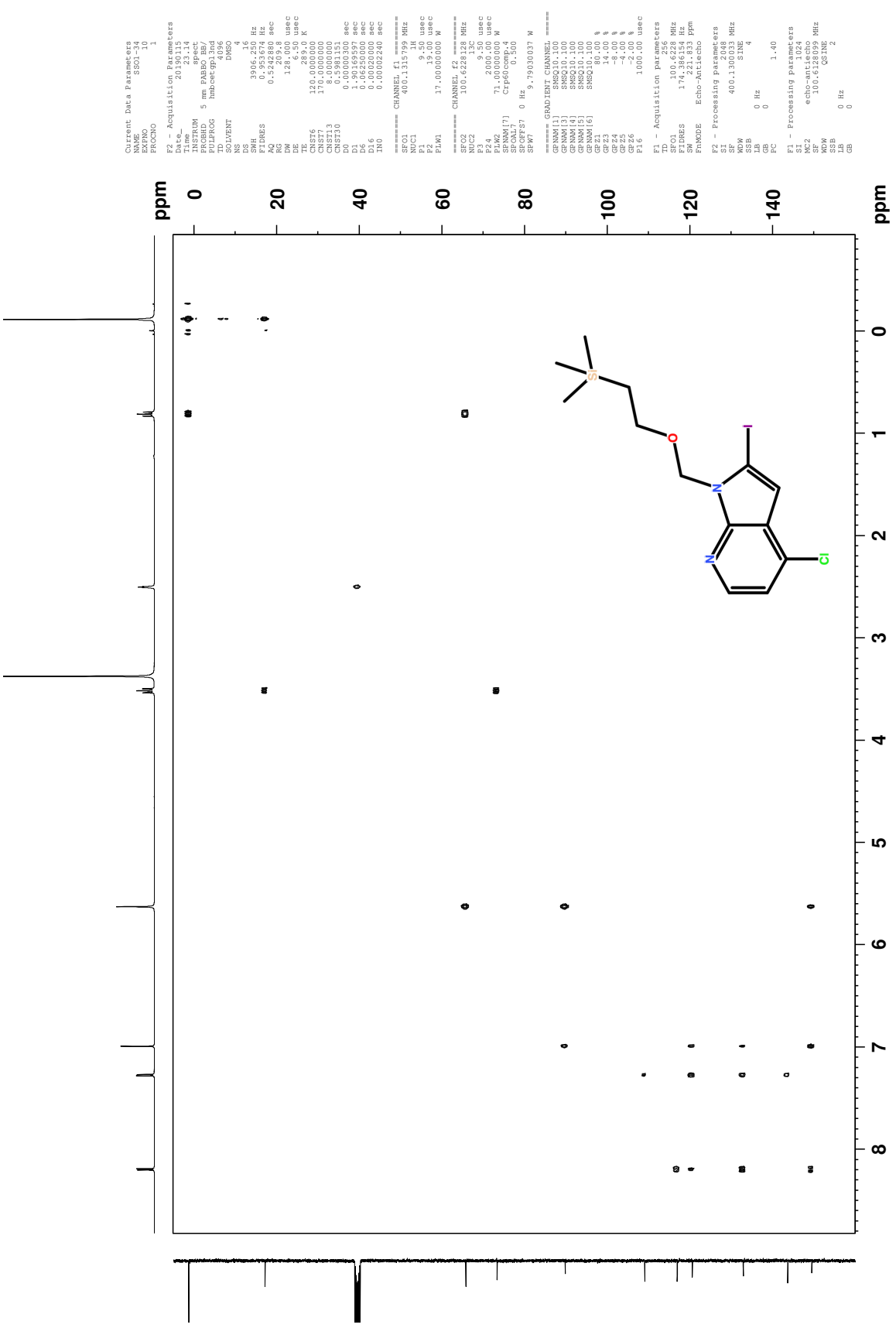

Figure B.5: HMBC spectrum of compound **2**.

Elemental Composition Report **Page 1**

Single Mass Analysis
Tolerance = 2.0 PPM / DBE: min = -2.0, max = 50.0
Element prediction: Off
Number of isotope peaks used for i-FIT = 3

Monoisotopic Mass, Even Electron Ions
7041 formula(e) evaluated with 15 results within limits (all results (up to 1000) for each mass)
Elements Used:
C: 0-100 H: 0-150 N: 0-8 O: 0-10 Si: 0-2 Cl: 0-3 I: 0-2

2019-17 38 (0.758) AM2 (Ar,35000.0,0.00,0.00); Cm (36:38)
1: TOF MS ASAP+

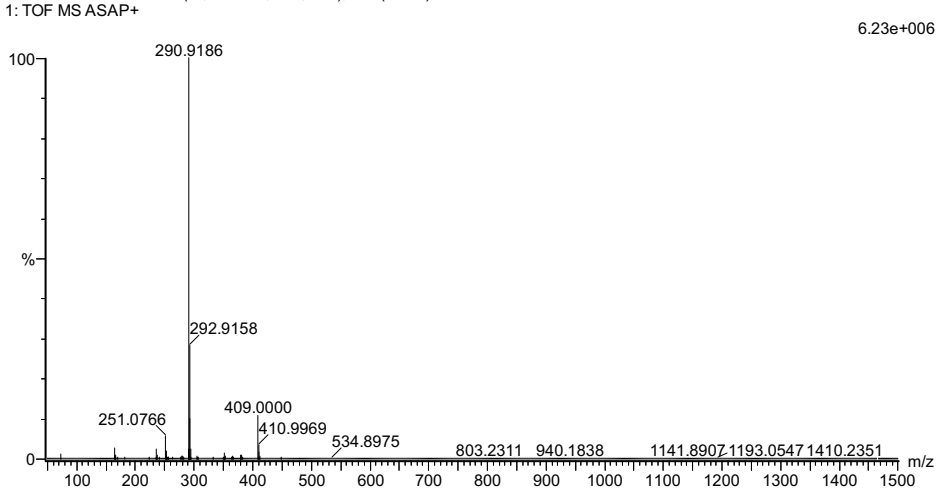

Minimum:				-2.0				
Maximum:		5.0	2.0	50.0				
Mass	Calc. Mass	mDa	PPM	DBE	i-FIT	Norm	Conf(%)	Formula
409.0000	409.0000	0.0	0.0	2.5	977.9	0.495	60.98	C6 H15 N8 O3 Cl I
	409.0000	0.0	0.0	5.5	978.5	1.094	33.49	C13 H19 N2 O Si Cl I
	409.0004	-0.4	-1.0	1.5	981.1	3.737	2.38	C5 H19 N8 Si2 Cl

Figure B.6: MS spectrum of compound **2**.

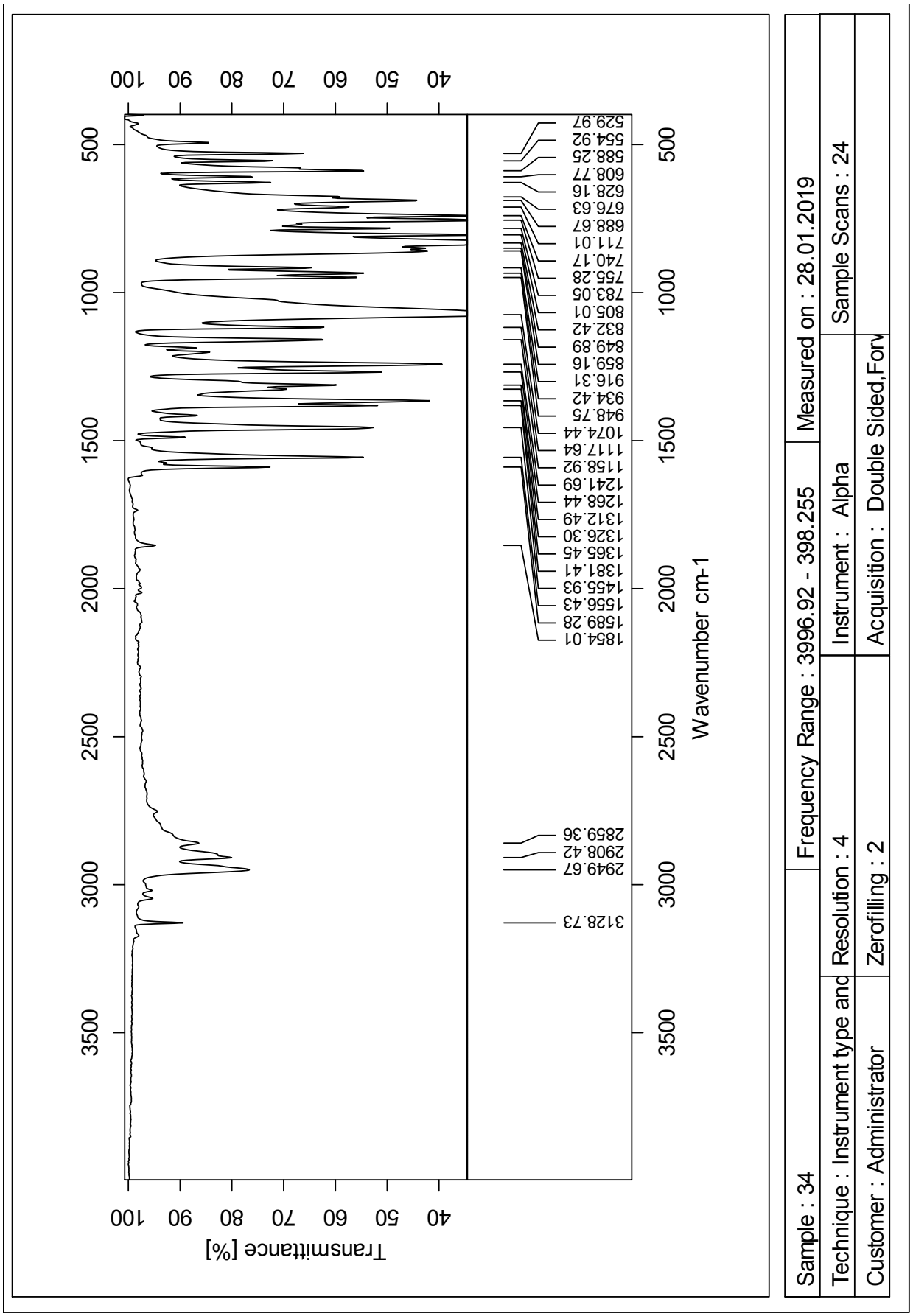

Figure B.7: IR spectrum of compound **2**.

Appendix C Compound 3

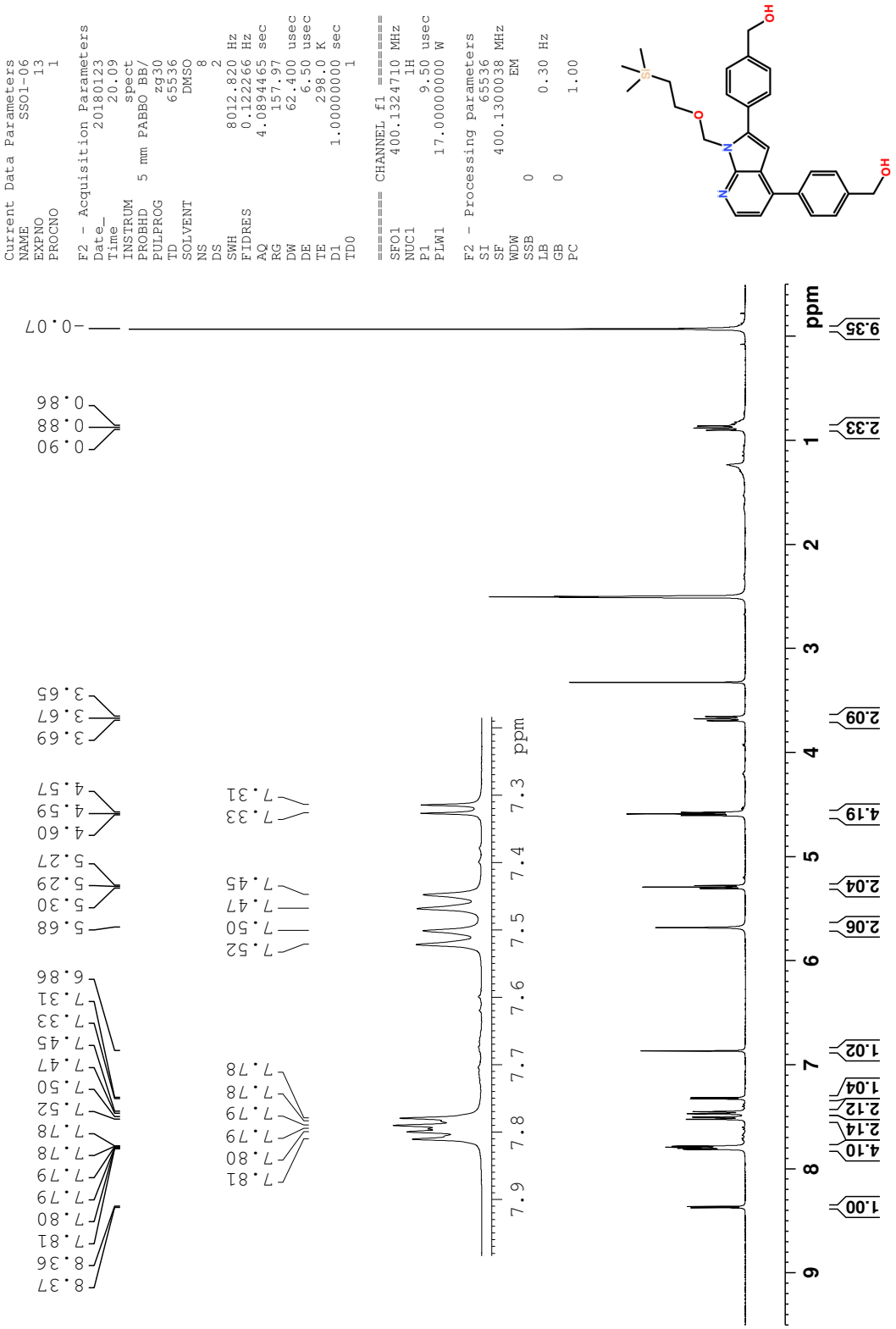

Figure C.1: ^{1}H NMR spectrum of compound **3**.

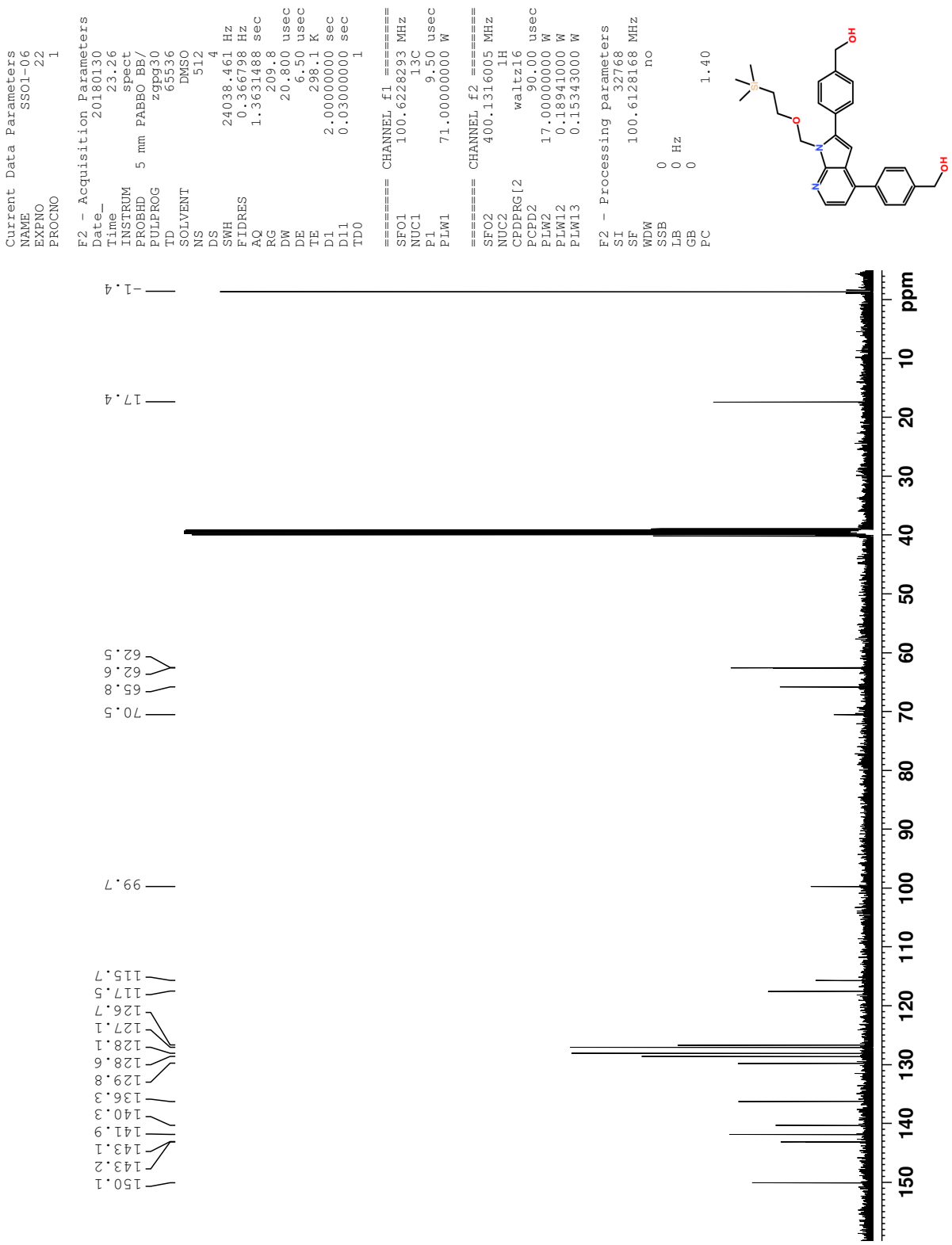

Figure C.2: ^{13}C NMR spectrum of compound **3**.

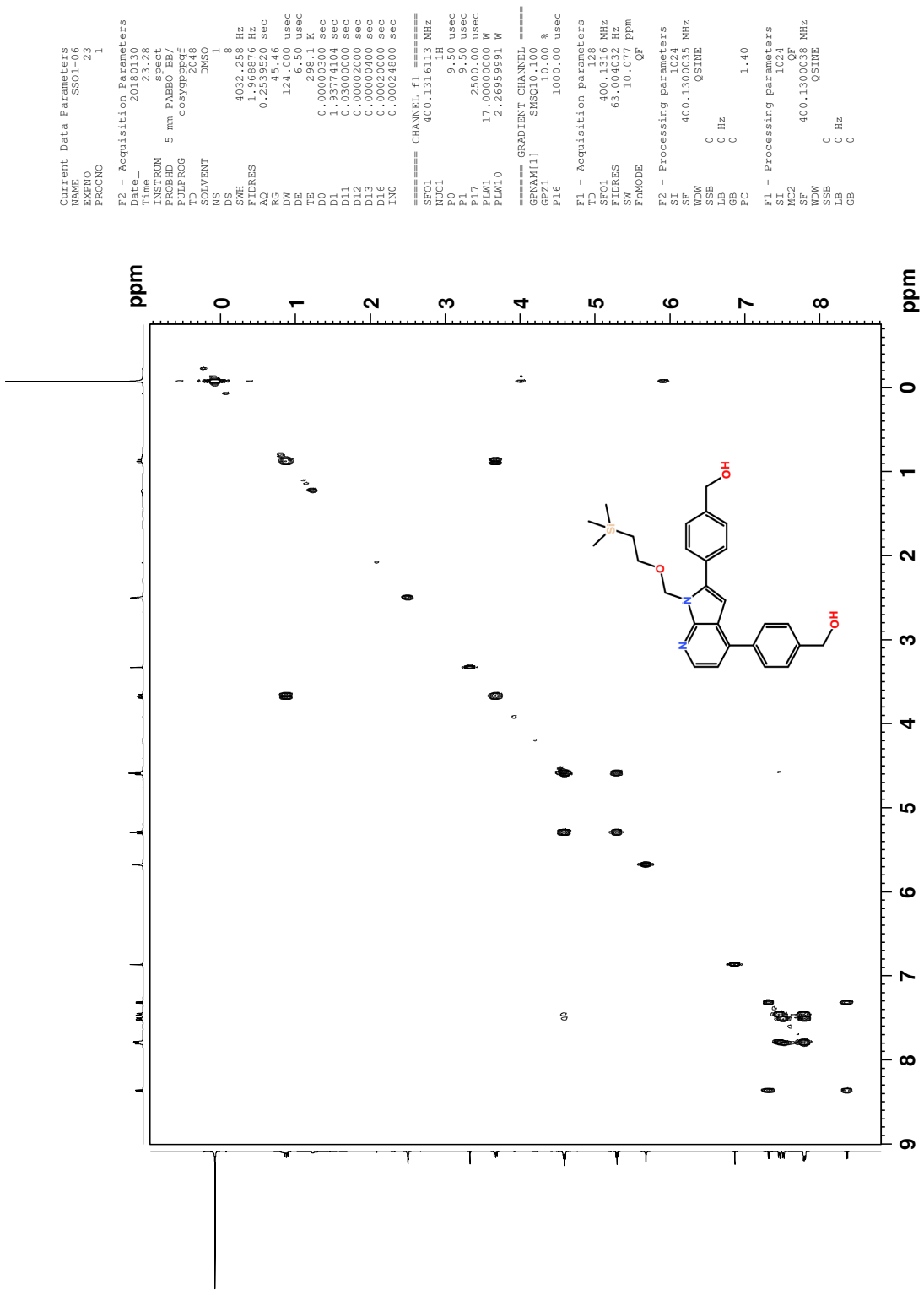

Figure C.3: COSY spectrum of compound **3**.

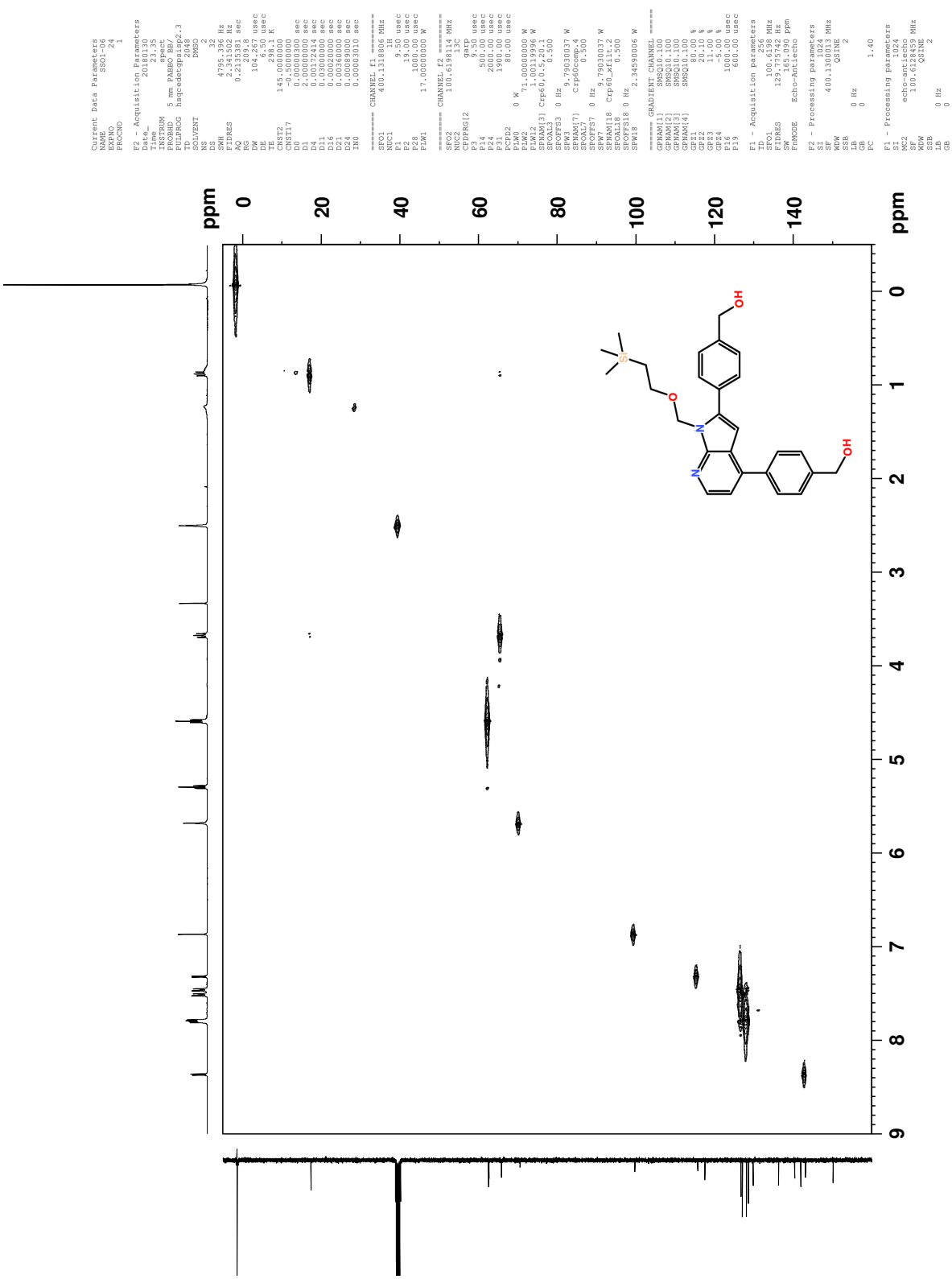

Figure C.4: HSQC spectrum of compound **3**.

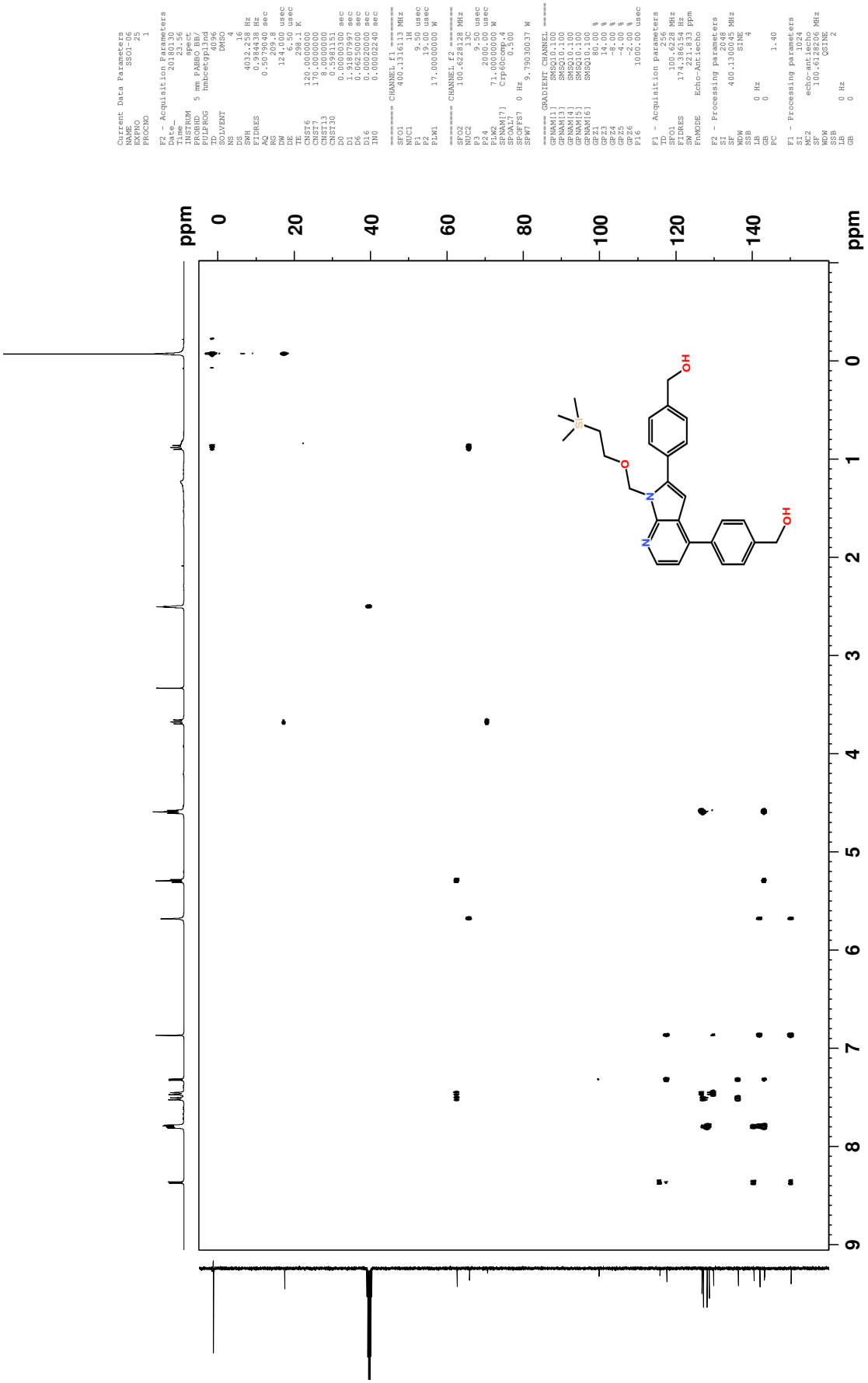

Figure C.5: HMBC spectrum of compound **3**.

Elemental Composition Report **Page 1**

Single Mass Analysis
Tolerance = 2.0 PPM / DBE: min = -2.0, max = 50.0
Element prediction: Off
Number of isotope peaks used for i-FIT = 3

Monoisotopic Mass, Even Electron Ions
2363 formula(e) evaluated with 7 results within limits (all results (up to 1000) for each mass)
Elements Used:
C: 0-100 H: 0-150 N: 0-10 O: 0-10 Si: 0-3
2019-14 154 (3.016) AM2 (Ar,35000.0,0.00,0.00); Cm (154:155)
1: TOF MS ASAP+

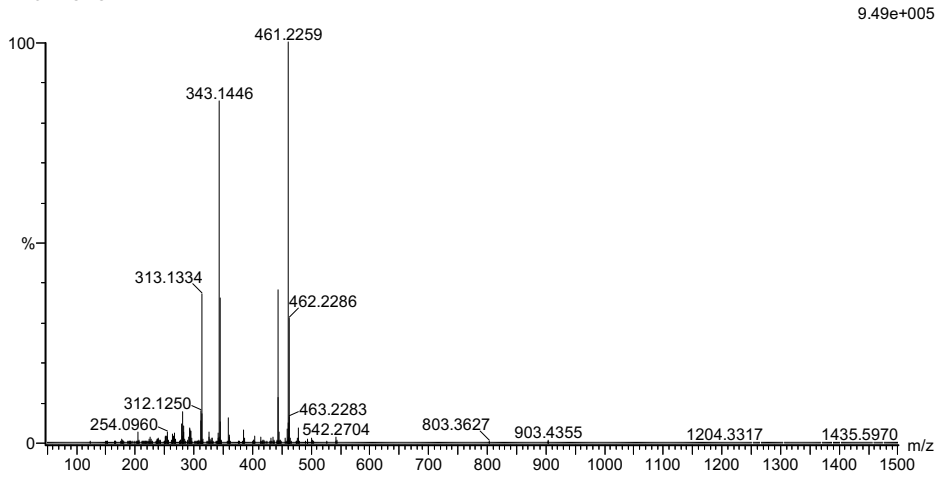

Minimum:				-2.0				
Maximum:		5.0	2.0	50.0				
Mass	Calc. Mass	mDa	PPM	DBE	i-FIT	Norm	Conf(%)	Formula
461.2259	461.2260	-0.1	-0.2	13.5	913.5	0.007	99.26	C27 H33 N2 O3 Si
	461.2261	-0.2	-0.4	10.5	919.2	5.633	0.36	C20 H29 N8 O5
	461.2256	0.3	0.7	0.5	924.1	10.557	0.00	C10 H37 N10 O5 Si3

Figure C.6: MS spectrum of compound **3**.

.

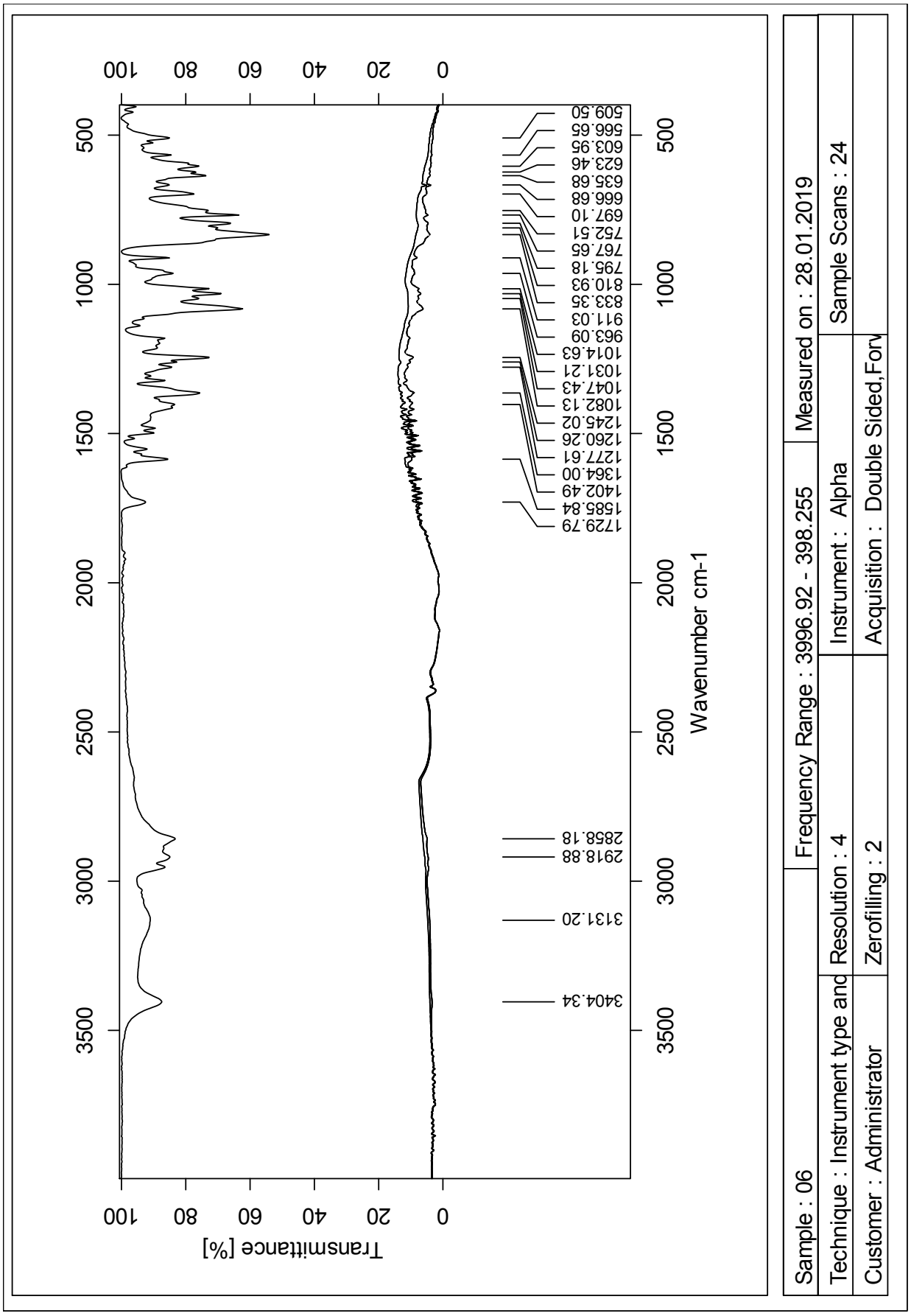

Figure C.7: IR spectrum of compound **3**.

Appendix D Compound 4

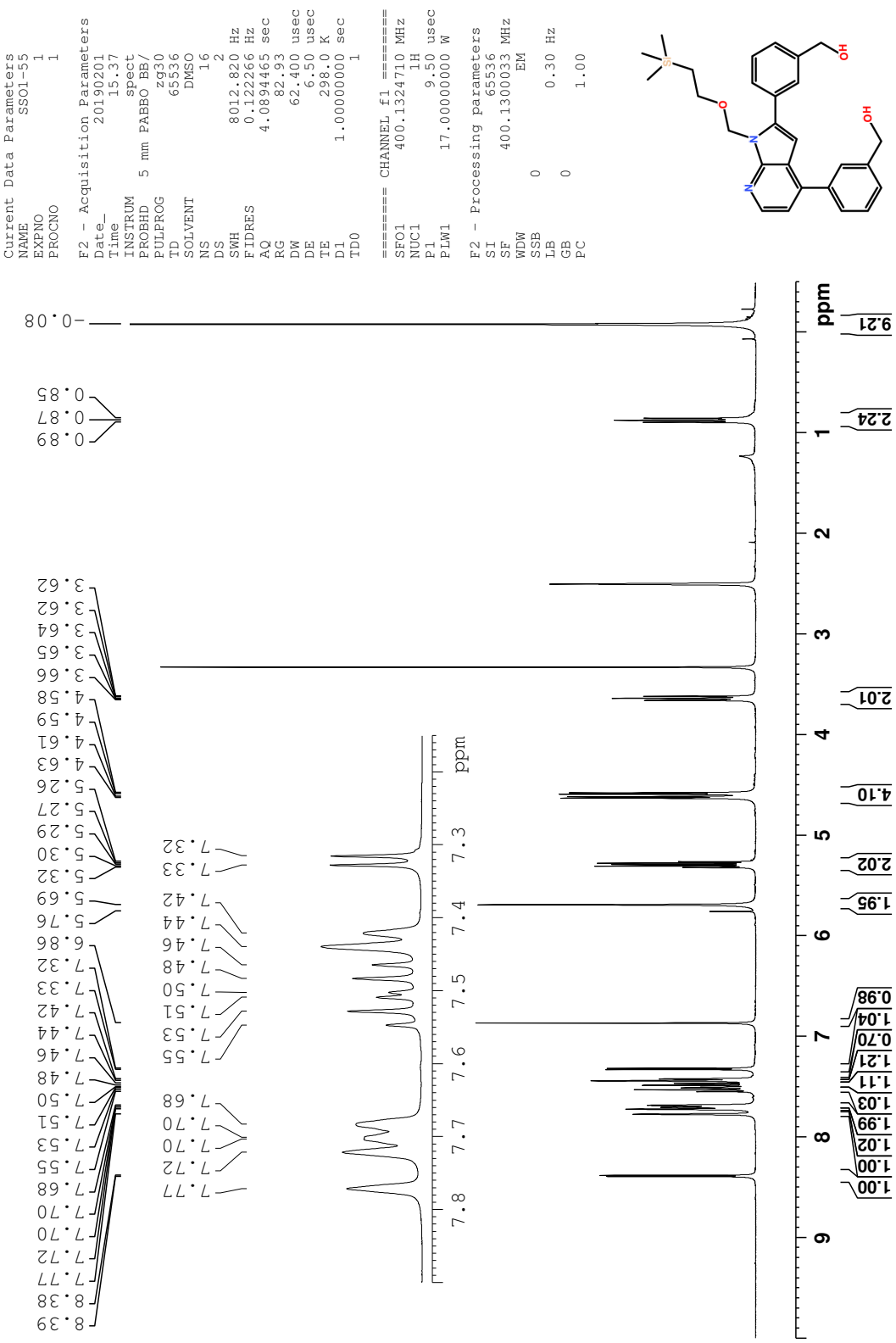

Figure D.1: ^{1}H NMR spectrum of compound **4**.

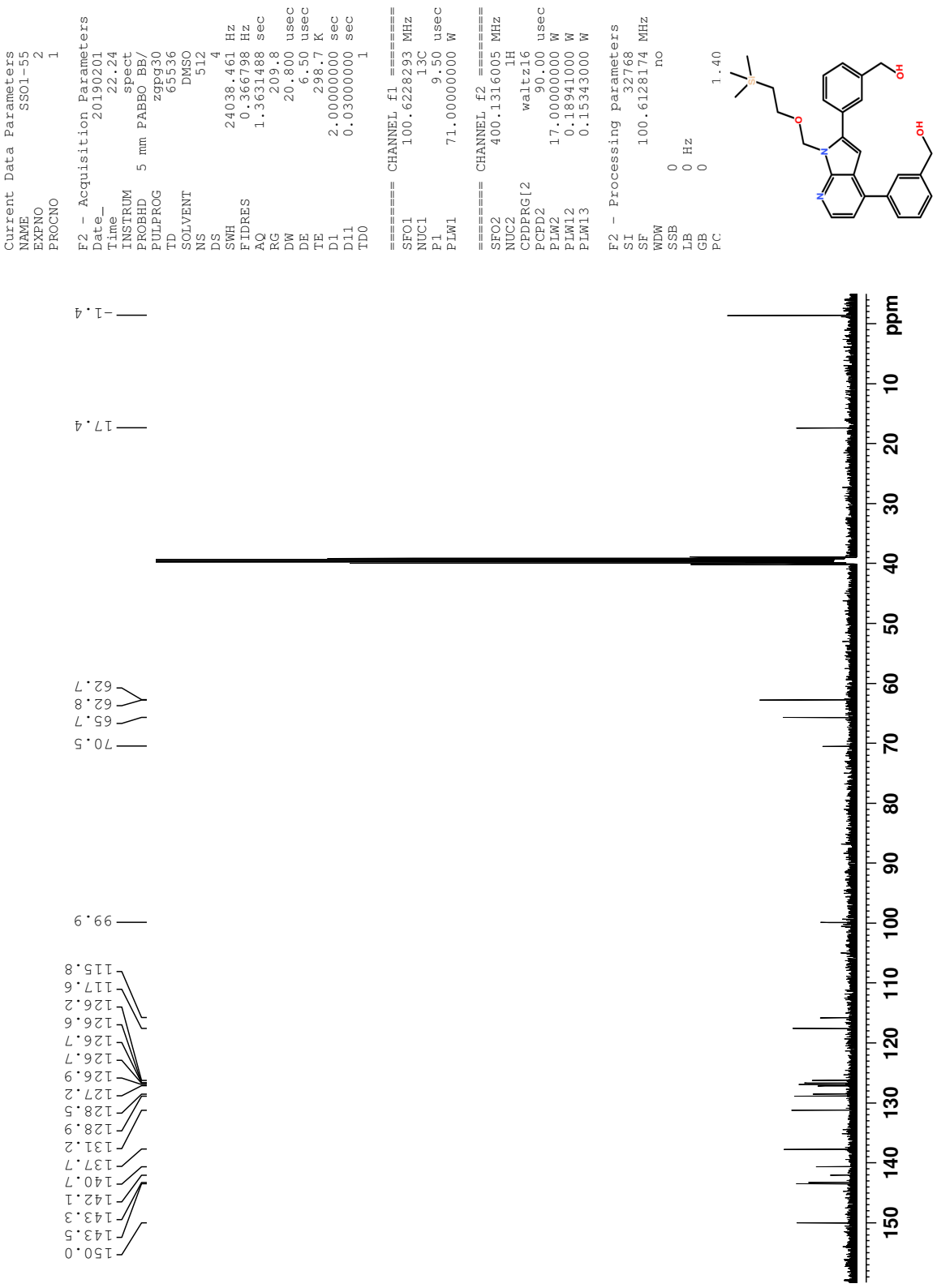

Figure D.2: ^{13}C NMR spectrum of compound **4**.

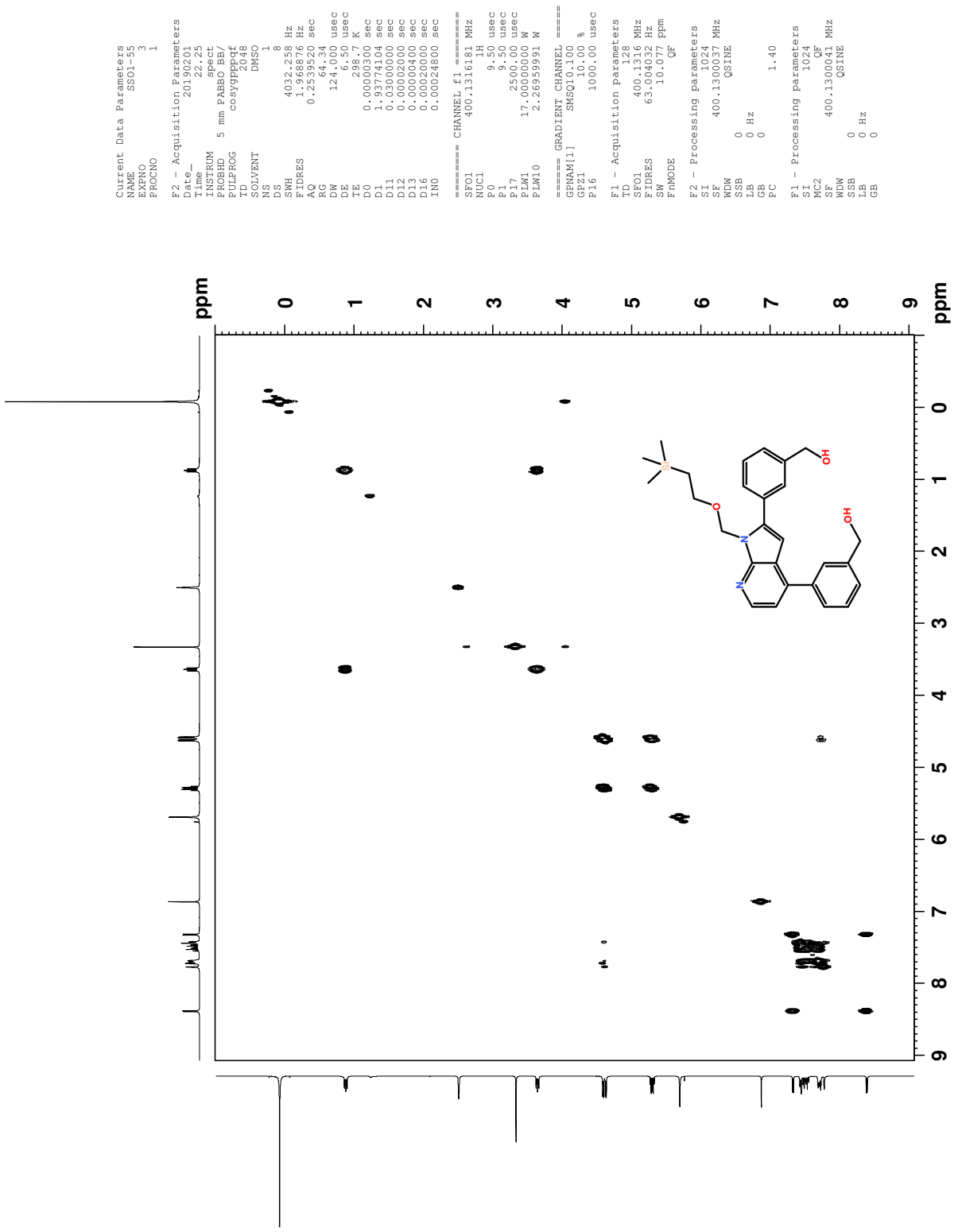

Figure D.3: COSY spectrum of compound **4**.

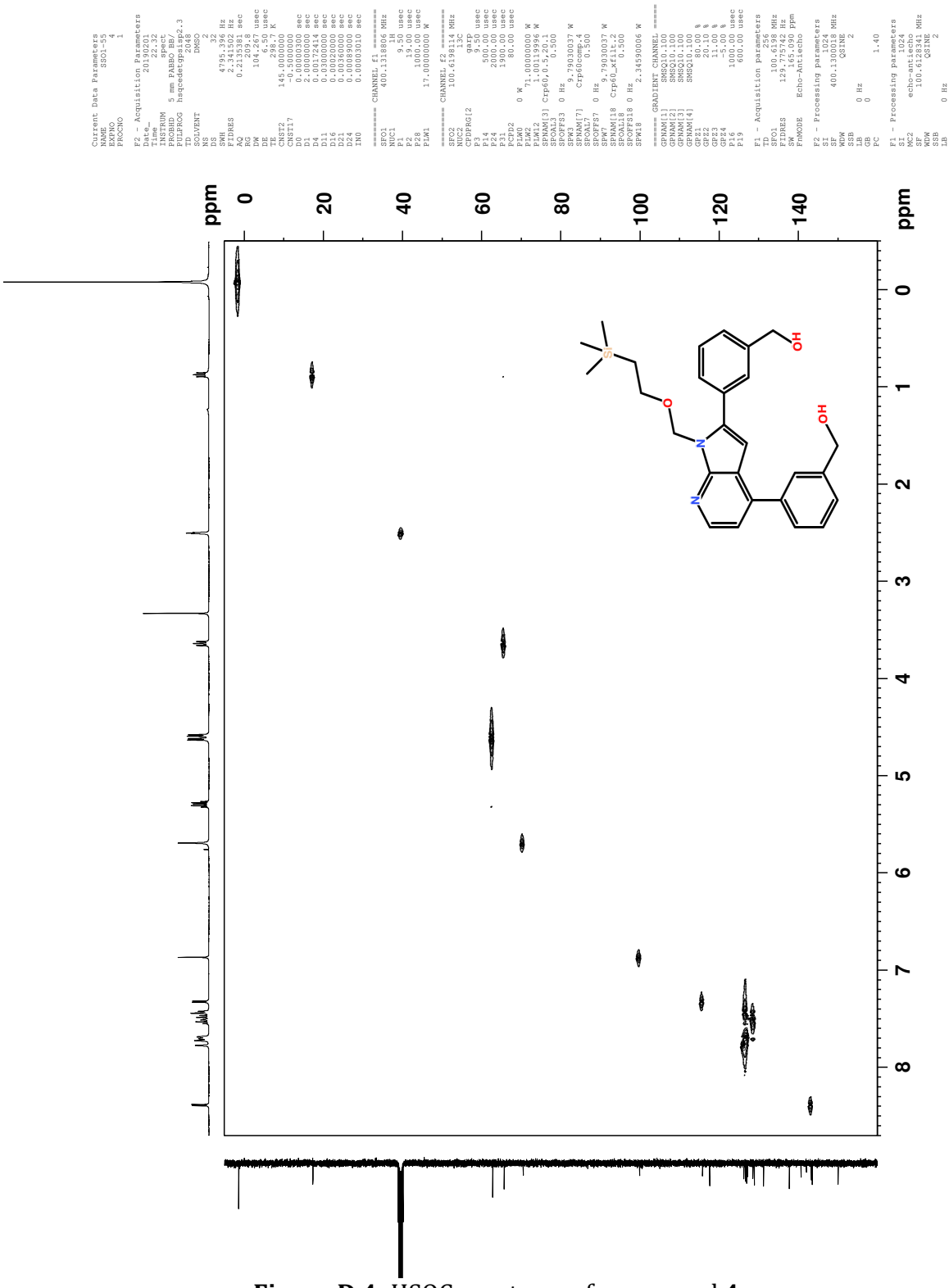

Figure D.4: HSQC spectrum of compound **4**.

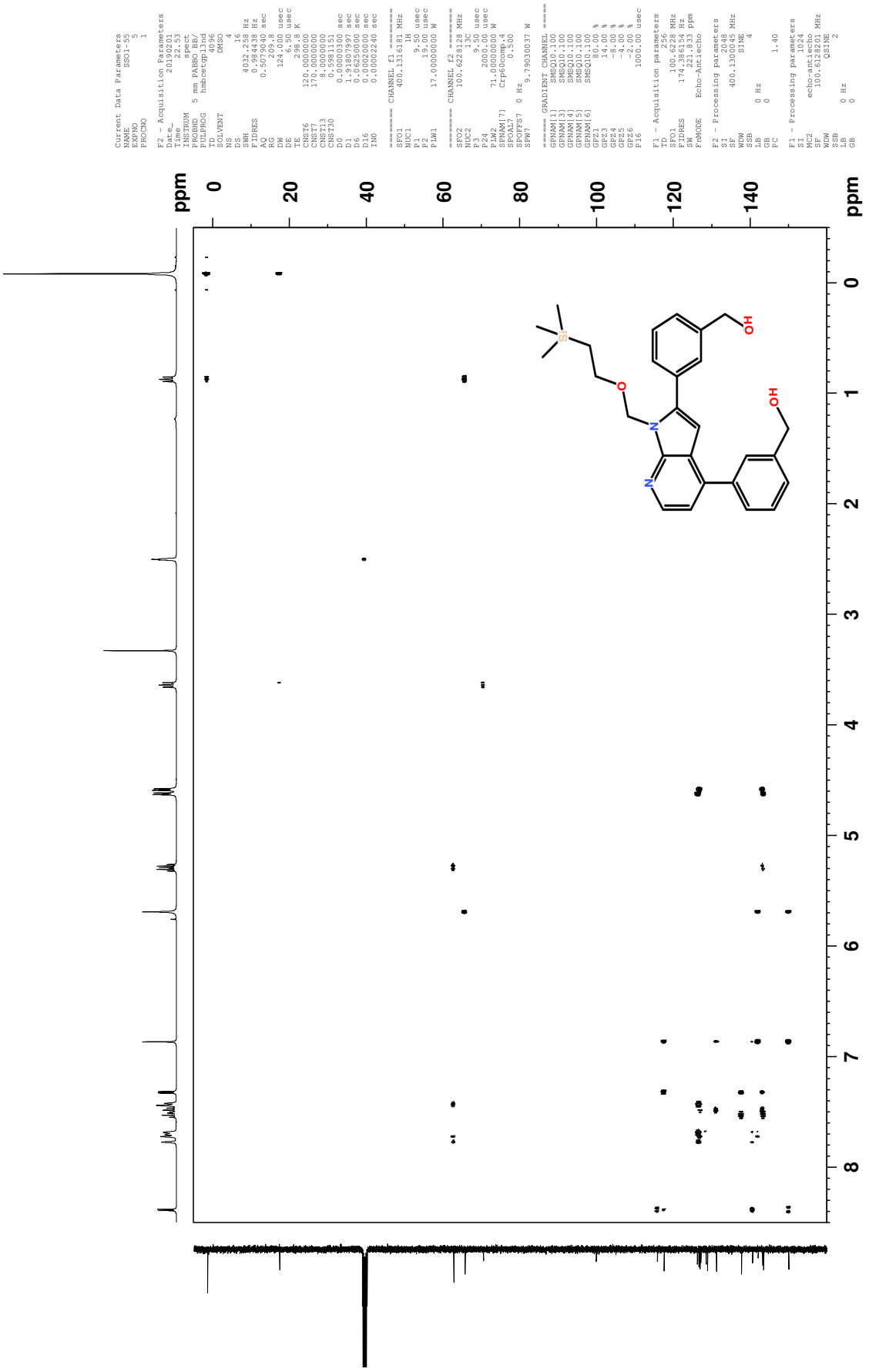

Figure D.5: HMBC spectrum of compound **4**.

Elemental Composition Report **Page 1**

Single Mass Analysis
Tolerance = 2.0 PPM / DBE: min = -2.0, max = 50.0
Element prediction: Off
Number of isotope peaks used for i-FIT = 3

Monoisotopic Mass, Even Electron Ions
5102 formula(e) evaluated with 8 results within limits (all results (up to 1000) for each mass)
Elements Used:
C: 0-100 H: 0-150 N: 0-10 O: 0-10 Na: 0-1 Si: 0-2 Au: 0-2

2019-41 152 (2.963) AM2 (Ar,35000.0,0.00,0.00); Cm (147:152)
1: TOF MS ASAP+

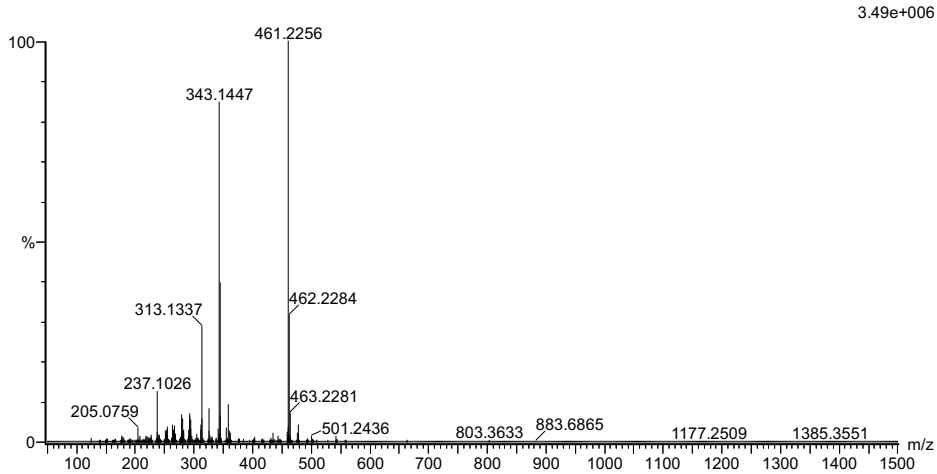

Minimum:				-2.0				
Maximum:		5.0	2.0	50.0				
Mass	Calc. Mass	mDa	PPM	DBE	i-FIT	Norm	Conf(%)	Formula
461.2256	461.2252	0.4	0.9	4.5	1089.1	7.300	0.07	C18 H37 N4 O6 Si2
	461.2252	0.4	0.9	1.5	1088.6	6.735	0.12	C11 H33 N10 O8 Si
	461.2260	-0.4	-0.9	13.5	1081.8	0.006	99.37	C27 H33 N2 O3 Si

Figure D.6: MS spectrum of compound **4**.

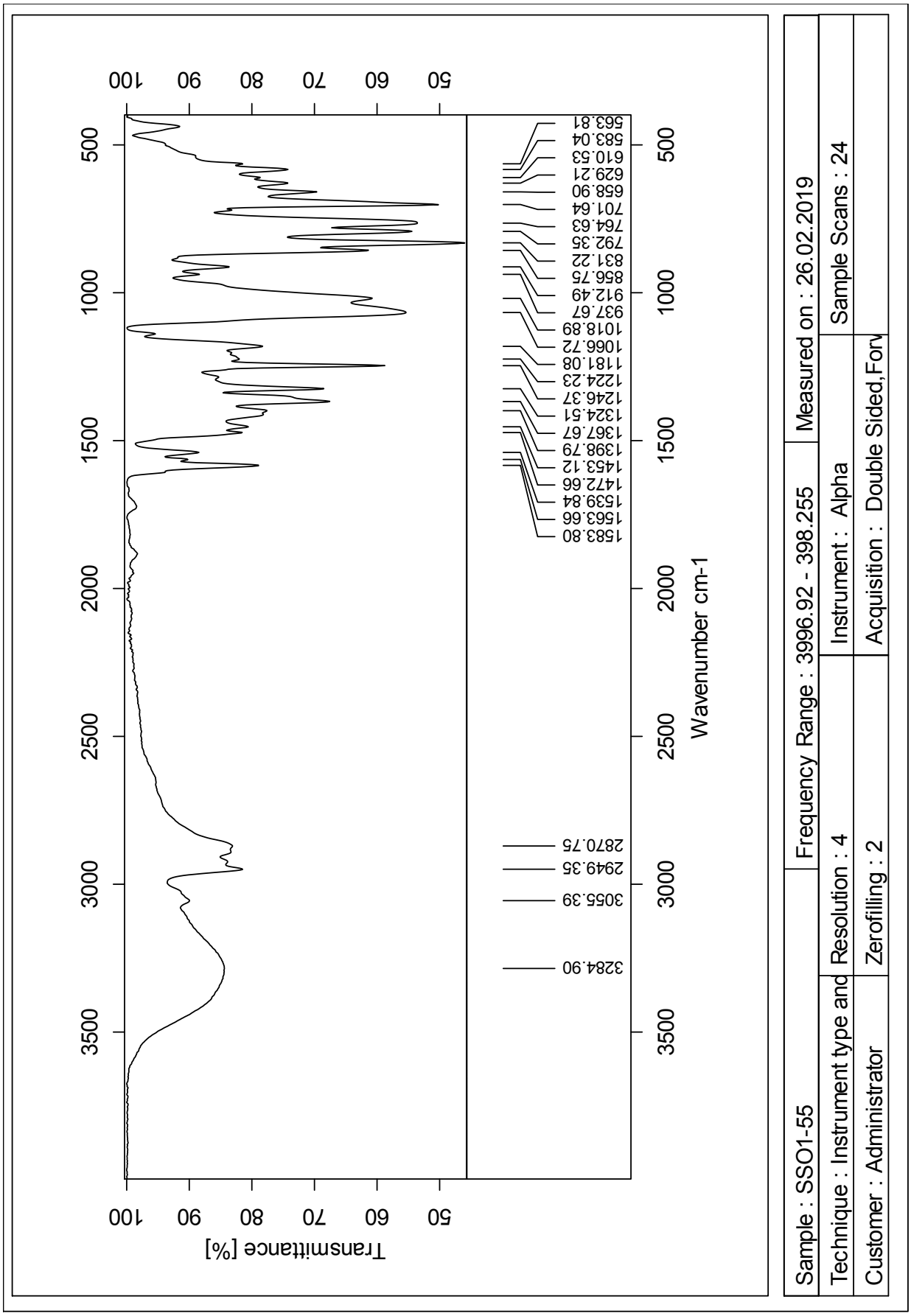

Figure D.7: IR spectrum of compound **4**.

Appendix E Compound 5

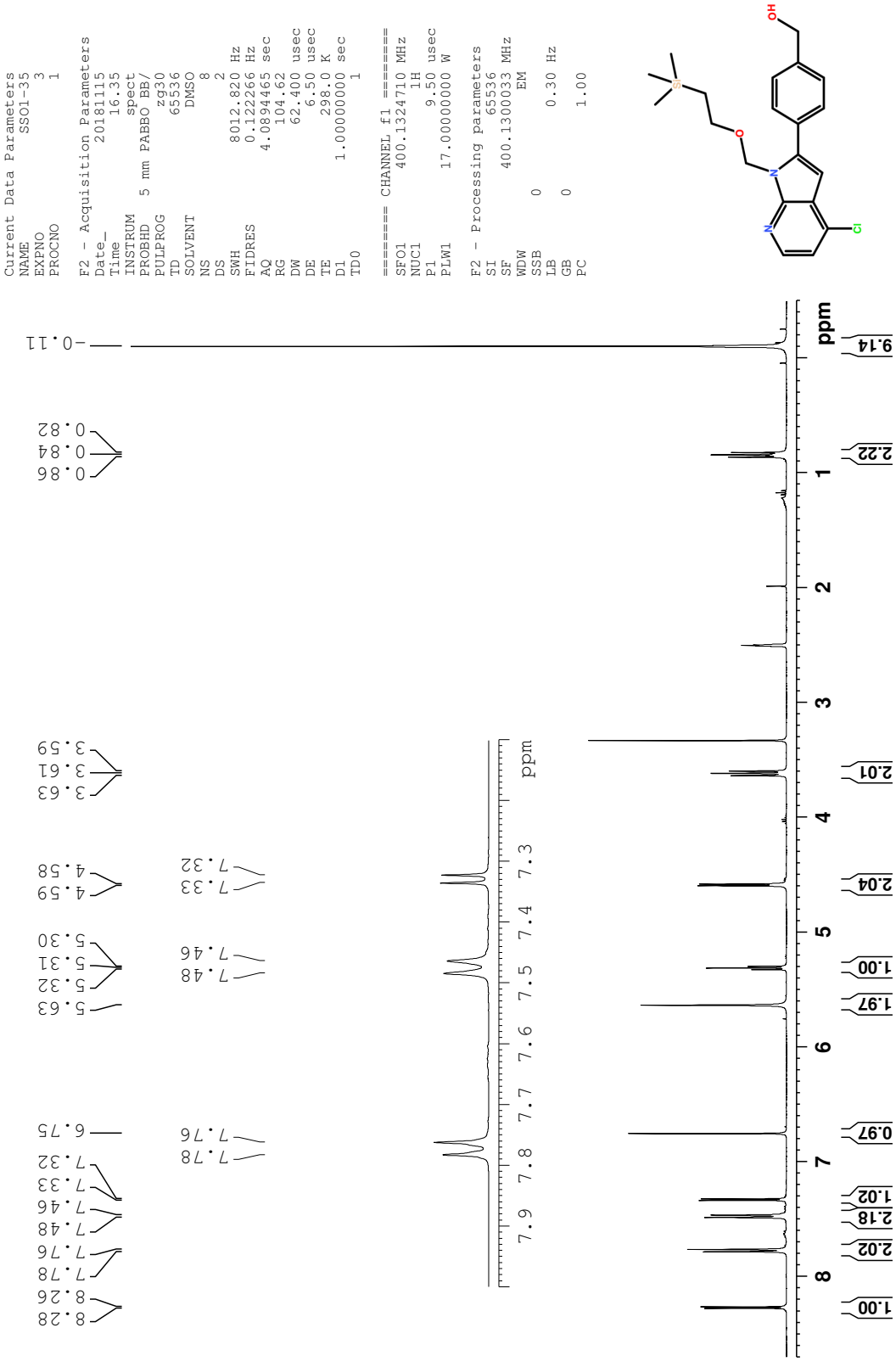

Figure E.1: ^{1}H NMR spectrum of compound **5**.

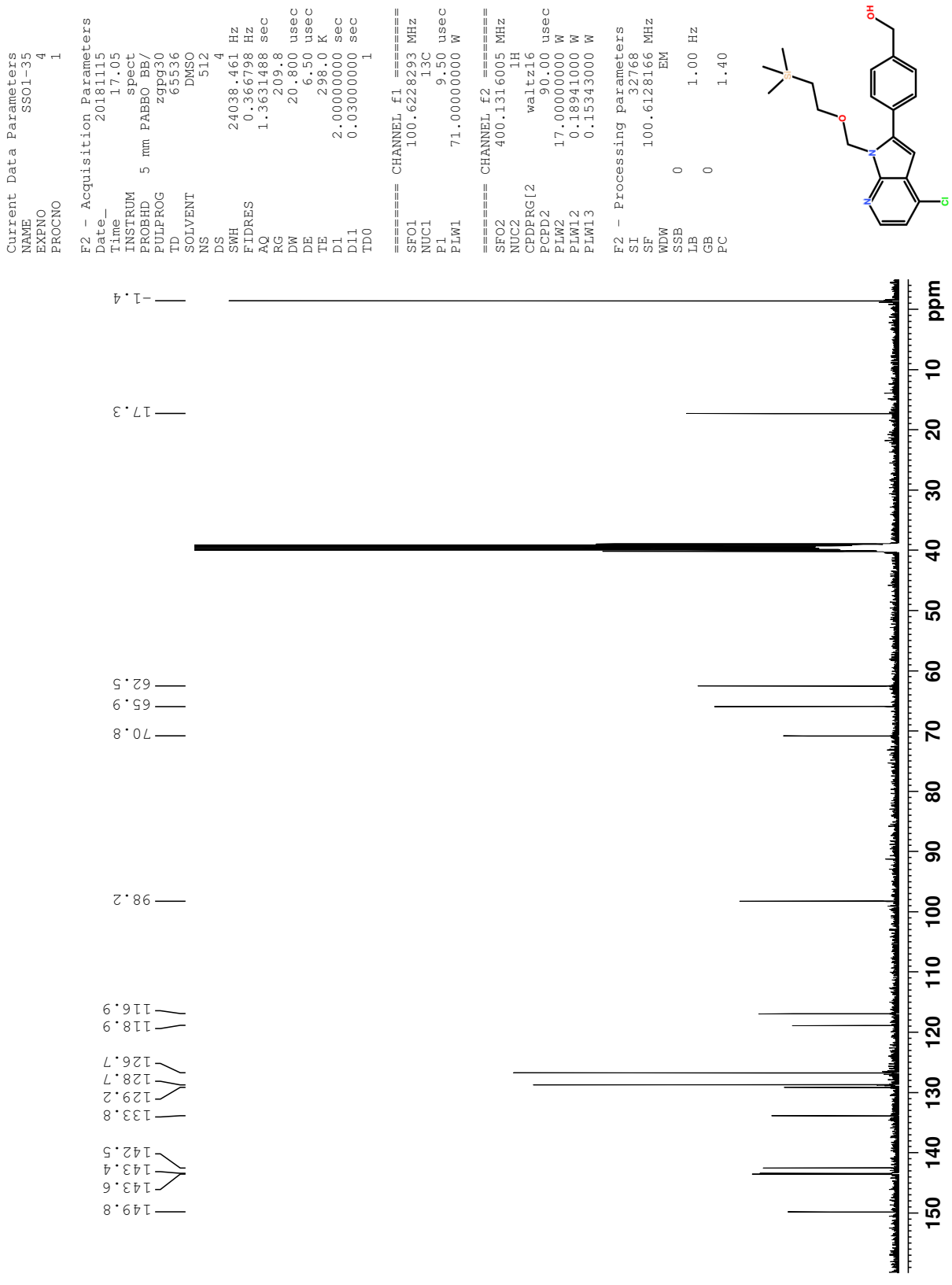

Figure E.2: ^{13}C NMR spectrum of compound **5**.

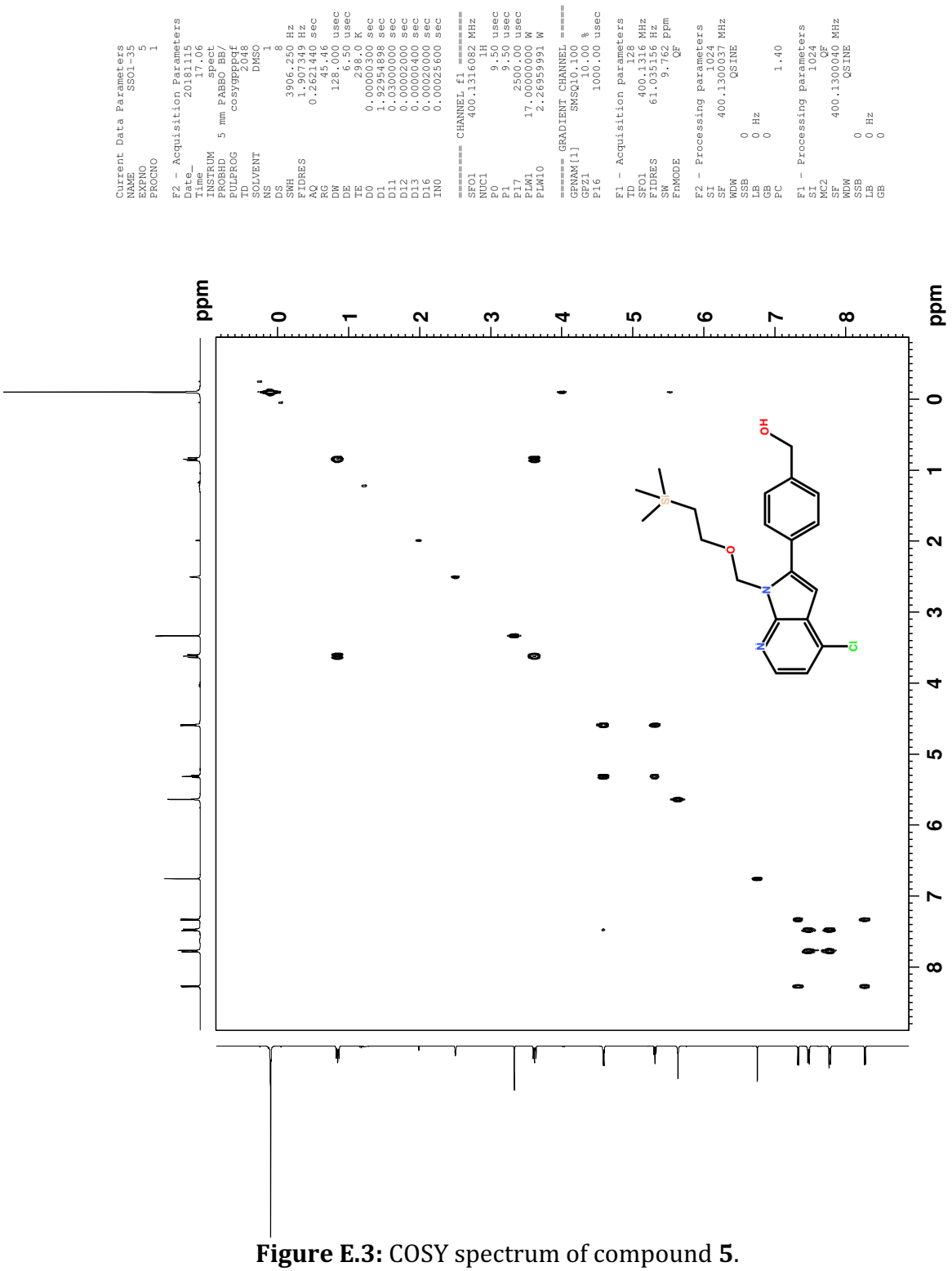

Figure E.3: COSY spectrum of compound **5**.

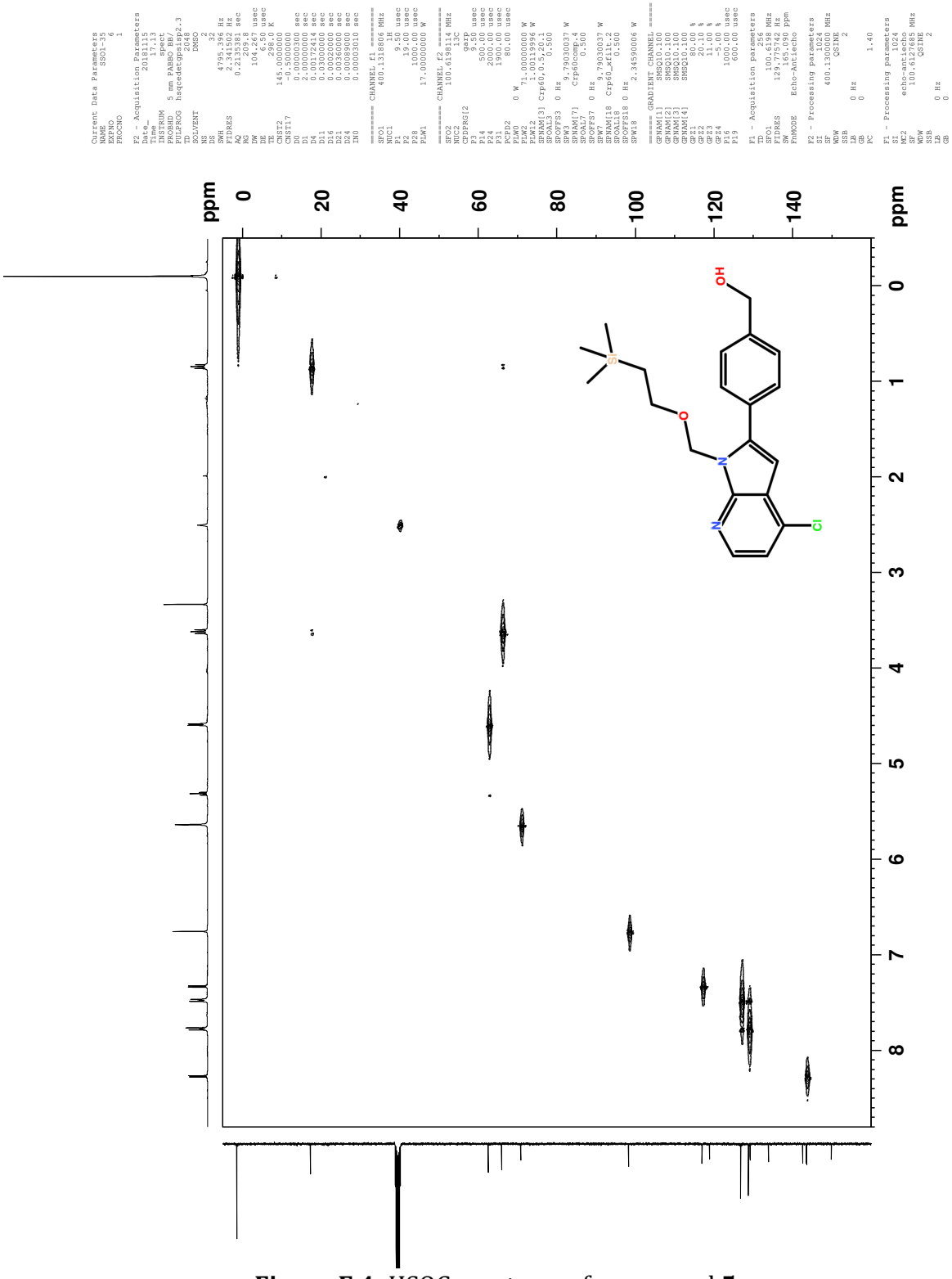

Figure E.4: HSQC spectrum of compound **5**.

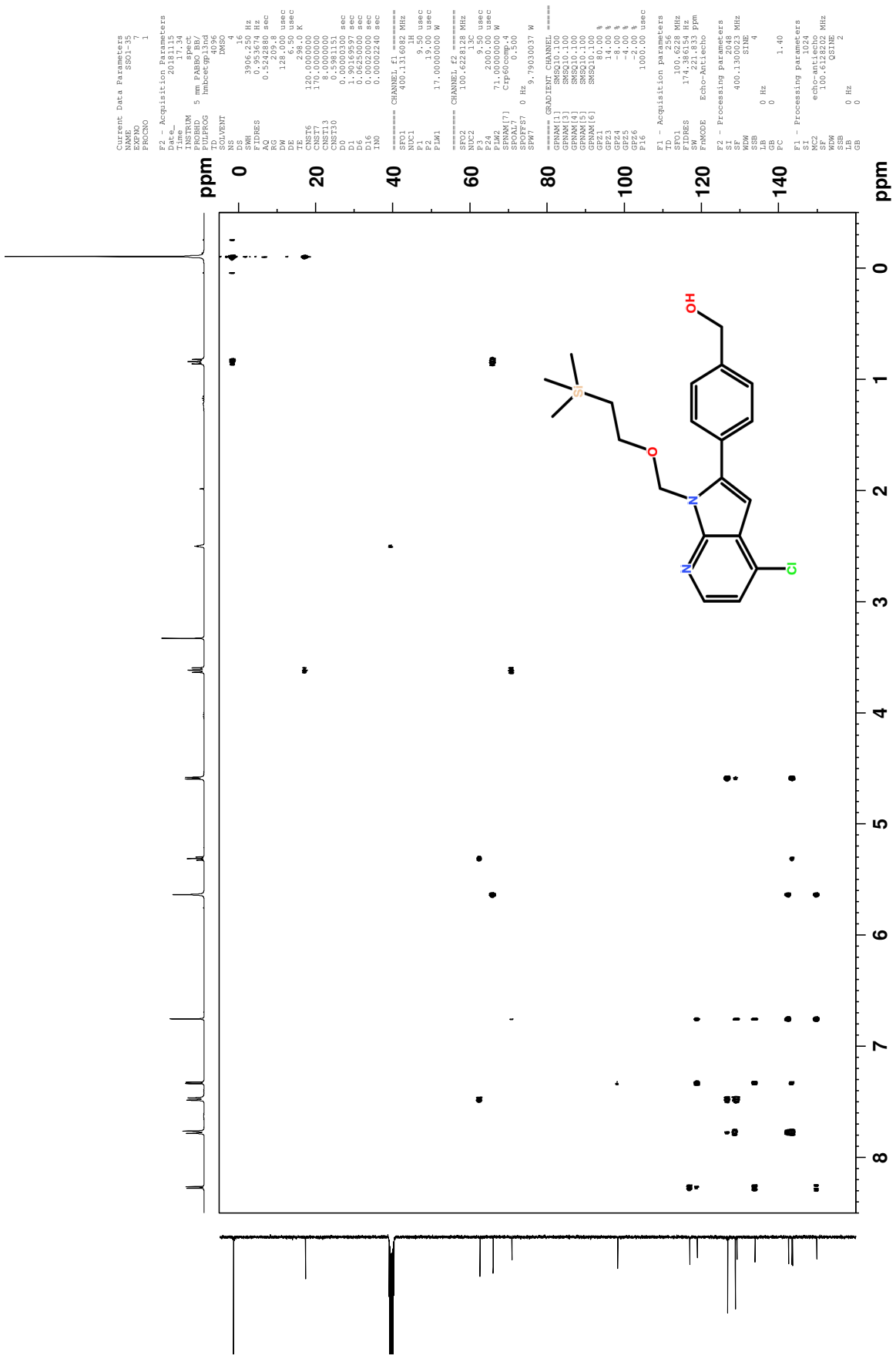

Figure E.5: HMBC spectrum of compound **5**.

Elemental Composition Report **Page 1**

Single Mass Analysis
Tolerance = 2.0 PPM / DBE: min = -2.0, max = 50.0
Element prediction: Off
Number of isotope peaks used for i-FIT = 3

Monoisotopic Mass, Even Electron Ions
7165 formula(e) evaluated with 10 results within limits (all results (up to 1000) for each mass)
Elements Used:
C: 0-100 H: 0-150 N: 0-10 O: 0-10 Si: 0-3 Cl: 0-3 Au: 0-2

2019-13 71 (1.395) AM2 (Ar,35000.0,0.00,0.00); Cm (67:72)
1: TOF MS ASAP+

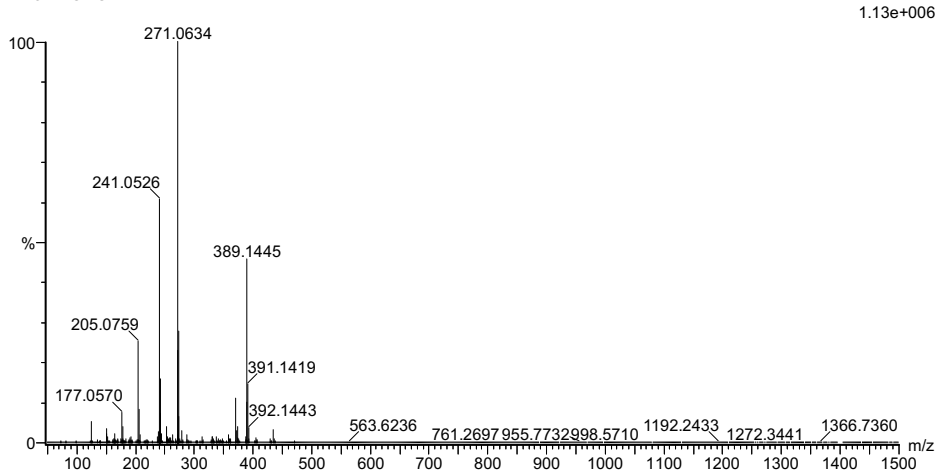

Minimum:				-2.0				
Maximum:		5.0	2.0	50.0				
Mass	Calc. Mass	mDa	PPM	DBE	i-FIT	Norm	Conf(%)	Formula
389.1445	389.1453	-0.8	-2.1	6.5	1073.1	0.685	50.41	C13 H22 N8 O4 Cl
	389.1439	0.6	1.5	1.5	1073.6	1.178	30.80	C12 H26 N4 O8 Cl
	389.1443	0.2	0.5	0.5	1074.7	2.303	9.99	C11 H30 N4 O5 Si2 Cl
	389.1452	-0.7	-1.8	9.5	1075.0	2.563	7.70	C20 H26 N2 O2 Si Cl

Figure E.6: MS spectrum of compound **5**.

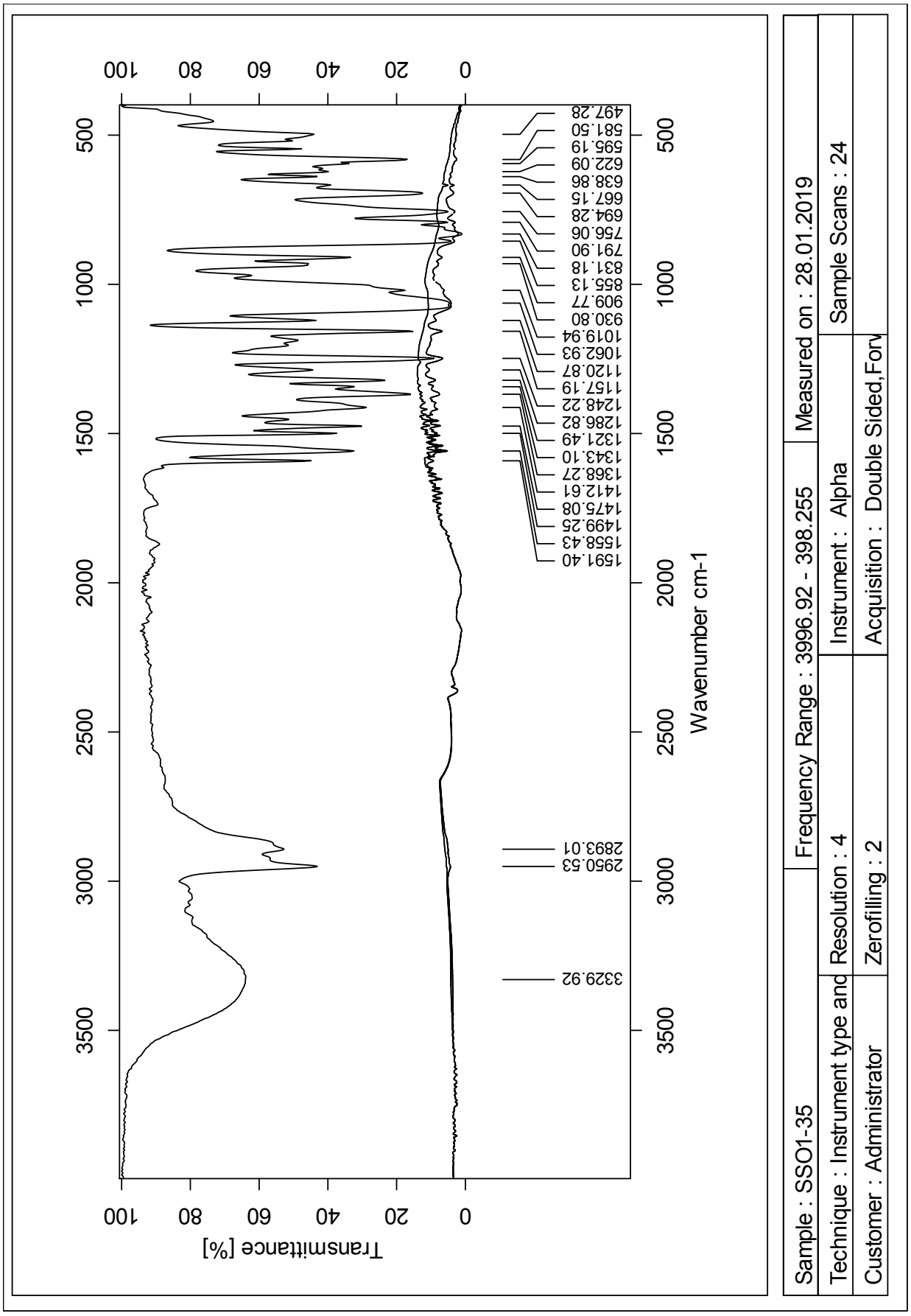

Figure E.7: IR spectrum of compound **5**.

Appendix F Compound 6

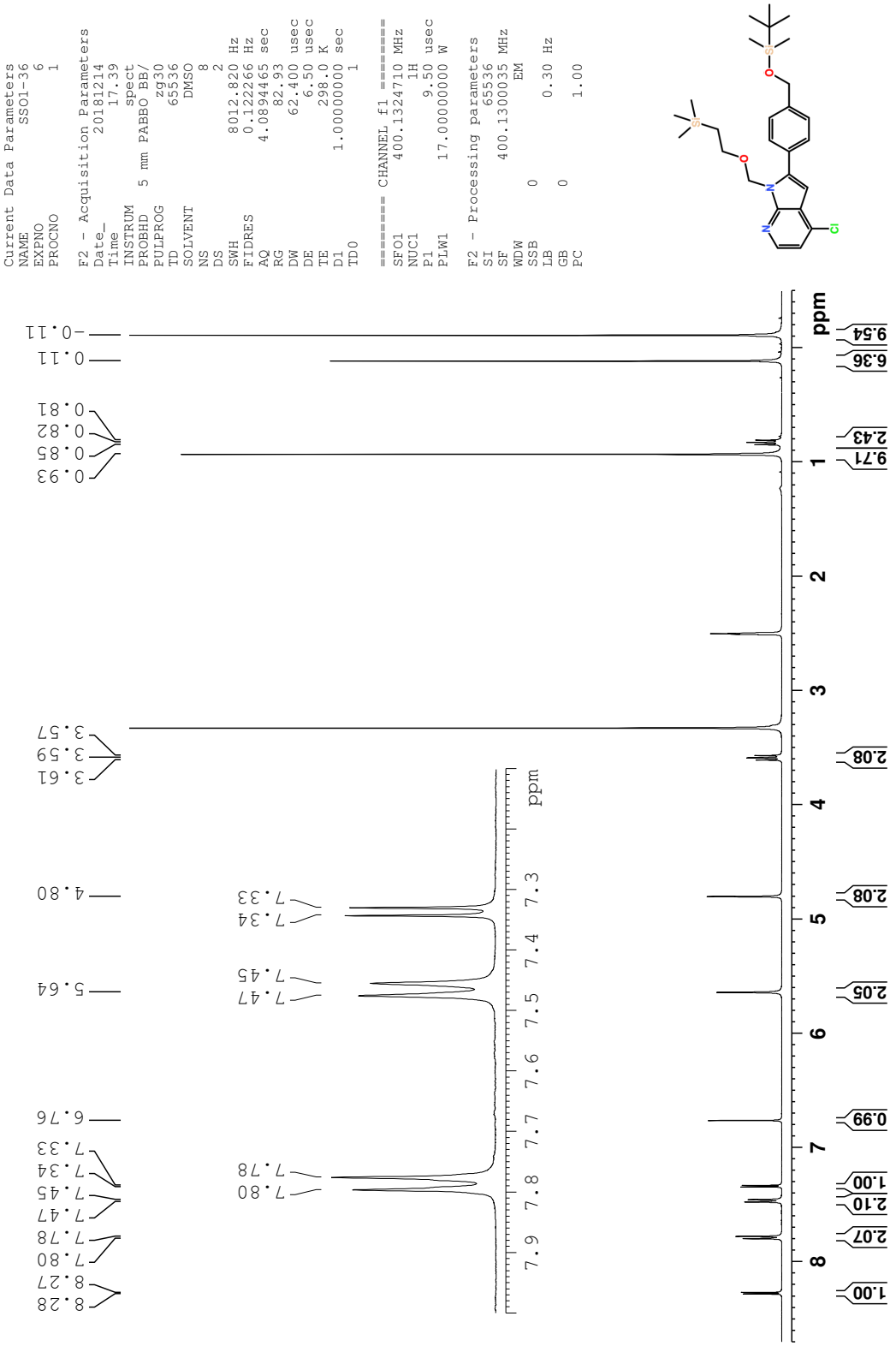

Figure F.1: ^{1}H NMR spectrum of compound **6.**

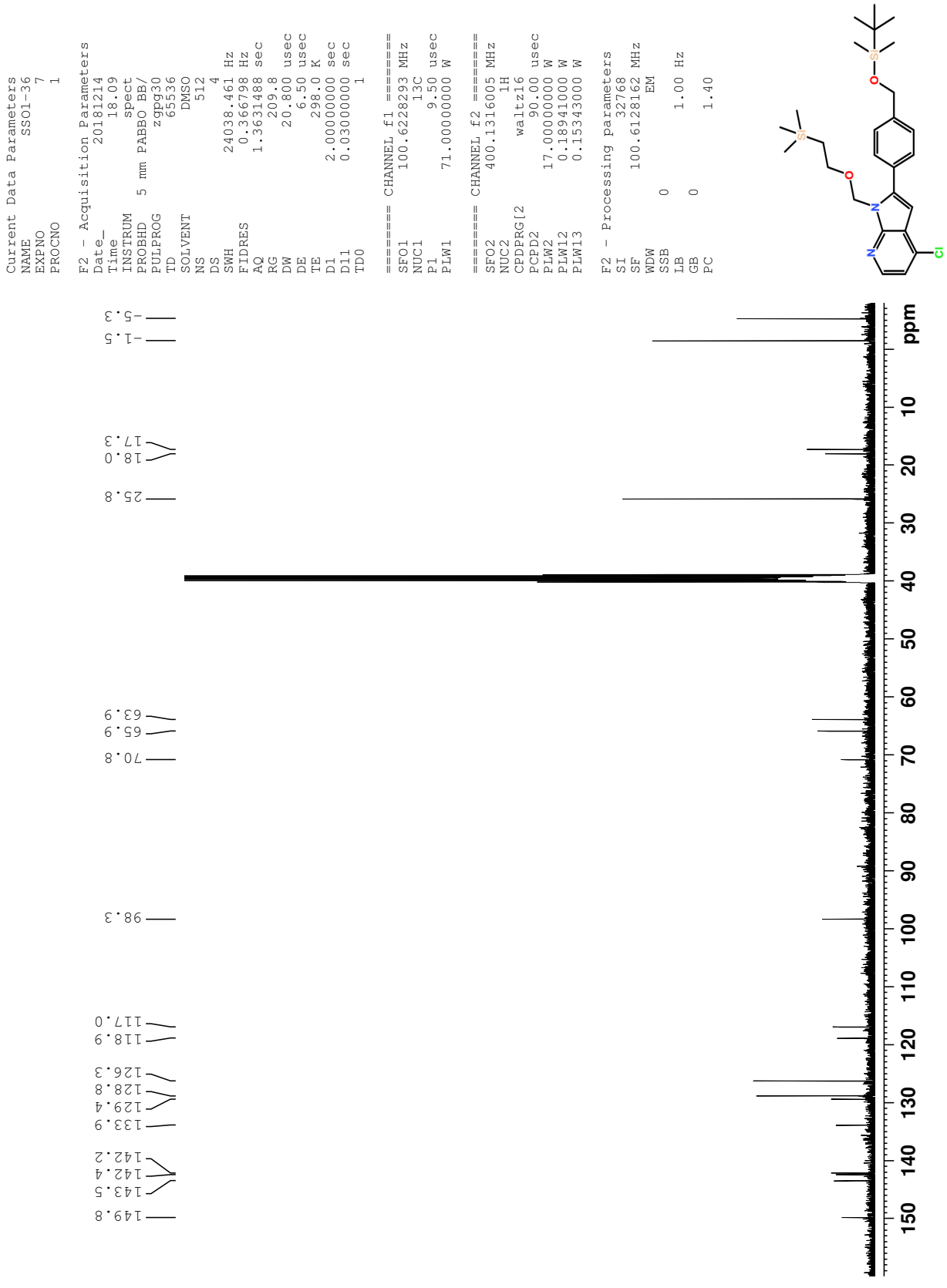

Figure F.2: ^{13}C NMR spectrum of compound **6.**

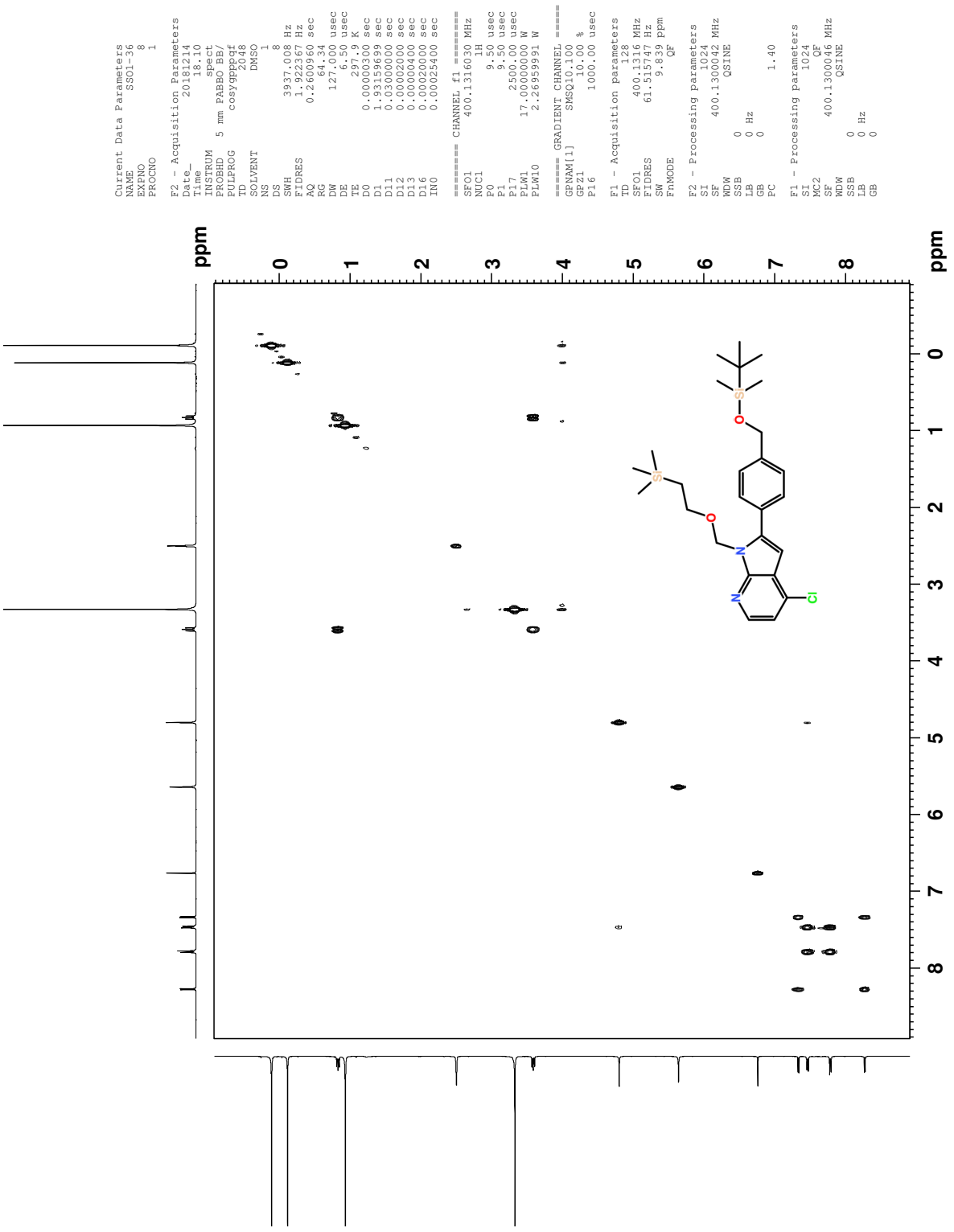

Figure F.3: COSY spectrum of compound **6.**

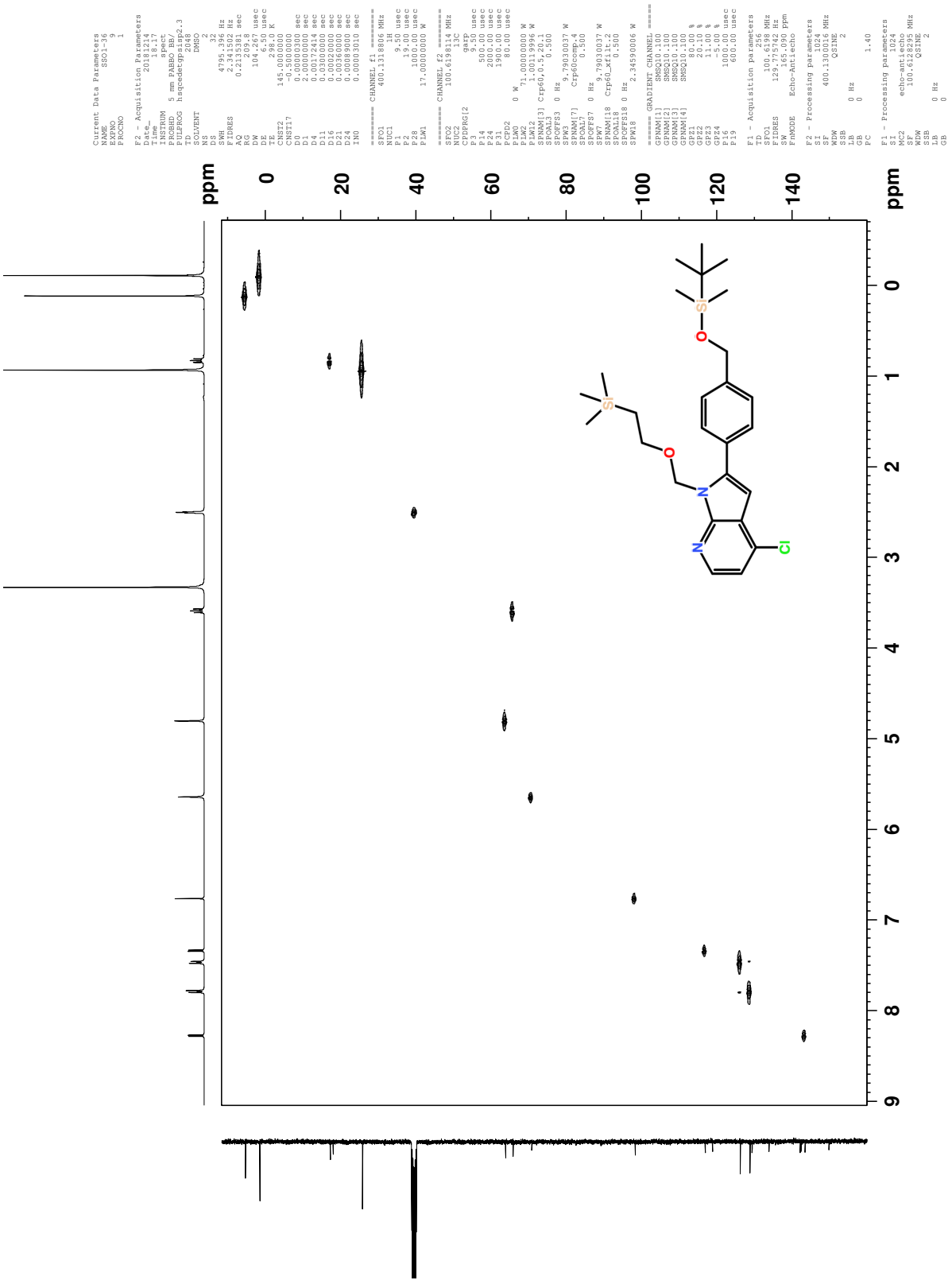

Figure F.4: HSQC spectrum of compound **6.**

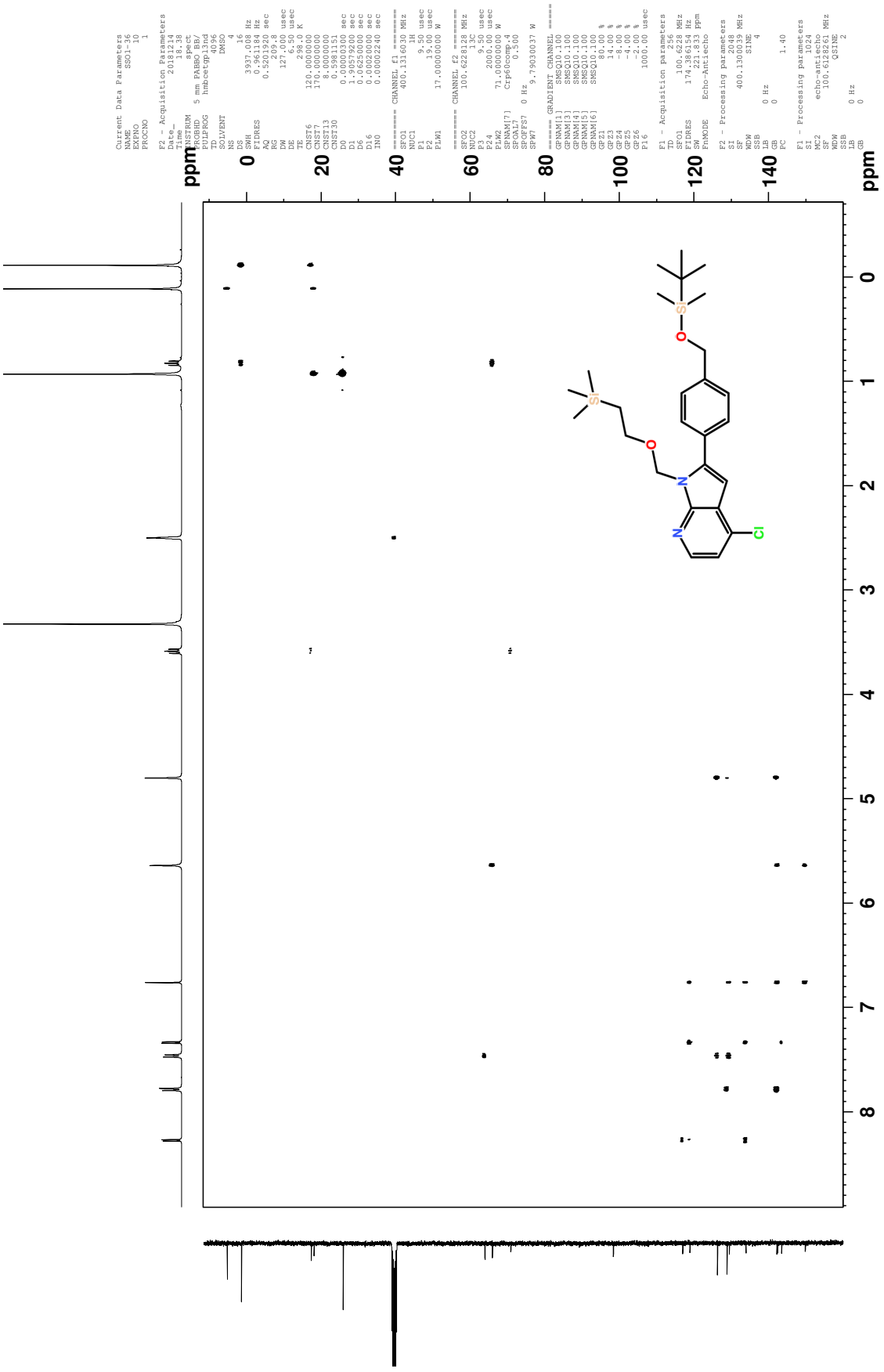

Figure F.5: HMBC spectrum of compound **6.**

Elemental Composition Report **Page 1**

Single Mass Analysis
Tolerance = 2.0 PPM / DBE: min = -2.0, max = 50.0
Element prediction: Off
Number of isotope peaks used for i-FIT = 3

Monoisotopic Mass, Even Electron Ions
8929 formula(e) evaluated with 11 results within limits (all results (up to 1000) for each mass)
Elements Used:
C: 0-100 H: 0-150 N: 0-10 O: 0-10 Si: 0-3 Cl: 0-3
2019-15 38 (0.758) AM2 (Ar,35000.0,0.00,0.00); Cm (35:38)
1: TOF MS ASAP+

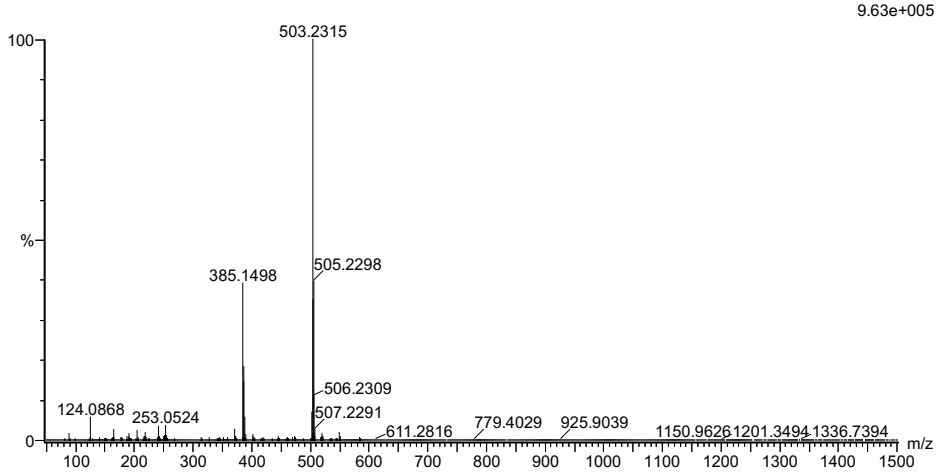

Minimum:				-2.0				
Maximum:		5.0	2.0	50.0				
Mass	Calc. Mass	mDa	PPM	DBE	i-FIT	Norm	Conf(%)	Formula
503.2315	503.2317	-0.2	-0.4	1.5	968.2	9.676	0.01	C15 H39 N6 O9 Si2
	503.2317	-0.2	-0.4	9.5	959.9	1.366	25.51	C26 H40 N2 O2 Si2 Cl
	503.2313	0.2	0.4	10.5	960.9	2.376	9.29	C27 H36 N2 O5 Cl

Figure F.6: MS spectrum of compound **6.**

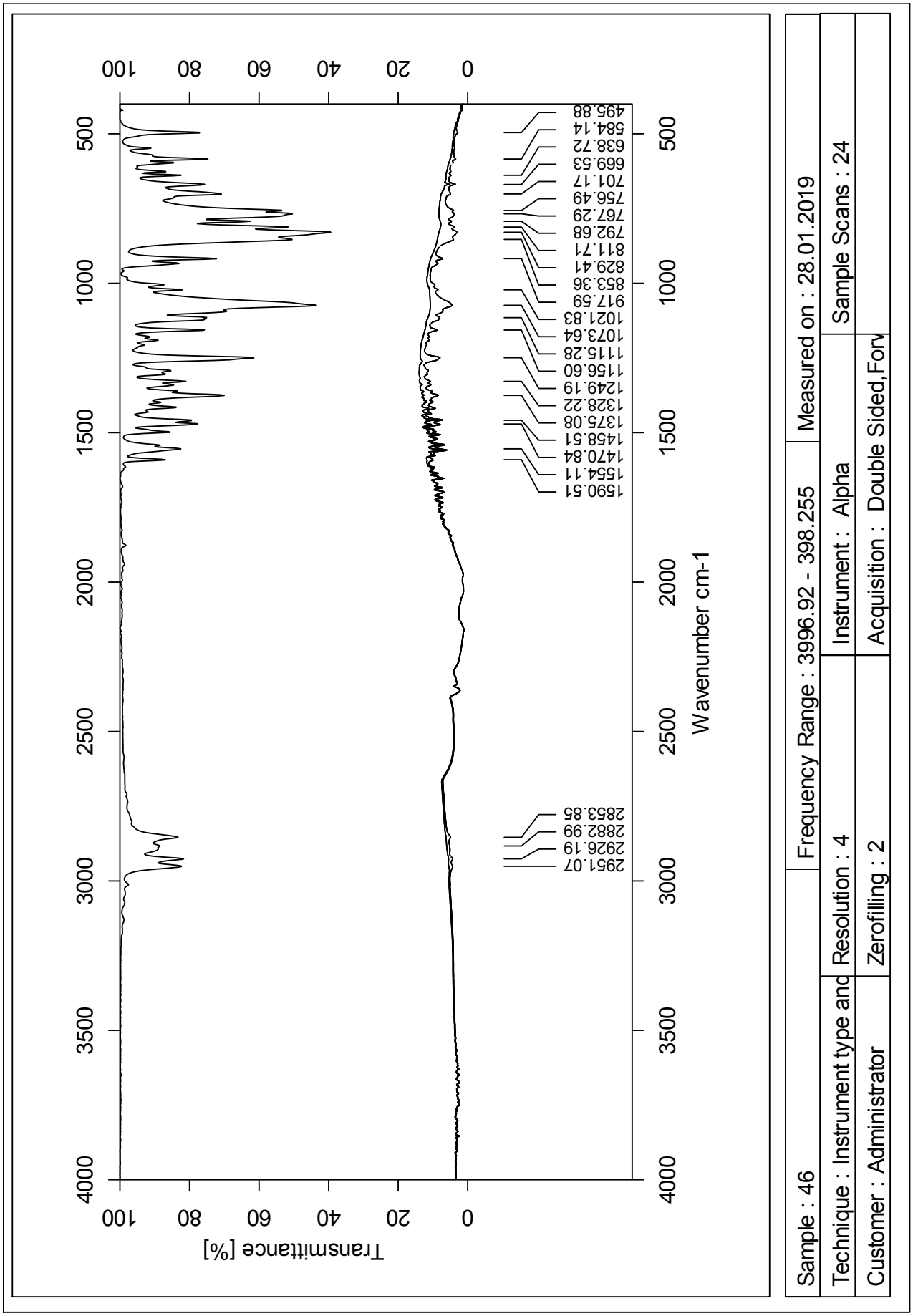

Figure F.7: IR spectrum of compound **6.**

Appendix G Compound 7

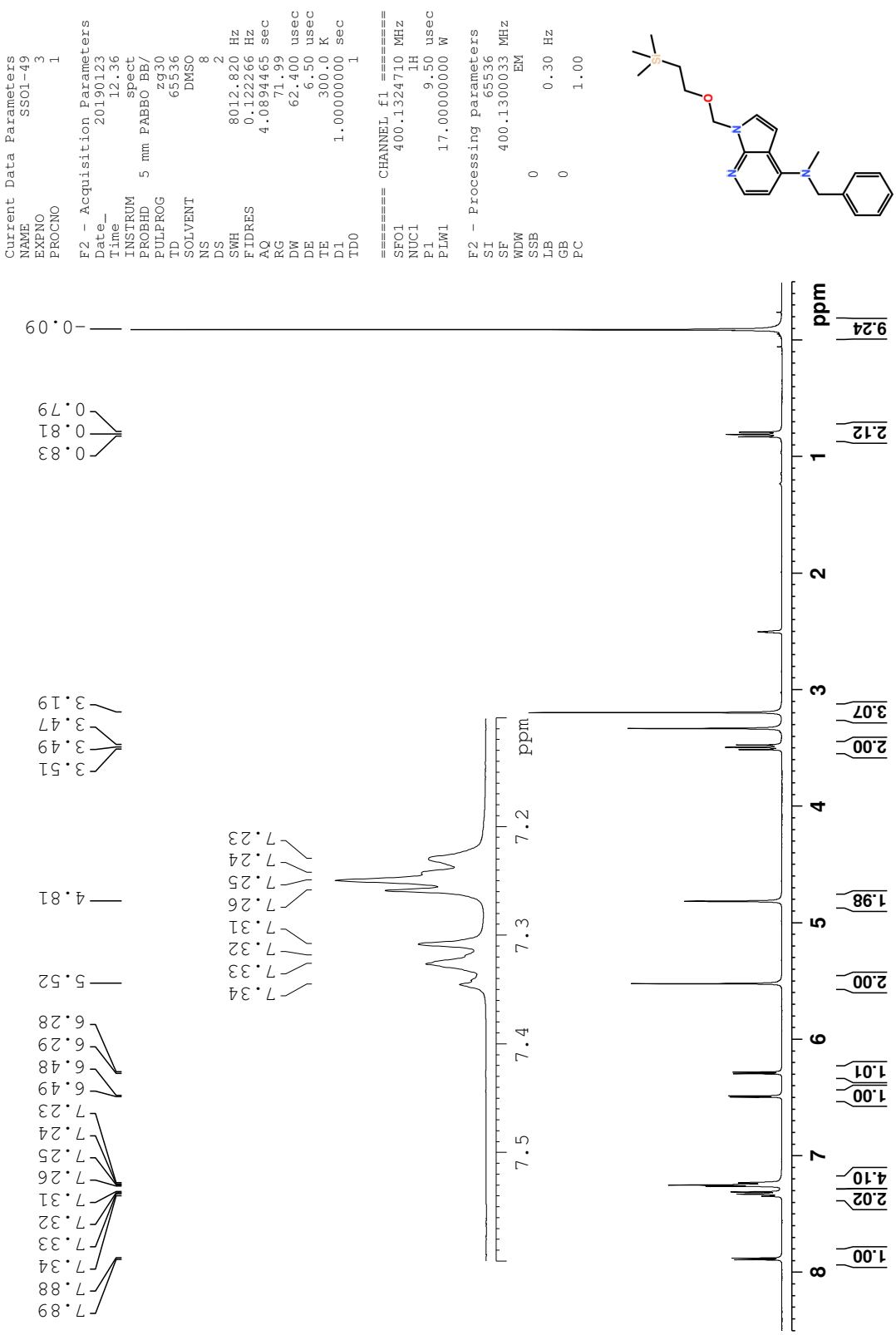

Figure G.1: ^{1}H NMR spectrum of compound **7.**

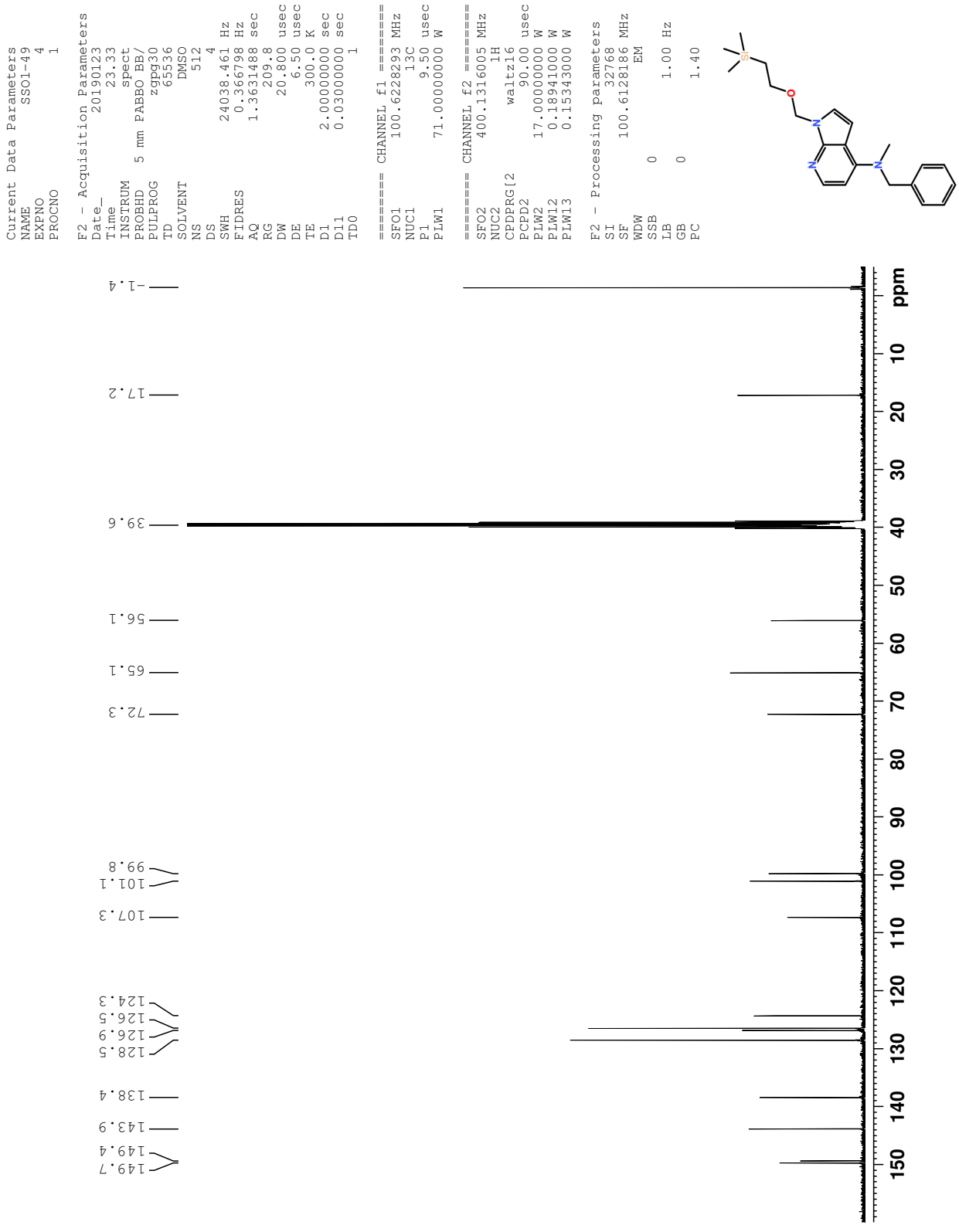

Figure G.2: ^{13}C NMR spectrum of compound **7.**

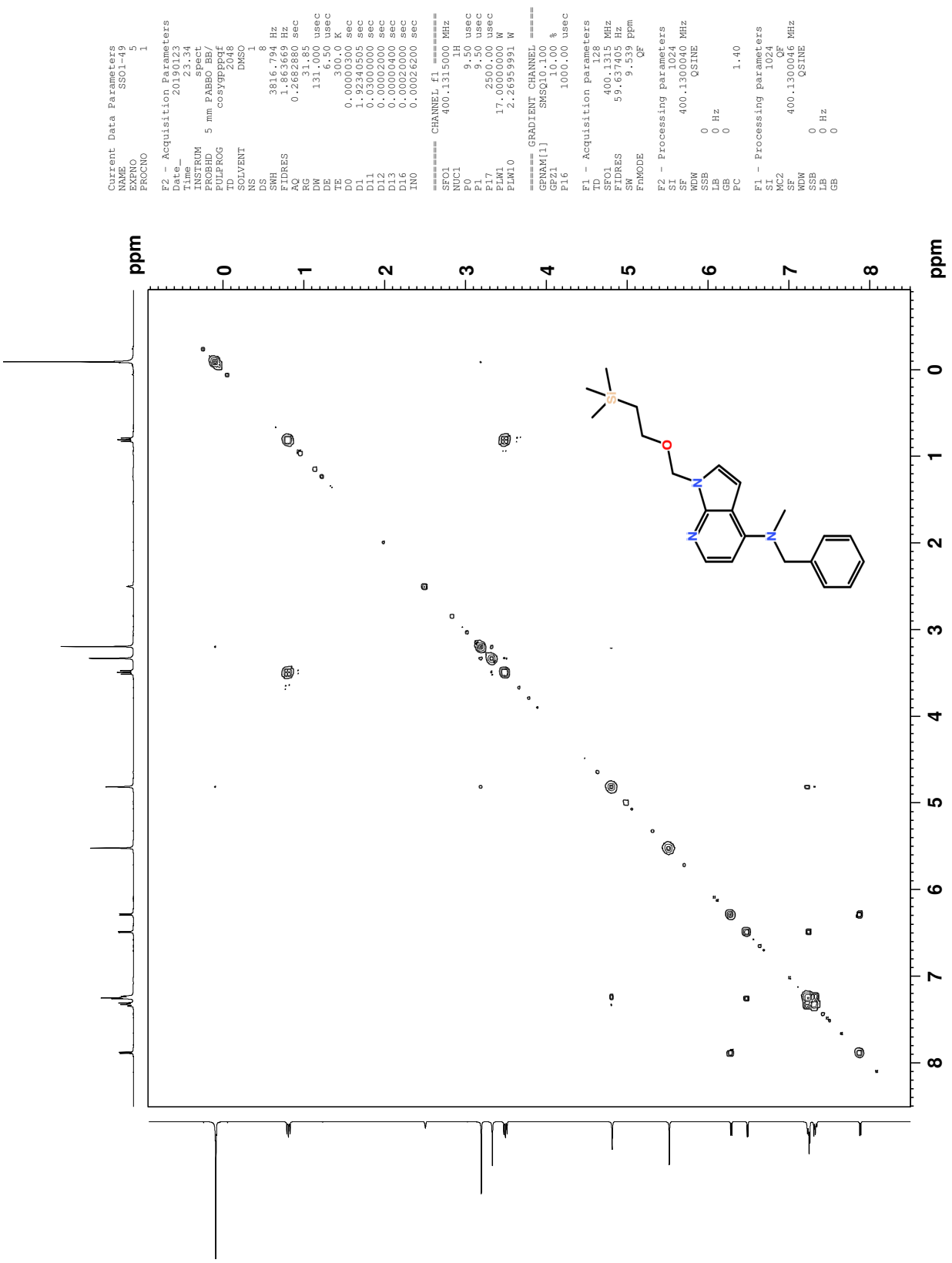

Figure G.3: COSY spectrum of compound **7.**

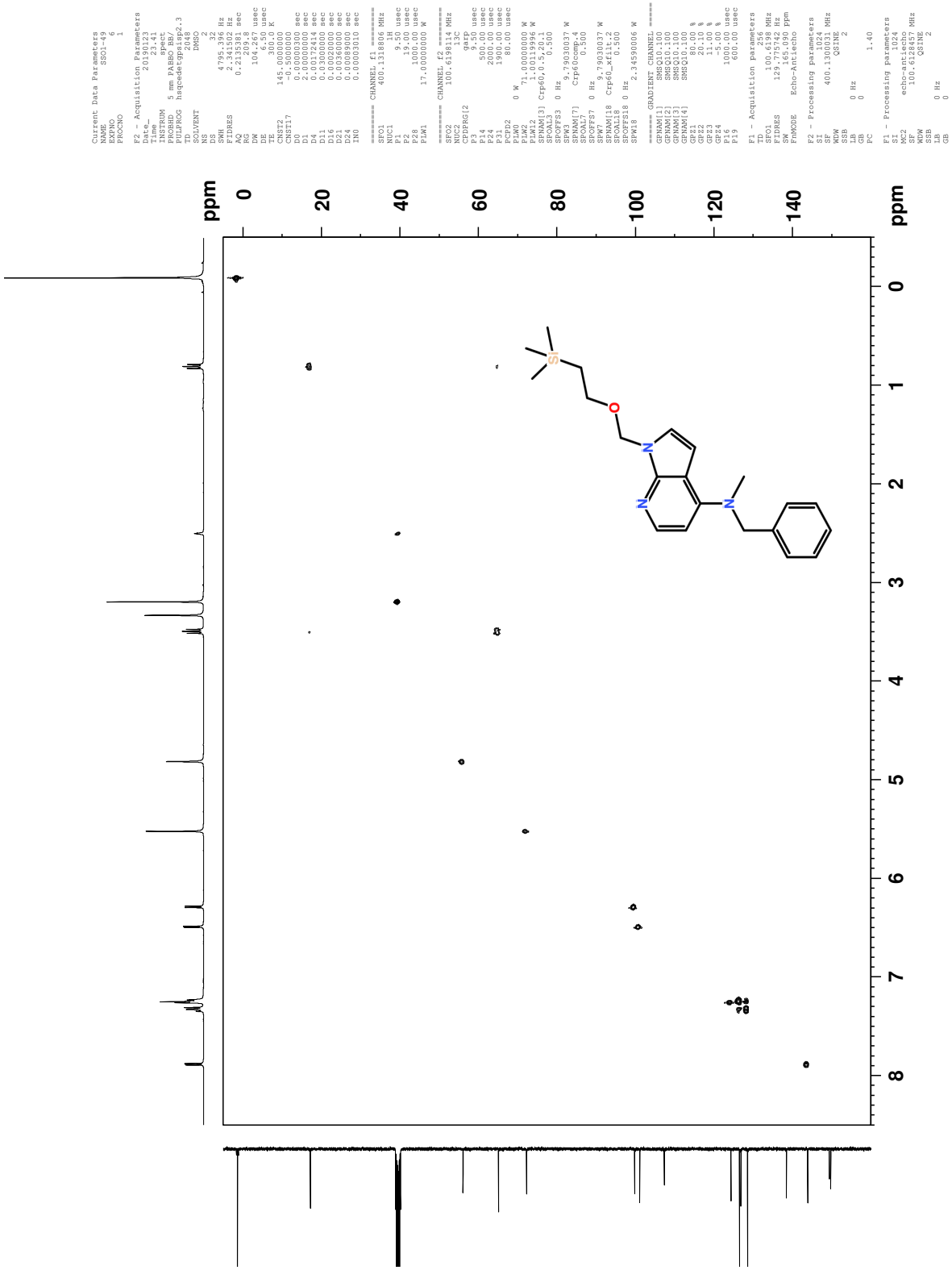

Figure G.4: HSQC spectrum of compound **7.**

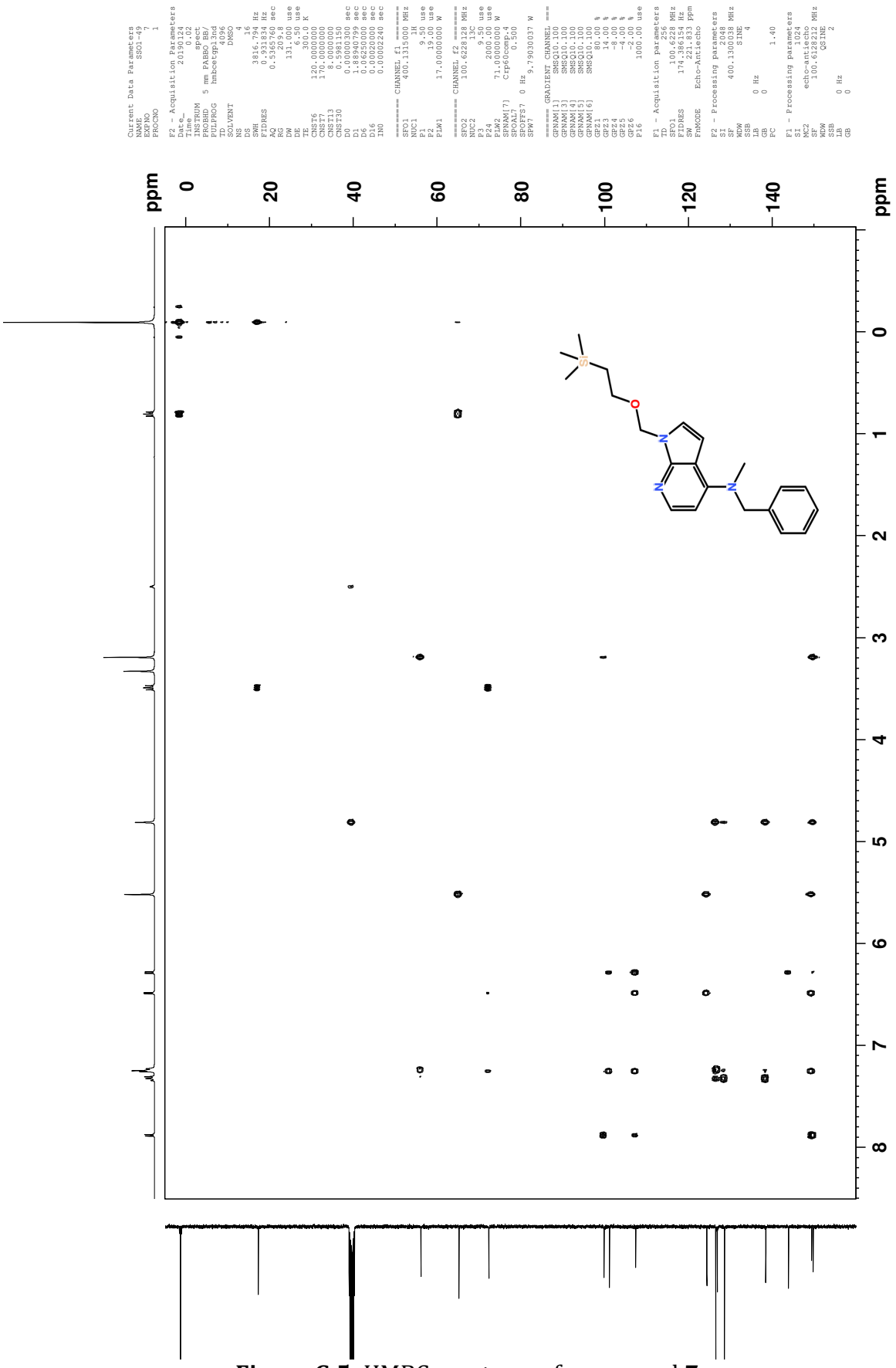

Figure G.5: HMBC spectrum of compound **7.**

Elemental Composition Report **Page 1**

Single Mass Analysis
Tolerance = 2.0 PPM / DBE: min = -2.0, max = 50.0
Element prediction: Off
Number of isotope peaks used for i-FIT = 3

Monoisotopic Mass, Even Electron Ions
3224 formula(e) evaluated with 4 results within limits (all results (up to 1000) for each mass)
Elements Used:
C: 0-100 H: 0-150 N: 0-10 O: 0-10 Na: 0-1 Au: 0-2 Si: 0-2

2019-43 43 (0.863) AM2 (Ar,35000.0,0.00,0.00); Cm (41:45)
1: TOF MS ASAP+

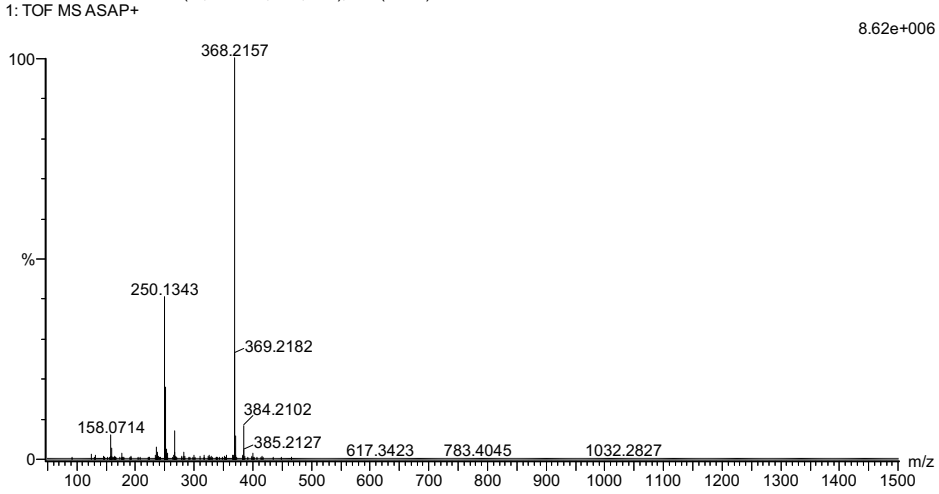

Minimum:				-2.0				
Maximum:		5.0	2.0	50.0				
Mass	Calc. Mass	mDa	PPM	DBE	i-FIT	Norm	Conf(%)	Formula
368.2157	368.2158	-0.1	-0.3	9.5	1489.8	0.000	99.97	C21 H30 N3 O Si
	368.2159	-0.2	-0.5	6.5	1500.3	10.502	0.00	C14 H26 N9 O3
	368.2161	-0.4	-1.1	2.5	1500.9	11.047	0.00	C16 H31 N3 O5 Na
	368.2163	-0.6	-1.6	5.5	1498.0	8.187	0.03	C13 H30 N9 Si2

Figure G.6: MS spectrum of compound **7.**

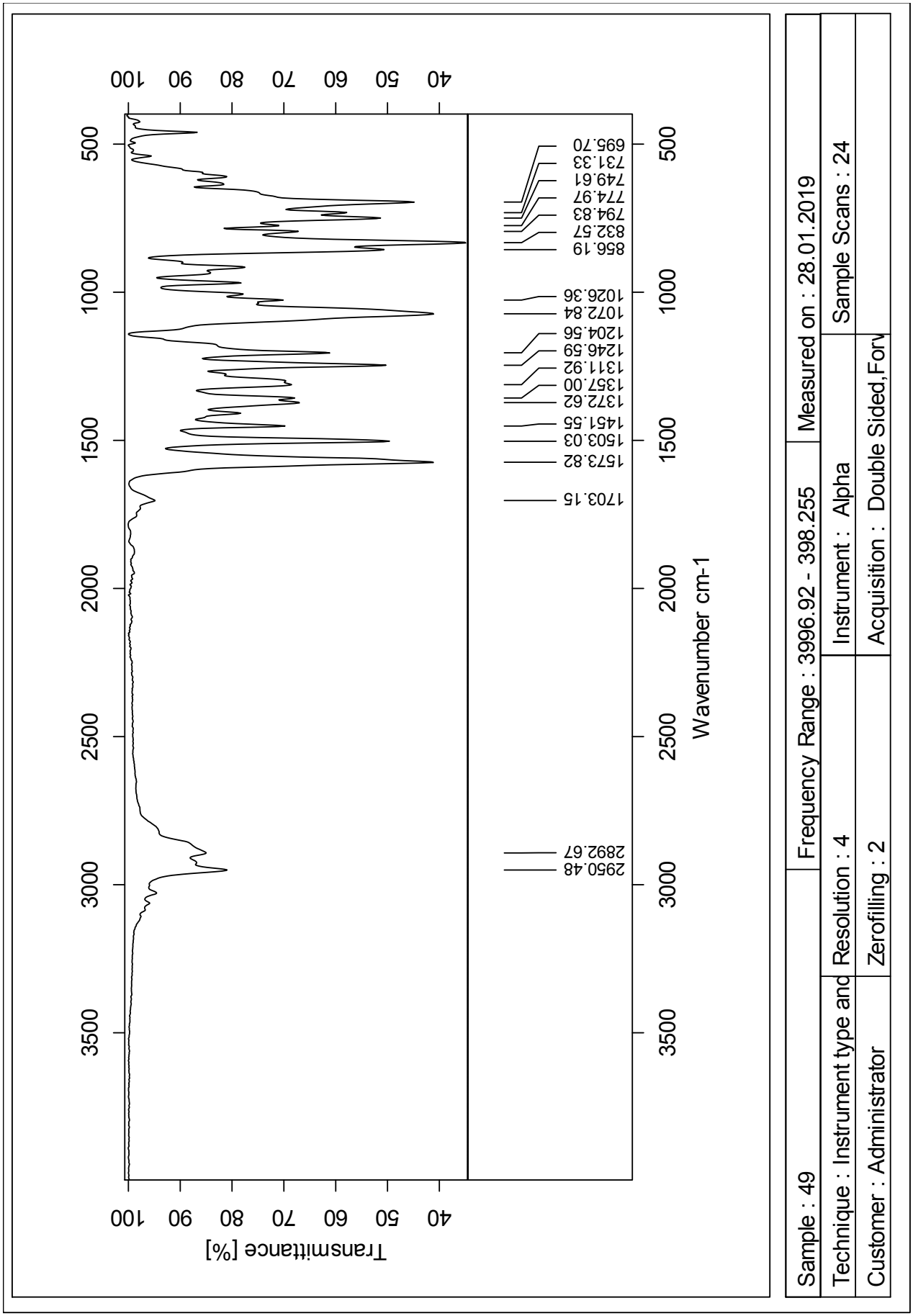

Figure G.7: IR spectrum of compound **7.**

L

Appendix H Compound 8

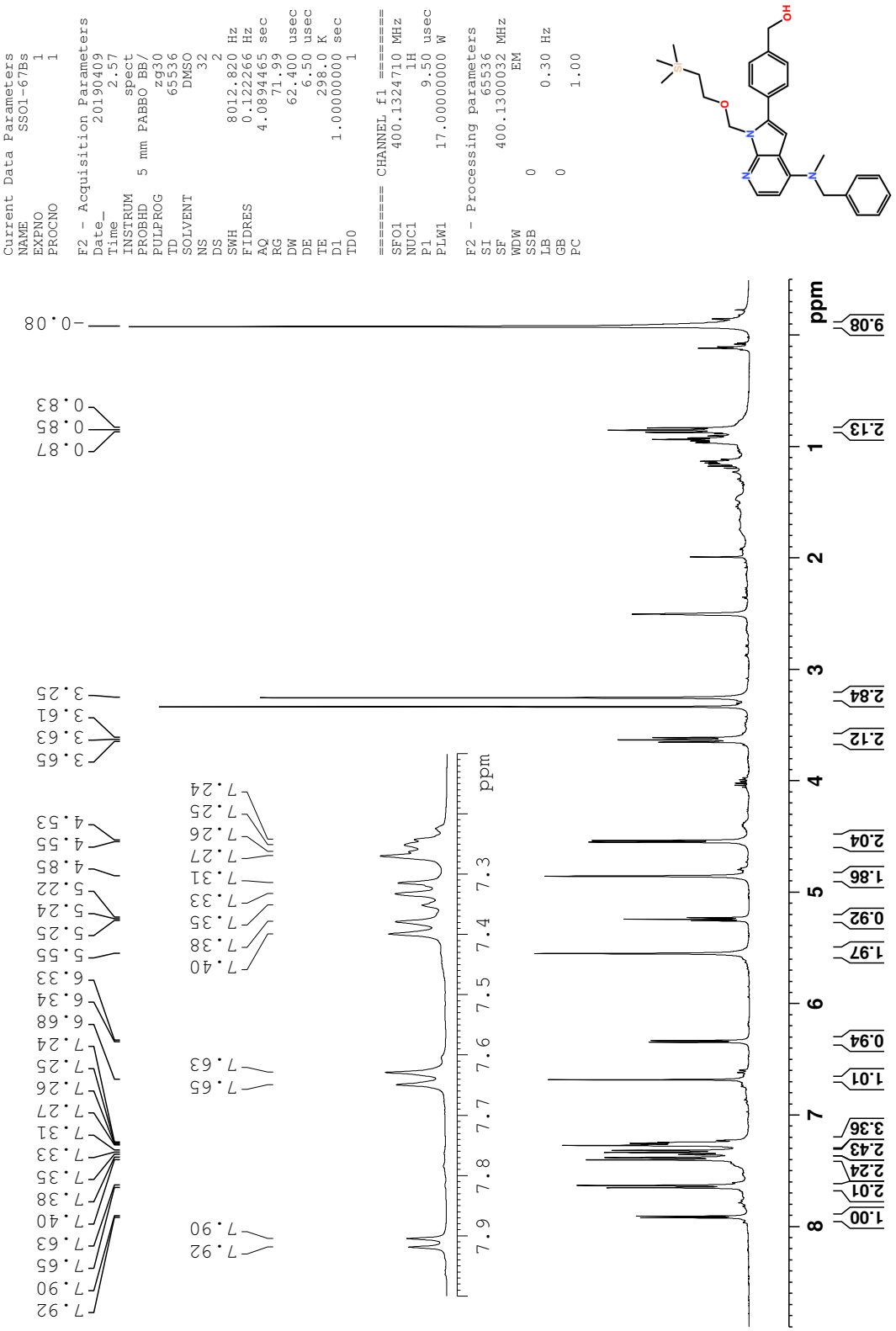

Figure H.1: ^{1}H NMR spectrum of compound **8.**

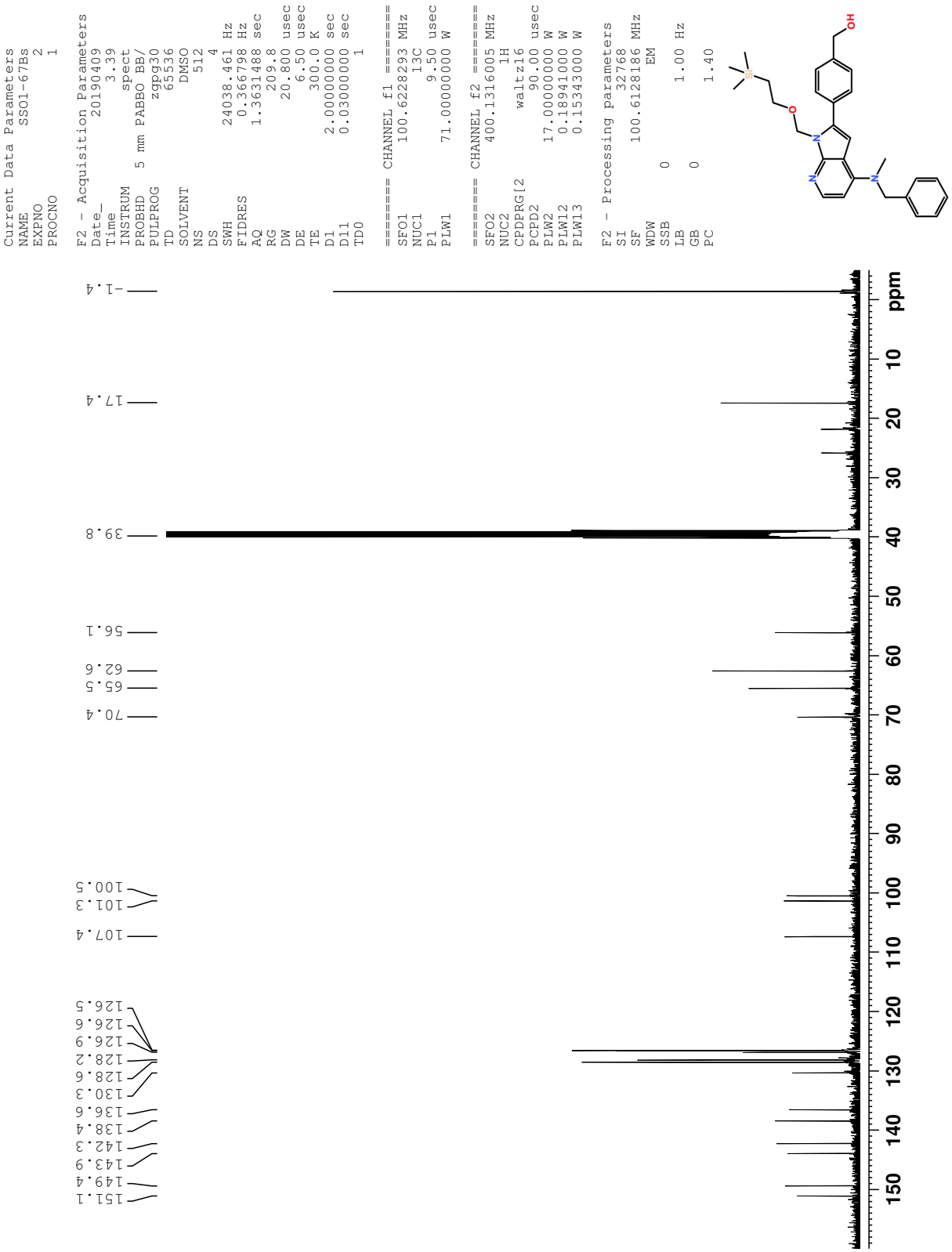

Figure H.2: ^{13}C NMR spectrum of compound **8.**

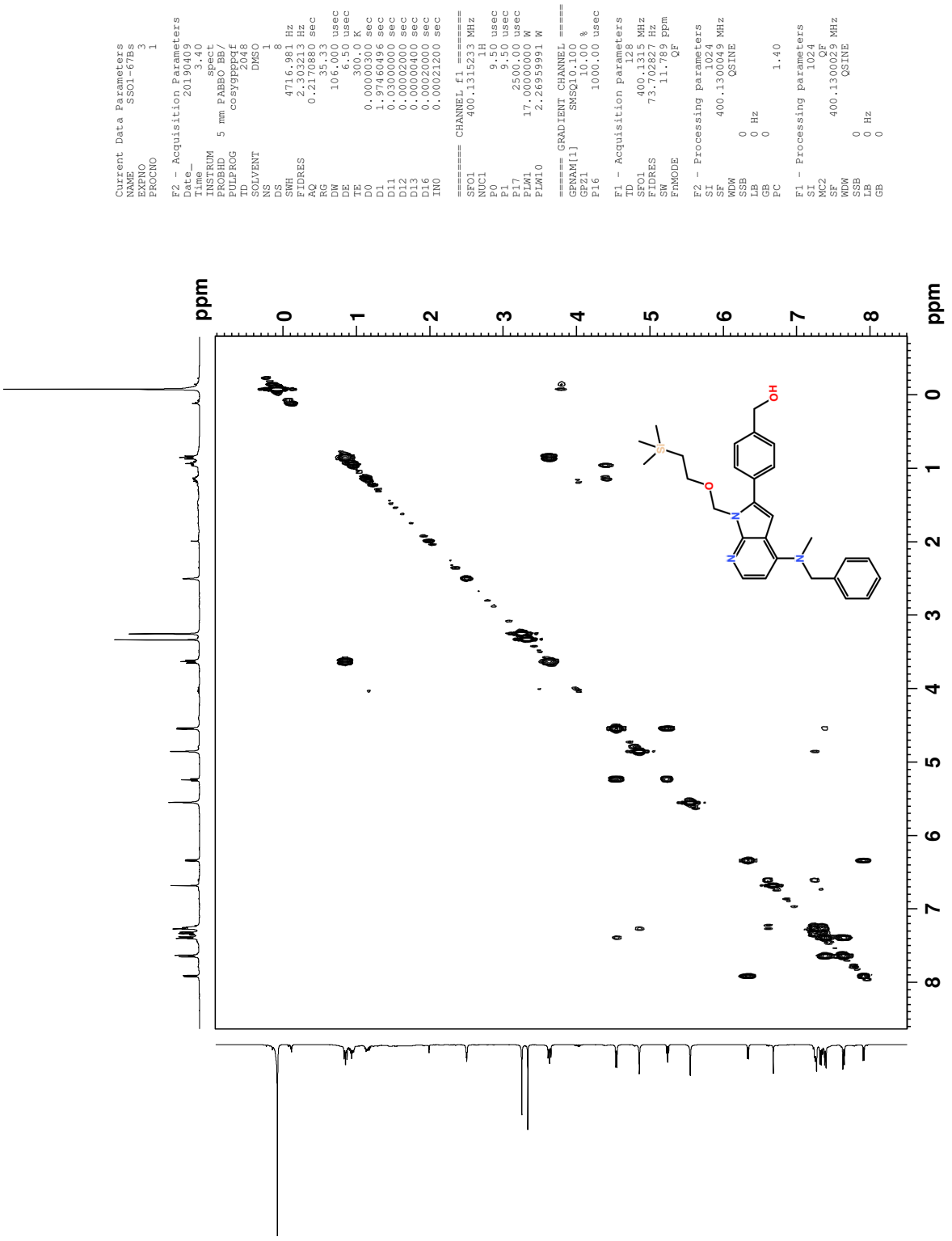

Figure H.3: COSY spectrum of compound **8.**

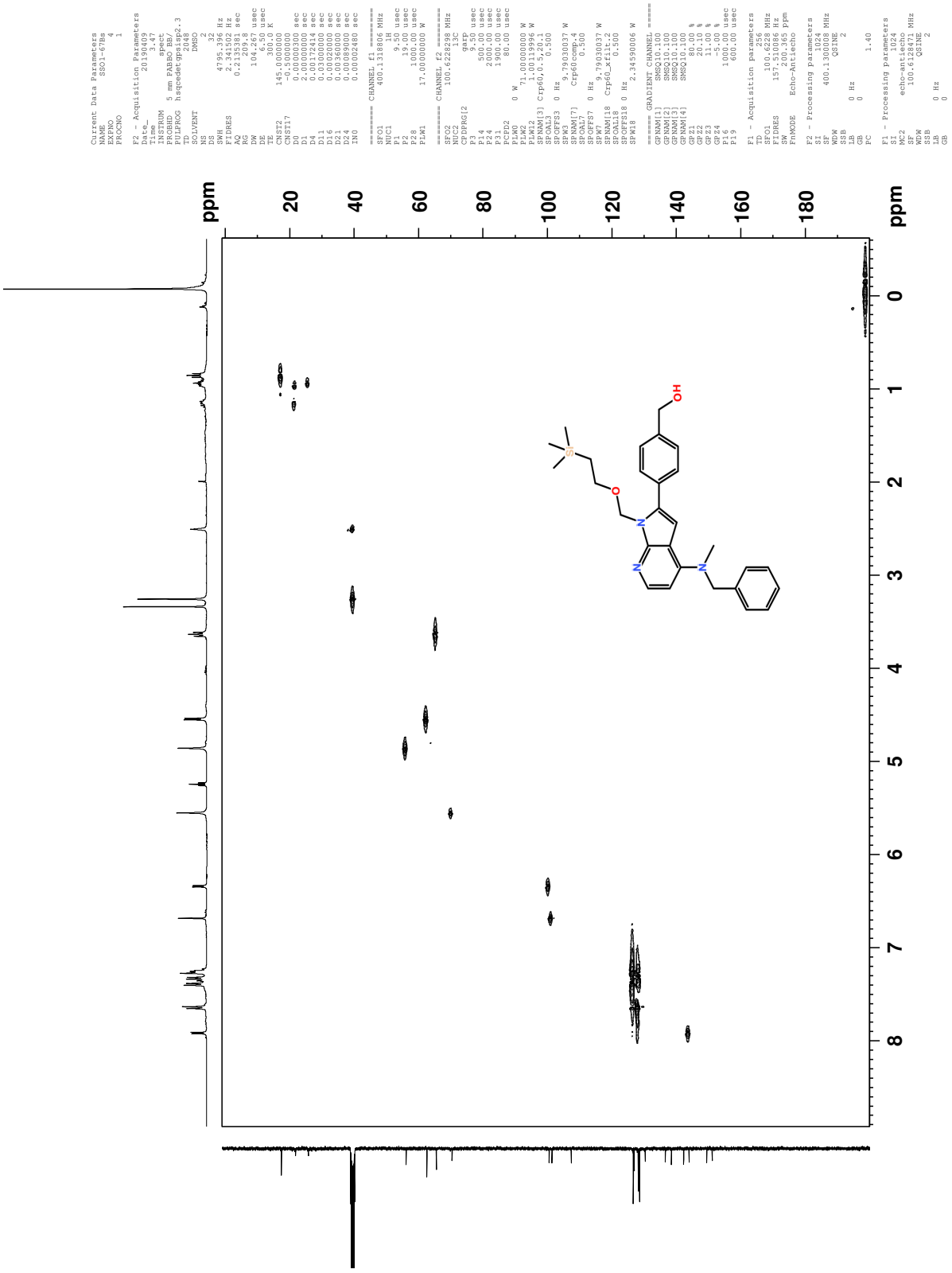

Figure H.4: HSQC spectrum of compound **8.**

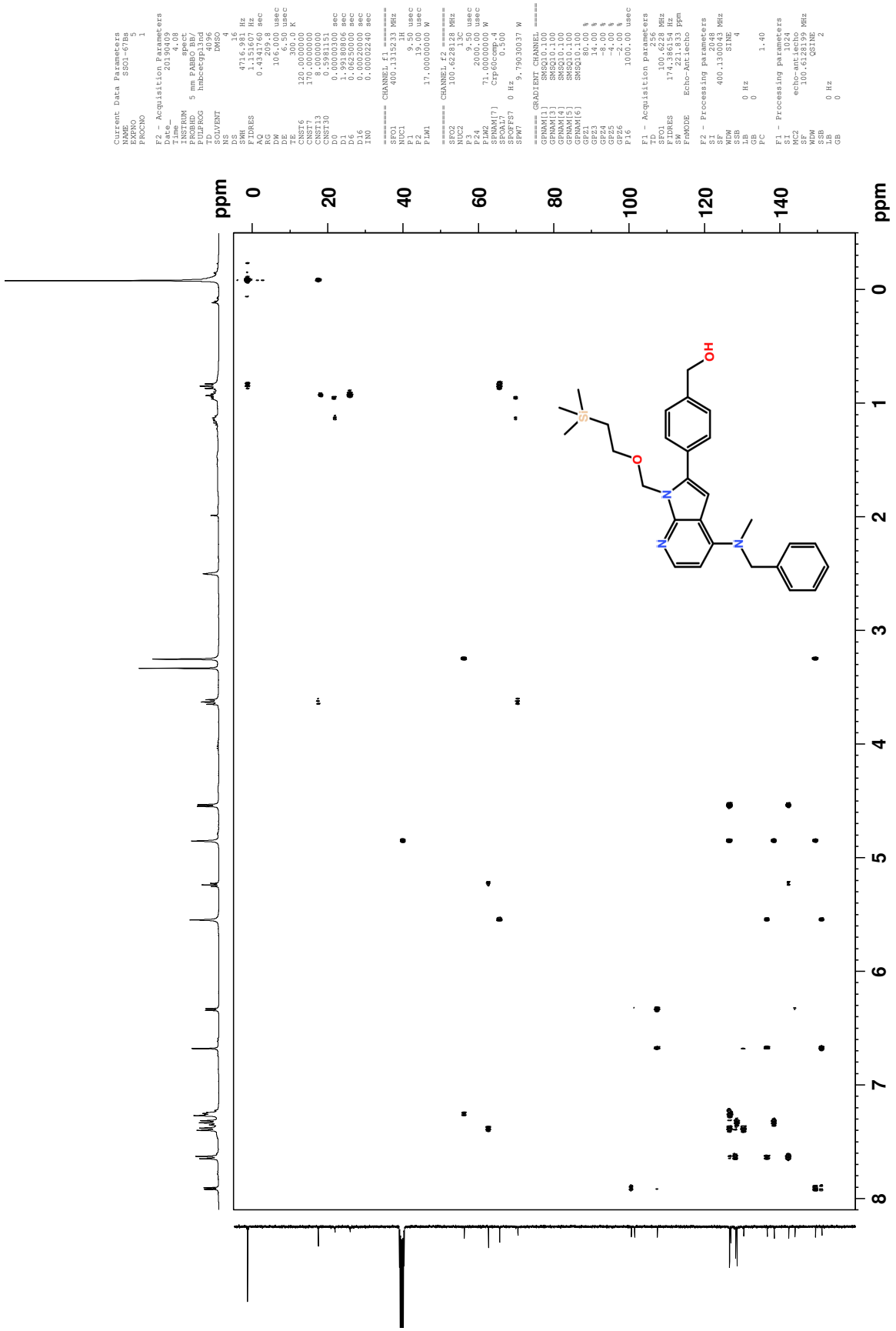

Figure H.5: HMBC spectrum of compound **8.**

Elemental Composition Report **Page 1**

Single Mass Analysis
Tolerance = 2.0 PPM / DBE: min = -50.0, max = 50.0
Element prediction: Off
Number of isotope peaks used for i-FIT = 3

Monoisotopic Mass, Even Electron Ions
2390 formula(e) evaluated with 3 results within limits (all results (up to 1000) for each mass)
Elements Used:
C: 0-100 H: 0-150 N: 0-5 O: 0-10 Si: 0-2
2019-259 173 (3.378) AM2 (Ar,35000.0,0.00,0.00); Cm (171:176)
1: TOF MS ASAP+

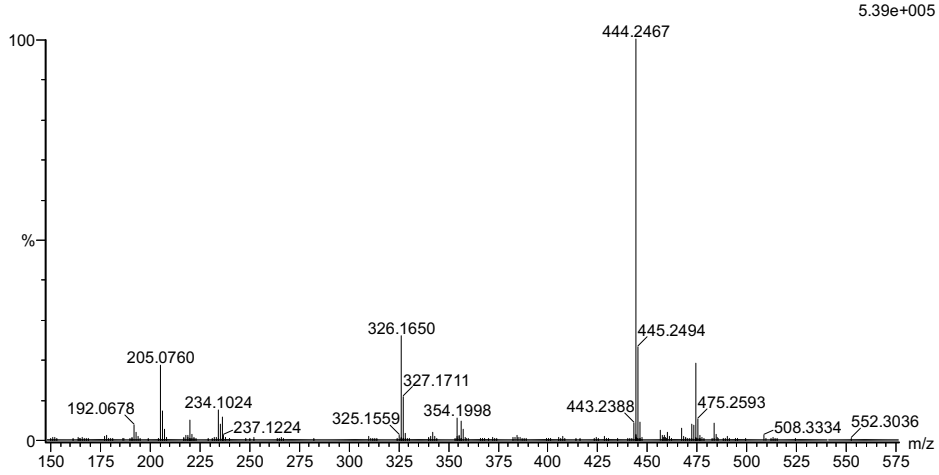

Minimum:				-50.0				
Maximum:		5.0	2.0	50.0				
Mass	Calc. Mass	mDa	PPM	DBE	i-FIT	Norm	Conf(%)	Formula
474.2571	474.2568	0.3	0.6	4.5	701.1	3.548	2.88	C19 H40 N5 O5 Si2
	474.2577	-0.6	-1.3	13.5	698.9	1.328	26.49	C28 H36 N3 O2 Si
	474.2564	0.7	1.5	5.5	697.9	0.348	70.63	C20 H36 N5 O8

Figure H.6: MS spectrum of compound **8.**

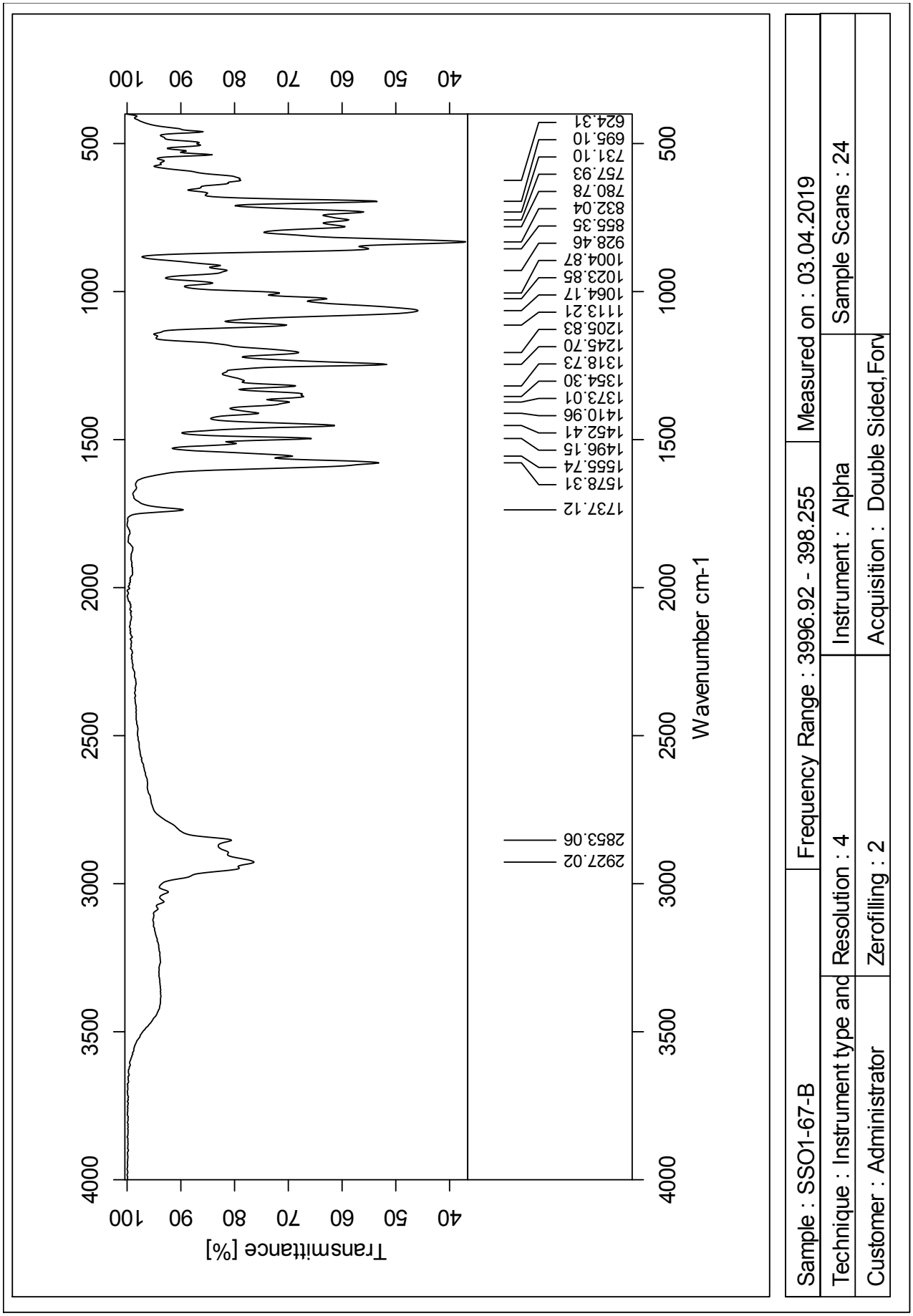

Figure H.7: IR spectrum of compound **8.**

Appendix I Compound 9

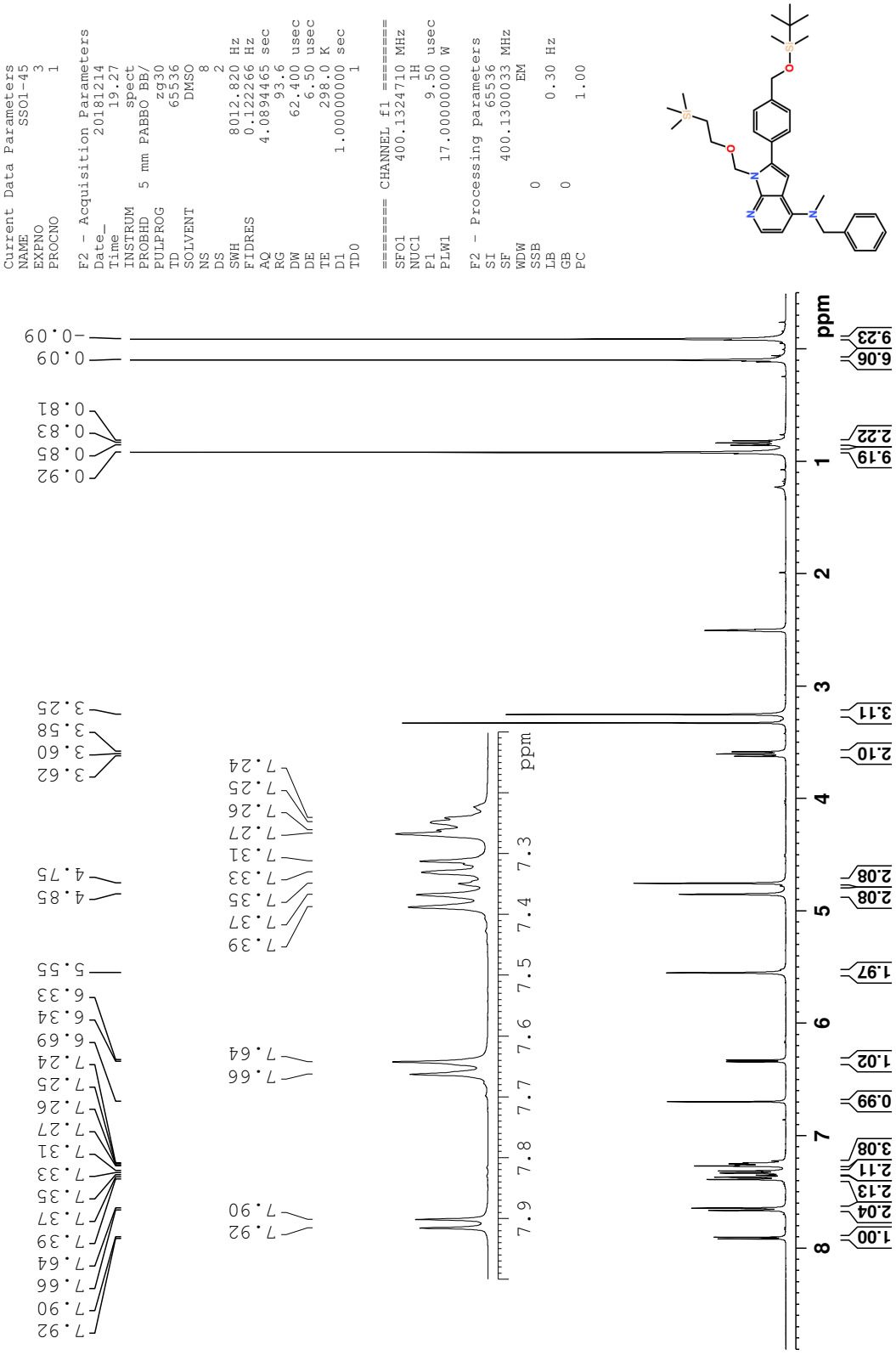

Figure I.1: ^{1}H NMR spectrum of compound **9.**

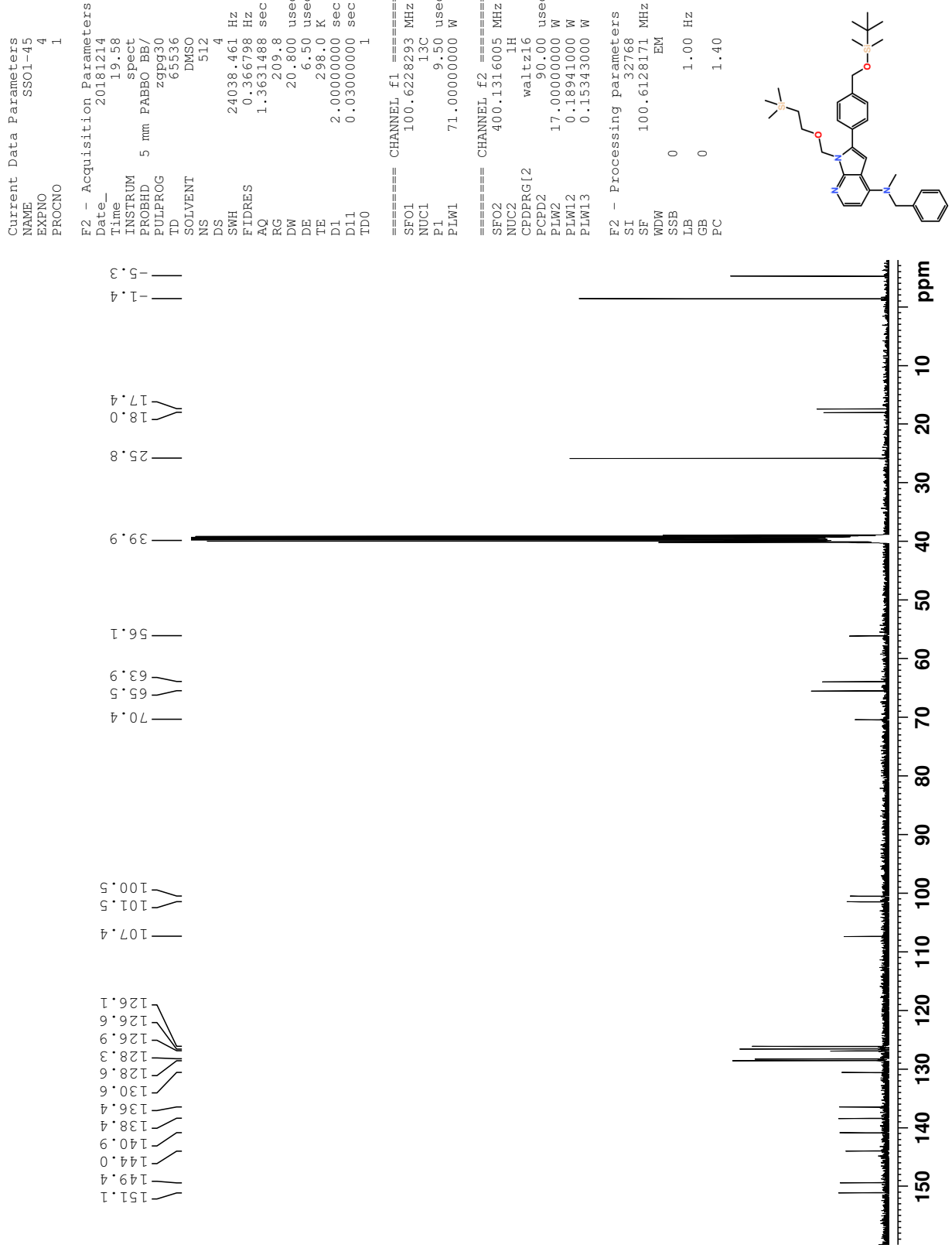

Figure I.2: ^{13}C NMR spectrum of compound **9.**

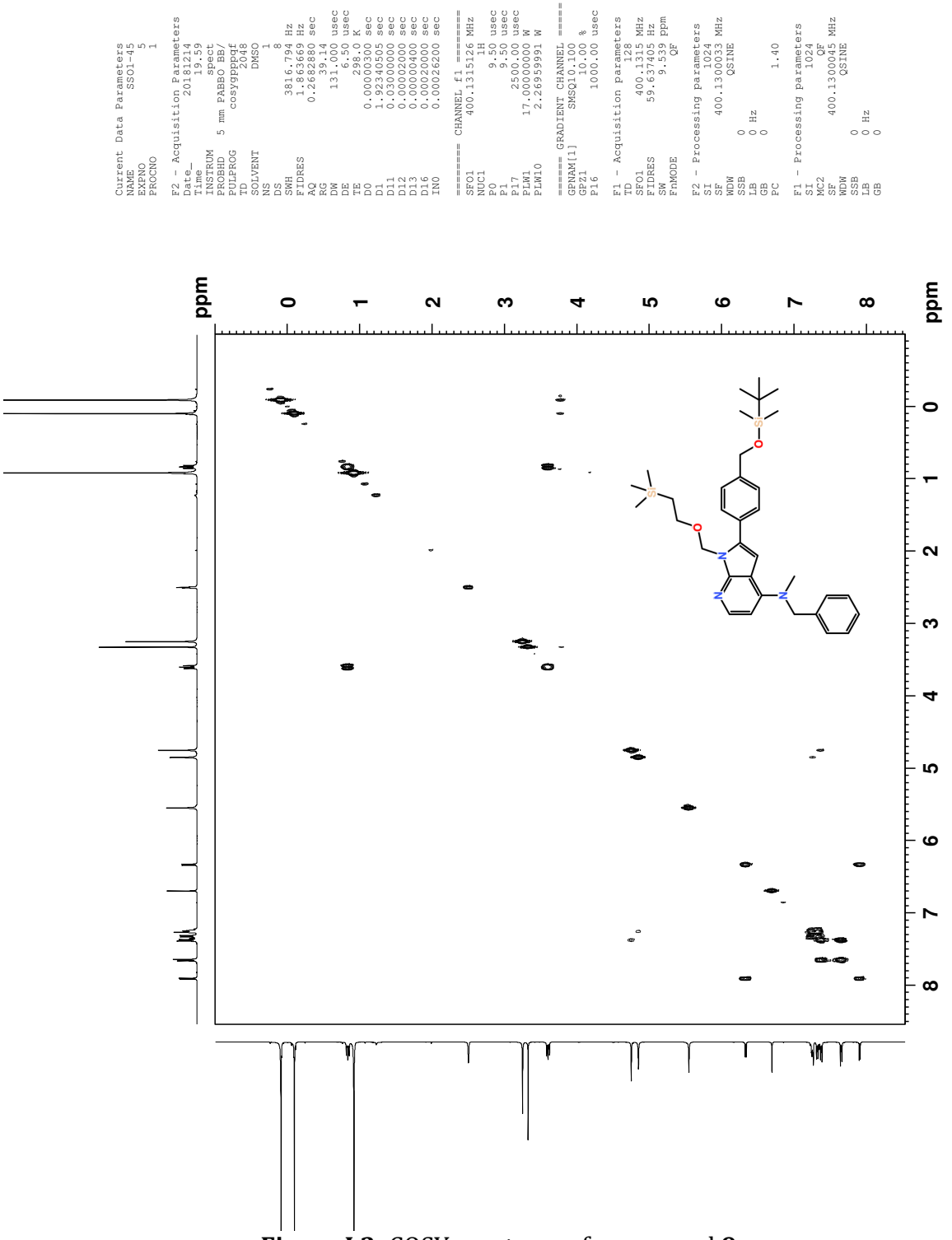

Figure I.3: COSY spectrum of compound **9.**

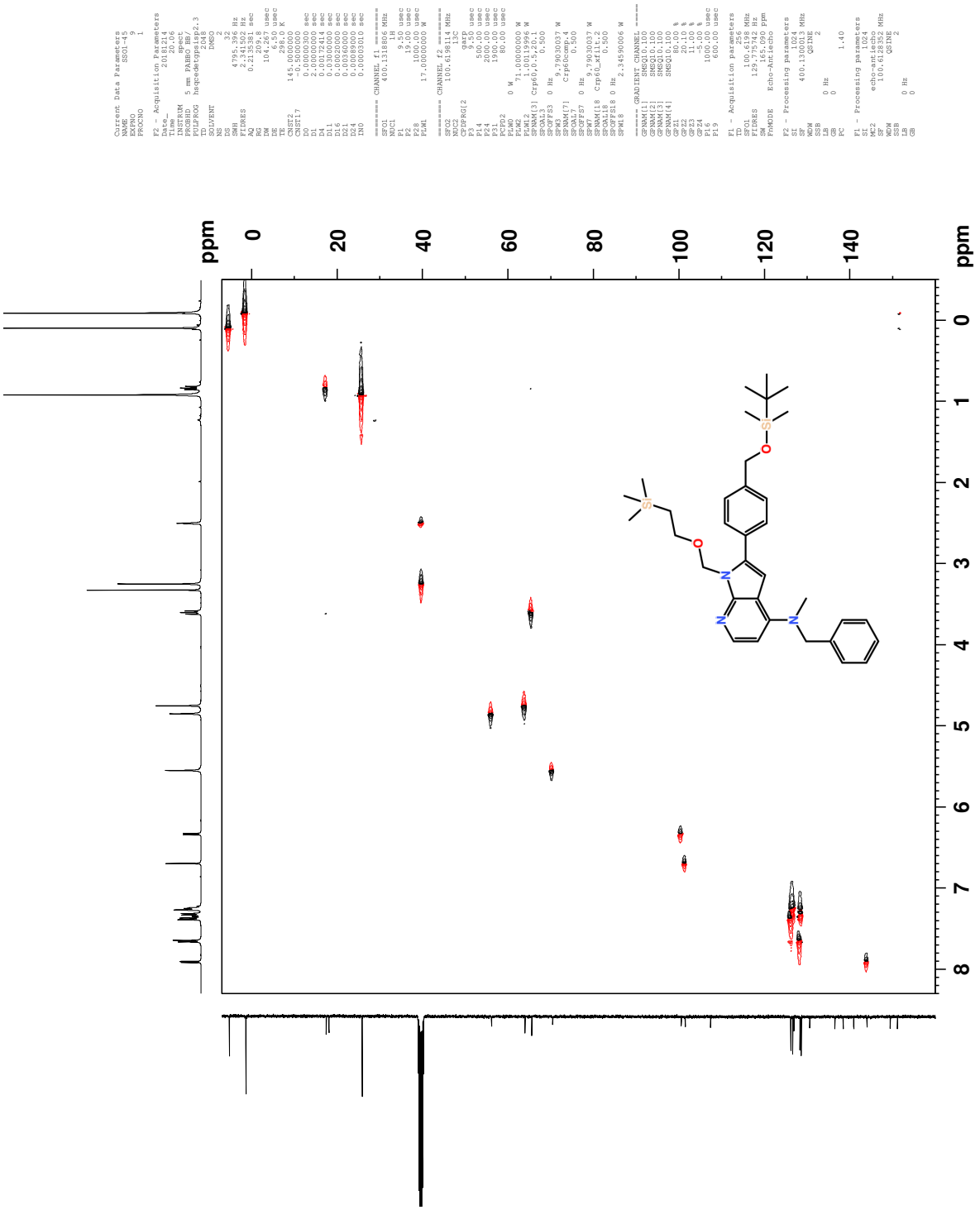

Figure I.4: HSQC spectrum of compound **9.**

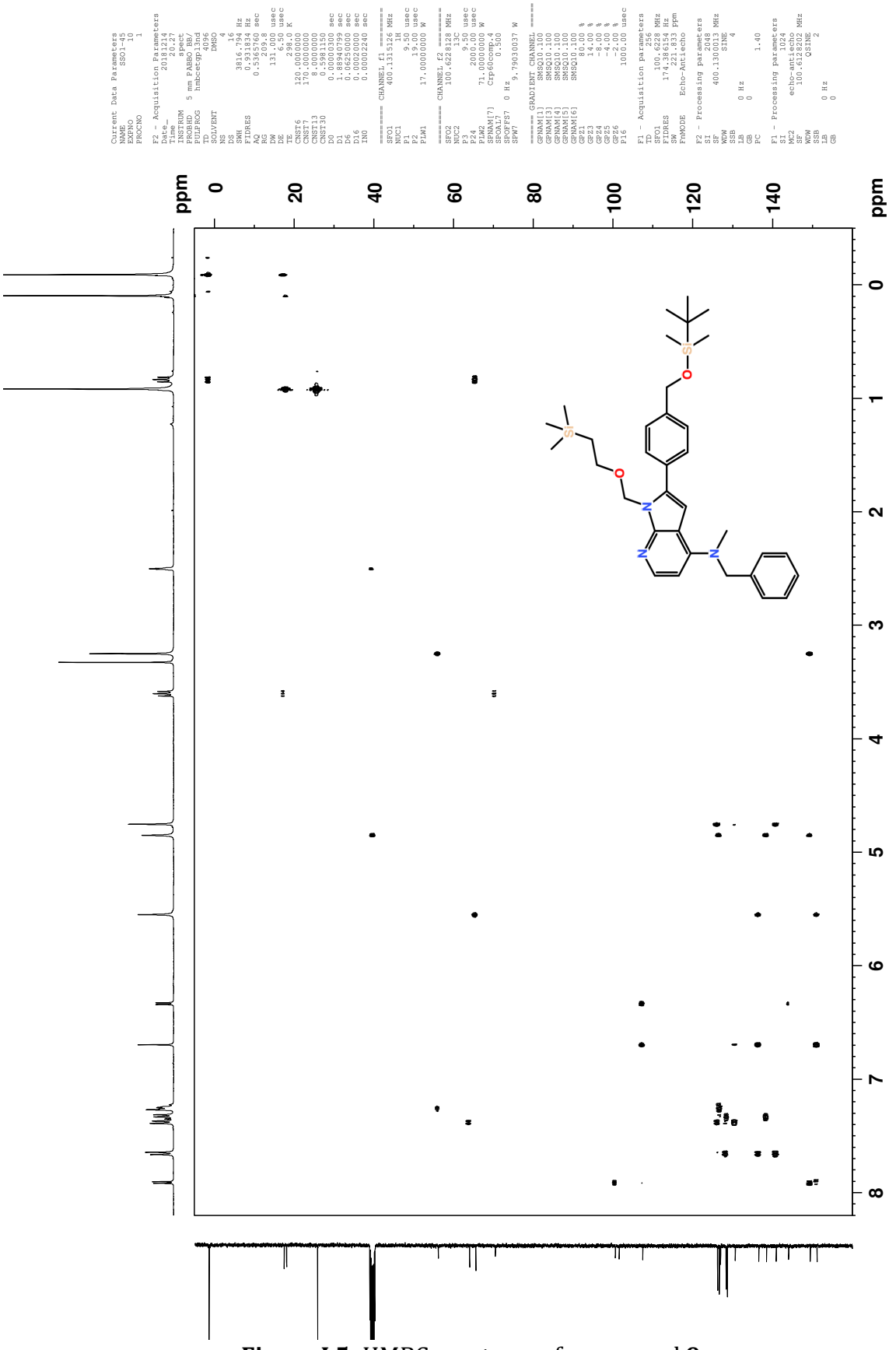

Figure I.5: HMBC spectrum of compound **9.**

Elemental Composition Report **Page 1**

Single Mass Analysis
Tolerance = 2.0 PPM / DBE: min = -2.0, max = 50.0
Element prediction: Off
Number of isotope peaks used for i-FIT = 3

Monoisotopic Mass, Even Electron Ions
9046 formula(e) evaluated with 9 results within limits (all results (up to 1000) for each mass)
Elements Used:
C: 0-100 H: 0-150 N: 0-8 O: 0-10 Si: 0-3 Cl: 0-3
2019-16 139 (2.723) AM2 (Ar,35000.0,0.00,0.00); Cm (137:139)
1: TOF MS ASAP+

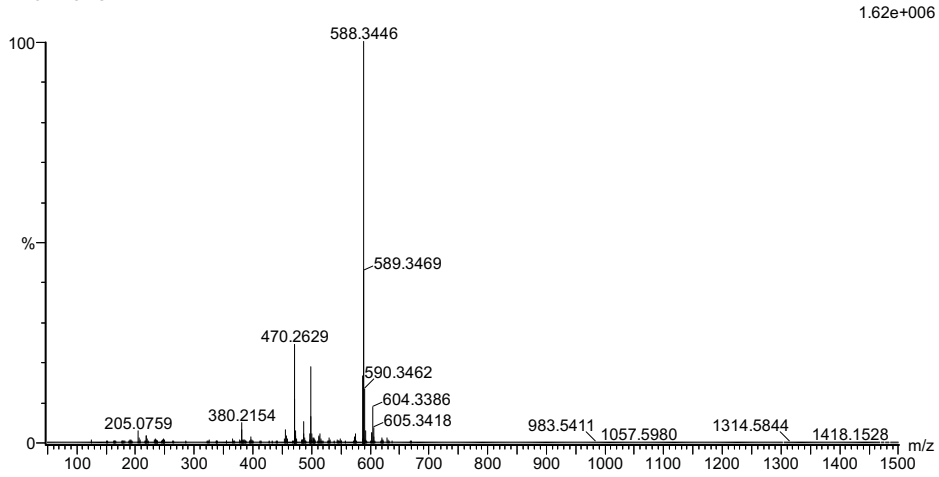

Minimum:				-2.0				
Maximum:		5.0	2.0	50.0				
Mass	Calc. Mass	mDa	PPM	DBE	i-FIT	Norm	Conf(%)	Formula
588.3446	588.3442	0.4	0.7	13.5	829.2	0.004	99.58	C34 H50 N3 O2 Si2
	588.3437	0.9	1.5	14.5	835.4	6.142	0.22	C35 H46 N3 O5
	588.3451	-0.5	-0.8	19.5	835.4	6.225	0.20	C36 H42 N7 O
	588.3456	-1.0	-1.7	9.5	840.5	11.291	0.00	C34 H51 N O5 Cl
	588.3447	-0.1	-0.2	0.5	841.0	11.827	0.00	C25 H55 N3 O8 Si Cl
	588.3451	-0.5	-0.8	-0.5	841.1	11.845	0.00	C24 H59 N3 O5 Si3 Cl
	588.3451	-0.5	-0.8	4.5	842.9	13.705	0.00	C28 H56 N5 Si2 Cl2
	588.3447	-0.1	-0.2	5.5	843.4	14.138	0.00	C29 H52 N5 O3 Cl2
	588.3438	0.8	1.4	-0.5	843.5	14.305	0.00	C27 H60 N O4 Si2 Cl2

Figure I.6: MS spectrum of compound **9.**

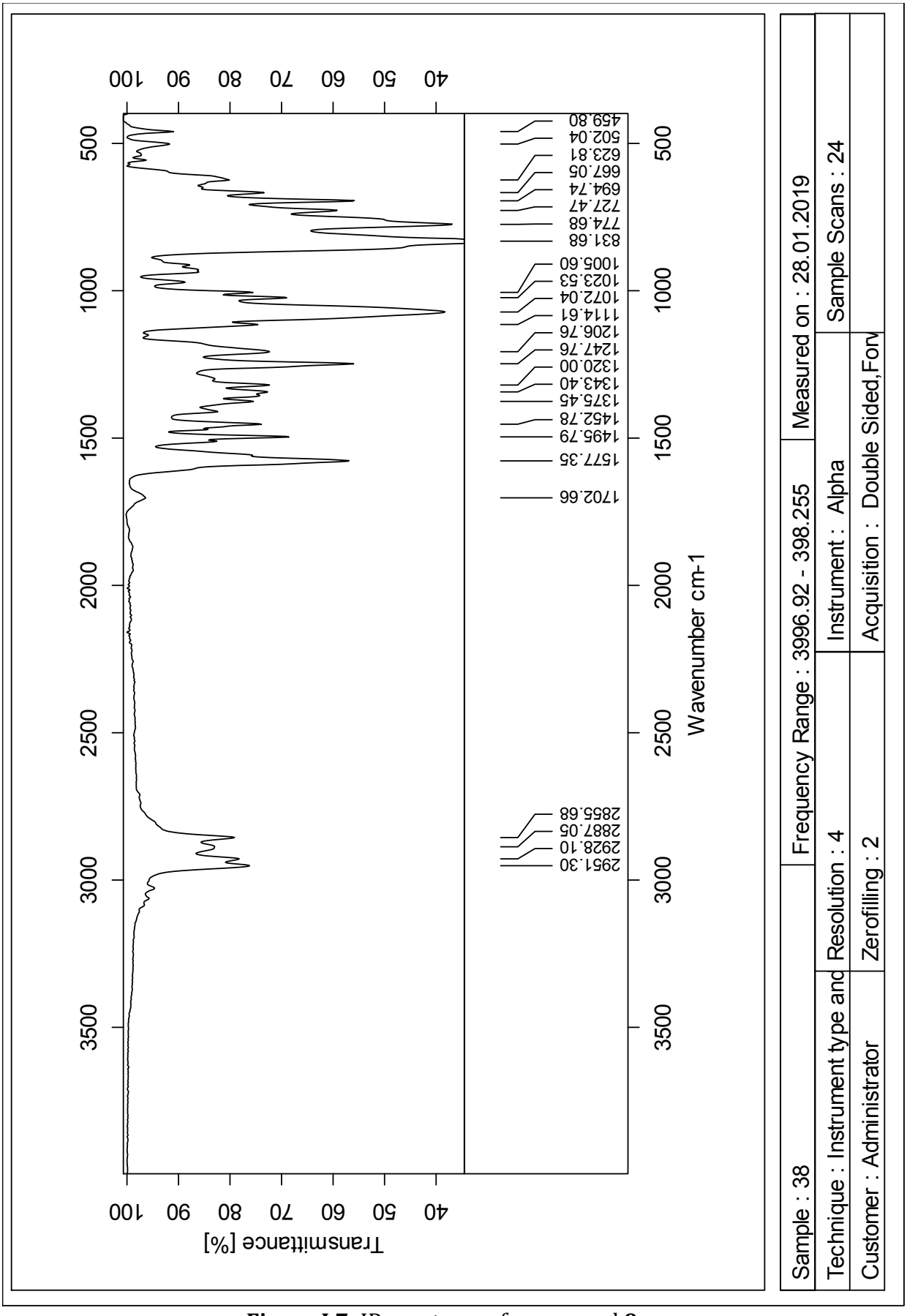

Figure I.7: IR spectrum of compound **9.**

Appendix J Compound 10

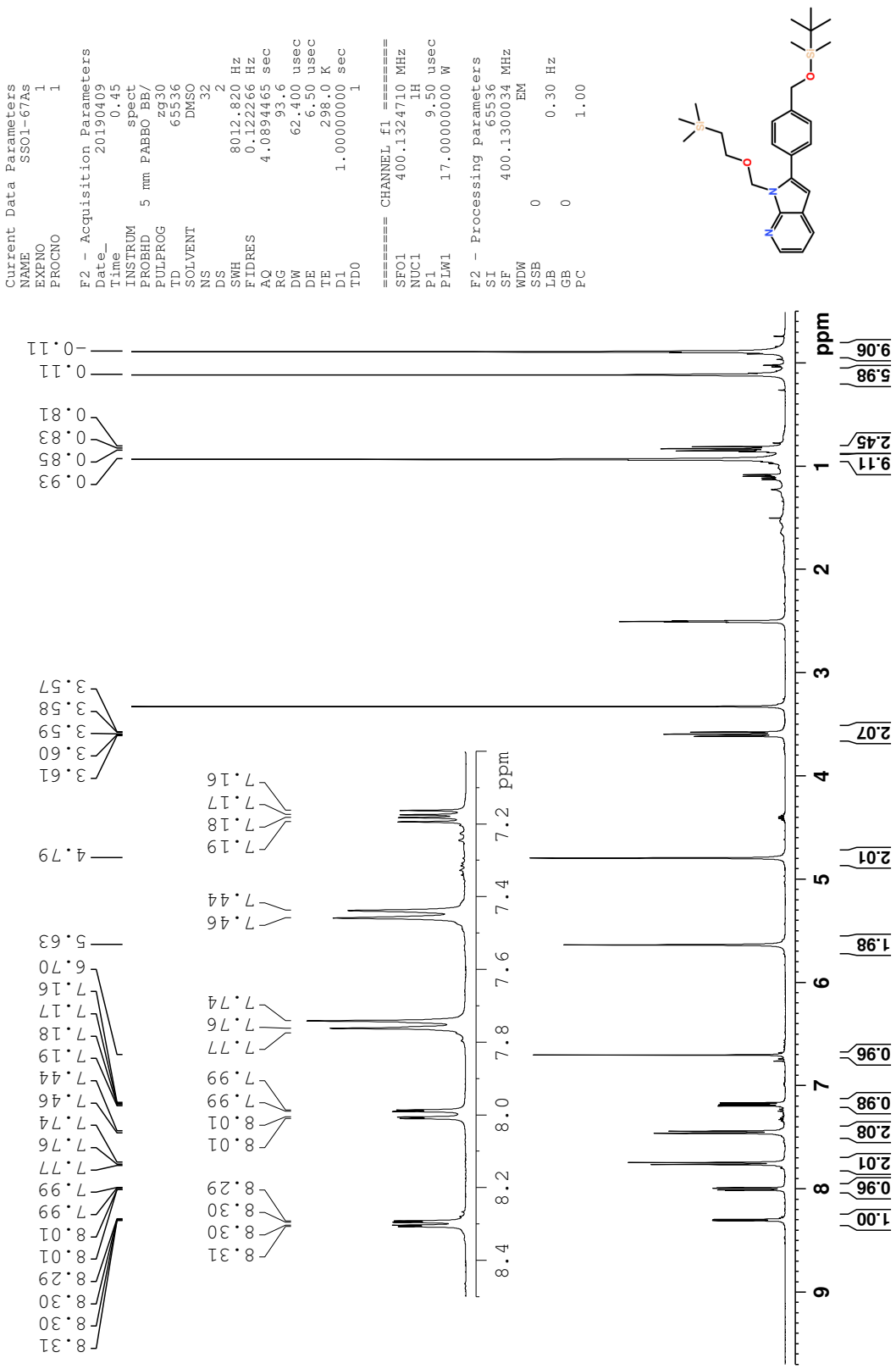

Figure J.1: ^{1}H NMR spectrum of compound **10.**

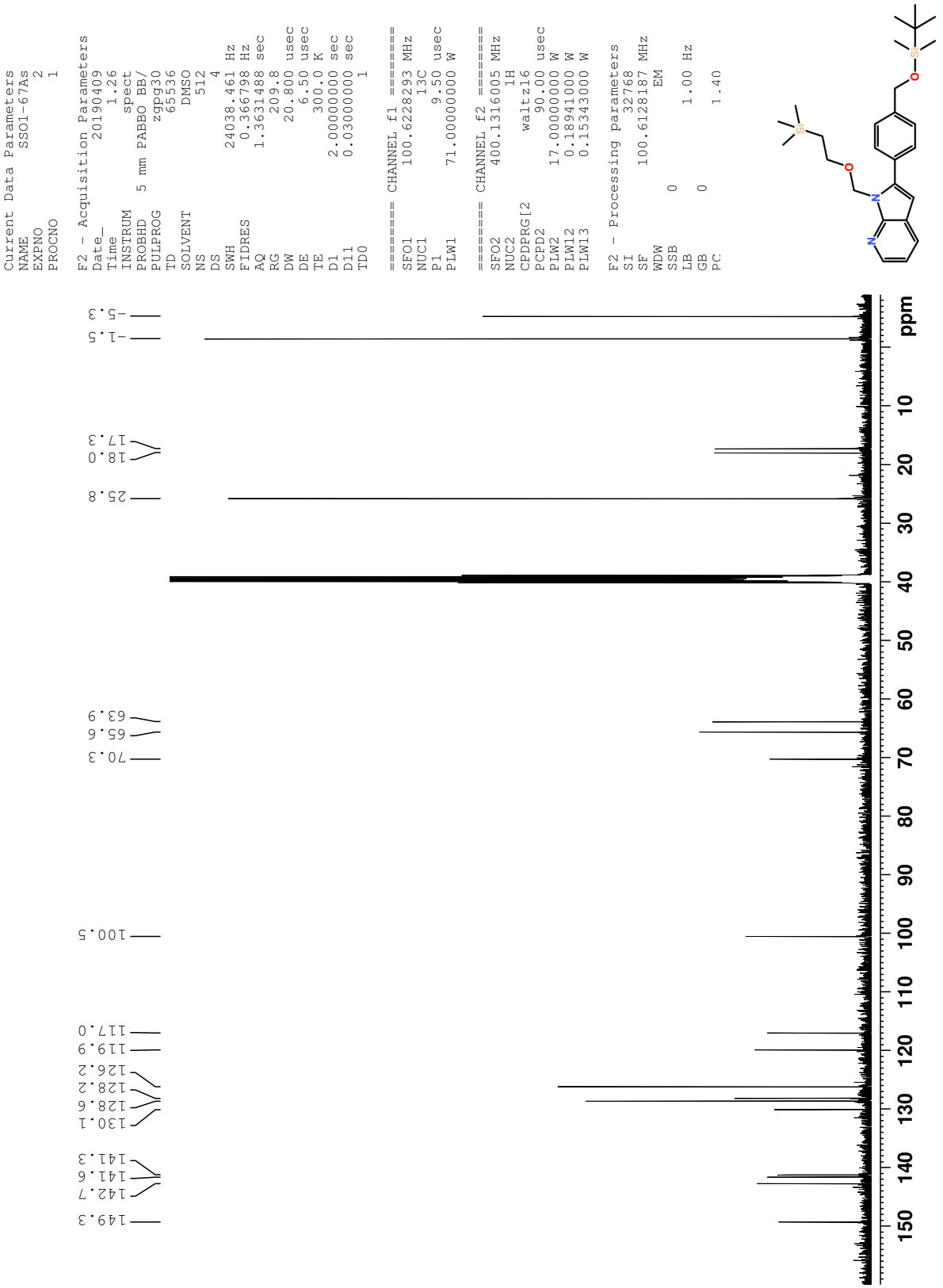

Figure J.2: ^{13}C NMR spectrum of compound **10.**

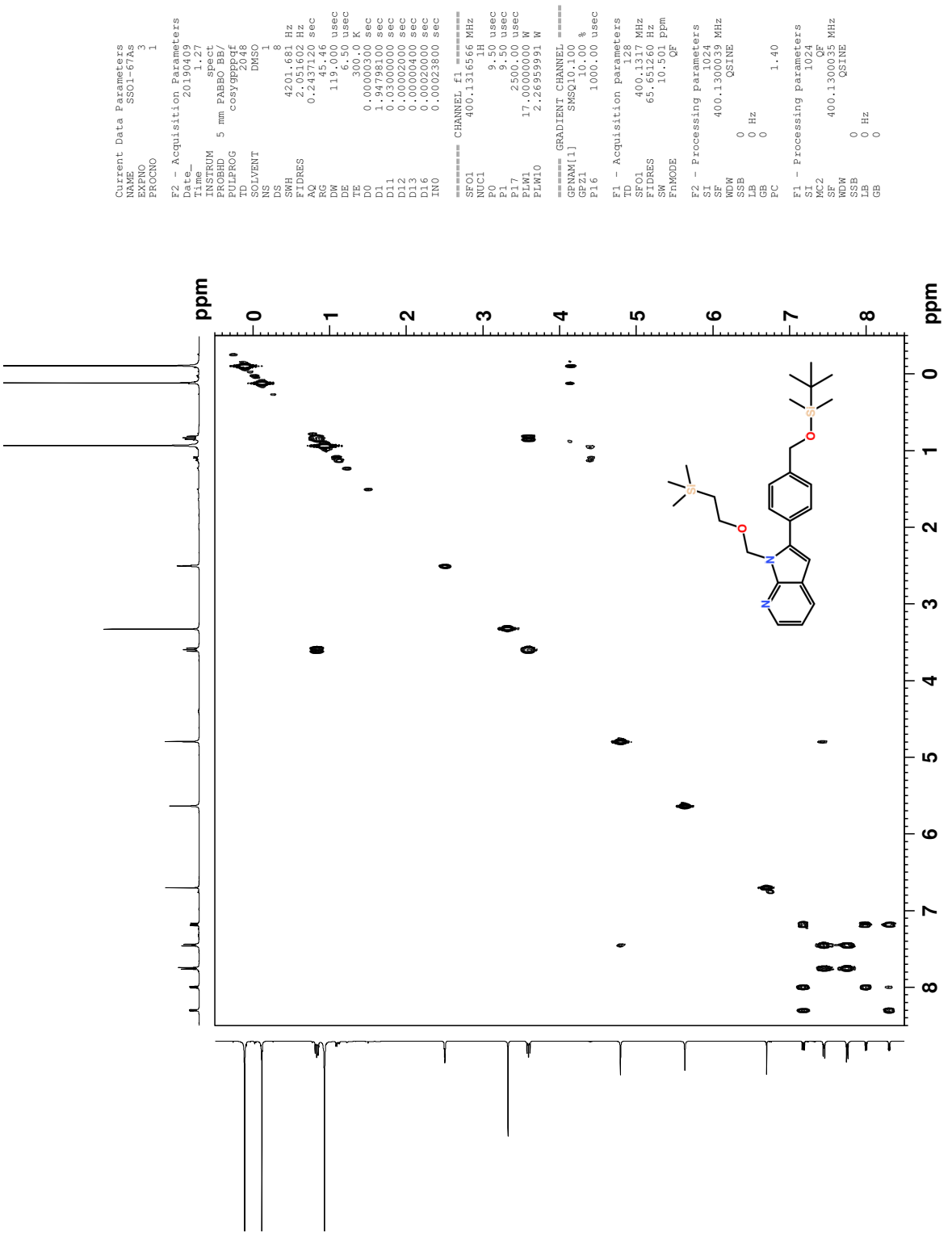

Figure J.3: COSY spectrum of compound **10.**

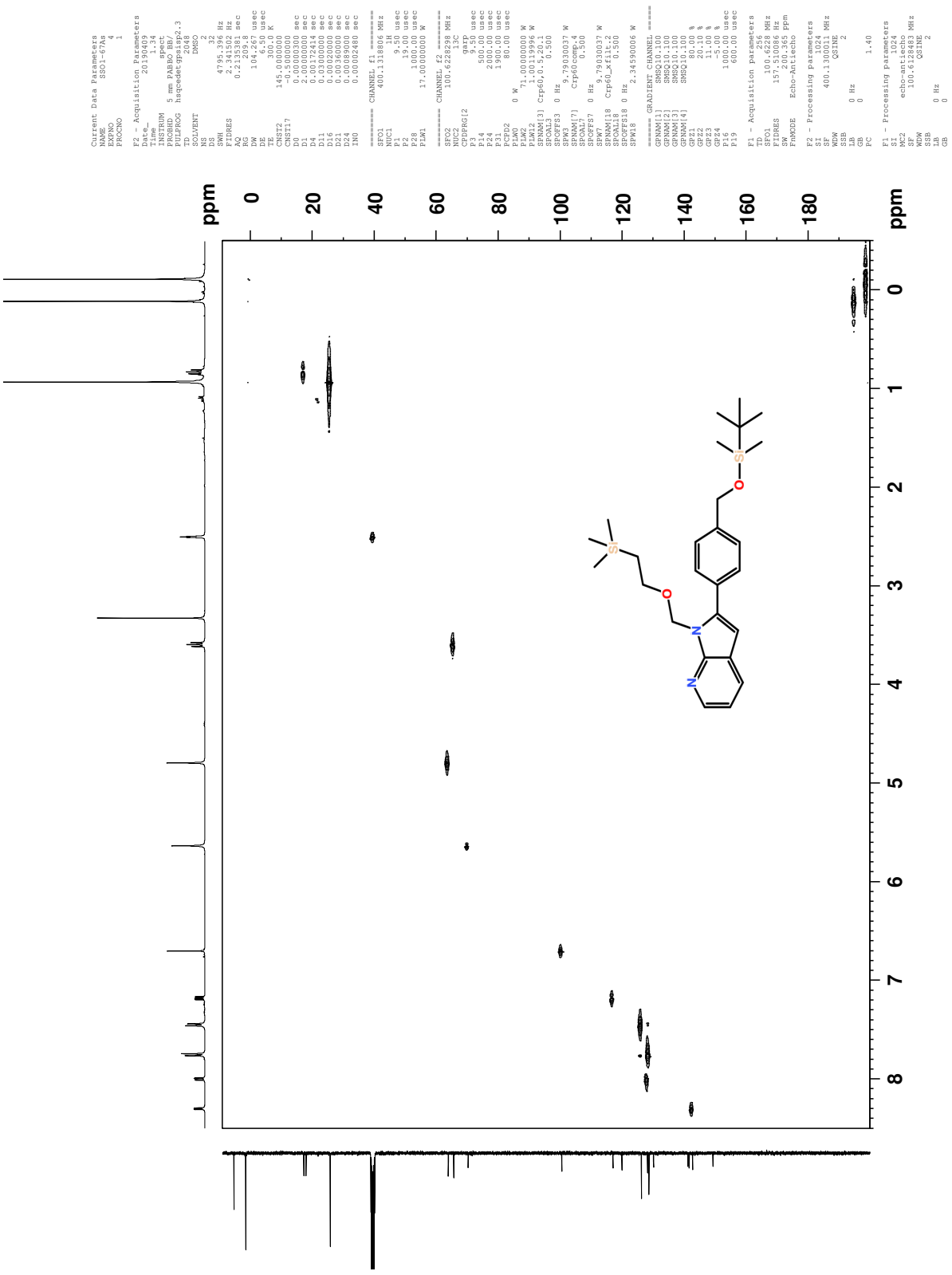

Figure J.4: HSQC spectrum of compound **10.**

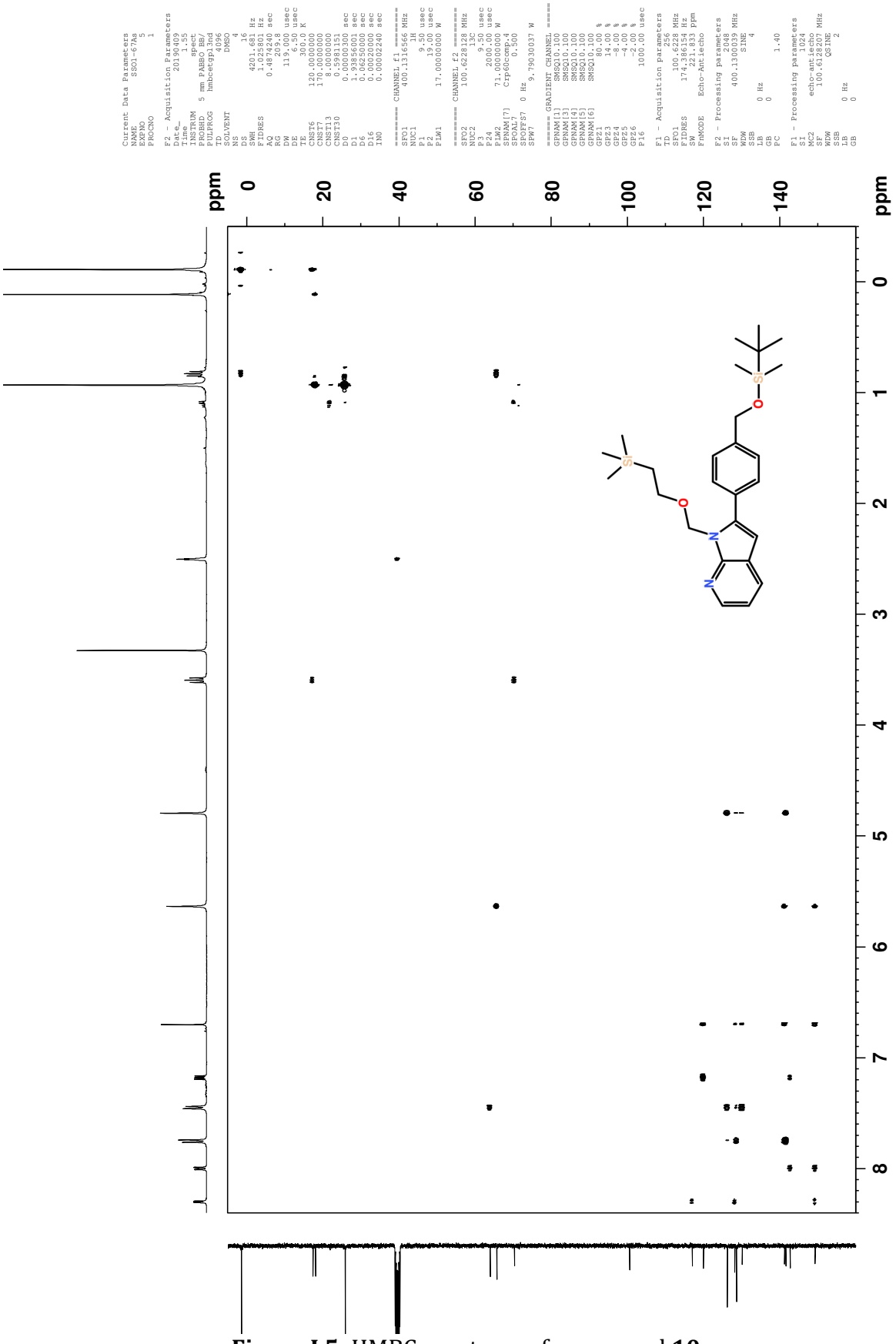

Figure J.5: HMBC spectrum of compound **10.**

Elemental Composition Report **Page 1**

Single Mass Analysis
Tolerance = 2.0 PPM / DBE: min = -50.0, max = 50.0
Element prediction: Off
Number of isotope peaks used for i-FIT = 3

Monoisotopic Mass, Even Electron Ions
4333 formula(e) evaluated with 4 results within limits (all results (up to 1000) for each mass)
Elements Used:
C: 0-100 H: 0-150 N: 0-10 O: 0-10 Si: 0-2

2019-258 122 (2.396) AM2 (Ar,35000.0,0.00,0.00); Cm (112:125)
1: TOF MS ASAP+

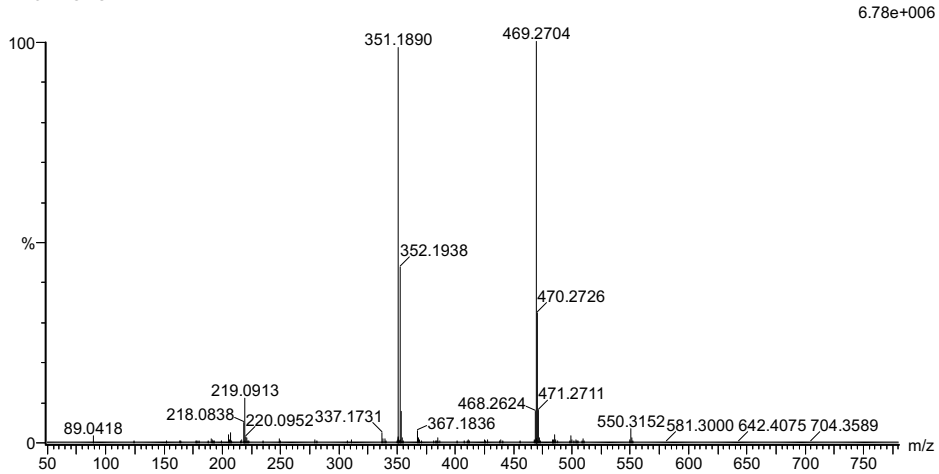

Mass	Calc. Mass	mDa	PPM	DBE	i-FIT	Norm	Conf(%)	Formula
Minimum:				-50.0				
Maximum:		5.0	2.0	50.0				
469.2704	469.2702	0.2	0.4	10.5	1286.4	8.963	0.01	C27 H37 N2 O5
	469.2707	-0.3	-0.6	9.5	1282.5	5.106	0.61	C26 H41 N2 O2 Si2
	469.2707	-0.3	-0.6	6.5	1277.4	0.007	99.35	C19 H37 N8 O4 Si
	469.2698	0.6	1.3	-2.5	1285.5	8.098	0.03	C10 H41 N10 O7 Si2

Figure J.6: MS spectrum of compound **10.**

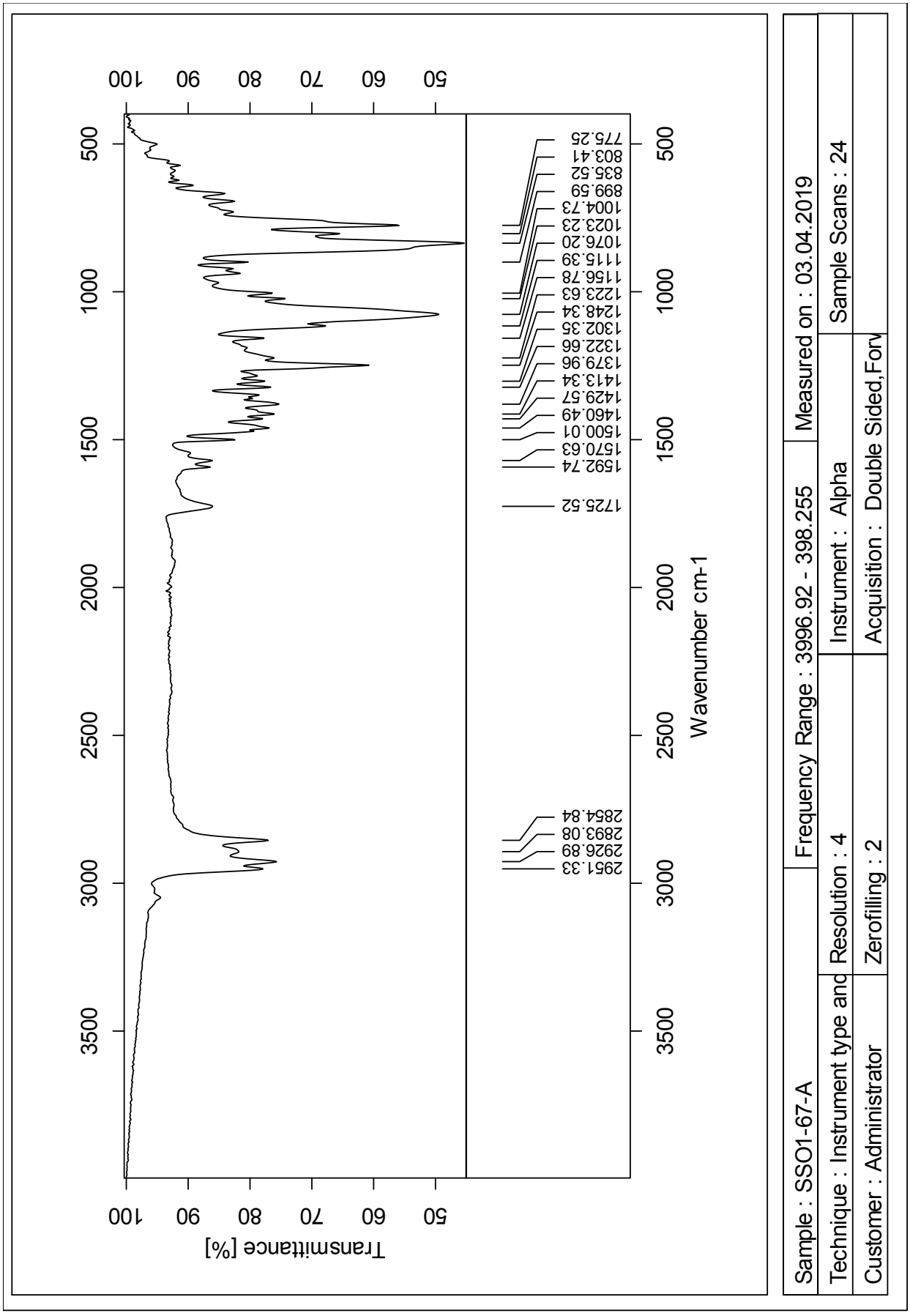

Figure J.7: IR spectrum of compound **10.**

Appendix K Compound 11

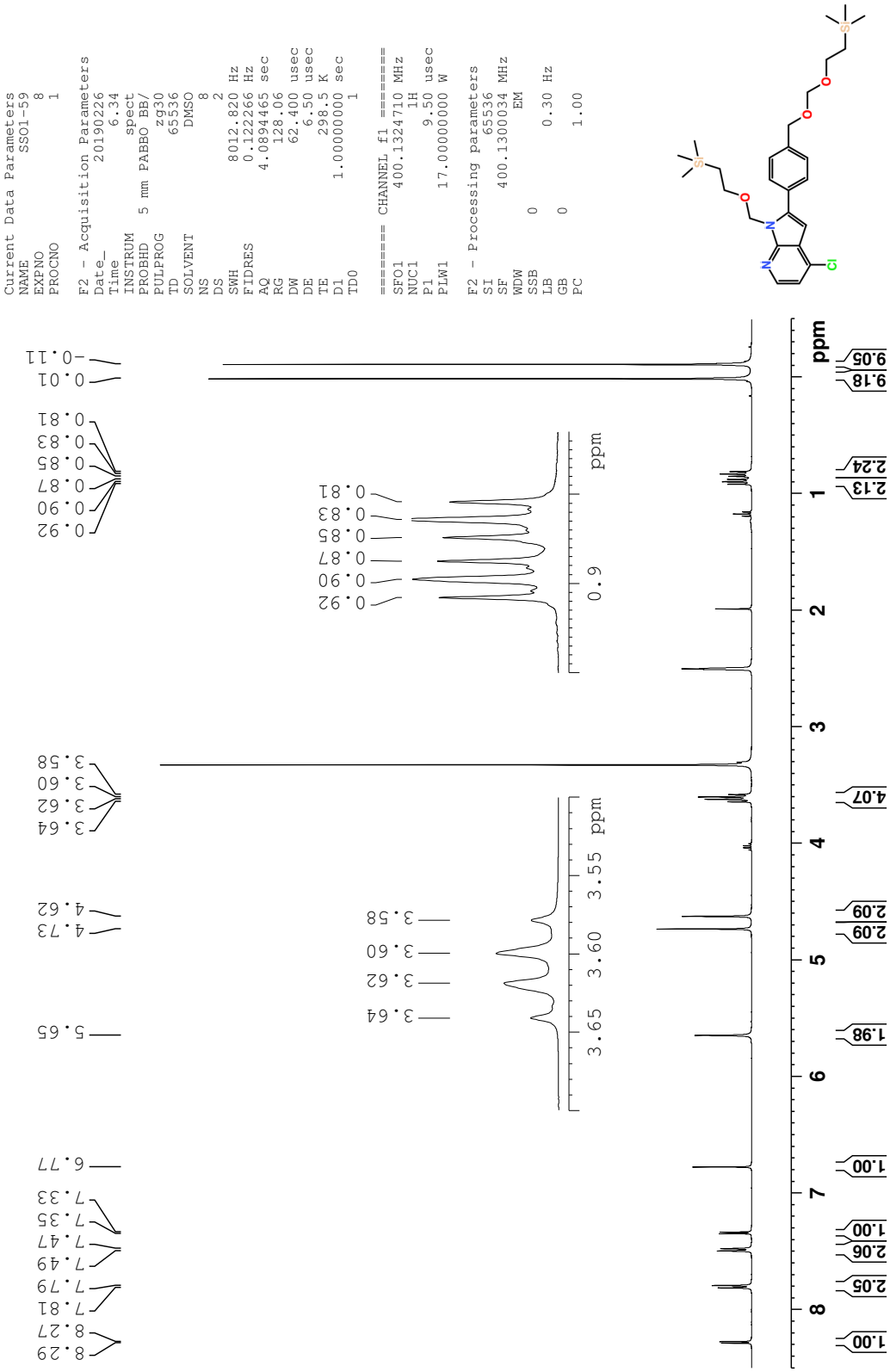

Figure K.1: [1]H NMR spectrum of compound **11.**

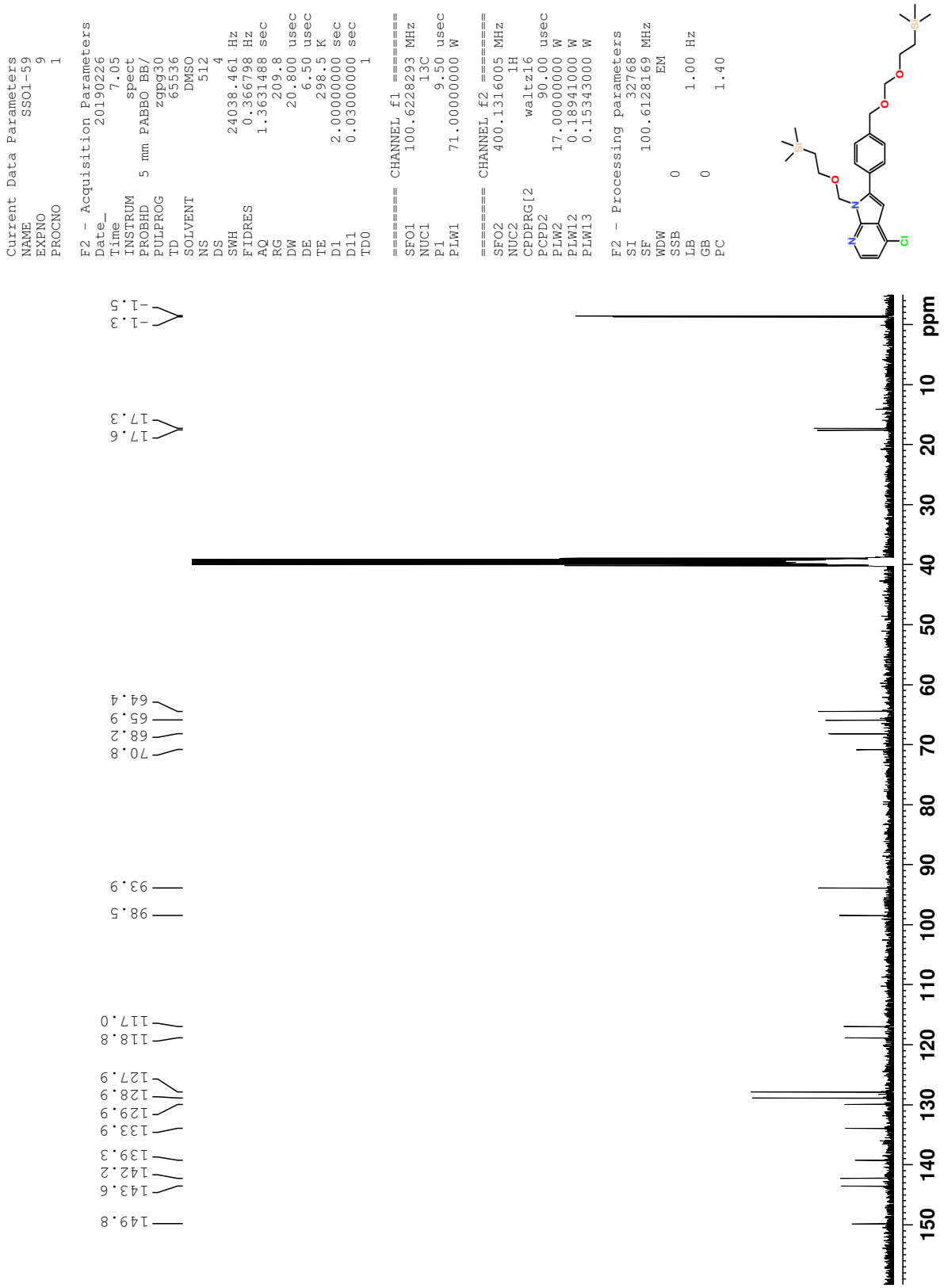

Figure K.2: ^{13}C NMR spectrum of compound **11.**

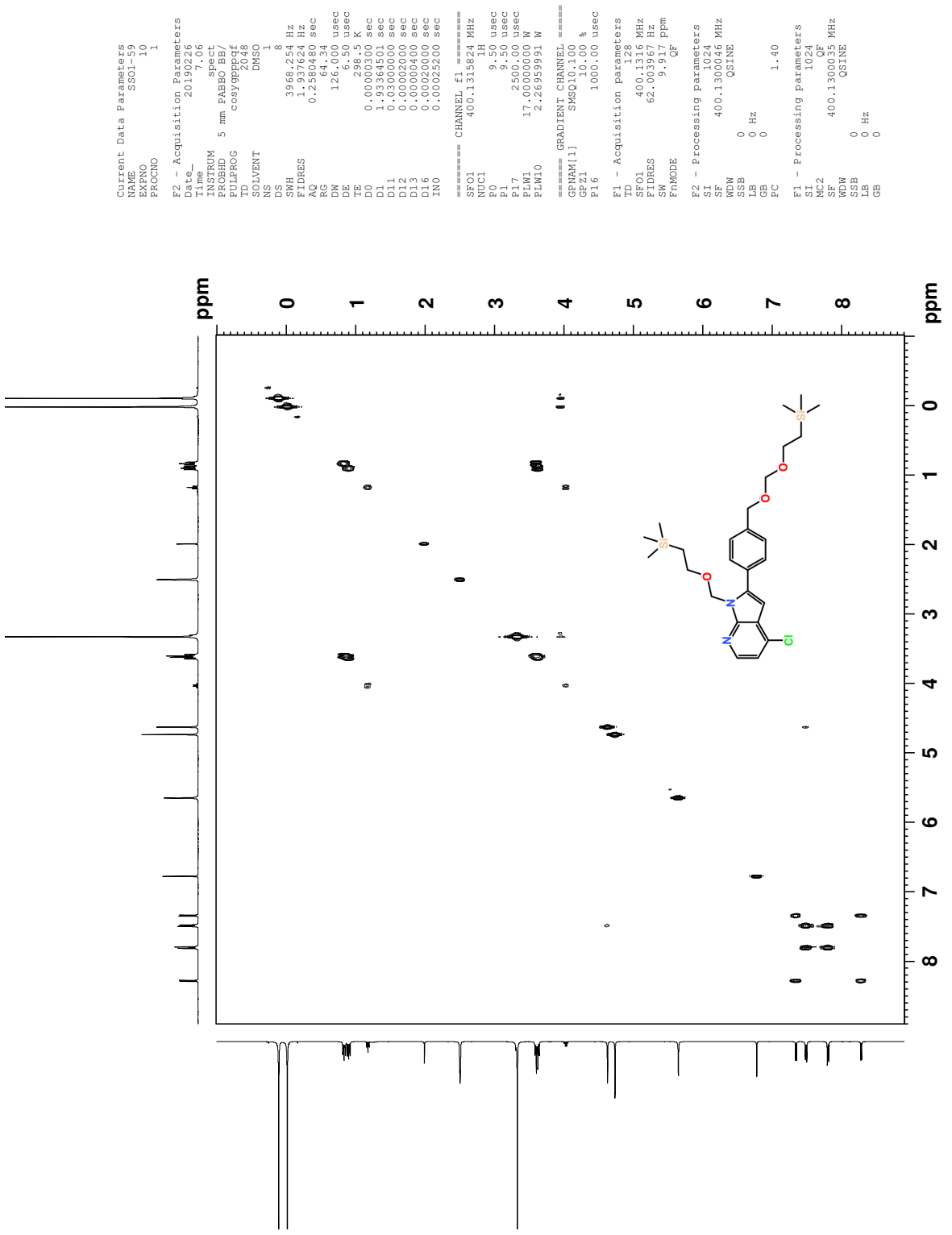

Figure K.3: COSY spectrum of compound **11.**

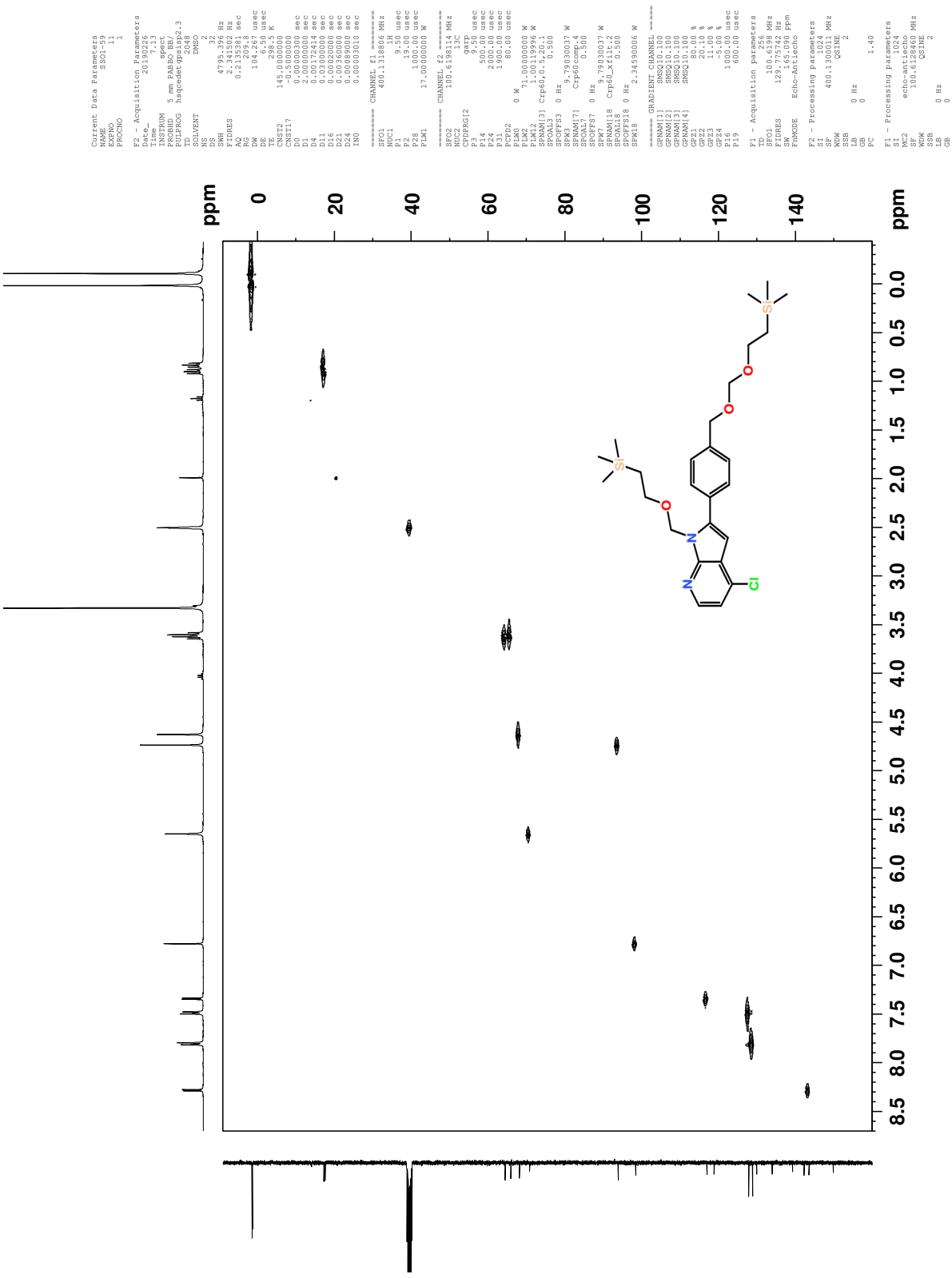

Figure K.4: HSQC spectrum of compound **11.**

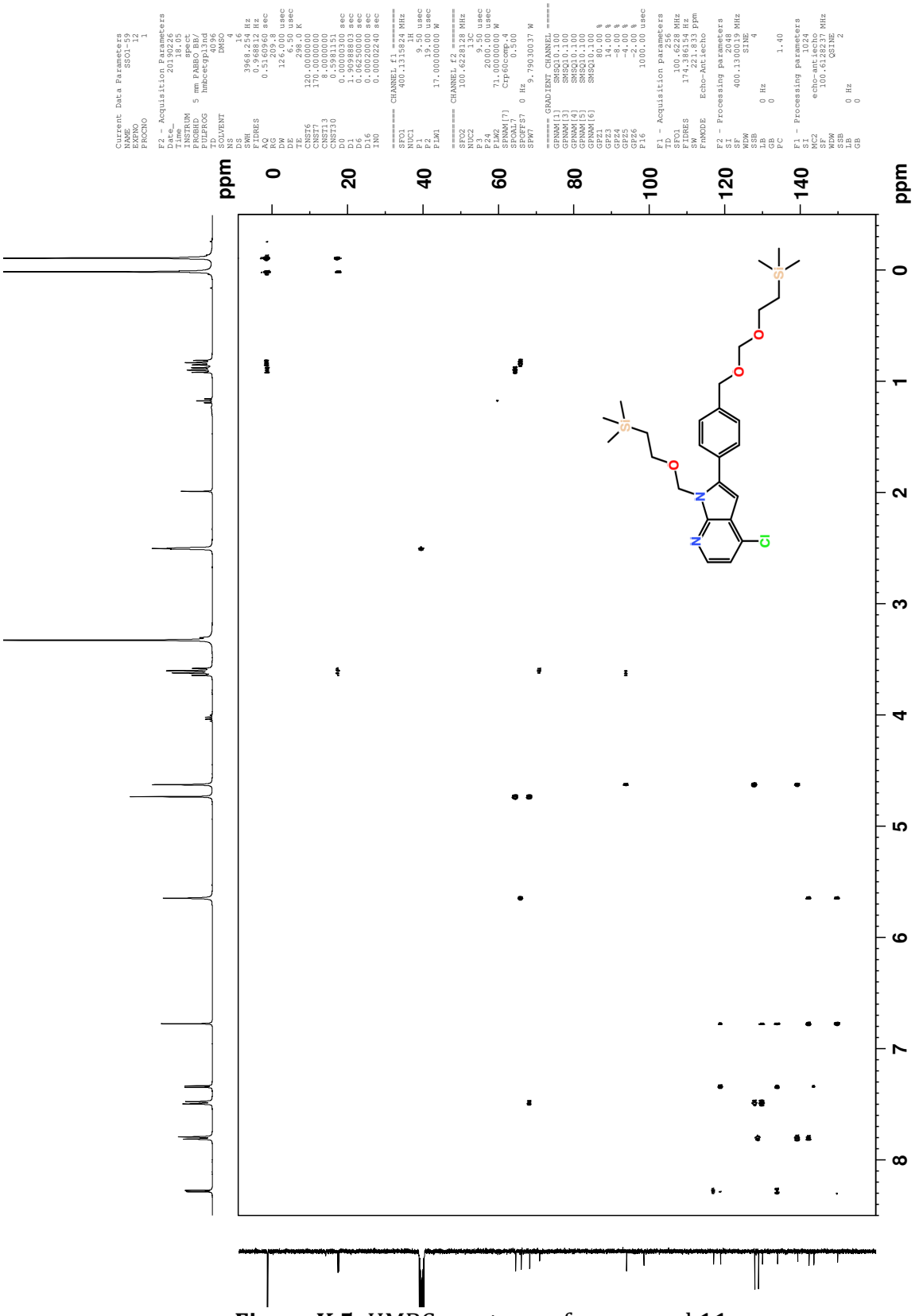

Figure K.5: HMBC spectrum of compound **11.**

Elemental Composition Report **Page 1**

Single Mass Analysis
Tolerance = 2.0 PPM / DBE: min = -2.0, max = 50.0
Element prediction: Off
Number of isotope peaks used for i-FIT = 3

Monoisotopic Mass, Even Electron Ions
3359 formula(e) evaluated with 8 results within limits (all results (up to 1000) for each mass)
Elements Used:
C: 0-100 H: 0-150 N: 0-10 O: 0-5 Si: 0-2 Cl: 0-2
2019-136 80 (1.567) AM2 (Ar,35000.0,0.00,0.00); Cm (76:80)
1: TOF MS ASAP+

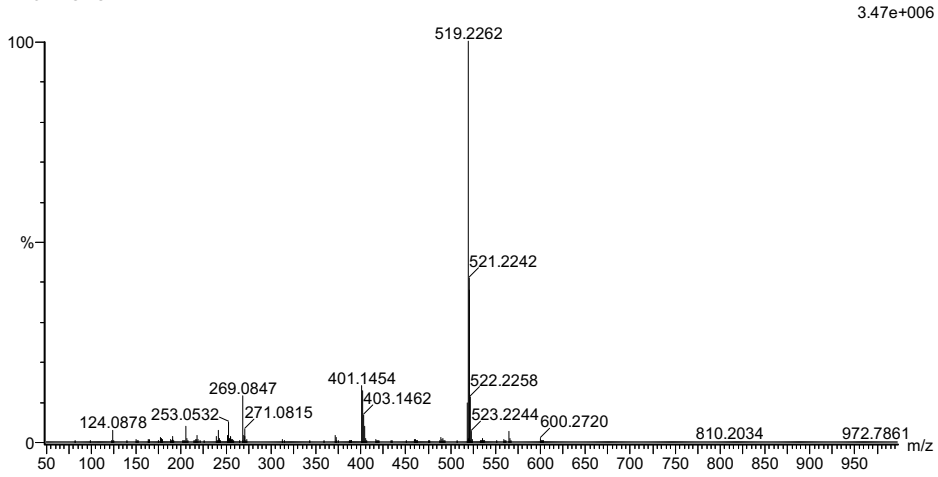

Minimum:				-2.0				
Maximum:		5.0	2.0	50.0				
Mass	Calc. Mass	mDa	PPM	DBE	i-FIT	Norm	Conf(%)	Formula
519.2262	519.2266	-0.4	-0.8	6.5	1063.3	2.030	13.13	C19 H36 N8 O5 Si Cl
	519.2266	-0.4	-0.8	9.5	1061.4	0.144	86.57	C26 H40 N2 O3 Si2 Cl

Figure K.6: MS spectrum of compound **11.**

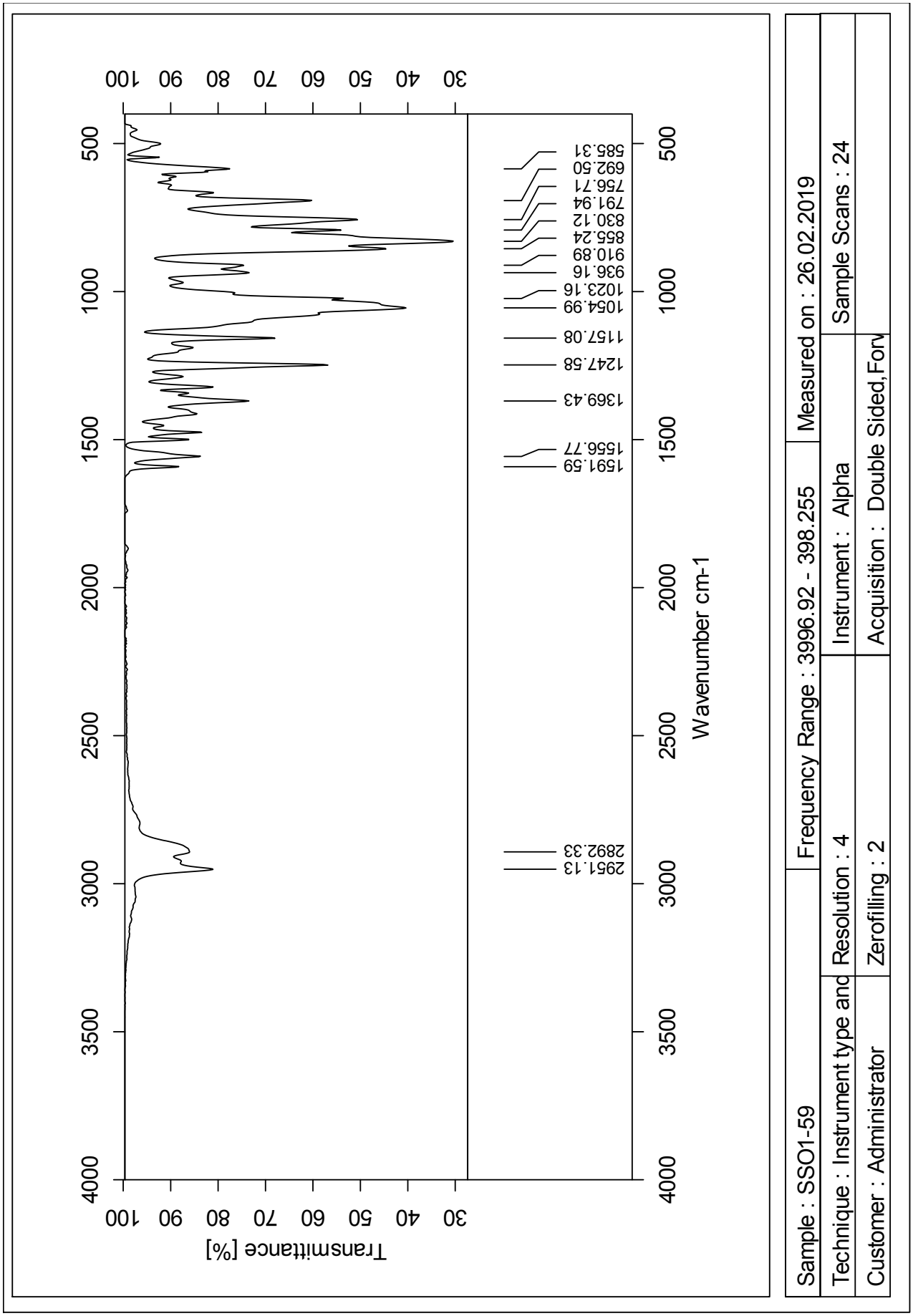

Figure K.7: IR spectrum of compound **11.**

Appendix L Compound 12

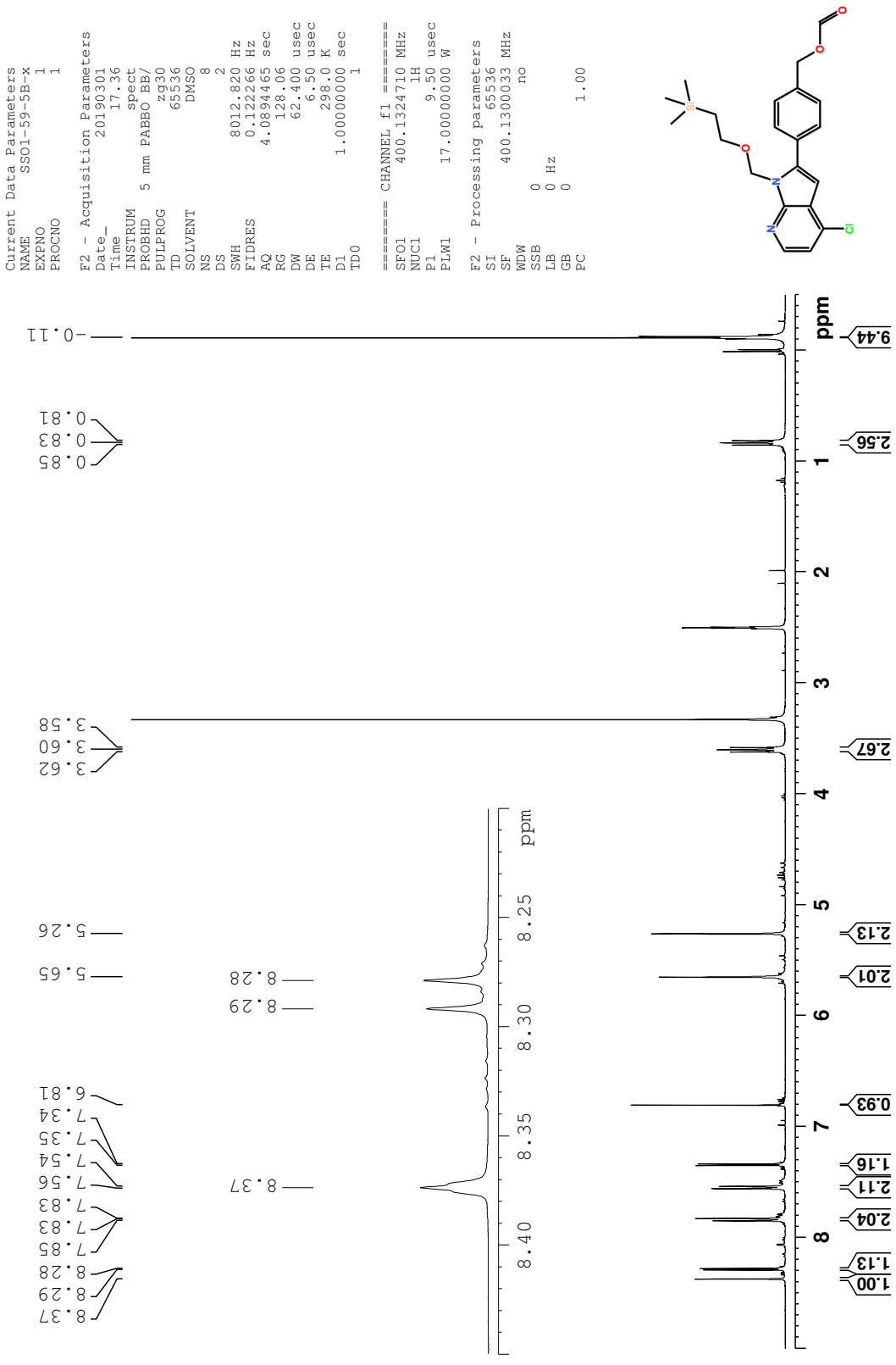

Figure L.1: ^{1}H NMR spectrum of compound **12.**

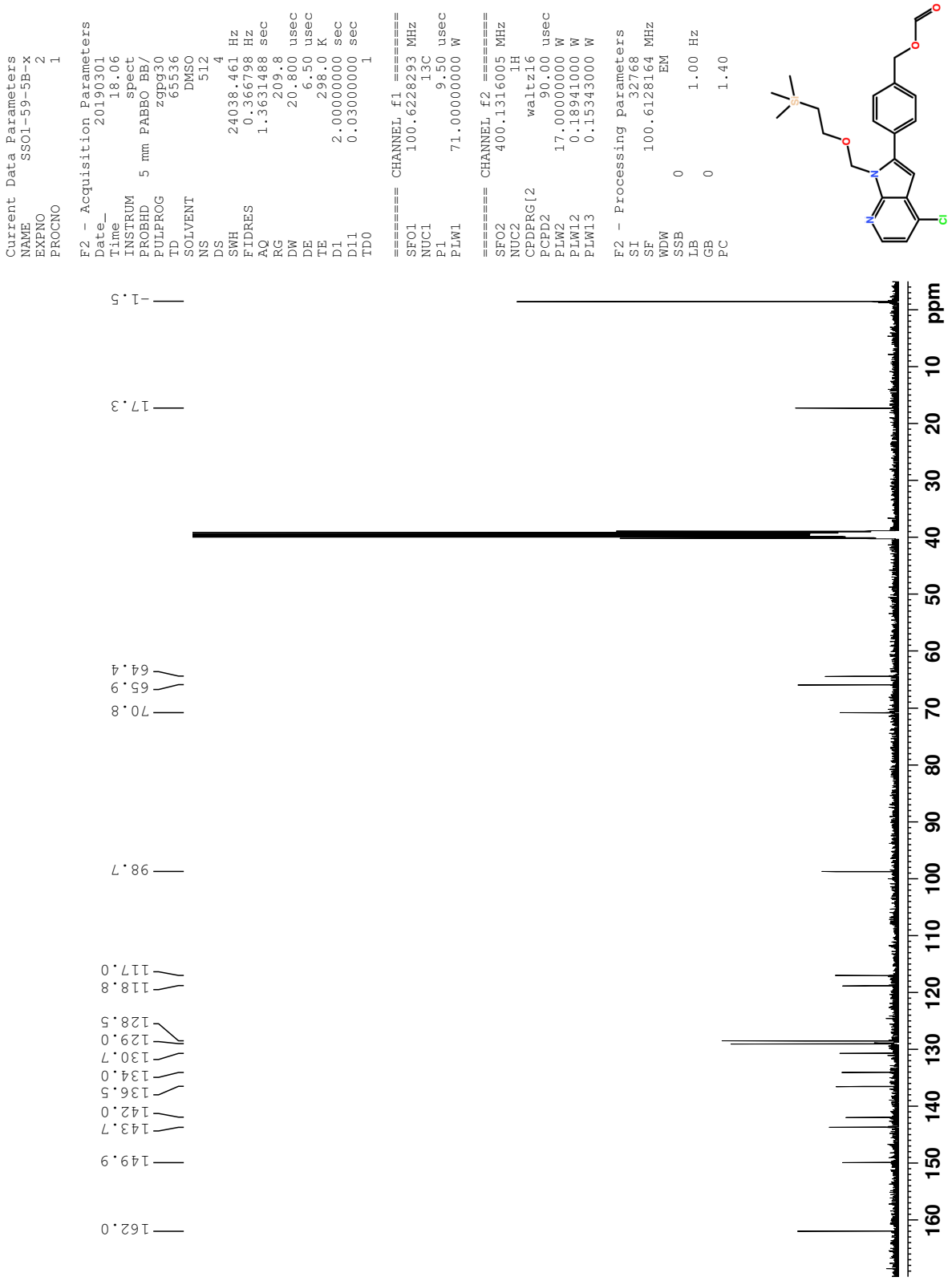

Figure L.2: ^{13}C NMR spectrum of compound **12.**

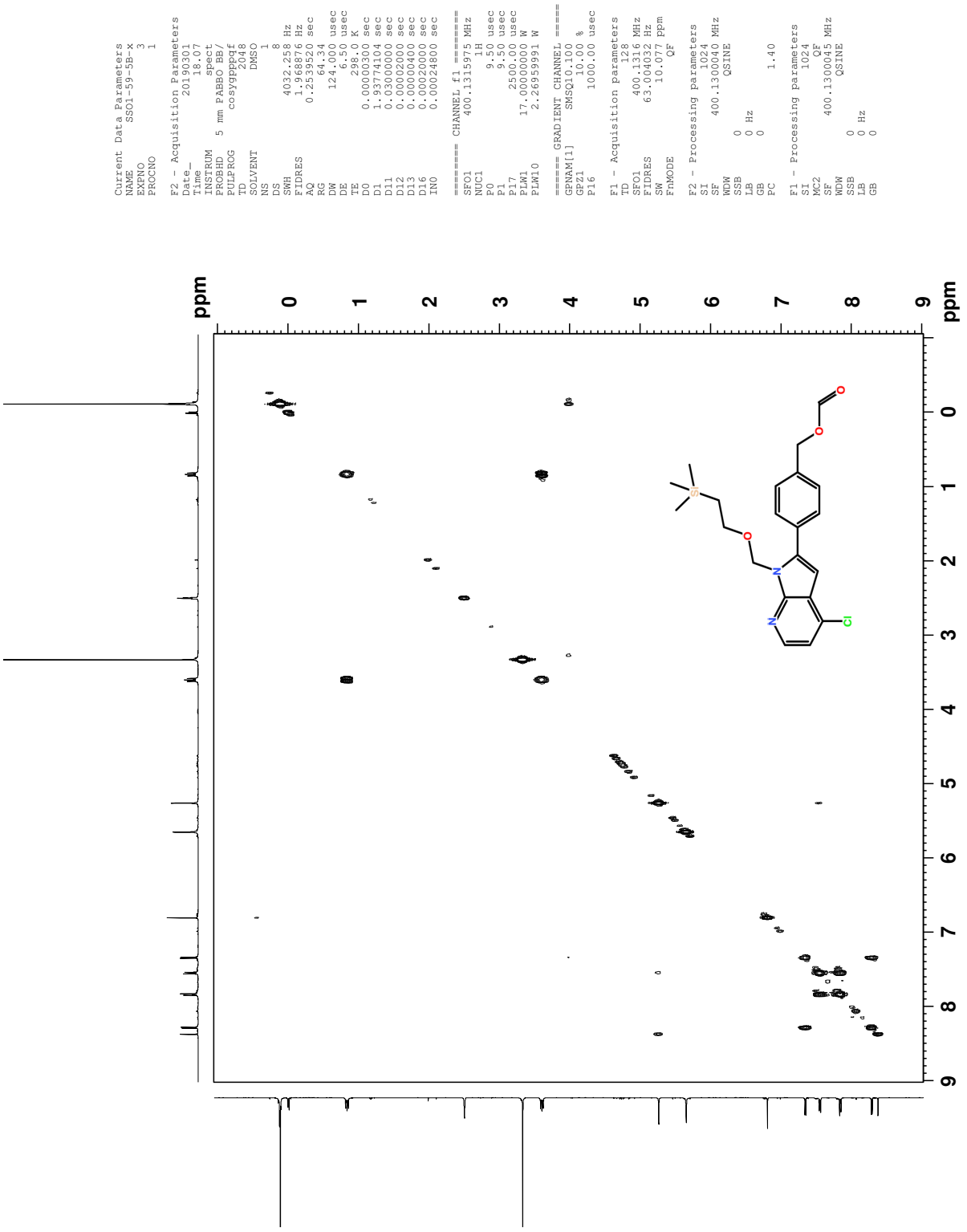

Figure L.3: COSY spectrum of compound **12.**

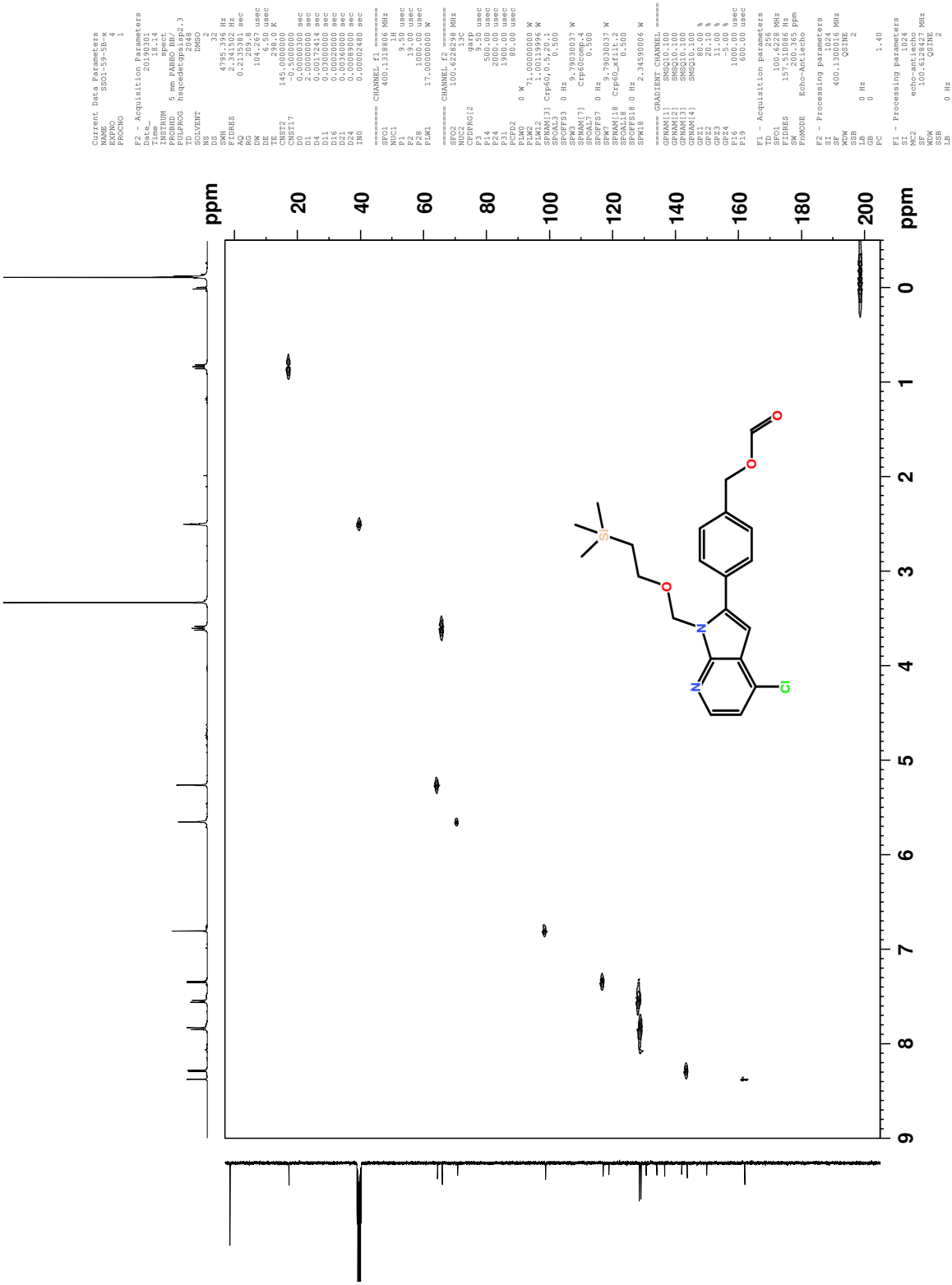

Figure L.4: HSQC spectrum of compound **12.**

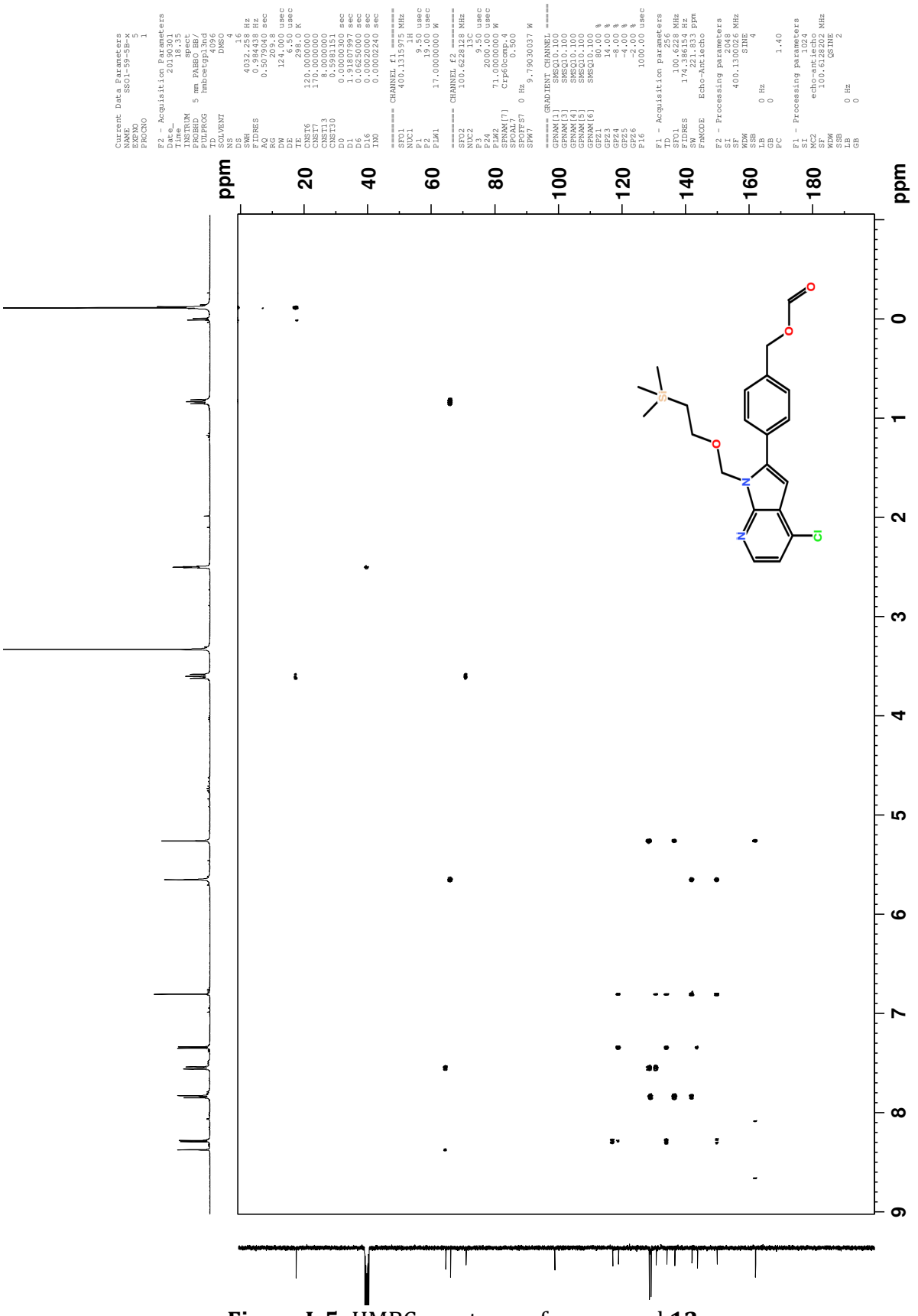

Figure L.5: HMBC spectrum of compound **12.**

Elemental Composition Report **Page 1**

Single Mass Analysis
Tolerance = 2.0 PPM / DBE: min = -2.0, max = 50.0
Element prediction: Off
Number of isotope peaks used for i-FIT = 3

Monoisotopic Mass, Even Electron Ions
2488 formula(e) evaluated with 4 results within limits (all results (up to 1000) for each mass)
Elements Used:
C: 0-100 H: 0-150 N: 0-5 O: 0-10 Cl: 0-2 Si: 0-2

2019-151 140 (2.740) AM2 (Ar,35000.0,0.00,0.00); Cm (140:149)
1: TOF MS ASAP+

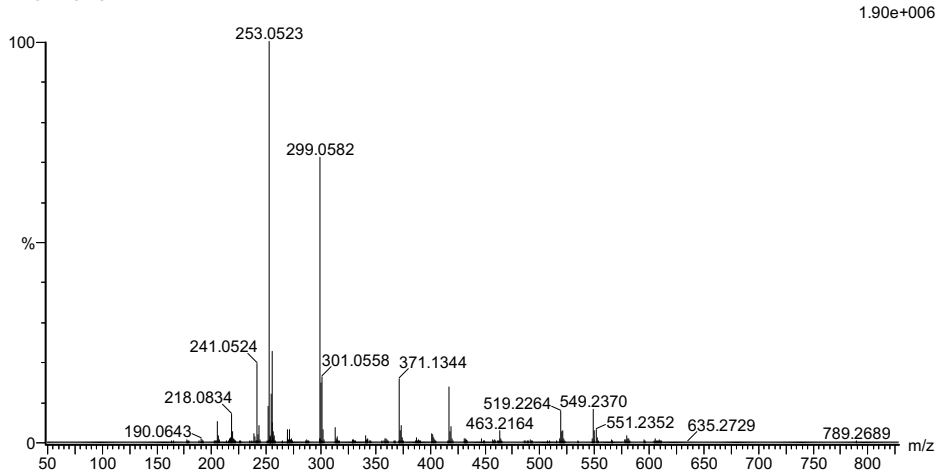

Minimum:				-2.0				
Maximum:		5.0	2.0	50.0				
Mass	Calc. Mass	mDa	PPM	DBE	i-FIT	Norm	Conf(%)	Formula
417.1398	417.1401	-0.3	-0.7	5.5	932.0	7.053	0.09	C17 H29 O8 Si2
	417.1401	-0.3	-0.7	10.5	925.6	0.708	49.28	C21 H26 N2 O3 Cl Si
	417.1392	0.6	1.4	24.5	937.5	12.616	0.00	C31 H17 N2
	417.1392	0.6	1.4	1.5	925.6	0.681	50.63	C12 H30 N4 O6 Cl Si2

Figure L.6: MS spectrum of compound **12.**

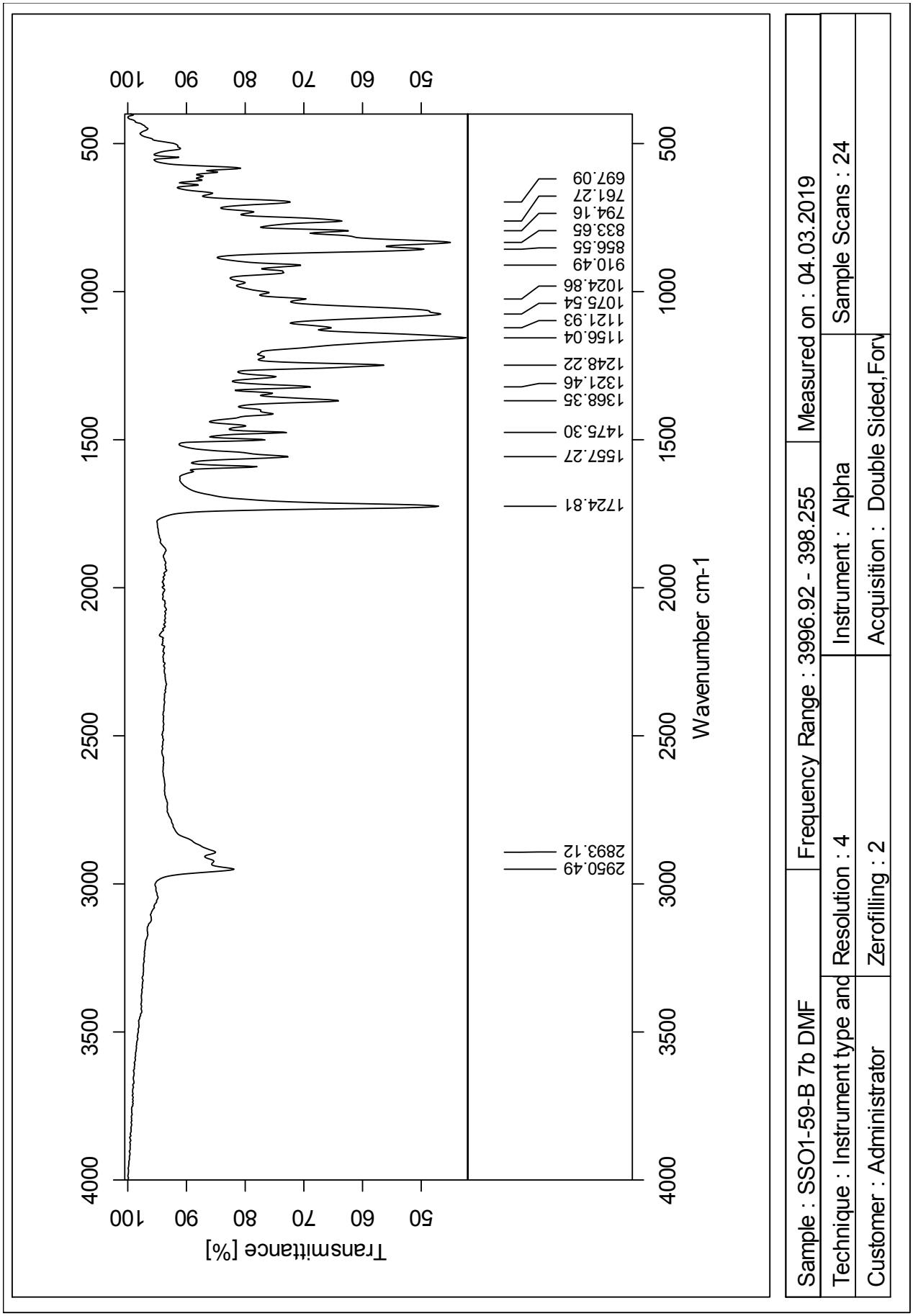

Figure L.7: IR spectrum of compound **12.**

XC

Appendix M Compound 13

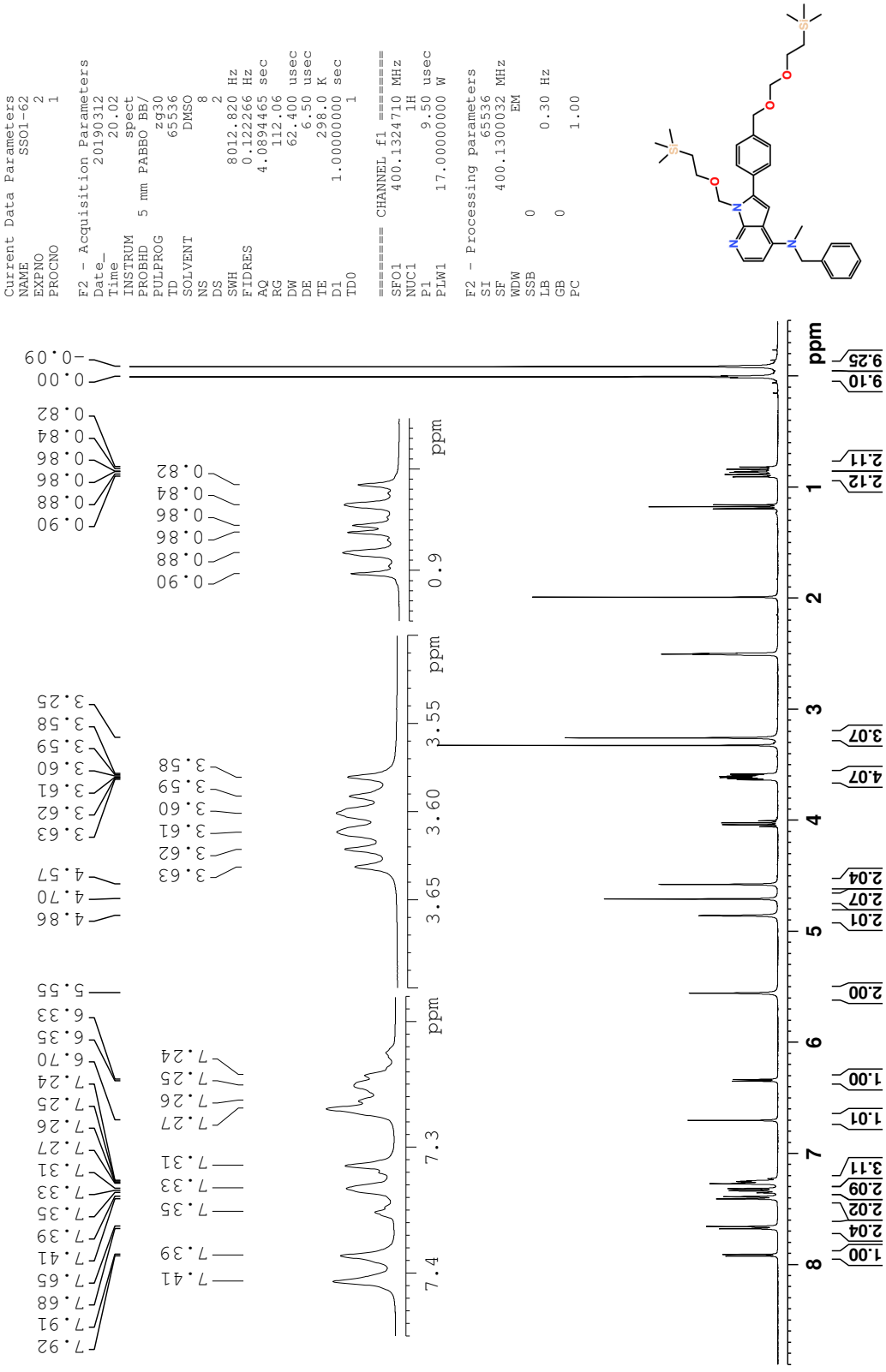

Figure M.1: ^{1}H NMR spectrum of compound **13.**

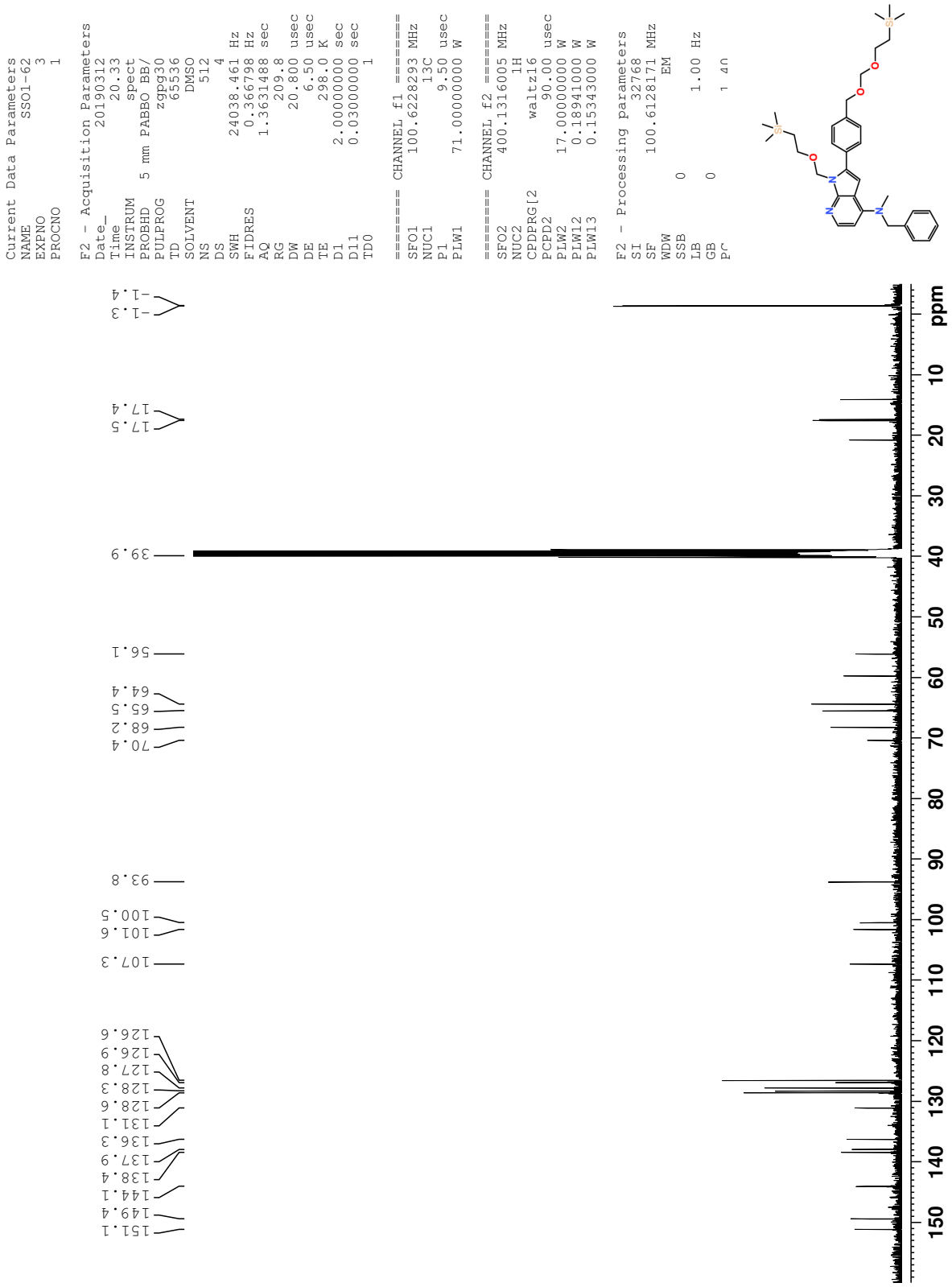

Figure M.2: ^{13}C NMR spectrum of compound **13.**

Figure M.3: COSY spectrum of compound **13.**

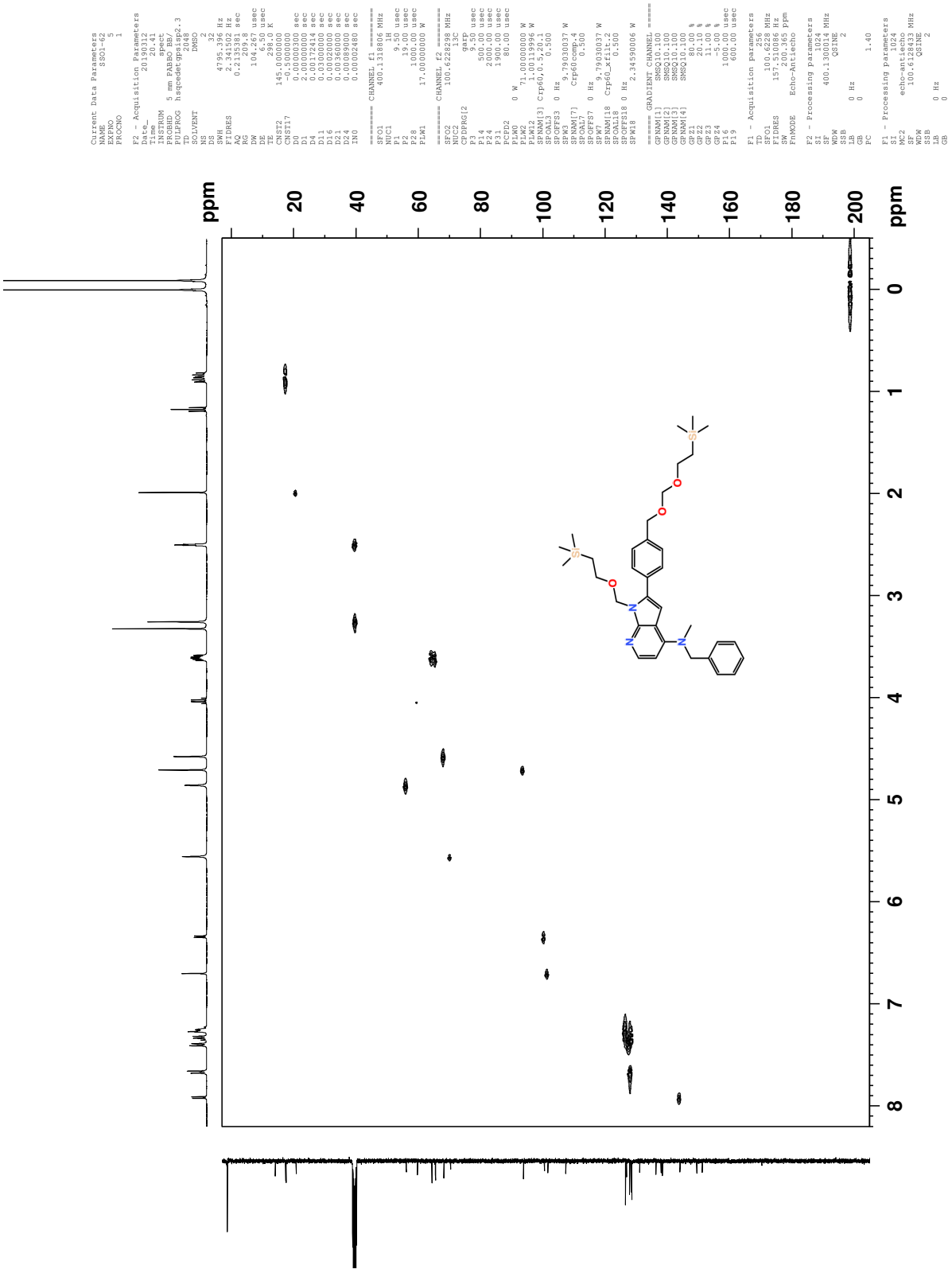

Figure M.4: HSQC spectrum of compound **13.**

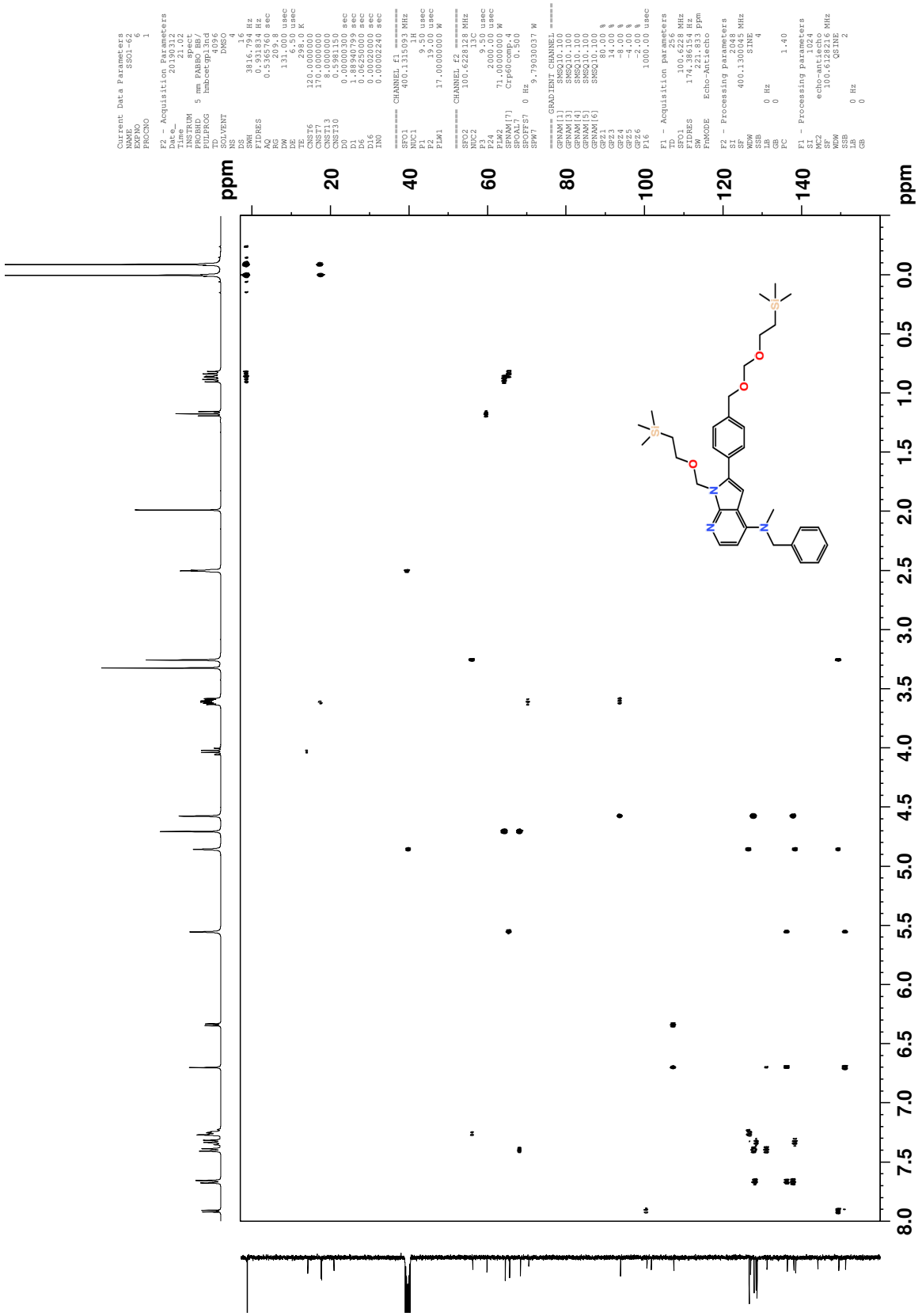

Figure M.5: HMBC spectrum of compound **13.**

Elemental Composition Report **Page 1**

Single Mass Analysis
Tolerance = 2.0 PPM / DBE: min = -2.0, max = 50.0
Element prediction: Off
Number of isotope peaks used for i-FIT = 3

Monoisotopic Mass, Even Electron Ions
1363 formula(e) evaluated with 3 results within limits (all results (up to 1000) for each mass)
Elements Used:
C: 0-100 H: 0-150 N: 0-5 O: 0-10 Si: 0-2
2019-147 144 (2.808) AM2 (Ar,35000.0,0.00,0.00); Cm (136:144)
1: TOF MS ASAP+

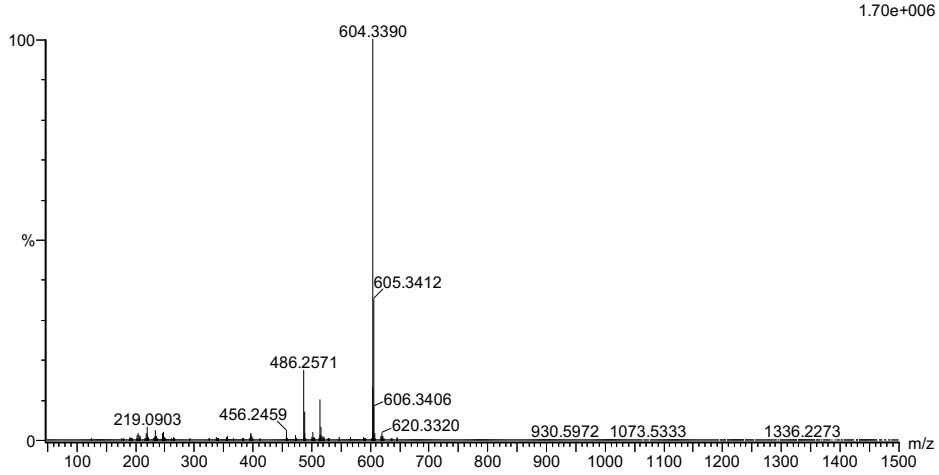

Minimum:				-2.0				
Maximum:		5.0	2.0	50.0				
Mass	Calc. Mass	mDa	PPM	DBE	i-FIT	Norm	Conf(%)	Formula
604.3390	604.3391	-0.1	-0.2	13.5	869.7	0.652	52.11	C34 H50 N3 O3 Si2
	604.3387	0.3	0.5	14.5	869.8	0.746	47.42	C35 H46 N3 O6
	604.3400	-1.0	-1.7	22.5	874.5	5.376	0.46	C43 H46 N Si

Figure M.6: MS spectrum of compound **13.**

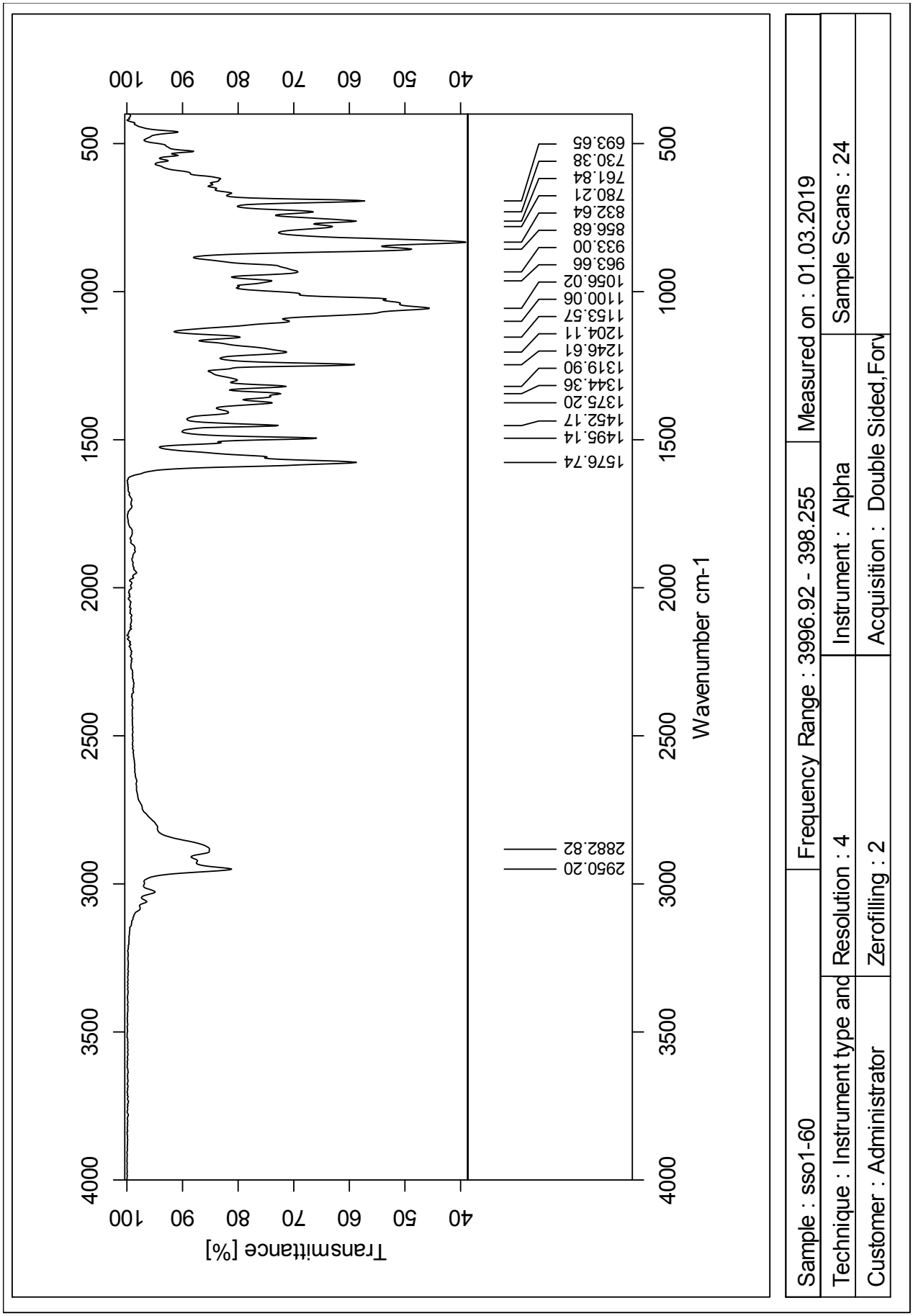

Figure M.7: IR spectrum of compound **13.**

Appendix N Compound 14

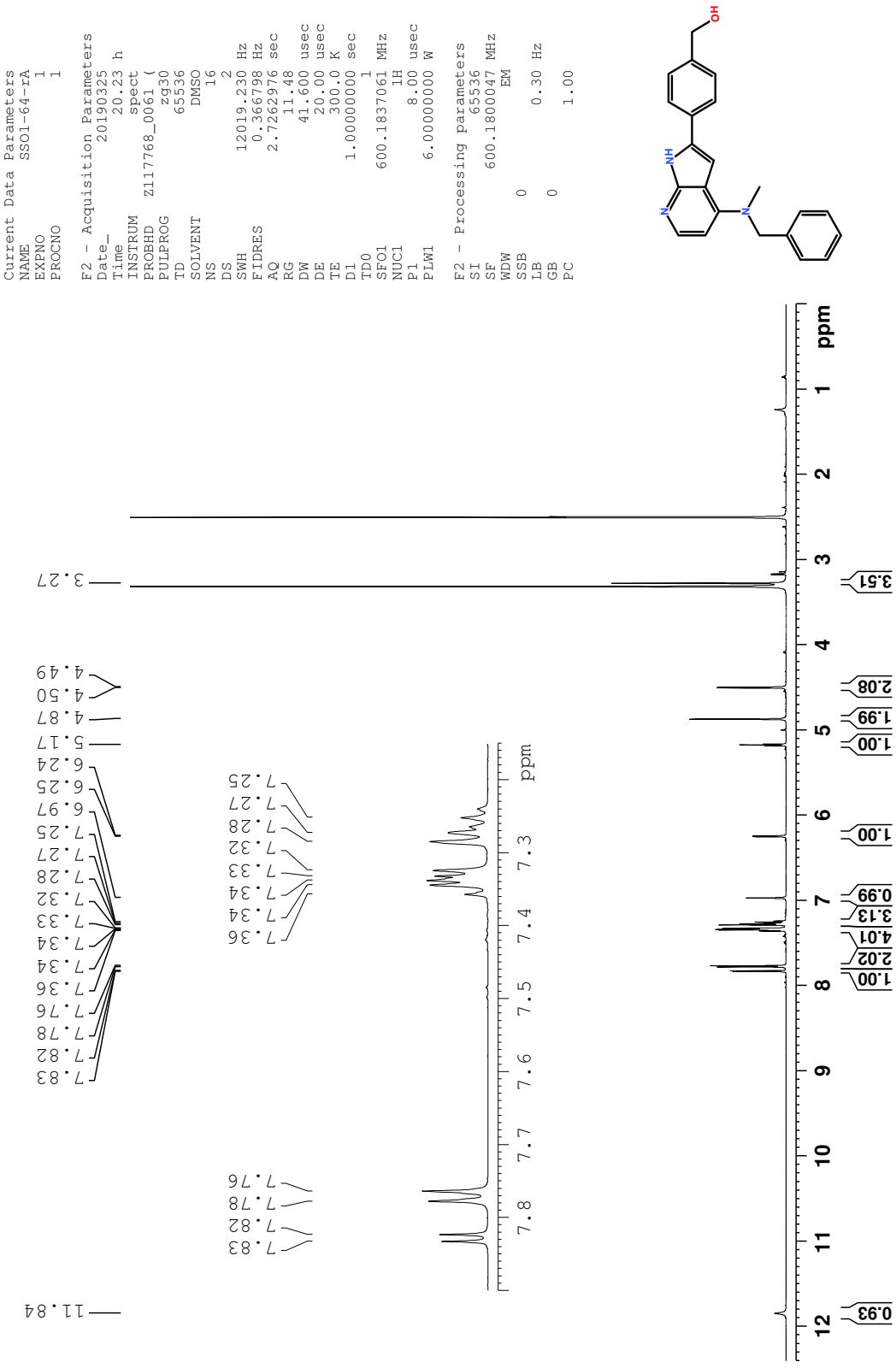

Figure N.1: ^{1}H NMR spectrum of compound **14.**

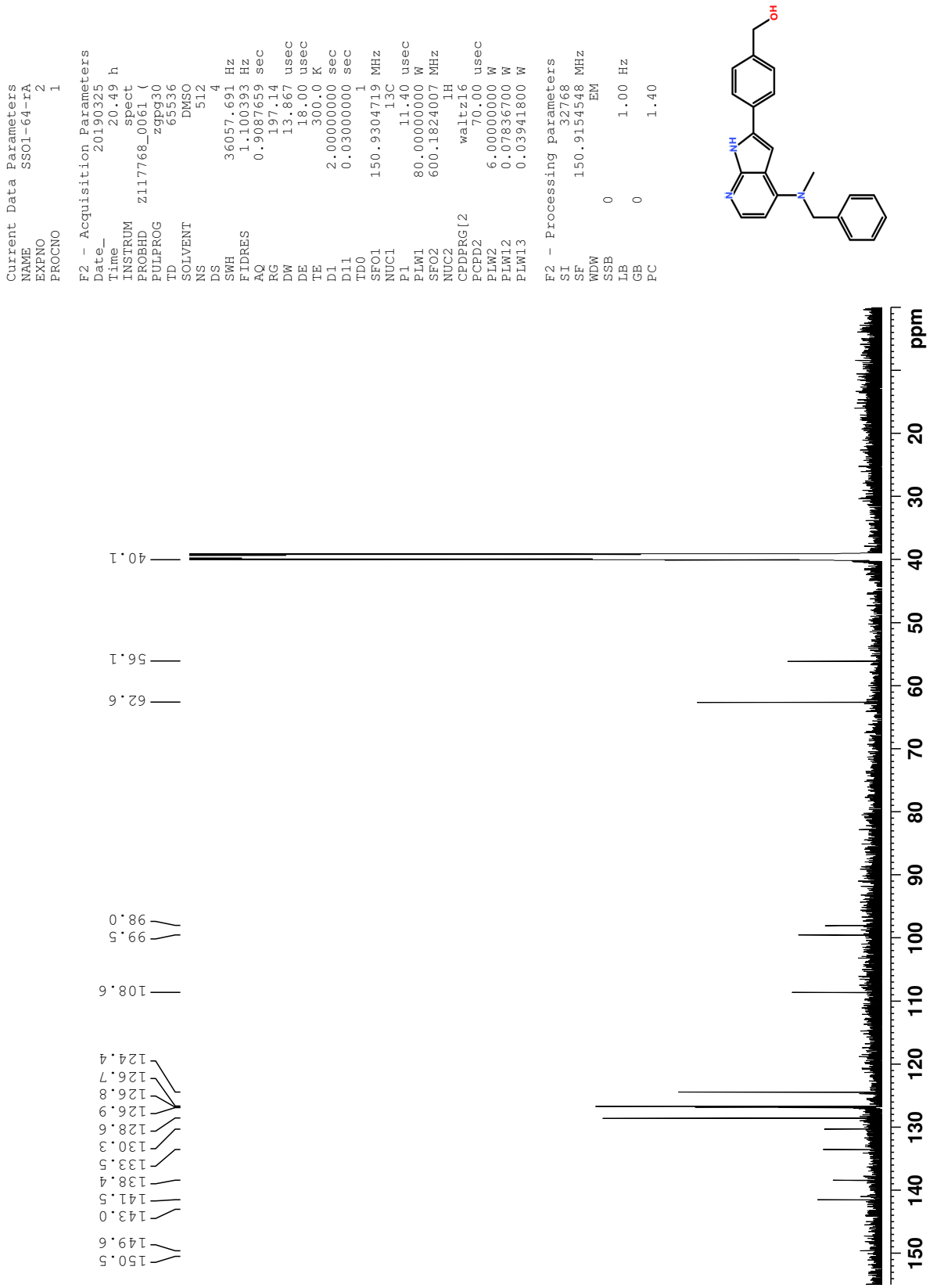

Figure N.2: ^{13}C NMR spectrum of compound **14.**

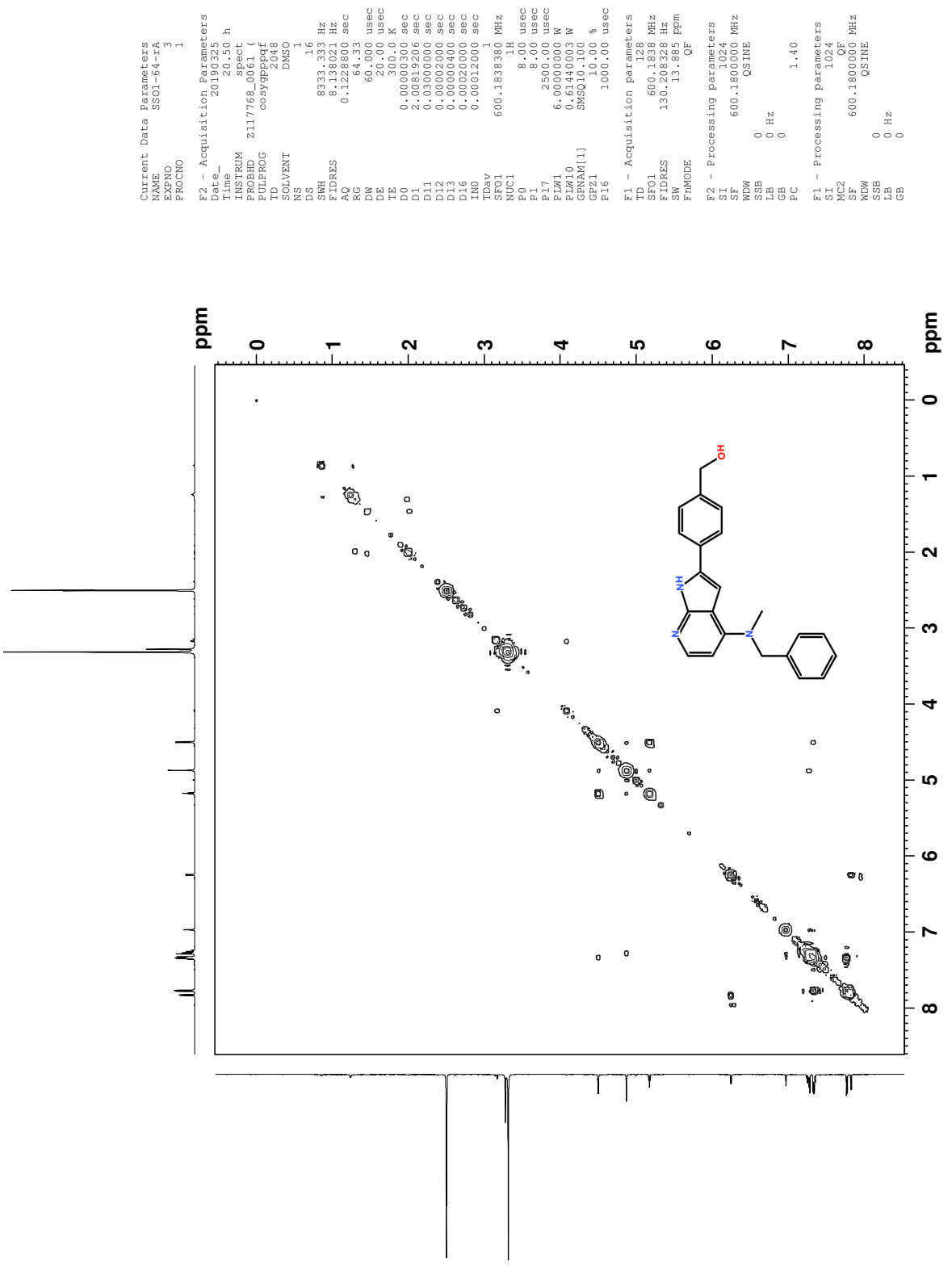

Figure N.3: COSY spectrum of compound **14.**

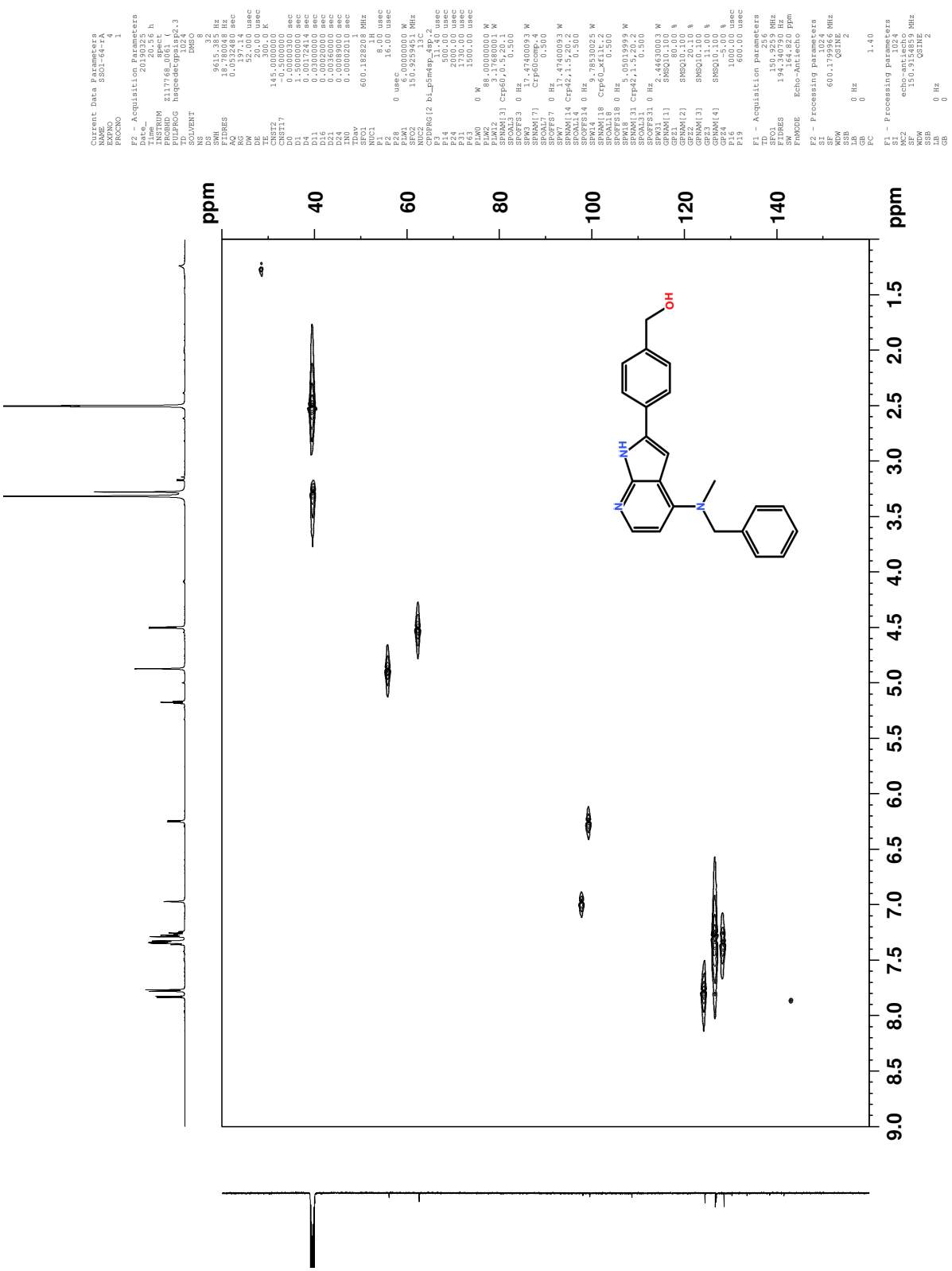

Figure N.4: HSQC spectrum of compound **14.**

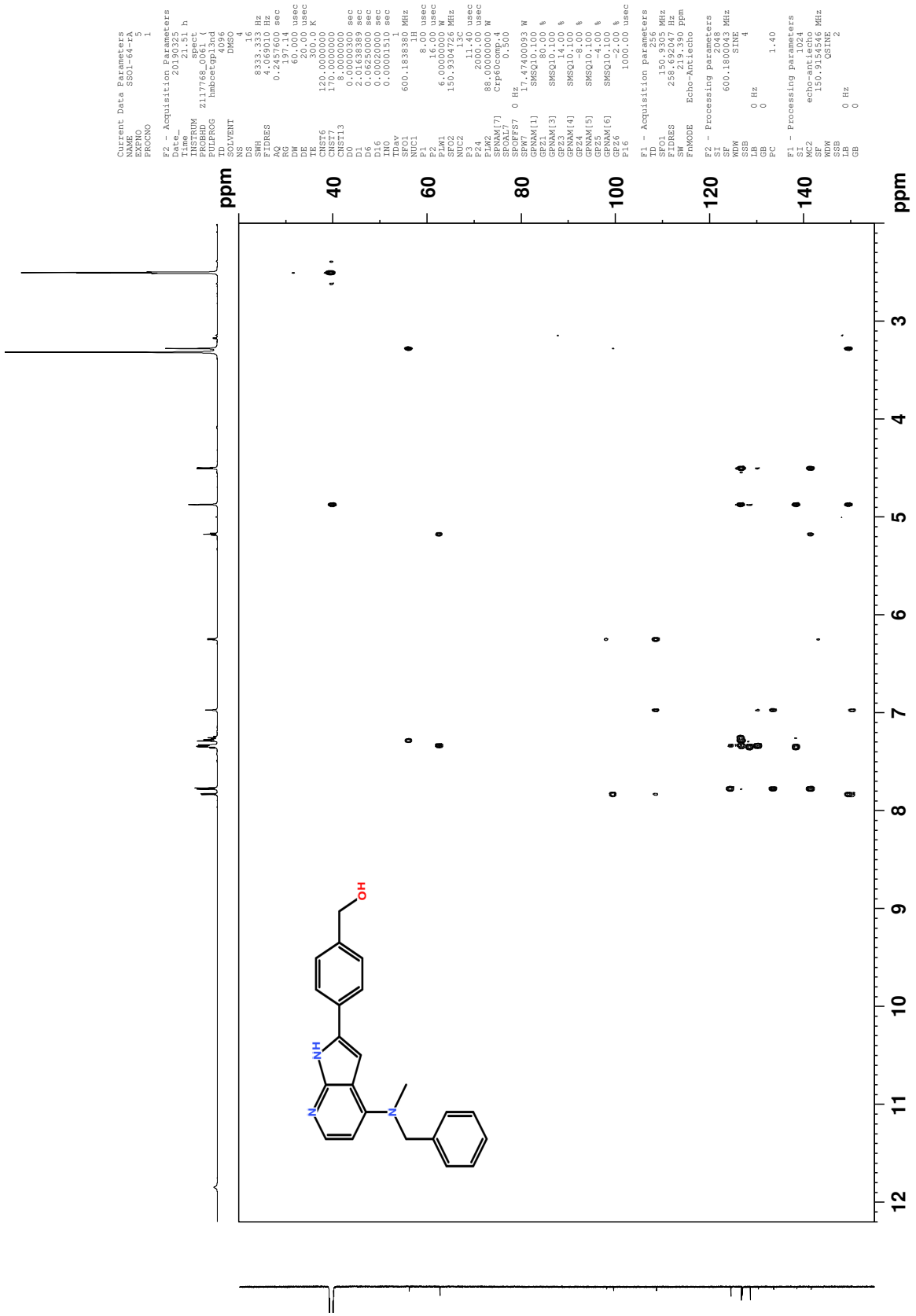

Figure N.5: HMBC spectrum of compound **14.**

Elemental Composition Report **Page 1**

Tolerance = 5.0 PPM / DBE: min = -50.0, max = 50.0
Element prediction: Off
Number of isotope peaks used for i-FIT = 3

Monoisotopic Mass, Even Electron Ions
803 formula(e) evaluated with 1 results within limits (all results (up to 1000) for each mass)
Elements Used:
C: 0-100 H: 0-150 N: 0-5 O: 0-5 Na: 0-1
2019-205 155 (3.034) AM2 (Ar,35000.0,0.00,0.00); Cm (153:156)
1: TOF MS ASAP+

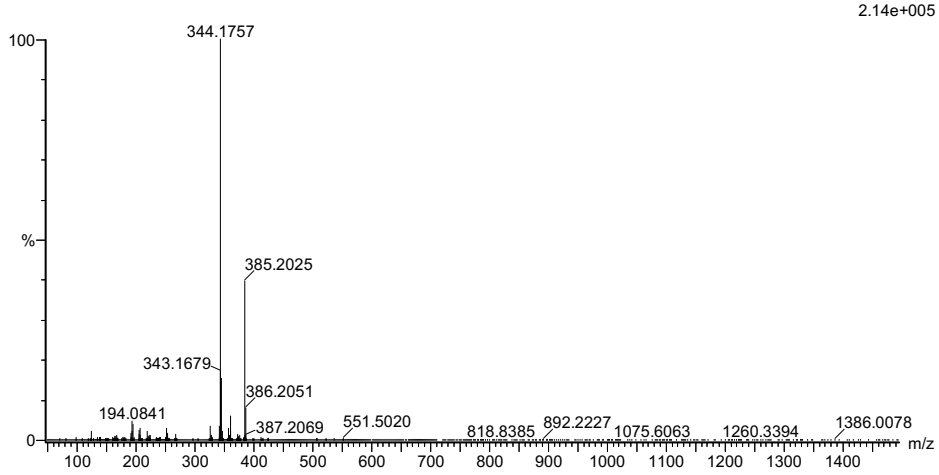

Minimum:	80.00				-50.0				
Maximum:	100.00		5.0	5.0	50.0				
Mass	RA	Calc. Mass	mDa	PPM	DBE	i-FIT	Norm	Conf(%)	Formula
344.1757	100.00	344.1763	-0.6	-1.7	13.5	823.5	n/a	n/a	C22 H22 N3 O

Figure N.6: MS spectrum of compound **14.**

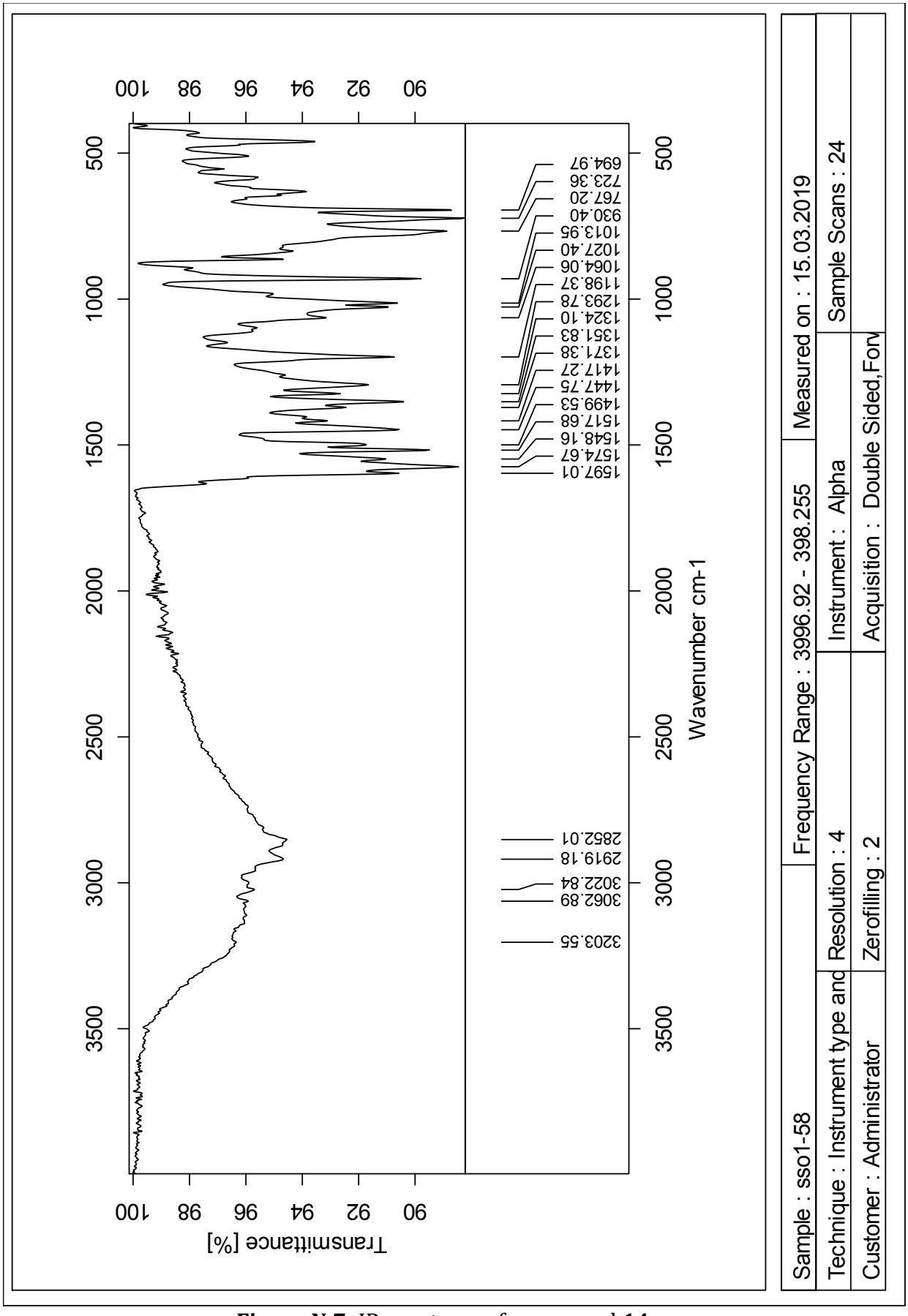

Figure N.7: IR spectrum of compound **14.**

Appendix O Compound 15

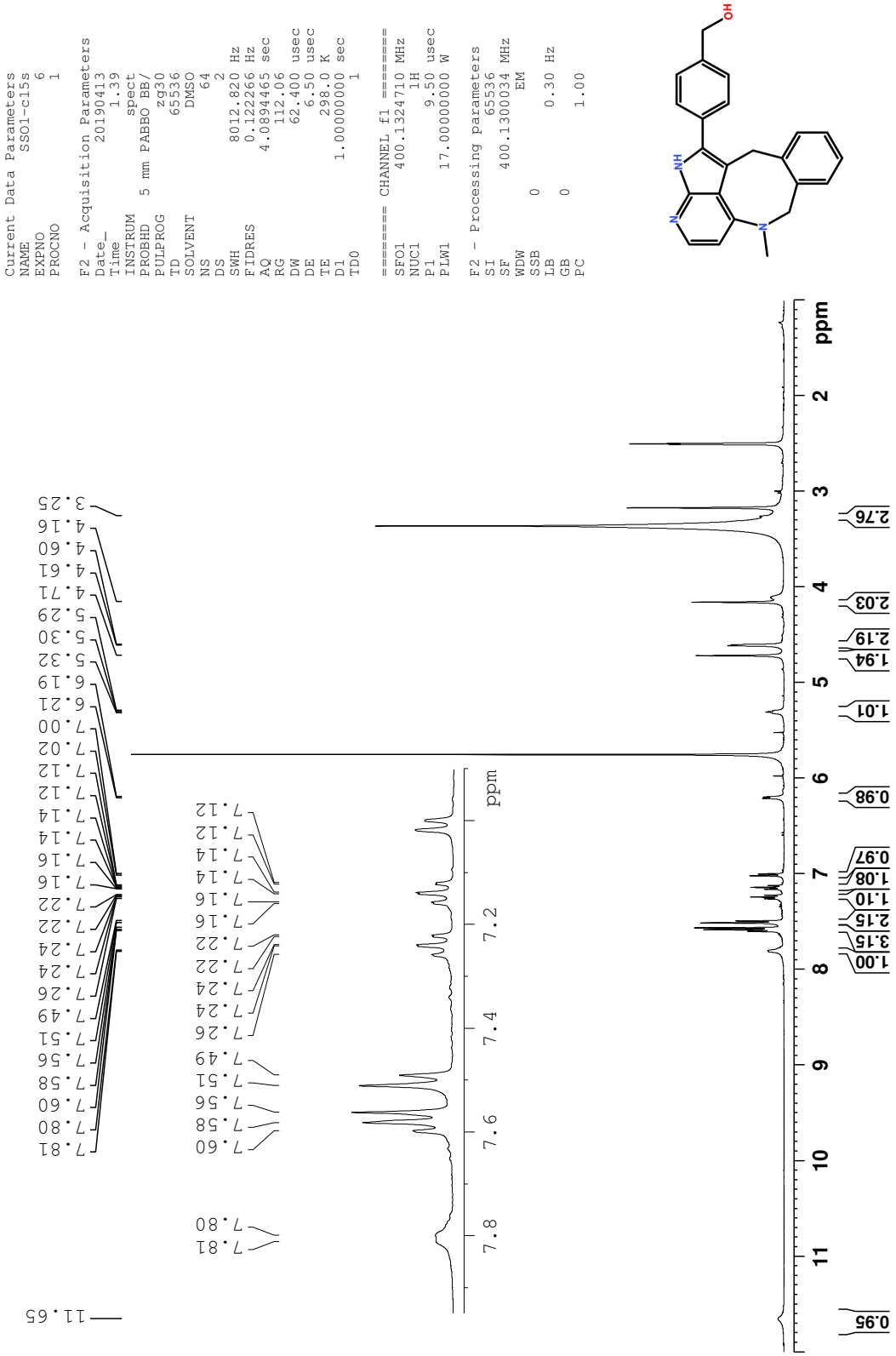

Figure O.1: ^{1}H NMR spectrum of compound **15.**

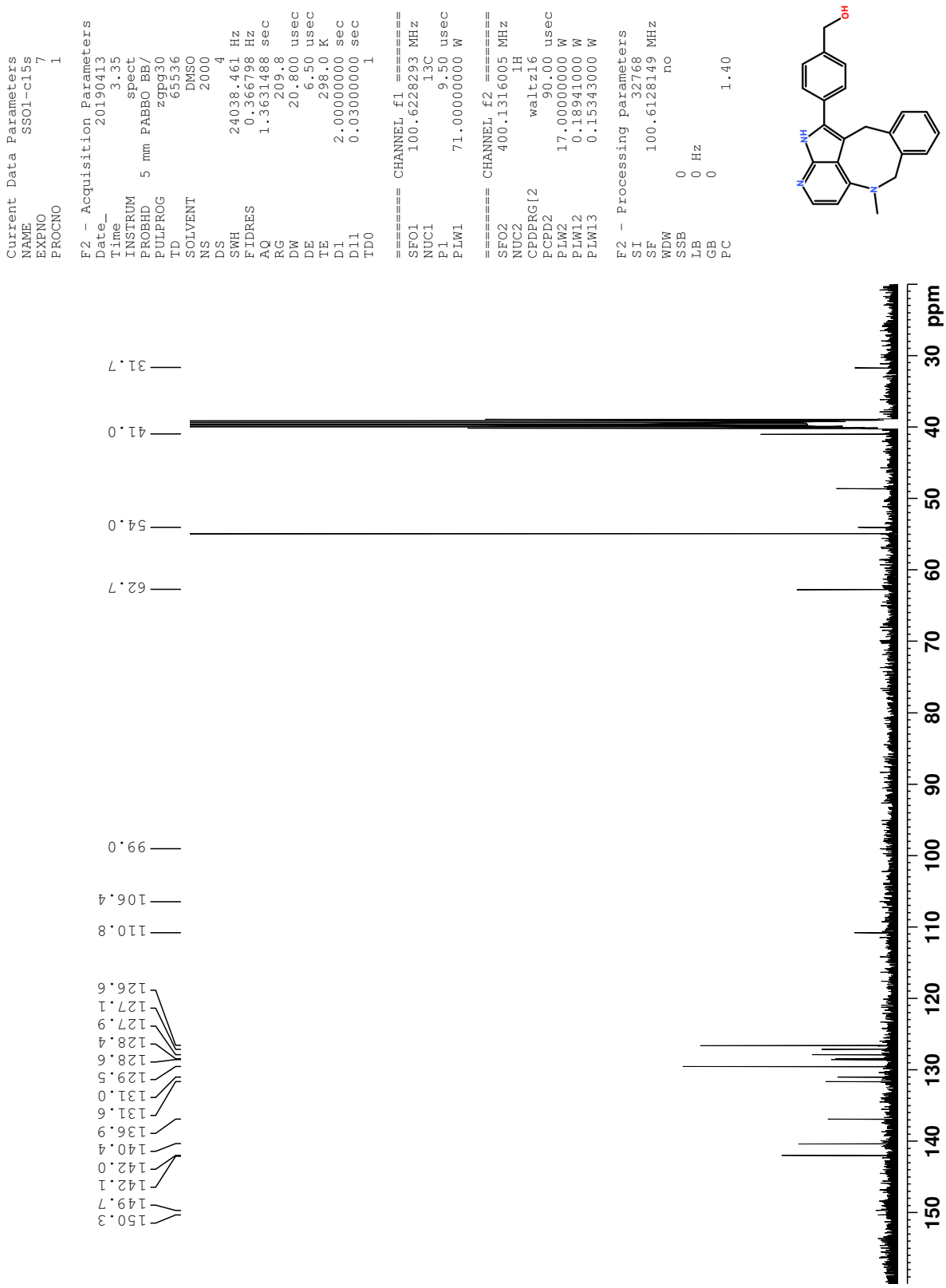

Figure O.2: ^{13}C NMR spectrum of compound **15.**

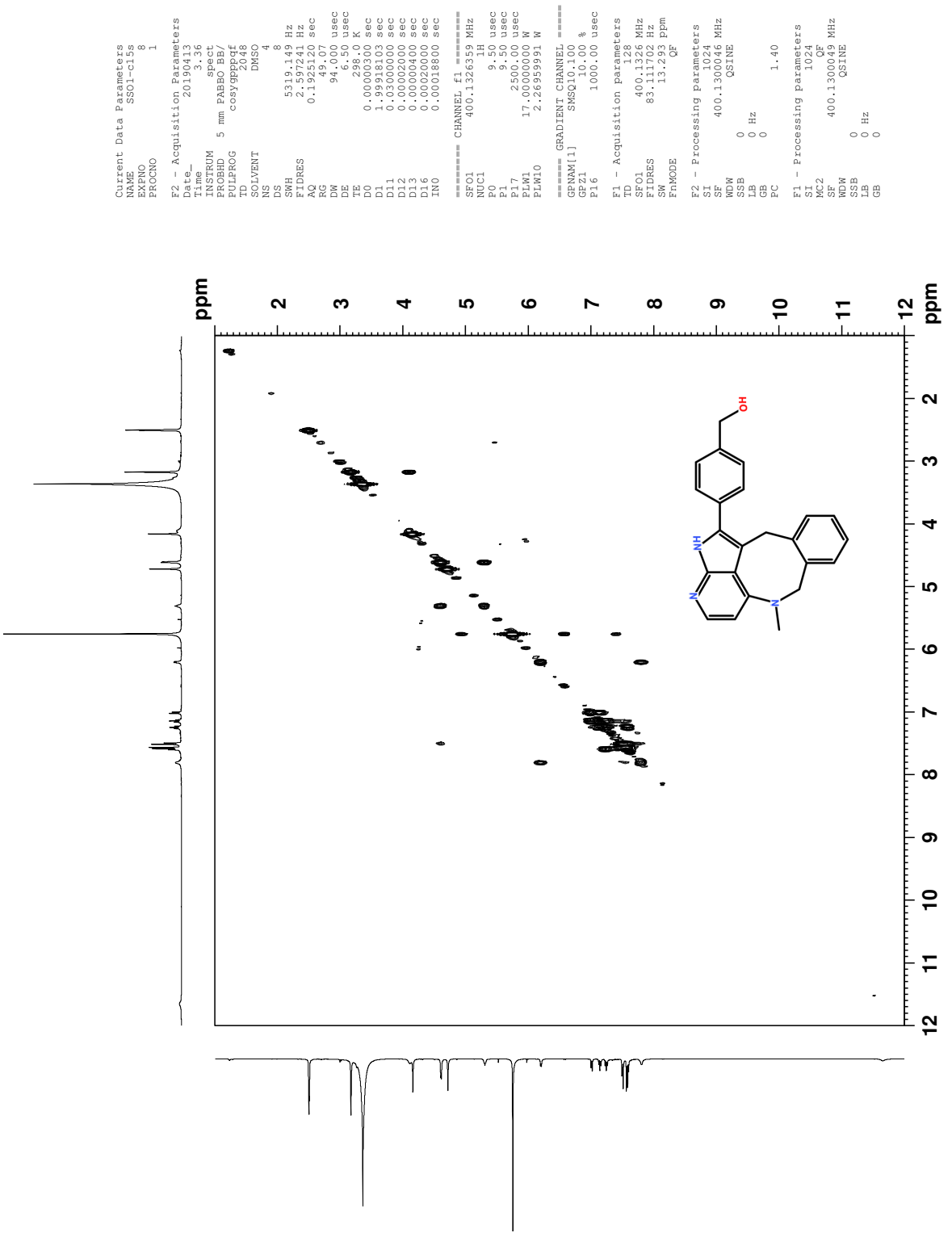

Figure O.3: COSY spectrum of compound **15.**

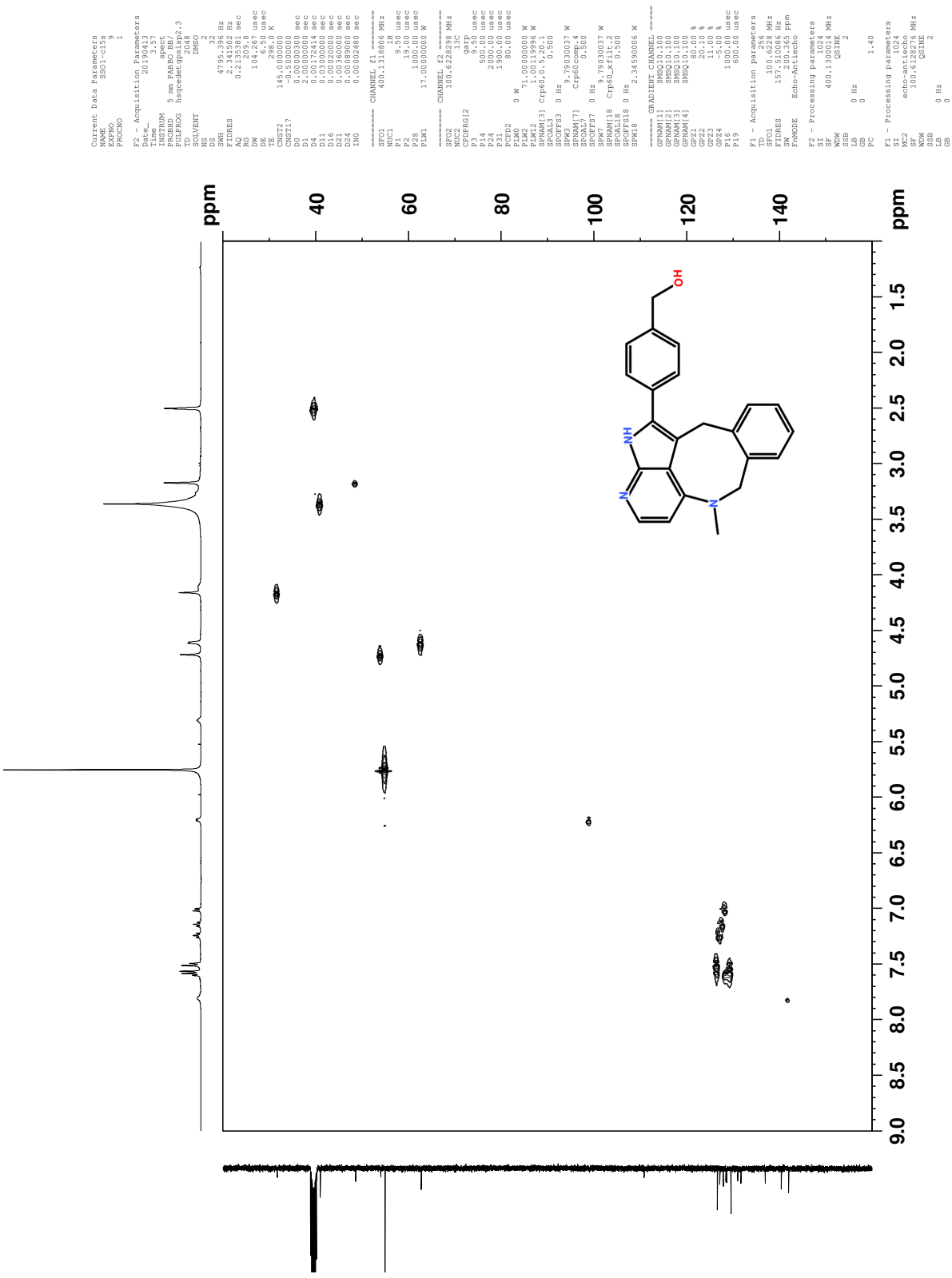

Figure 0.4: HSQC spectrum of compound **15.**

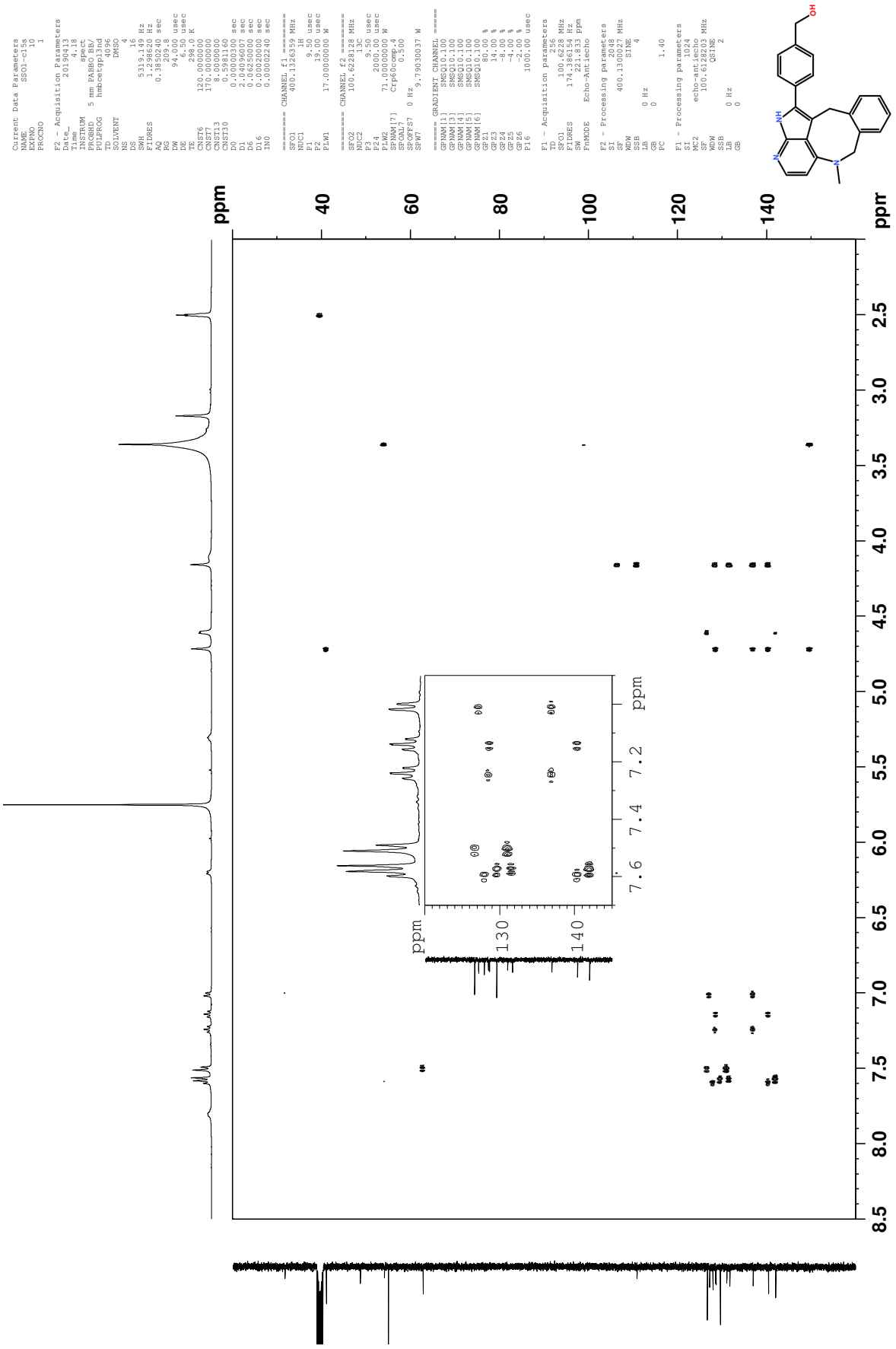

Figure O.5: HMBC spectrum of compound **15.**

Elemental Composition Report **Page 1**

Single Mass Analysis
Tolerance = 2.0 PPM / DBE: min = -50.0, max = 50.0
Element prediction: Off
Number of isotope peaks used for i-FIT = 3

Monoisotopic Mass, Even Electron Ions
3135 formula(e) evaluated with 2 results within limits (all results (up to 1000) for each mass)
Elements Used:
C: 0-100 H: 0-150 N: 0-10 O: 0-15 Na: 0-1
2019-261 188 (3.672) AM2 (Ar,35000.0,0.00,0.00); Cm (187:192)
1: TOF MS ASAP+

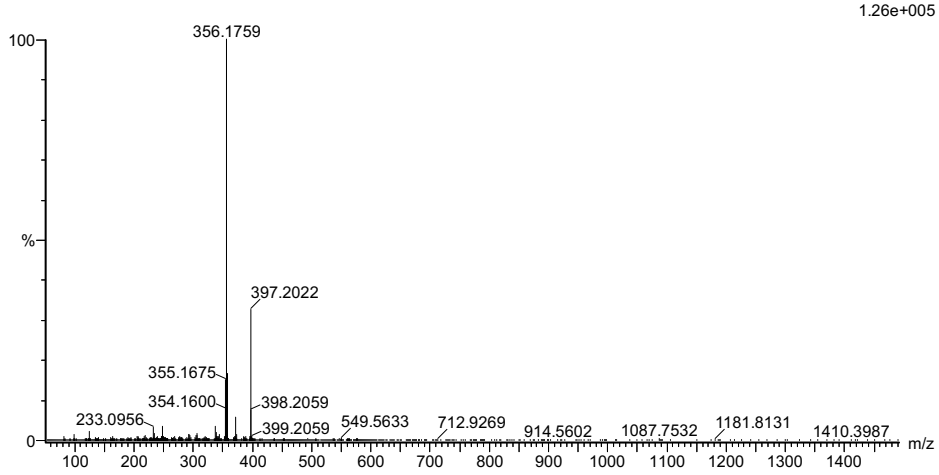

Minimum:				-50.0				
Maximum:		5.0	2.0	50.0				
Mass	Calc. Mass	mDa	PPM	DBE	i-FIT	Norm	Conf(%)	Formula
356.1759	356.1757	0.2	0.6	-1.5	796.7	0.413	66.17	C9 H27 N5 O8 Na
	356.1763	-0.4	-1.1	14.5	797.4	1.084	33.83	C23 H22 N3 O

Figure O.6: MS spectrum of compound **15.**

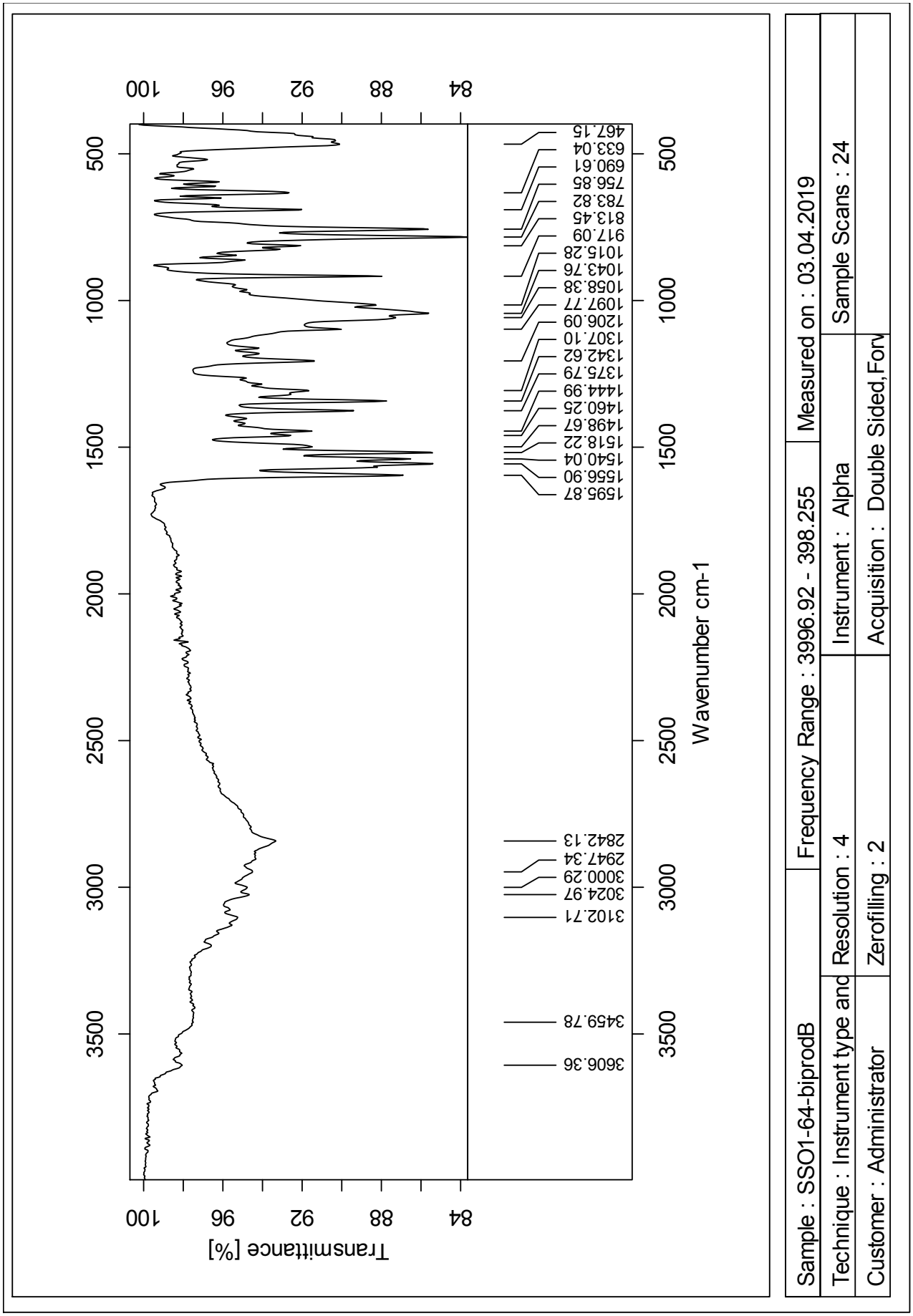

Figure 0.7: IR spectrum of compound **15.**

Appendix P Compound 16

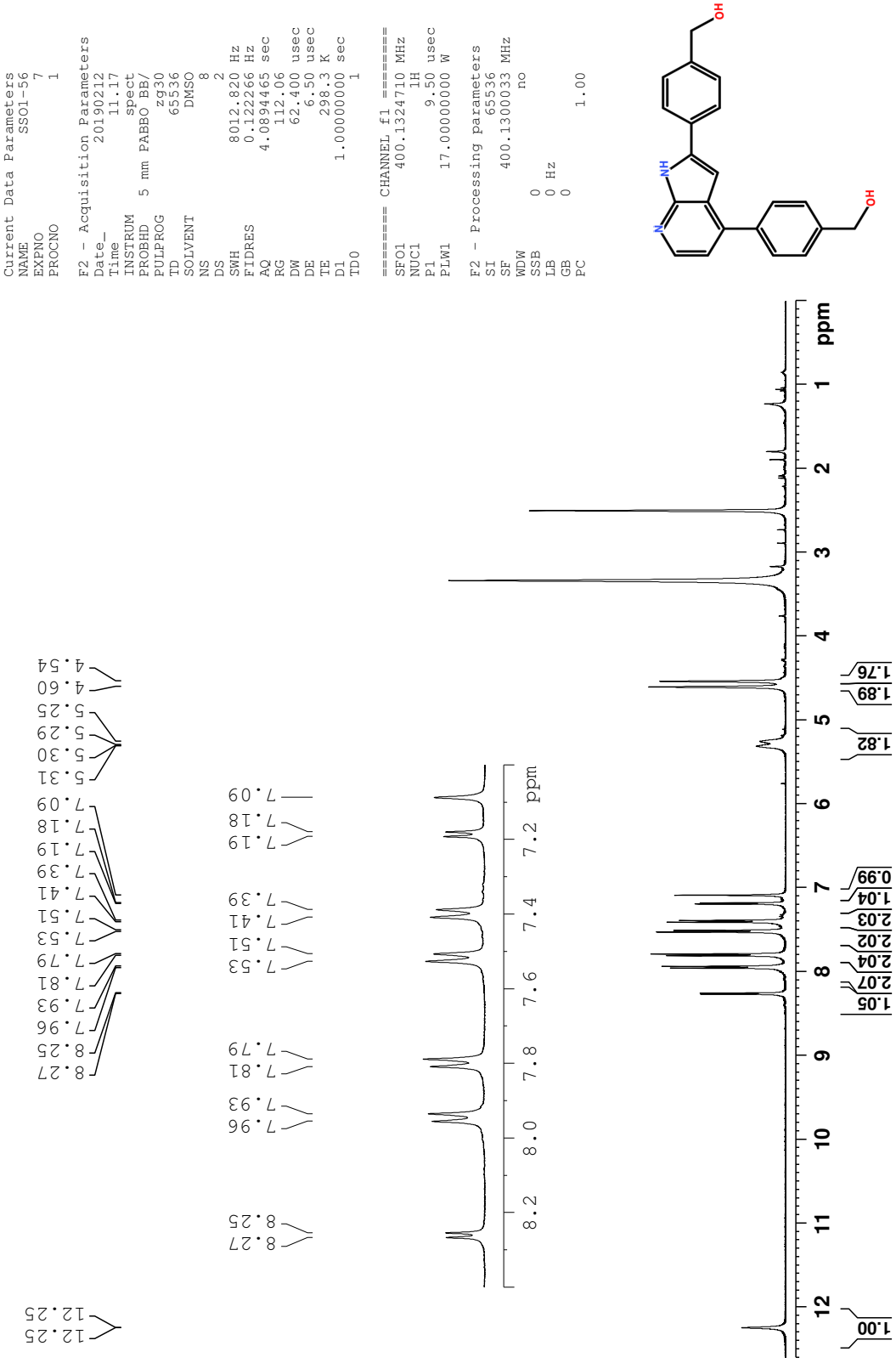

Figure P.1: ^{1}H NMR spectrum of compound **16.**

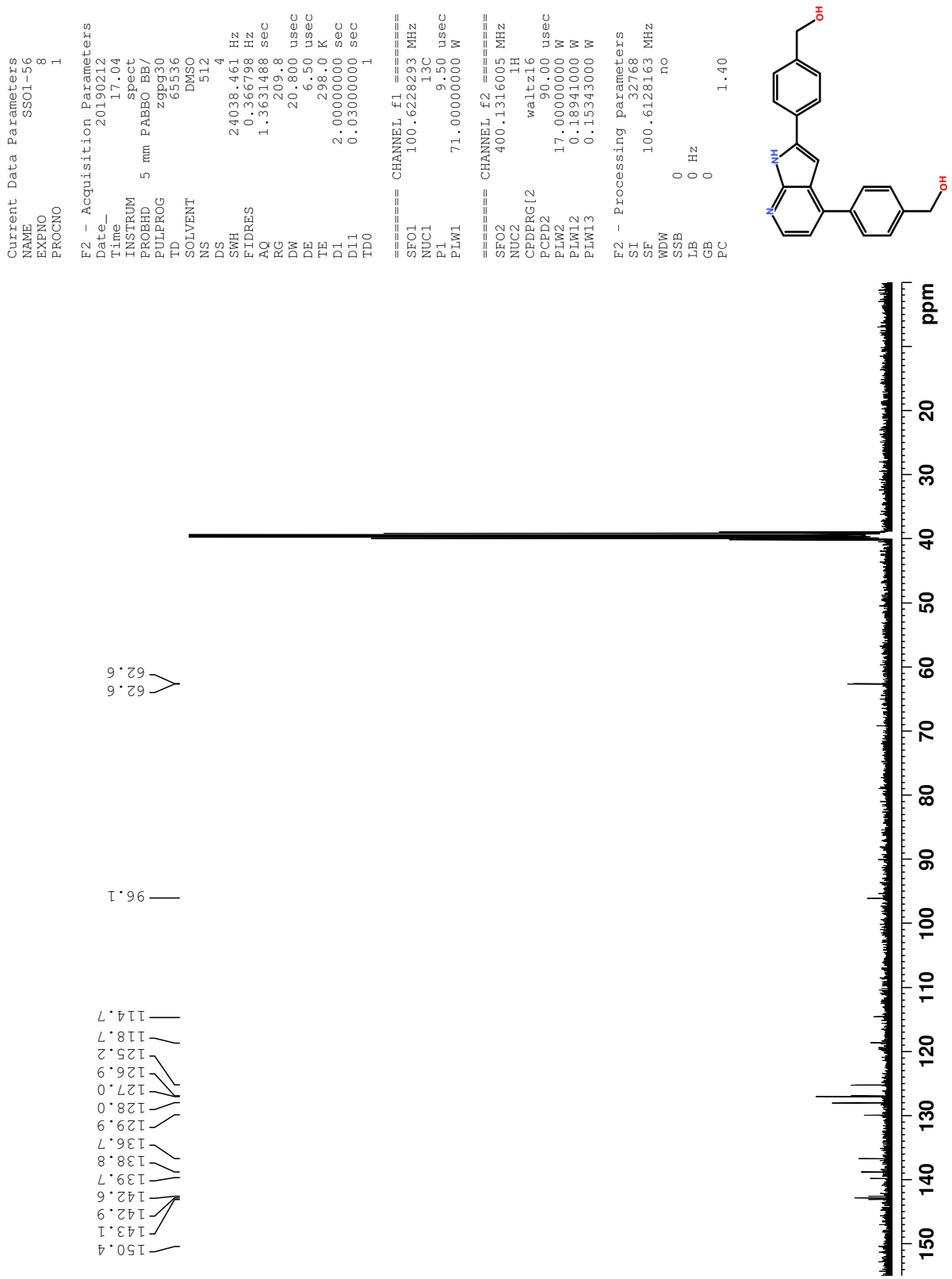

Figure P.2: ^{13}C NMR spectrum of compound **16.**

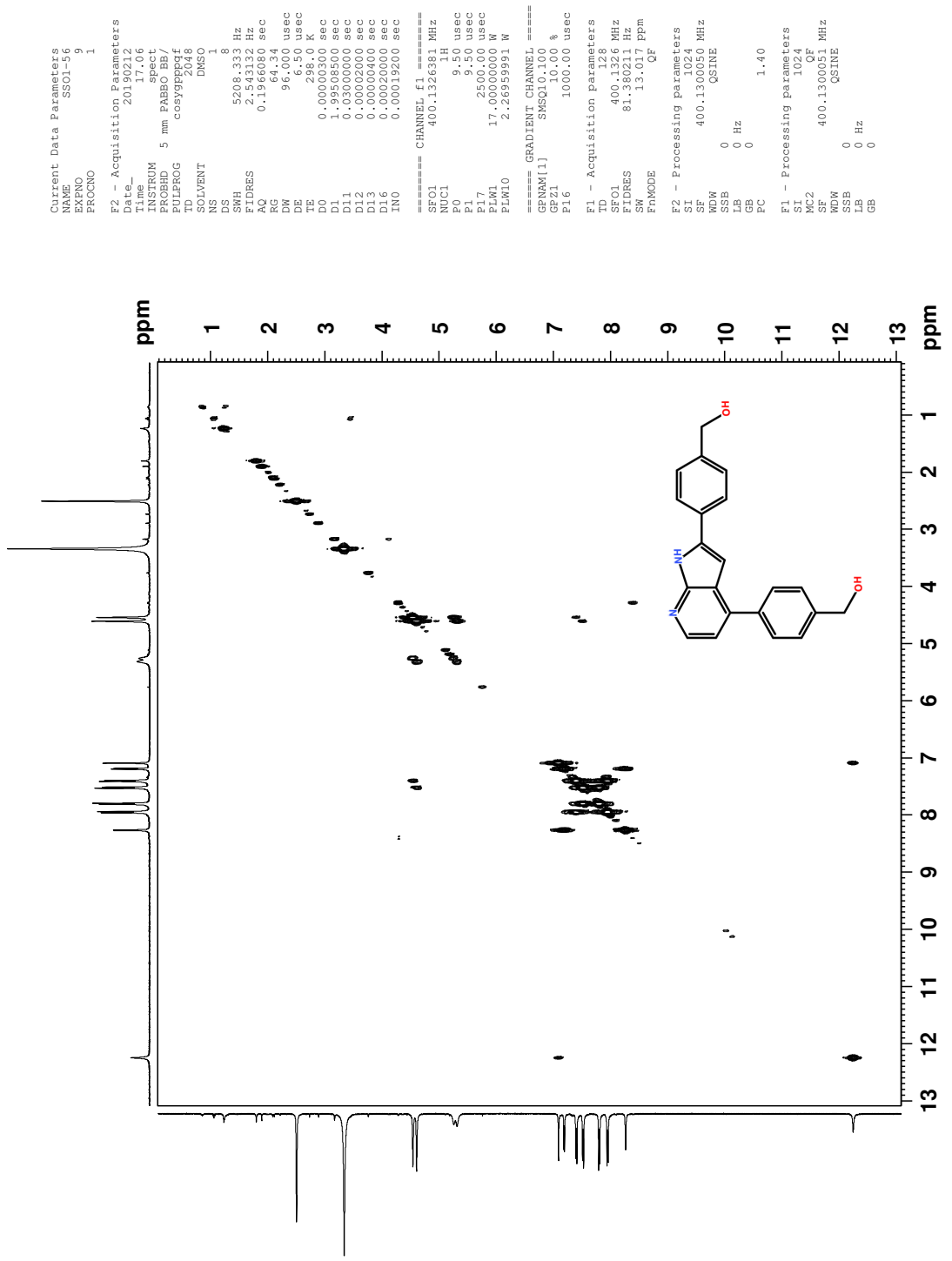

Figure P.3: COSY spectrum of compound **16.**

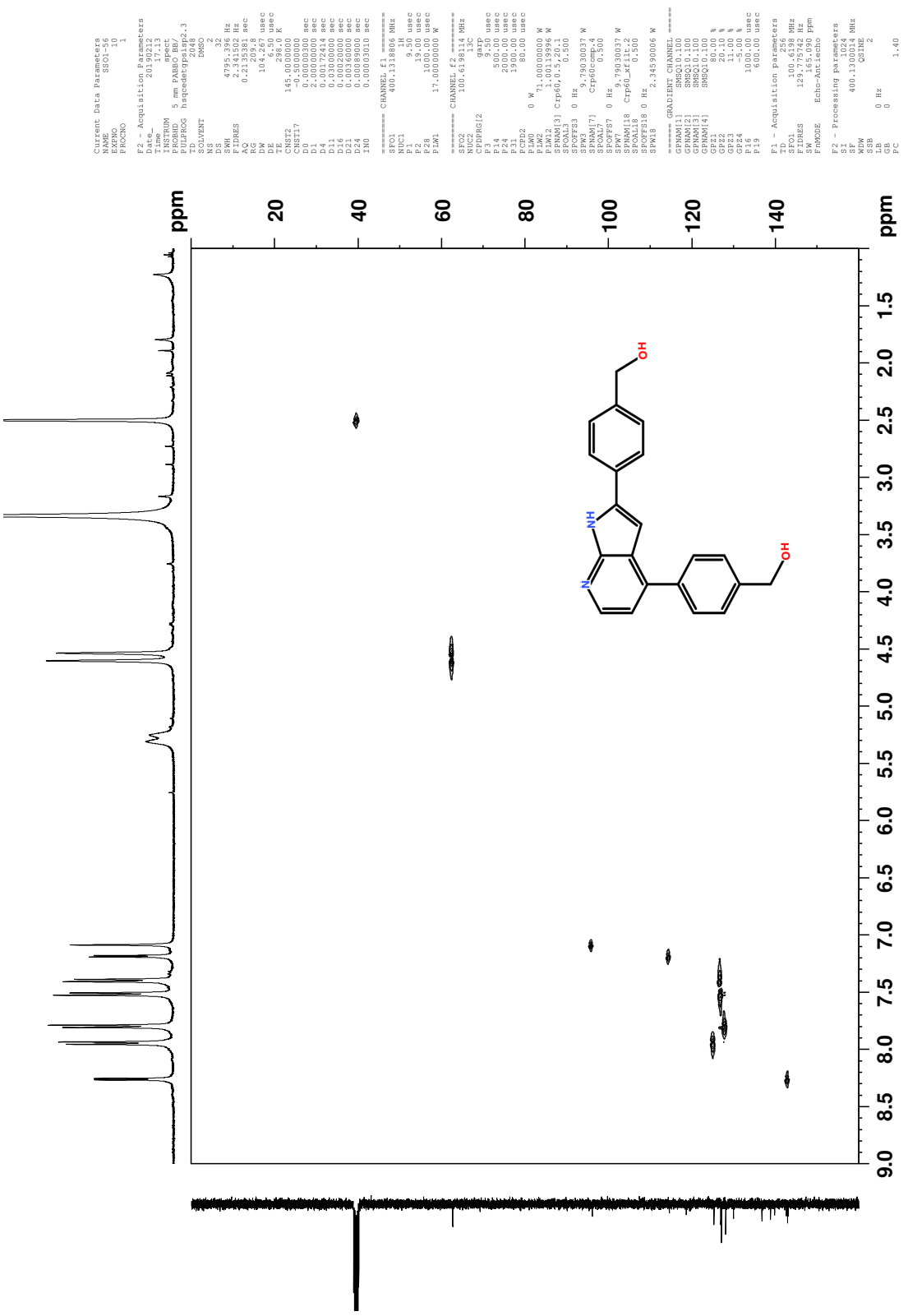

Figure P.4: HSQC spectrum of compound **16.**

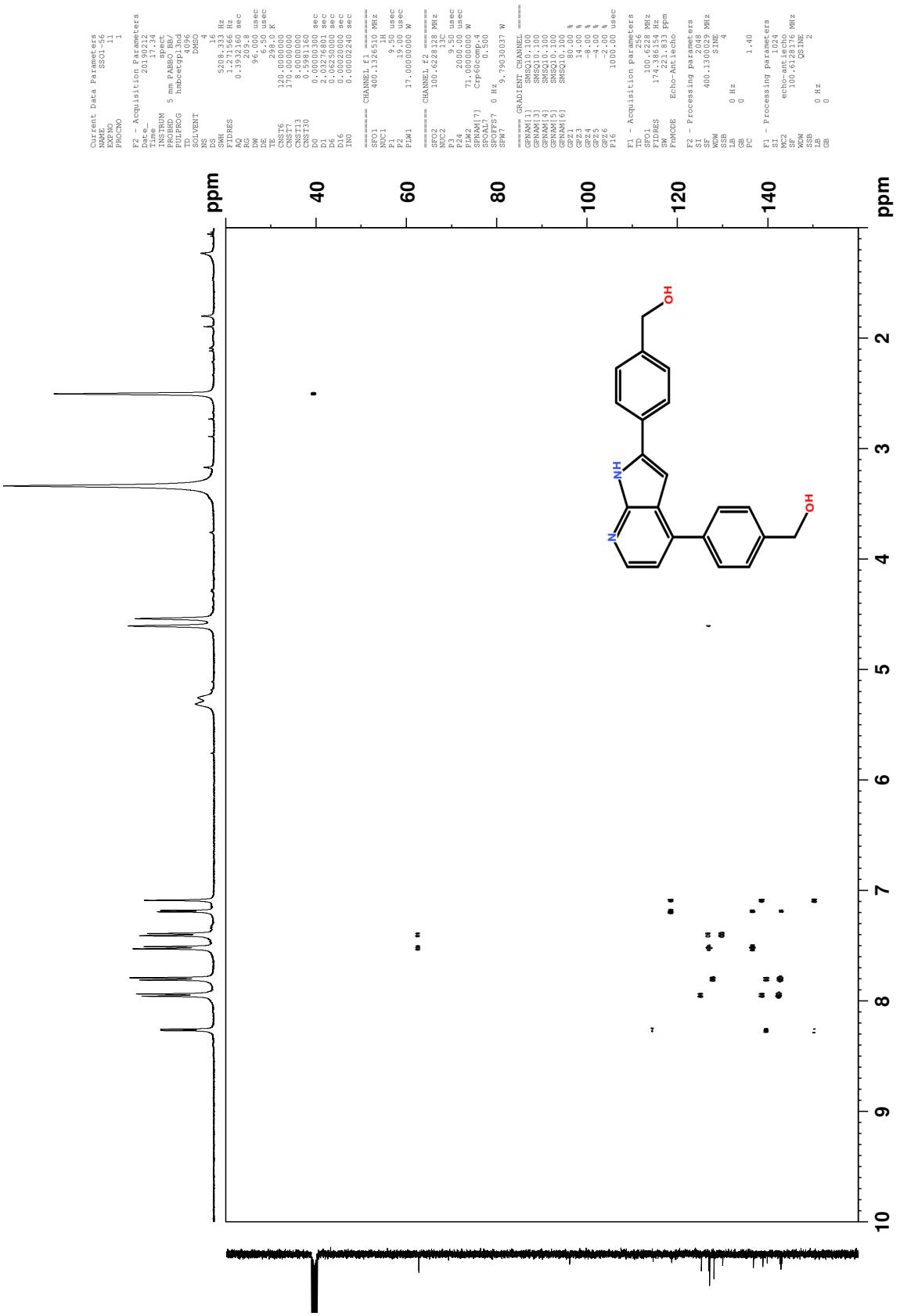

Figure P.5: HMBC spectrum of compound **16.**

Elemental Composition Report **Page 1**

Single Mass Analysis
Tolerance = 2.0 PPM / DBE: min = -2.0, max = 50.0
Element prediction: Off
Number of isotope peaks used for i-FIT = 3

Monoisotopic Mass, Even Electron Ions
2013 formula(e) evaluated with 5 results within limits (all results (up to 1000) for each mass)
Elements Used:
C: 0-100 H: 0-150 N: 0-10 O: 0-5 Si: 0-2 Cl: 0-2
2019-137 238 (4.635) AM2 (Ar,35000.0,0.00,0.00); Cm (234:239)
1: TOF MS ASAP+

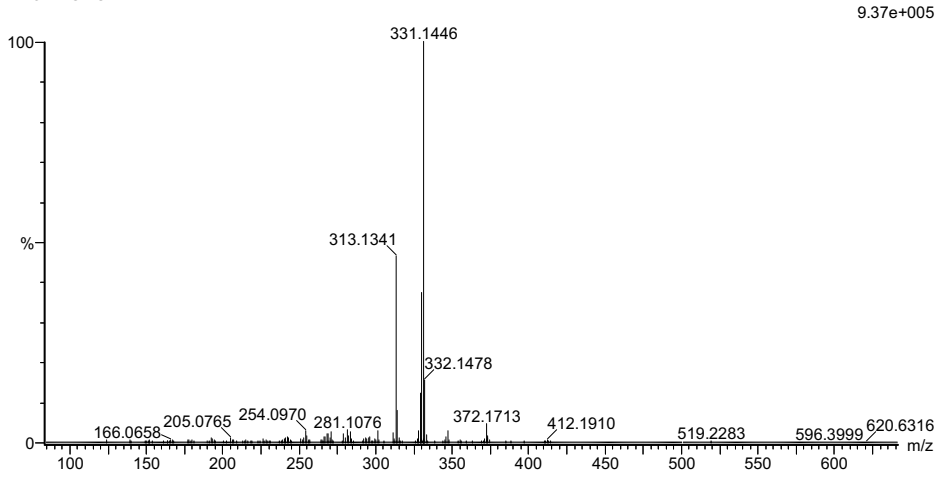

Minimum:				-2.0				
Maximum:		5.0	2.0	50.0				
Mass	Calc. Mass	mDa	PPM	DBE	i-FIT	Norm	Conf(%)	Formula
331.1446	331.1447	-0.1	-0.3	-1.5	1142.5	19.499	0.00	C13 H33 O Si2 Cl2
	331.1447	-0.1	-0.3	13.5	1123.0	0.000	100.00	C21 H19 N2 O2
	331.1443	0.3	0.9	-0.5	1142.7	19.722	0.00	C14 H29 O4 Cl2
	331.1442	0.4	1.2	0.5	1138.0	14.964	0.00	C4 H23 N10 O4 Si2
	331.1451	-0.5	-1.5	9.5	1135.2	12.158	0.00	C13 H19 N8 O Si

Figure P.6: MS spectrum of compound **16.**

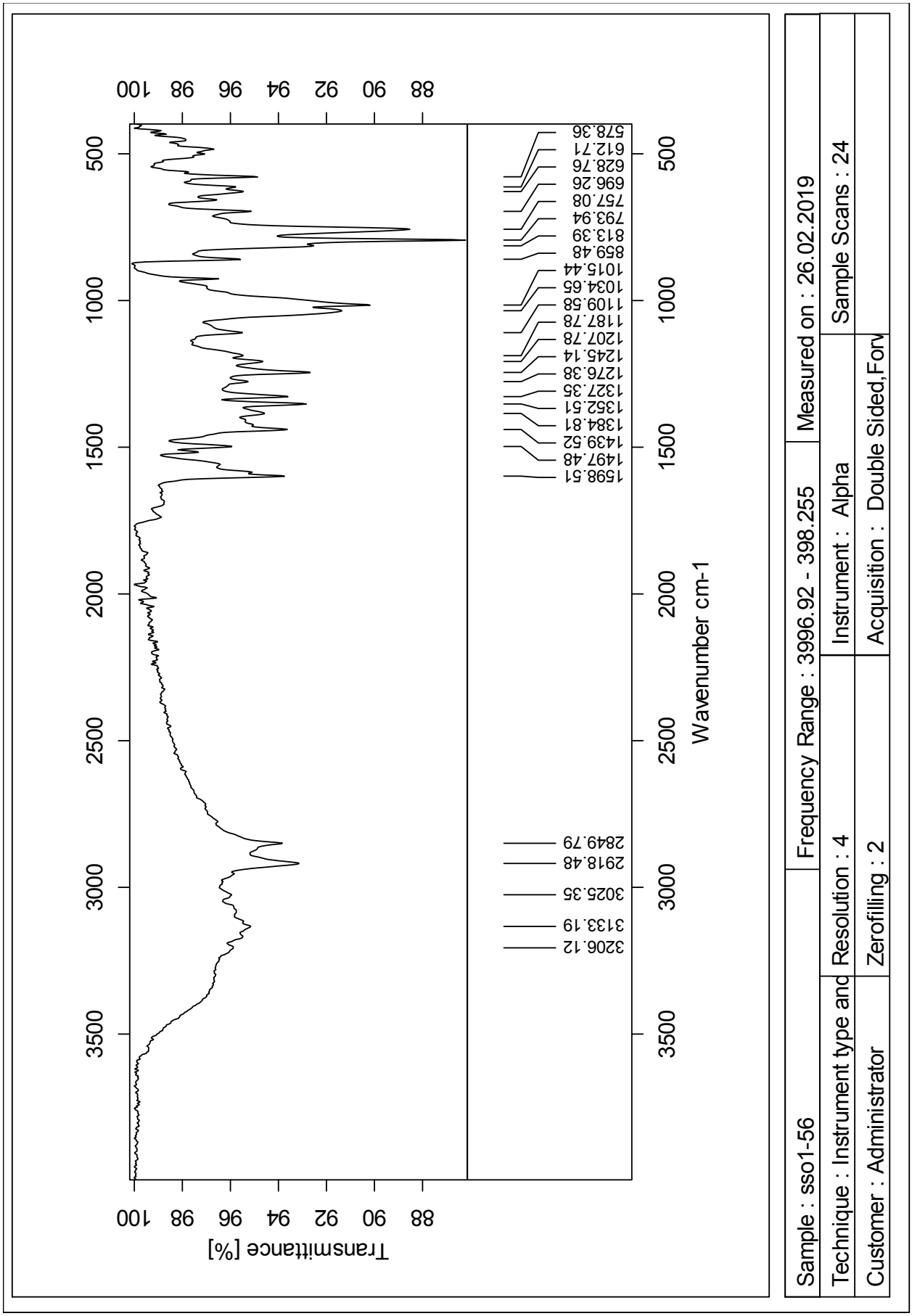

Figure P.7: IR spectrum of compound **16.**

Appendix Q Compound 17

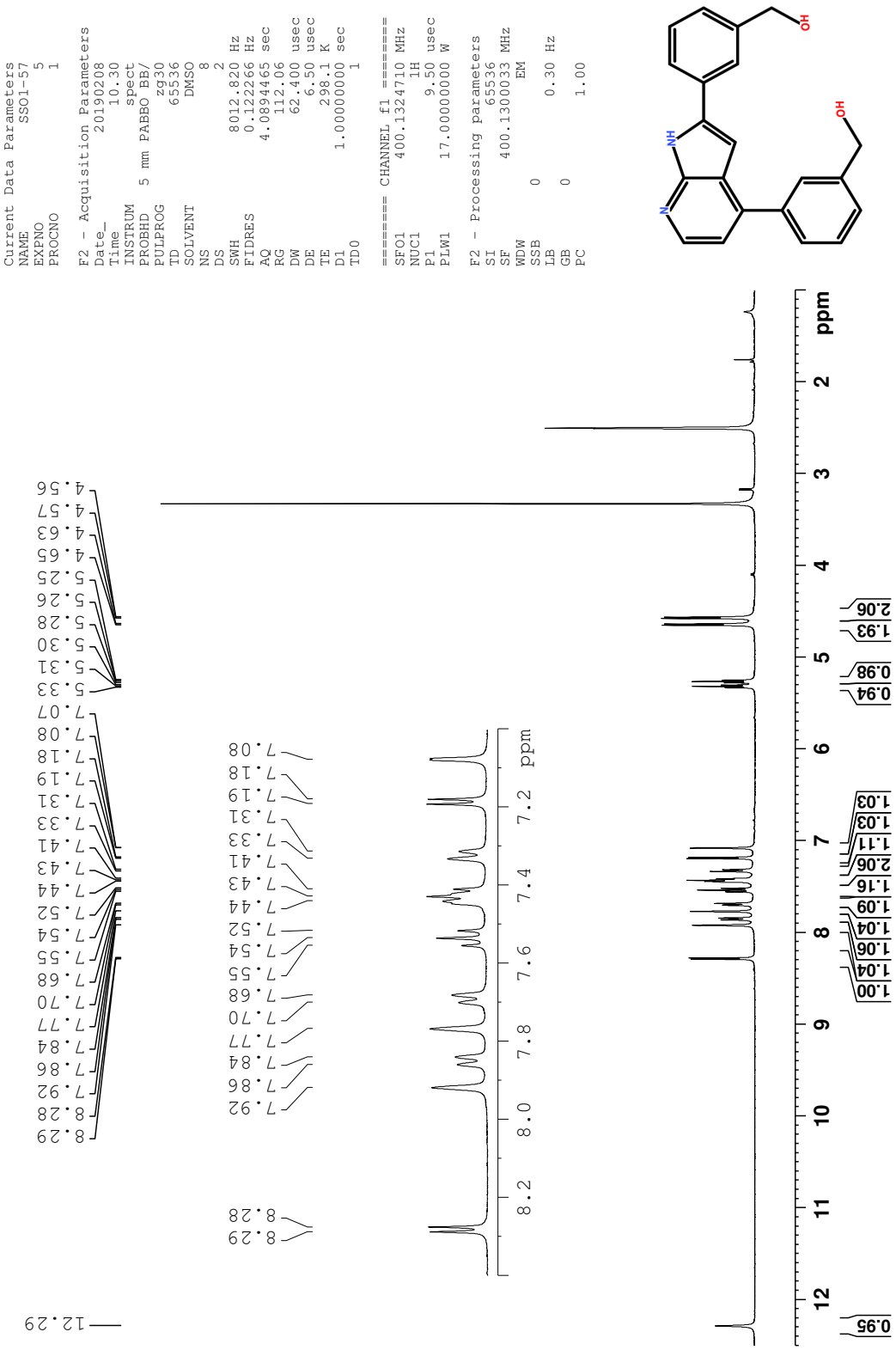

Figure Q.1: ^{1}H NMR spectrum of compound **17.**

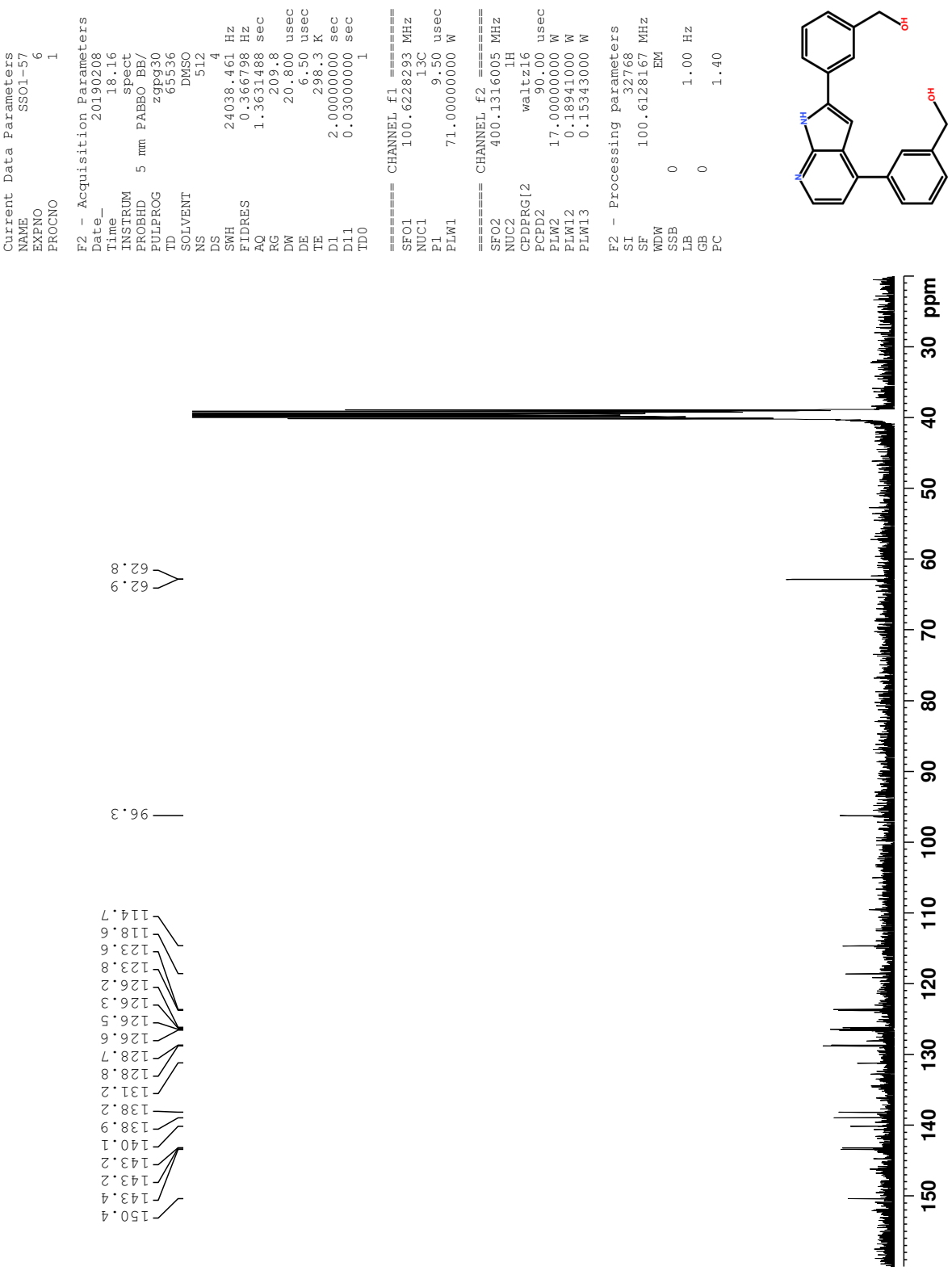

Figure Q.2: ^{13}C NMR spectrum of compound **17.**

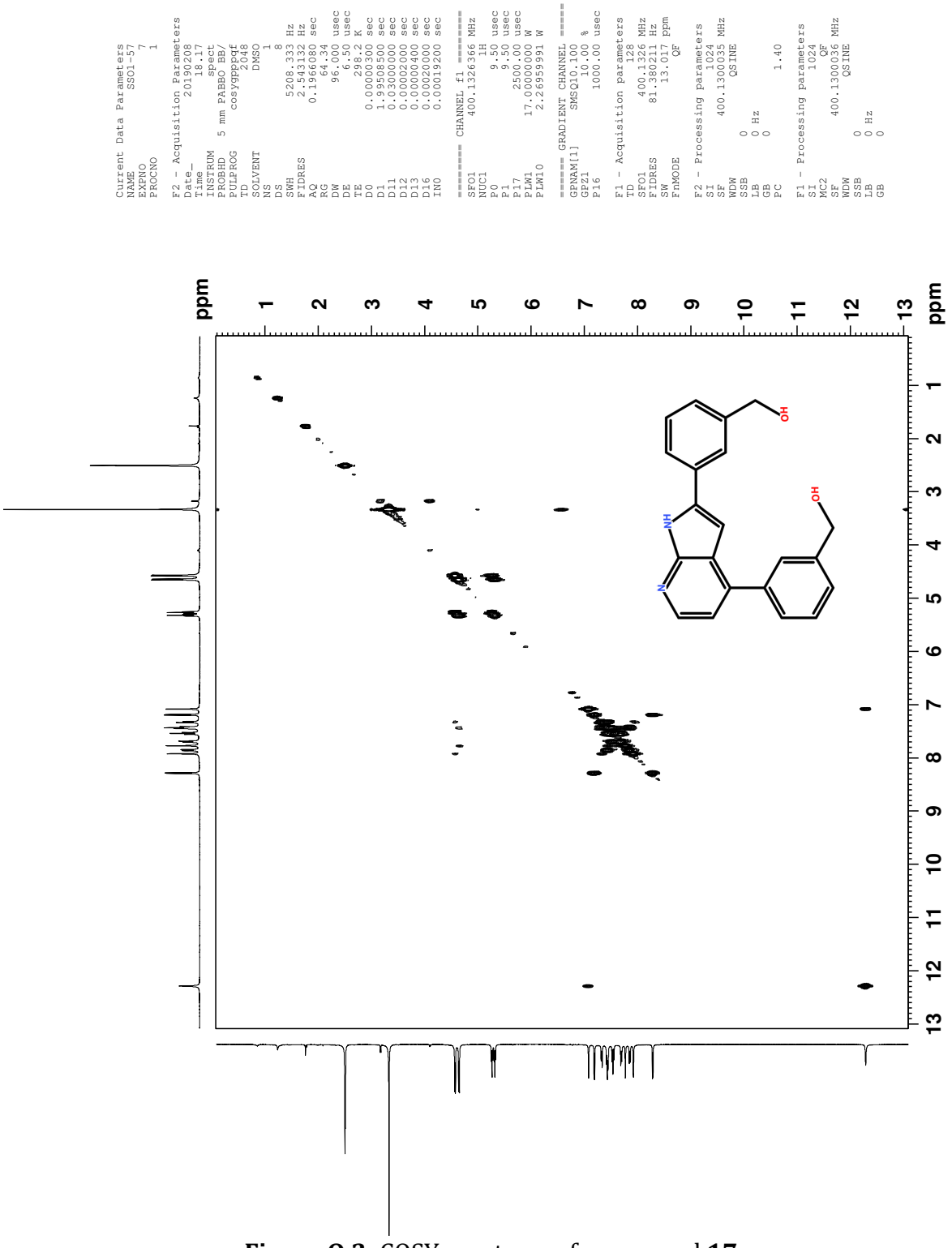

Figure Q.3: COSY spectrum of compound **17.**

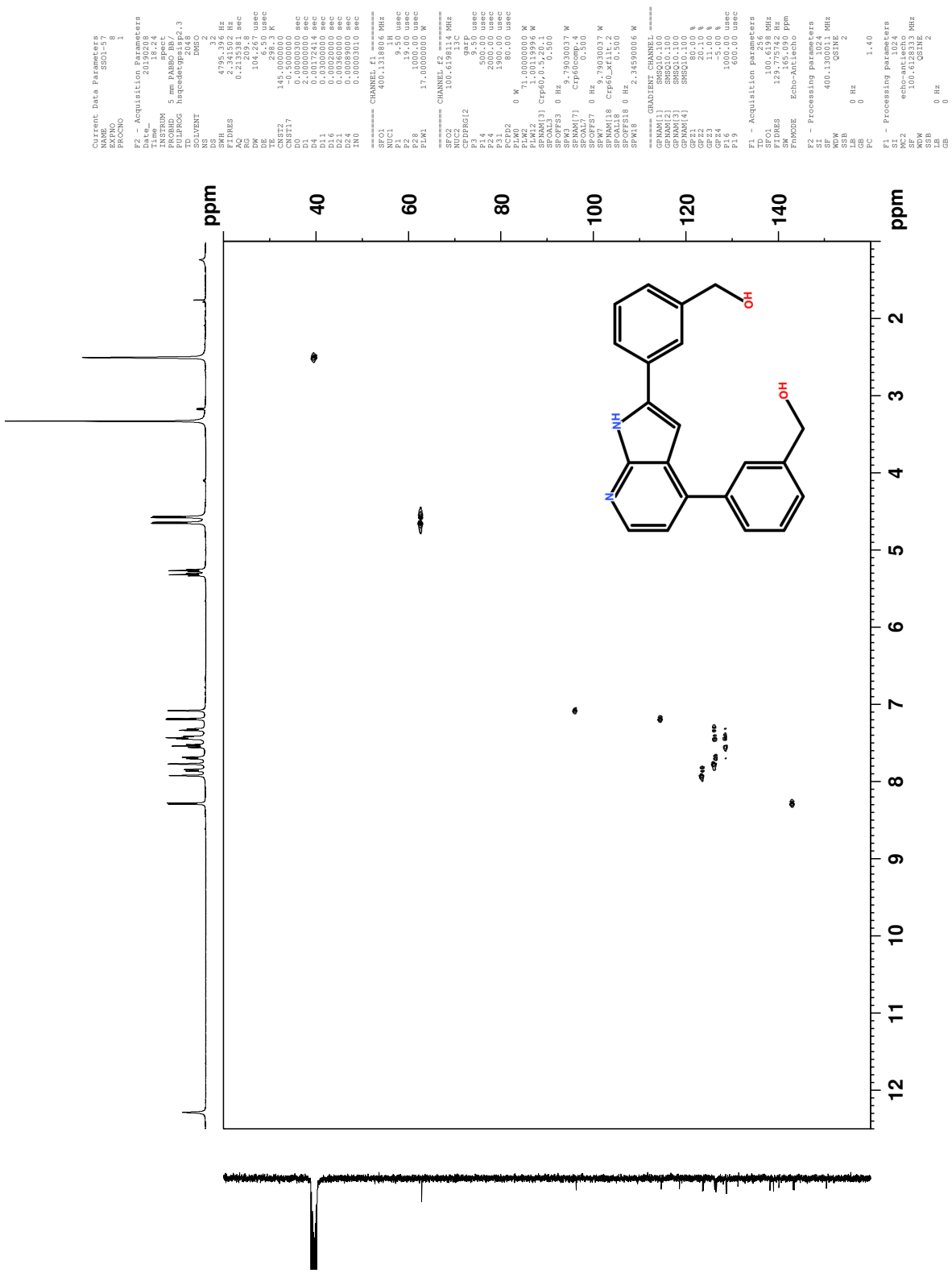

Figure Q.4: HSQC spectrum of compound **17.**

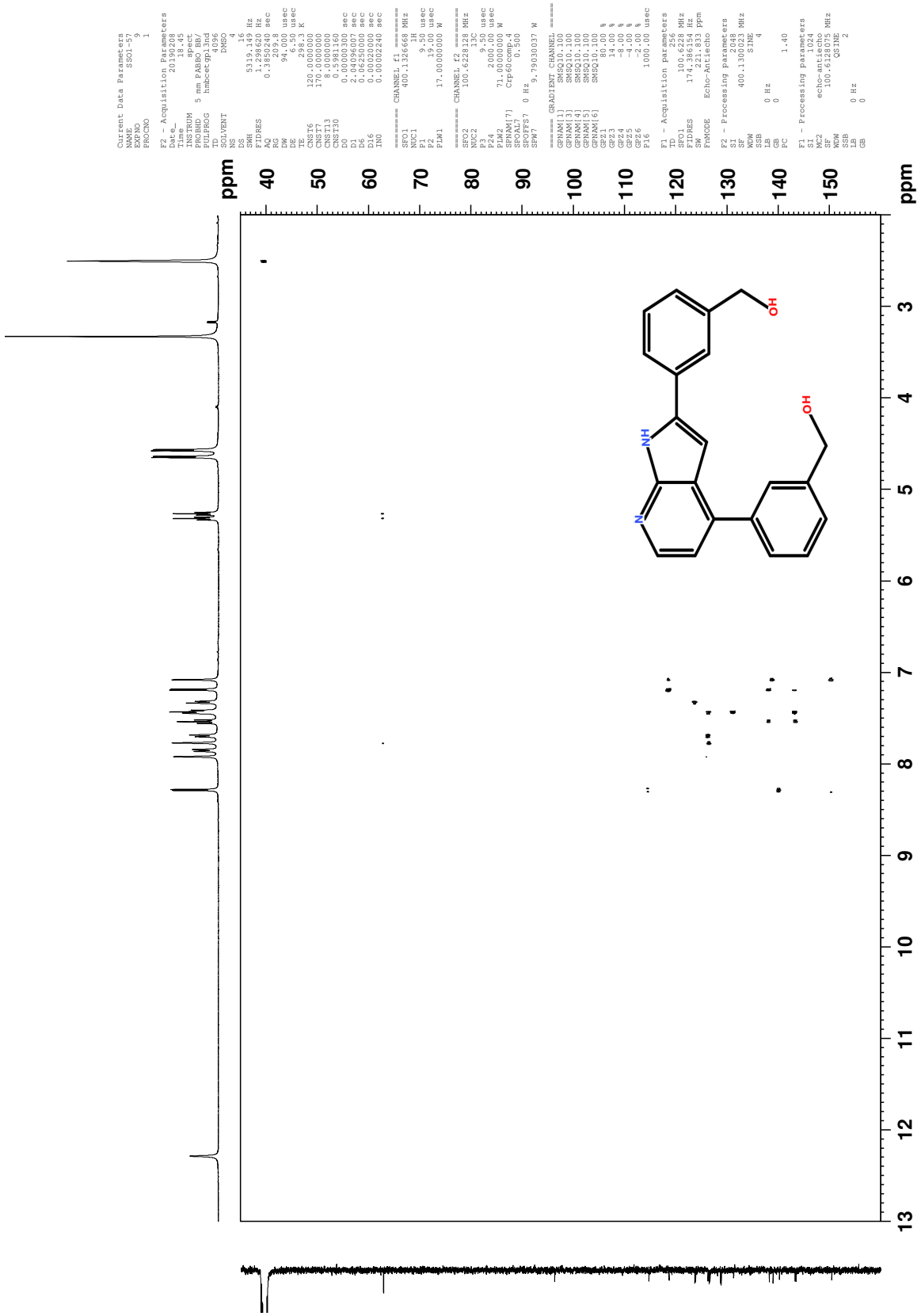

Figure Q.5: HMBC spectrum of compound **17.**

Elemental Composition Report **Page 1**

Single Mass Analysis
Tolerance = 2.0 PPM / DBE: min = -2.0, max = 50.0
Element prediction: Off
Number of isotope peaks used for i-FIT = 3

Monoisotopic Mass, Even Electron Ions
273 formula(e) evaluated with 1 results within limits (all results (up to 1000) for each mass)
Elements Used:
C: 0-100 H: 0-150 N: 0-10 O: 0-5
2019-138 179 (3.499) AM2 (Ar,35000.0,0.00,0.00); Cm (172:179)
1: TOF MS ASAP+

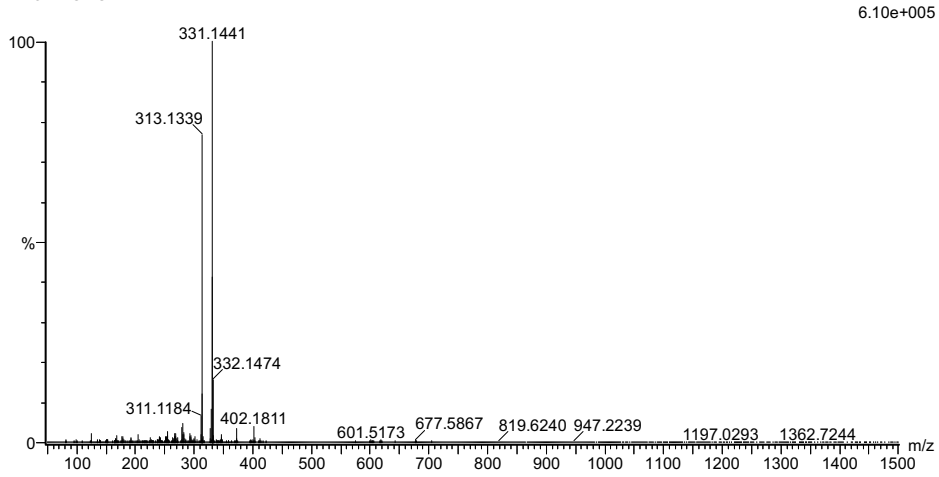

Minimum:				-2.0				
Maximum:		5.0	2.0	50.0				
Mass	Calc. Mass	mDa	PPM	DBE	i-FIT	Norm	Conf(%)	Formula
331.1441	331.1447	-0.6	-1.8	13.5	1108.7	n/a	n/a	C21 H19 N2 O2

Figure Q.6: MS spectrum of compound **17.**

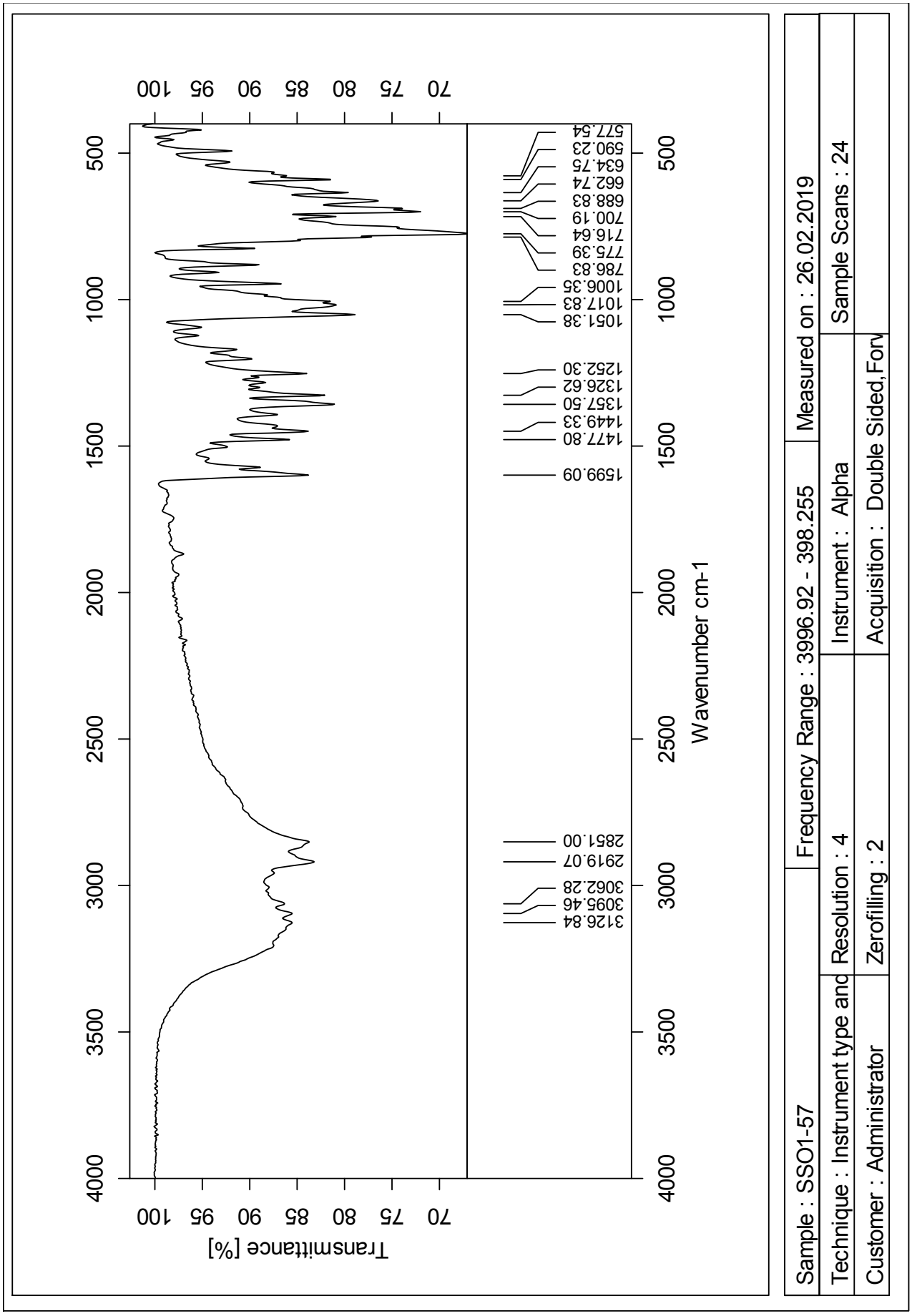

Figure Q.7: IR spectrum of compound **17.**

Selmer-Olsen, Sigrid Maria Elisabeth

Palladium Catalyzed Cross-Coupling Reactions on 7-Azaindoles in the Synthesis of CSF1R Inhibitors

NTNU
Kunnskap for ei betre verd